TESIS DE LA UNIVERSIDAD DE ZARAGOZA

2018

26

David Arnas Martínez

Necklace Flower Constellations

Departamento

Instituto Universitario de Investigación en Matemáticas y sus Aplicaciones

Director/es

Eva Tresaco Vidaller
Antonio Elipe Sánchez

ISSN 2254-7606

Prensas de la Universidad Universidad Zaragoza

ISSN 2254-7606

Universidad Zaragoza
1542

Tesis Doctoral

NECKLACE FLOWER CONSTELLATIONS

Autor

David Arnas Martínez

Director/es

Eva Tresaco Vidaller
Antonio Elipe Sánchez

UNIVERSIDAD DE ZARAGOZA

Instituto Universitario de Investigación en Matemáticas y sus Aplicaciones

2018

NECKLACE FLOWER CONSTELLATIONS

David Arnas Martínez

Instituto Universitario de Investigación
de Matemáticas
y Aplicaciones
Universidad Zaragoza

IUMA - Universidad de Zaragoza

Universidad de Zaragoza

Departamento de Matemáticas – I.U.M.A

NECKLACE FLOWER CONSTELLATIONS

Memoria presentada por

DAVID ARNAS MARTÍNEZ

para optar al Grado de

Doctor por la Universidad de Zaragoza

Dirigida por los doctores

Antonio Carmelo Elipe Sánchez, Universidad de Zaragoza (España)

Eva Tresaco Vidaller, Universidad de Zaragoza (España)

Over the course of the years
there is just one thing to fear,
a fragile courage without will
proclaiming terror as its king.

A lo largo de la vida
hay tan sólo que temer
a una frágil valentía
que convierta al miedo en rey.

David Arnas

Contents

Acknowledgments

First of all, I would like to thank Eva Tresaco and Antonio Elipe for giving me the opportunity to start my career as a Ph.D. student and researcher at Centro Universitario de la Defensa - Zaragoza. You were the first people that believed in me to research and study in my all time passion: space. Moreover, I have to thank them for giving me the freedom to develop this research in the direction I wanted. Second, I would also like to thank to all the components at Universidad the Zaragoza and Centro Universitario de la Defensa that helped me during my first steps in this new work and life: starts are never easy, but many people helped me to ease that journey.

On the other hand, I would like to thank the Spanish Ministry of Economy and Competitiveness, and the support they provided to this work through project number ESP2013–44217–R and scholarship BES–2014–068470. These projects allowed me to develop the work presented in this manuscript and to perform my two short stays during this process.

In that regard, I would also like to thank the people that welcomed and helped me during these short stays. For me, these were two wonderful experiences where I was able to learn many different things. In particular, I would like to thank Daniele Mortari from Texas A&M for his unlimited enthusiasm and imagination. Thanks to him, I was introduced to many interesting problems, including Flower Constellations (the main subject of this work), the k-vector, and star identification. On the other hand, I would also like to thank Itziar Barat, Berthyl Duesmann and the EOP-PES team at ESA-ESTEC for their warm welcome and the opportunity they gave me to work with them and learn from an splendid team. Thanks to them, I was able to greatly improve my insight in mission analysis and satellites in general.

Finally, I would like to thank my parents for their great support and patience during all these months of work. They have helped me in everything they could, enjoying and suffering all the good and bad news that I encounter during this period. Without their constant support, this work would have never been finished.

Introduction

The use of satellites provide countless possibilities including a great variety of missions such as Earth and space observation, telecommunications or global positioning systems. Moreover, many missions require multiple satellites working cooperatively to achieve a common mission, that is, a satellite constellation. In that sense, in the last years an increasing number of space missions have benefit from the advantages that satellite constellations provide, such as the improvement on the performance of the system, or the reduction of the costs associated with the mission. Examples of such missions are GPS, Galileo, Glonass, Iridium, A-train [1] or X-Tandem [2]. However, the simultaneous study of multiple satellites, and more importantly, the relations that appear in the internal structure of the constellation, increases the complexity of the problem to solve, but it also enhances the use of the available satellites, and the ability to expand the possibilities of design at our disposal.

Satellite constellation design has been since its beginning a process that required a high number of iterations due to the lack of established models for the generation and study of constellations. This situation resulted in the necessity of specific studies for each particular mission, being unable of extrapolate the results from one mission to another.

Fortunately, in the last decades, several satellite constellation design methodologies have appeared, such as Walker Constellations [3] for circular orbits or the design of Draim [4] for elliptic orbits. Later, in 2004, Mortari introduced the Flower Constellation Theory [5, 6, 7], which includes in its formulation both circular and elliptic orbits, and contains the former designs of Walker and Draim. The theory was later improved by Avendaño and Davis in the 2D Lattice [8] and 3D Lattice [9] theories which simplifies the formulation and makes the configuration independent of any reference frame. Other more recent examples of satellite constellation design include the Helix constellation [2] for very safe formation flying, polar constellations for discontinuous coverage [10] or the definition of constellations in clusters [11].

However, although being an interesting subject both academically and from the point of view of the industry, satellite constellation design has not been treated extensively in the literature. This has been caused, in most cases, by the high inversion required to position constellations with a large number of satellites in orbit. Nevertheless, this is a situation that is highly probable to change in the short term due to the interest of an increasing number of companies to position large constellations in orbit, with missions for Earth observation and telecommunications. Additionally, each passing year, more and more universities, research centers and companies are beginning to launch their first missions using the concept of micro and nano satellites. This kind of mission allows to deploy small spacecrafts requiring a very low budget, which has widen the possibilities of the use of the space

for scientific and commercial purposes. For these reasons, the advancement in satellite constellation design can be a key factor in this near future, allowing to reduce the costs of future missions and simplify the design process.

In that regard, and compared to other satellite constellation designs, Flower Constellations have had a more in depth treatment from very different perspectives. This includes the study of the relations that appeared in the configuration of the constellation [12, 13], the application of Flower Constellations to global positioning [14], or the evaluation and design of this constellations under orbital perturbations and its posterior station keeping [15, 16].

As a whole, Flower Constellations present very interesting properties. First of all, they can be defined in any rotating frame of reference. This can seem a very simple statement, but, in reality it leads to a lot of freedom in the design of constellations, being able to take advantage of the configuration that the constellation presents in one reference frame and applied it to the design of the constellation. An example of this is the ability to generate constellations where there is no possible collision between the satellites. This can be easily done by finding a reference frame in which the track of the satellites has no intersections. However, for many applications, the Earth Fixed is considered due to its advantages for many missions, specially for Earth observation. In this reference system, the resultant orbits acquire a shape that reminds the one of the petals of a flower, which is the reason why these constellations take their name.

Other extremely important property of Flower Constellations is the uniformity of the distribution. That way, and with the introduction of Lattice Flower Constellations, a general methodology was presented for the generation of all possible uniform distributions that a set of satellites can acquire. In fact, this uniform distributions introduce a new element in design: the existence of inherent structures in the constellation that are maintained over time, a property that is interesting for Earth observation and telecommunications. These structures are caused by the high number of symmetries that the constellations present, which is also one of the primary characteristics of the Lattice Flower Constellation theory.

Lattice Flower Constellations have deep foundations in Number Theory, that is, the relations that appear between integer numbers. This, at first glance, may seem an unnatural manner to perform distribution in a real space, the orbits. However, this is far for true. The reality is that since we have an integer number of satellites that is positioned in an integer number of orbits, these integer relations appear naturally, which makes the Lattice Flower constellations the proper tool to deal with the problem of satellite distribution.

However, in a Lattice Flower Constellation, the possible configurations that the theory provides is proportional to the number of satellites in the constellation, and thus, it imposes a great limitation in the design of small constellations. In order to solve this limitation, Casanova introduced the concept of necklace for the 2D Lattice formulation [17, 18] where the condition for maintaining the uniformity and symmetries of the configurations was presented. A necklace is just the selection of a subset of elements from a set of available positions. This modification of the theory allowed to expand the possibilities of design of Lattice Flower Constellations. However, necklaces were not included directly in the formulation of the constellation and its computation was difficult to handle in a computer. This resulted in the impossibility to automatize the computation of the different configurations, and the requirement to calculate all the available positions instead of just the real locations of the satellites. Thus, a new design framework was required to solve these difficulties.

In that respect, and in order to solve all these previous difficulties, this work introduces the Necklace Flower Constellation Theory. This new design framework constitutes the generalization of the methodology presented in 2D Lattice Flower Constellations using necklaces [17, 18] and the Lattice Flower Constellations themselves, and includes in its definition all the former Lattice Flower Constellations. This methodology allows to define constellations based on a fictitious constellation that has the only purpose to increase the configuration space in which we can search for uniform and symmetric distributions. In addition, and contrary to what happened in previous works, necklaces are part of the formulation, which allows to expand the fictitious constellation as much as we desire since we are not longer require to compute the positions of all the fictitious satellites. This provides a powerful tool for optimization problems, since it speeds the process significantly [19, 20, 21]. Furthermore, The Necklace Flower Constellations theory not only allows to generate uniform distributions in an early design of the constellation, but also allows the study of other problems of great interest in celestial mechanics. Examples of that are the sequence of launches for constellation building, or the determination of the possible reconfigurations available in case of failure of some satellites of the distribution.

Unfortunately, Lattice and Necklace Flower Constellations perform their design in the inertial frame of reference, not providing a clear process to control their design in the Earth Fixed frame of reference. This is an issue in some missions, especially Earth observation, telecommunications and global positioning, since having control of the design in the Earth Fixed frame of reference is, in many cases, of great importance. Thus, in order to overcome this problem, the Ground-Track Constellations are introduced in addition to the Flower Constellation methodology.

Ground-Track Constellations [22, 23] are a new methodology of design where the distribution of the constellation is performed directly in the Earth Fixed frame of reference (although it can be in any other reference system). In particular, the constellation is distributed in a set of previously defined ground-tracks that contain the satellites of the constellation at a given instant. Moreover, instead of using classical elements to define the constellation, time is selected as the distribution parameter, providing a simple manner to define the time of pass between two satellites over particular regions of the Earth. Thus, Ground-Track Constellations provide an alternative design methodology that complements the Flower Constellation theory.

On the other hand, and in order to improve the long term maintenance of the constellation defined, an alternative definition of Ground-Track Constellations is presented, which allows to include the effects of orbital perturbations directly in the definition of the constellation. In particular, all orbital parameters must be modified in the initial design of the orbit to minimize the effect of orbital perturbations [24, 25, 26, 27, 28]. However, since the along track and across track distance between satellites is selected as design parameter, the definition and the study of the evolution of the constellation structure is simplified. In that respect, a general methodology to define repeating ground-track constellations under perturbations is presented. This methodology allows to improve the maintenance of the structure of the constellation and is especially devised for the use alongside the Ground-Track Constellations methodology.

This work is structured as follows. The first chapter includes an introduction to celestial mechanics and the orbital parameters. Then, a summary of the 2D and 3D Lattice Flower Constellation theory is presented, showing an example of application for each formulation. Once this introduction is done, the concept of necklace is introduced and with it, the 2D Lattice Flower Constellations using necklaces. The chapter finishes with the description of Burnside's lemma which is used in

some parts of this work for counting the number of possibilities of design that the Necklace Flower Constellations can create.

The second chapter focuses on the study of the 2D Necklace Flower Constellations, a generalization of the 2D Lattice Flower Constellations using necklaces. This chapter includes the complete formulation of this design methodology as well as a set of theorems that allows to count the number of different possibilities of design that the 2D Necklace Flower Constellations provide.

The third chapter includes the 3D Necklace Flower Constellations, which is a generalization of all the previous Lattice Flower Constellations. This chapter also introduces the concept of generating necklaces in several variables at the same time and how they affect to the distribution generated.

The forth chapter first introduces the 4D Lattice Flower Constellations, a generalization of the 2D and 3D Lattice Flower Constellations where the semi-major axis of the orbits is included as a distribution parameter for the constellation. As it will be seen, the inclusion of the semi-major axis as a variable has deeper implications in the constellation design. Then, the 4D Necklace Flower Constellations is presented as the furthermost generalization of the Lattice and Necklace Flower Constellations theory.

The fifth chapter presents the n-dimensional congruent lattices using necklaces. This methodology allows to generate uniform and congruent distribution in a n-dimensional space subjected to modular arithmetic in all its variables. This theory represents the foundations in which the Lattice and Necklace Flower Constellations are based. In that respect, the chapter includes the proof of existence and uniqueness of the distributions obtained, providing the constraints in the parameters of distribution that allows to avoid duplicities in the design. Moreover, the theory includes counting theorems for the most interesting cases of study of this kind of distributions.

The sixth chapter deals with the alternative formulation of the Ground-Track Constellations. This design methodology allows to define constellations in a given number of ground-tracks, each one with a set of satellites. In particular, two definitions of this methodology are presented, one devised for a keplerian formulation and the other for a perturbed motion of the constellation. In addition, several examples of this new design technique are presented in order to show in a clearer way the methodology and also provide examples of design possibilities.

The seventh chapter includes a general and simple methodology for the design of repeating ground-track constellations under the effects of orbital perturbations. In that regard, the Earth gravitational potential is treated with special interest, since it is the most important perturbation for the majority of Earth space missions. This methodology is specially useful when dealing with constellations defined with the Ground-Track Constellations methodology.

The eighth and final chapter introduces the formulation to transform 2D Necklace Flower Constellations into Ground-Track Constellations. This allows to perform the constellation design using the two formulations at the same time, providing information of the distribution in both the inertial and Earth Fixed frames of reference. Additionally, this chapter includes a complete example of satellite constellation design based on three different payloads, which allows to show the possibilities and potential that the theory presented in this work provides. This example includes the definition of the nominal orbits of the constellation, two possible launching strategies and the control strategy for the mission.

Introducción

El uso de satélites proporciona un número incontable de posibilidades que incluyen una gran variedad de misiones, como la observación de la Tierra y el espacio, las telecomunicaciones o los sistemas de posicionamiento global. Además, muchas misiones requieren de varios satélites trabajando conjuntamente para alcanzar una misión común, esto es, una constelación de satélites. En ese sentido, en los últimos años, un número creciente de misiones espaciales se han beneficiado de las ventajas que las constelaciones de satélites proporcionan, tales como la mejora del comportamiento del sistema, o la reducción de los costes asociados con la misión. Ejemplos de estas misiones son GPS, Galileo, Glonass, Iridium, A-train [1] o X-Tandem [2]. Sin embargo, el estudio simultáneo de múltiples satélites, y de forma más importante, las relaciones que aparecen en la estructura interna de la constelación, aumenta la complejidad del problema tratado, aunque también permite un mejor aprovechamiento de los satélites disponibles, y la habilidad de expandir las posibilidades de diseño a nuestro alcance.

El diseño de constelaciones de satélites ha sido desde sus inicios un proceso que requería un gran número de iteraciones debido a la falta de modelos establecidos para la generación y estudio de constelaciones. Esta situación generaba la necesidad de estudios específicos para cada misión particular, no pudiendo extrapolar los resultados de una misión a otra.

Afortunadamente, en las últimas décadas, han aparecido varias metodologías de diseño de constelaciones, tales como las Walker Constellations [3] para órbitas circulares, o el diseño de Draim [4] para órbitas elípticas. Más tarde, en 2004, Mortari presentó la teoría de las Flower Constellations [5, 6, 7] que incluía en su formulación tanto órbitas circulares y elípticas, y que contenía los anteriores diseños de Walker y Draim. La teoría fue posteriormente mejorada por Avendaño y Davis con las teorías de las 2D Lattice [8] y 3D Lattice [9], que simplificaron la formulación e hicieron la configuración independiente de ningún sistema de referencia. Otros ejemplos más recientes de diseño de constelaciones de satélites incluyen la constelación tipo Helix [2] para formaciones de vuelo muy seguras, constelaciones polares para cobertura discontinua [10], o la definición de constelaciones en cúmulos [11].

Sin embargo, aunque el tema es interesante desde un punto de vista académico e industrial, el diseño de constelaciones de satélites no ha sido tratado extensamente en la literatura. Esto ha sido debido en muchos casos a la gran inversión requerida para inyectar constelaciones con un gran número de satélites en órbita. No obstante, esta situación tiene una gran probabilidad de cambio a corto plazo dado el interés de un creciente número de empresas de posicionar grandes constelaciones en órbita, con misiones para la observación de la Tierra y las telecomunicaciones. Además, cada año que pasa, un mayor número de universidades, centros de investigación y compañías están empezando a lanzar

sus primeras misiones utilizando los conceptos de micro y nano satélites. Este tipo de misiones permite el despliegue de pequeños satélites los cuales tienen unos costes muy reducidos, lo que ha incrementado las posibilidades de uso del espacio para fines científicos y comerciales. Por estas razones, el avance en el diseño de constelaciones puede ser un factor de gran importancia en este futuro cercano, consiguiendo reducir los costes de las futuras misiones y simplificando el proceso de diseño.

En este sentido, y comparado con otros diseños de constelaciones de satélites, las Flower Constellations han tenido un tratamiento más exhaustivo desde muy diferentes perspectivas. Esto incluye el estudio de las relaciones que aparecen en la configuración de la constelación [12, 13], la aplicación de las Flower Constellations para posicionamiento global [14], o la evaluación y diseño de estas constelaciones bajo perturbaciones orbitales y su posteior mantenimiento [15, 16].

En su conjunto, las Flower Constellations presentan propiedades muy interesantes. Primero de todo, pueden ser definidas en cualquier sistema de referencia. Esto puede parecer una propiedad muy simple, pero en realidad, proporciona una gran libertad en el diseño de constelaciones, permitiendo beneficiarse de la configuración que la constelación presenta en un sistema de referencia, y aplicarlo al diseño general de la constelación. Un ejemplo de ello es la posibilidad de definir constelaciones donde no hay colisiones posibles entre los satélites. Esto puede realizarse fácilmente encontrando un sistema de referencia donde la trayectoria de los satellites no tenga intersecciones. Sin embargo, en muchas aplicaciones, el sistema de referencia sujeto a Tierra es seleccionado dadas sus ventajas en muchas misiones, especialmente en observación de la Tierra. En este sistema de referencia, las órbitas resultantes adquieren una forma que recuerda a las de los pétalos de una flor, que es de donde proviene el nombre de estas constelaciones.

Otra propiedad muy importante de las Flower Constellations es la uniformidad en la distribución. De esta forma, y con la introducción de las Lattice Flower Constellations, se presentó una metodología general para la generación de todas las posibles distribuciones uniformes que un conjunto de satélites pueden adquirir. De hecho, estas distribuciones uniformes introducen un nuevo elemento en el diseño: la existencia de estructuras inherentes en la constelación que son mantenidas en el tiempo, una propiedad que es interesante para la observación de la Tierra y telecomunicaciones. Estas estructuras están causadas por el gran número de simetrías que las constelaciones presentan, que es también una de las principales características de la teoría de las Lattice Flower Constellations.

La base de las Lattice Flower Constellations tiene profundas raíces en la Teoría de Números, esto es, en las relaciones que aparecen entre los números enteros. Esto, en un primer vistazo, puede parecer una manera antinatural de realizar una distribución en el espacio real, las órbitas. Sin embargo, esto está lejos de la realidad. En verdad, dado que se tiene un número entero de satélites que están posicionados en un número entero de órbitas, estas relaciones entre enteros aparecen de forma natural, lo que hace de las Lattice Flower Constellations la herramienta adecuada para tratar con el problema de distribución de satélites.

No obstante, en una Lattice Flower Constellation, las posibles configuraciones que la teoría puede proporcionar son proporcionales al número de satélites en la constelación, y por tanto, impone una gran limitación en el diseño de constelaciones pequeñas. Para resolver estas limitaciones, el concepto de necklace fue introducido por Casanova para la formulación de las 2D Lattice [17, 18], donde la condición para el mantenimiento de la uniformidad y simetría de la configuración fue presentado. Un necklace es simplemente la selección de un subconjunto de elementos de un conjunto de posiciones

admisibles. Esta modificación de la teoría permite expandir las posibilidades de diseño de las Lattice Flower Constellations. Sin embargo, los necklaces no estaban incluídos directamente en la formulación de la constelación y su computación era difícil de manejar por un ordenador. Esto resultó en la imposibilidad de automatizar la computación de las diferentes configuraciones, y la necesidad de calcular todas las posiciones admisibles en vez de sólo las posiciones reales de los satélites. Es por ello que un nuevo marco de diseño era requerido para resolver estas dificultades.

A ese respecto, y con objeto de solventar los anteriores problemas, este trabajo introduce la teoría de las Necklace Flower Constellations. Este nuevo marco de diseño constituye la generalización de la metodología presentada en las '2D Lattice Flower Constellations using necklaces' [17, 18] y las mismas Lattice Flower Constellations, e incluye en su definición todas las Lattice Flower Constellations anteriores. Esta metodología permite definir constelaciones basadas en una constelación ficticia que tiene como único propósito incrementar el espacio de configuracion en el que se pueden buscar distribuciones simétricas y uniformes. Adicionalmente, y contrariamente a lo que ocurría en trabajos anteriores, los necklaces son parte de la formulación, lo que permite expandir la constelación ficticia tanto como deseemos dado que ya no se requiere el cálculo de las posiciones de todos los satélites ficticios. Esto proporciona una herramienta muy potente para problemas de optimización, dado que incrementa la velocidad del proceso significativamente [19, 20, 21]. Además, la teoría de las Necklace Flower Constellations no sólo genera distribuciones uniformes en un primer diseño de la constelación, sino que también permite el estudio de otros problemas de gran interés en mecánica celeste. Ejemplos de ello son la secuencia de lanzamientos para la formación de constelaciones o la determinación de las posibles reconfiguraciones disponibles en caso de fallo de algún satélite de la distribución.

Desafortunadamente, las Lattice y Necklace Flower Constellations realizan su diseño en el sistema de referencia inercial, no proporcionando un proceso claro con el que controlar su diseño en el sistema de referencia Earth Fixed. Esto es un problema en determinadas misiones, especialmente en observación de la Tierra, telecomunicaciones y posicionamiento global, dado que tener control en el sistema de referencia Earth Fixed durante el diseño es, en muchos casos, de extrema importancia. Por tanto, y para superar este problema, las Ground-Track Constellations son introducidas complementariamente a la metodología de las Flower Constellations.

Las Ground-Track Constellations [22, 23] son una nueva metodología de diseño donde la distribución de la constelación se realiza directamente en el sistema de referencia Earth Fixed (aunque puede hacerse en cualquier otro sistema de referencia). En particular, la constelación se distribuye en un conjunto de trazas previamente definidas que contienen los satélites de la constelación en un momento dado. Además, en lugar de utilizar elementos clásicos para definir la constelación, el tiempo se selecciona como el parámetro de distribución, proporcionando una forma sencilla de definir el tiempo de paso entre dos satélites sobre determinadas regiones de la Tierra. Por tanto, las Ground-Track Constellations proporcionan una metodología de diseño alternativo que complementa a la teoría de las Flower Constellations.

Por otro lado, y para mejorar el mantenimiento a largo plazo de las constelaciones definidas, se presentta una definición alternativa de las Ground-Track Constellations, que permite incluir los efectos de perturbaciones orbitales directamente en la definición de la constelación. En particular, todos los parámetros orbitales han de ser modificados en el diseño inicial de la órbita para minimizar el efecto de las perturbaciones orbitales [24, 25, 26, 27, 28]. Sin embargo, dado que la distancia a lo largo y a través de la traza es seleccionada como parámetro de diseño, la definición y el estudio

de la evolución de la estructura de la constelación se simplifica. A este respecto, se presenta una metodología general para la definición de constelaciones de repetición de traza. Esta metodología permite mejorar el mantenimiento de la estructura de la constelación y está especialmente disñada para su uso conjunto con la metodología de las Ground-Track Constellations.

Este trabajo está estructurado como sigue. El primer capítulo incluye una introducción a la mecánica celeste y a los parámetros orbitales. Después, se presenta un resumen de las teorías de las 2D y 3D Lattice Flower Constellations, mostrando ejemplos de aplicación de cada formulación. Una vez hecha esta introducción, el concepto de necklace se introduce y con él, las 2D Lattice Flower Constellations utilizando necklaces. El capítulo termina con la descripción del lema de Burnside, el cuál es utilizado en algunas partes de este trabajo para contar el número de posibilidades de diseño que las Necklace Flower Constellations pueden generar.

El segundo capítulo se centra en el estudio de las 2D Necklace Flower Constellations, que son la generalización de las 2D Lattice Flower Constellations usando necklaces. Este capítulo incluye la completa formulación de esta metodología de diseño además de un conjunto de teoremas para el conteo del número de diferentes posibilidades de diseño que las 2D Necklace Flower Constellations proporcionan.

El tercer capítulo incluye las 3D Necklace Flower Constellations, que es una generalización de las anteriores Lattice Flower Constellations. Este capítulo también introduce el concepto de la generación de necklaces en varias variables al mismo tiempo y cómo afecta esto a la distribución generada.

El cuarto capítulo introduce por primera vez las 4D Lattice Flower Constellations, una generalización de las 2D y 3D Lattice Flower Constellations en donde el semieje mayor de las órbitas es incluído como parámetro de distribuicón para la constelación. Tal y como se verá, la inclusión del semieje mayor como variable tiene unas implicaciones más profundas en el diseño de constelaciones. Después, las 4D Necklace Flower Constellations son presentadas como la última generalización de la teoría de las Lattice and Necklace Flower Constellations.

El quinto capítulo presenta los n-dimensional congruent lattices using necklaces. Esta metodología permite la generación de distribuciones uniformes y congruentes en un espacio n-dimensional sujeto a aritmética modular en todas sus variables. Esta teoría representa los cimientos en los que las Lattice y Necklace Flower Constellations están basadas. A ese respecto, el capítulo incluye las demostraciones de existencia y unicidad de las distribuciones obtenidas, proporcionando los límites que presentan los parámetros de ditribución y que evitan las duplicidades en el diseño. Además, la teoría incluye teoremas de conteo para los casos más interesantes de estudio de este tipo de distribuciones.

El sexto capítulo trata la formulación alternativa de las Ground-Track Constellations. Esta metodología de diseño permite la definición de constelaciones en un conjunto dado de trazas, cada una con un conjunto de satélites. En concreto, se presentan dos definiciones para esta metodología, una pensada para una formulación kepleriana, y la otra para constelaciones en las que se considera un movimiento perturbado. Además, se presentan varios ejemplos de aplicación de esta nueva técnica de diseño en el que se muesta claramente la metodología así como las posibilidades de diseño que permite.

El séptimo capítulo incluye una metodología simple y general para el diseño de constelaciones de repetición de traza bajo los efectos de perturbaciones orbitales. En este sentido, el potencial gravitatorio terrestre es tratado con especial interés, dado que es la perturbación más importante para la mayoría de misiones espaciales. Esta metodología es especialmente útil para su uso junto a la metodología de las Ground-Track Constellations.

El octavo y último capítulo introduce la formulación que permite transformar las 2D Necklace Flower Constellations en las Ground-Track Constellations. Esto permite generar el diseño de constelaciones simultáneamente en el sistema de referencia inercial y rotante. Adicionalmente, este capítulo incluye un ejemplo completo de diseño de una constelación de satélites basado en tres cargas de pago diferentes, lo que permite mostrar las posibilidades y el potencial que la teoría presentada en este trabajo proporciona. Este ejemplo incluye la definición de las órbitas nominales de la constelación, dos posibles estrategias de lanzamiento, y la estrategia de control para la misión.

Chapter 1

Preliminaries

This first chapter serves as a initial point from which the research presented in this work departs. It contains the basic concepts and theories that will be used extensively during this work. First, an introduction in orbital mechanics is done, starting with the derivation of the equations in the Kepler's problem, and the presentation of the classical formulation. Then, a summary of the perturbation theory is introduced in order to add the effects of orbital perturbations to the classical formulation, being the Earth oblateness the most important perturbation to consider. That way, the foundations of orbital mechanics are shown as a reference of the entire document.

Second, the Lattice Flower Constellation Theory is summarized, including the formulation of the 2D and 3D Lattice Flower Constellations. In addition, the necklace problem is introduced, and the 2D Lattice Flower Constellations using necklaces is presented.

Finally, Burnside's Lemma is shown, as it is used in several theorems introduced in this work. In particular, Burnside's Lemma is required for the determination of the number of possibilities of design that the Necklace Flower Constellation theory can provide.

1.1 Kepler's problem: Classical Formulation

The keplerian movement is the basic physic model in celestial mechanics and constitutes the first order approximation to the real problem. This model only considers the interaction between two massive bodies, treated as material points with isotropic density and whose sizes are negligible compared with the distances of the problem. Although this is a set of very restrictive hypothesis for the problem, it is extremely close to reality as the sizes of celestial bodies are much smaller than the distances between them.

The classical formulation of Kepler's problem is based on Newton's laws applied to the gravitational force. It departs from the observation that two mass bodies suffer, between them, an attractive force that is directly proportional to their masses and inversely proportional to the square of the distance between them, that is:

$$\begin{aligned} m_1\ddot{\boldsymbol{x}}_1 &= -G\frac{m_1 m_2}{\| \boldsymbol{x}_1 - \boldsymbol{x}_2 \|^2}\frac{\boldsymbol{x}_1 - \boldsymbol{x}_2}{\| \boldsymbol{x}_1 - \boldsymbol{x}_2 \|}, \\ m_2\ddot{\boldsymbol{x}}_2 &= -G\frac{m_1 m_2}{\| \boldsymbol{x}_2 - \boldsymbol{x}_1 \|^2}\frac{\boldsymbol{x}_2 - \boldsymbol{x}_1}{\| \boldsymbol{x}_2 - \boldsymbol{x}_1 \|}, \end{aligned} \tag{1.1}$$

where G is the universal gravitational constant, m_1 and m_2 are the masses of the two particles and $\boldsymbol{x}_1$, $\boldsymbol{x}_2$, $\ddot{\boldsymbol{x}}_1$ y $\ddot{\boldsymbol{x}}_2$ are the positions and accelerations of the particles in an inertial frame of reference.

As it can be seen, the acceleration experienced by a point positioned in the center of masses of the system is zero because there is no external force perturbing the system and as such, the system is inertial with respect of this center of masses. Moreover, if the mass of one of the bodies is much bigger than the other (such as the planets orbiting the Sun or satellites in the gravitational field of another celestial body), the center of masses of the system can be approximated by the one of the heaviest body (the primary body). Thus, the origin of the inertial frame of reference can be positioned in the center of masses of the primary body, and then using Equation (1.1), we obtain the following expression:

$$\ddot{\boldsymbol{r}} = -\mu \frac{\boldsymbol{r}}{r^3}, \tag{1.2}$$

where $\mu = G(M_\oplus + m_2) \approx GM_\oplus$ and $M_\oplus$ are the primary body gravitational constant and its mass, whilst $\boldsymbol{r}$ is the radio-vector from the origin of the inertial frame to the particle that is being studied.

1.1.1 Constants of motion

One important property presented in Equation (1.2) is that the force always points to the origin of the frame of reference, a property that is called central force. Particles moving under a central force have some interesting properties.

First, the angular momentum of the particle is constant. Let $\boldsymbol{h}$ be the angular momentum of a particle defined as:

$$\boldsymbol{h} = \boldsymbol{r} \times \dot{\boldsymbol{r}}, \tag{1.3}$$

where $\boldsymbol{r}$ is the position and $\dot{\boldsymbol{r}}$ is the velocity of the particle. It is easy to prove that $\boldsymbol{h}$ is constant over time:

$$\dot{\boldsymbol{h}} = \dot{\boldsymbol{r}} \times \dot{\boldsymbol{r}} + \boldsymbol{r} \times \dot{\dot{\boldsymbol{r}}} = \boldsymbol{r} \times \dot{\boldsymbol{r}} - \frac{\mu}{r^3} (\boldsymbol{r} \times \boldsymbol{r}) = \boldsymbol{0}, \tag{1.4}$$

where $r = \| \boldsymbol{r} \|$. Moreover, we can observe that $\boldsymbol{h} \cdot \boldsymbol{r} = 0$ and $\boldsymbol{h} \cdot \boldsymbol{v} = 0$. This implies that, the movement lays in a plane that contains the origin of the reference frame, and that $\boldsymbol{h}$ is perpendicular both to the position $\boldsymbol{r}$ and the velocity $\dot{\boldsymbol{r}}$ of the particle in each instant.

Second, a central force generates a conservative field. We know that a force is conservative if its curl is zero. Let $\boldsymbol{u}_x$, $\boldsymbol{u}_y$ and $\boldsymbol{u}_z$ be the unitary vectors of the inertial frame of reference. Then, using Equation (1.2):

$$\nabla \times \ddot{\boldsymbol{r}} = \left(3\mu \frac{yz}{r^5} - 3\mu \frac{yz}{r^5}\right) \boldsymbol{u}_x + \left(3\mu \frac{xz}{r^5} - 3\mu \frac{xz}{r^5}\right) \boldsymbol{u}_y + \left(3\mu \frac{xy}{r^5} - 3\mu \frac{xy}{r^5}\right) \boldsymbol{u}_z = \boldsymbol{0}, \tag{1.5}$$

and thus, the gravitational force is conservative and there exists a potential associated with the force. Let V be the specific potential of a particle defined as:

$$V = \int_\infty^r \ddot{\boldsymbol{r}} \cdot d\boldsymbol{r} = -\mu \int_\infty^r \frac{\boldsymbol{r}}{r^3} d\boldsymbol{r} = -\frac{\mu}{r}. \tag{1.6}$$

As the force is conservative, the mechanical energy ξ, sum of the potential and kinetic energies, is constant, and thus:

$$\xi = \frac{v^2}{2} - \frac{\mu}{r}. \tag{1.7}$$

In addition, by computing the derivative of the unit vector that points the particle of study, we obtain:

$$\frac{d}{dt}\left(\frac{\boldsymbol{r}}{r}\right) = \frac{\boldsymbol{r} \times (\dot{\boldsymbol{r}} \times \boldsymbol{r})}{r^3} = \frac{\ddot{\boldsymbol{r}} \times \boldsymbol{h}}{\mu} = \frac{d}{dt}\left(\frac{\dot{\boldsymbol{r}} \times \boldsymbol{h}}{\mu}\right), \tag{1.8}$$

which leads us to the definition of another constant of the movement, the eccentricity:

$$\boldsymbol{e} = e\boldsymbol{u}_e = \frac{\dot{\boldsymbol{r}} \times \boldsymbol{h}}{\mu} - \frac{\boldsymbol{r}}{r}, \tag{1.9}$$

which is a vector contained in the plane of the movement and perpendicular to $\boldsymbol{h}$.

As it can be seen, there exist six degrees of freedom in the problem (three positions and three velocities) and we have obtained seven first integrals (constants in the movement). Thus, it is logical to think that these constants are not independent.

By computing the scalar product between the eccentricity and the angular momentum, we obtain that the product is always zero:

$$\boldsymbol{e} \cdot \boldsymbol{h} = 0, \tag{1.10}$$

which means that there is a relation between both vectors and, to be more precise, they are perpendicular to each other.

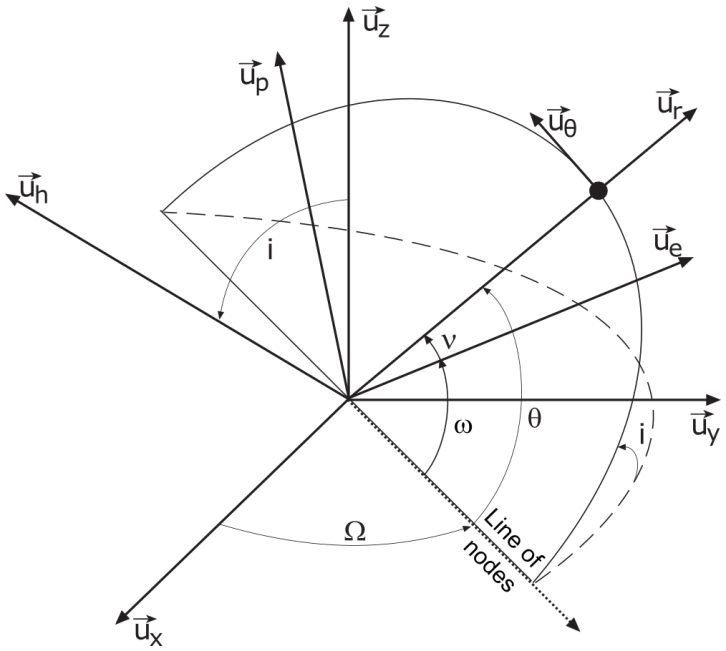

Figure 1.1: Orbital elements and reference systems.

On the other hand, as we said before, the movement is planar and thus, it is possible to define the dynamic of the particle in an inertial frame of reference fixed to that plane. Let $\boldsymbol{u}_r$, $\boldsymbol{u}_\theta$ and $\boldsymbol{u}_h$ be the unit vectors of this frame of reference (the orbital reference system) where $\boldsymbol{u}_r$ always points towards the particle, $\boldsymbol{u}_h$ is perpendicular to the orbital plane (where $\boldsymbol{u}_h = \boldsymbol{h}/ \parallel \boldsymbol{h} \parallel$) and $\boldsymbol{u}_\theta = \boldsymbol{u}_h \times \boldsymbol{u}_r$ (see Figure 1.1). Thus, the position, velocity and acceleration of the particle can be defined in polar coordinates (r, θ) as:

$$\begin{aligned} \boldsymbol{r} &= r\boldsymbol{u}_r, \\ \dot{\boldsymbol{r}} &= \dot{r}\boldsymbol{u}_r + r\dot{\theta}\boldsymbol{u}_\theta, \\ \ddot{\boldsymbol{r}} &= \left(\ddot{r} - \dot{\theta}^2 r\right)\boldsymbol{u}_r + \left(\ddot{\theta}r + 2\dot{\theta}\dot{r}\right)\boldsymbol{u}_\theta, \end{aligned} \tag{1.11}$$

Now, we apply these expressions to the angular momentum:

$$\boldsymbol{h} = h\boldsymbol{u}_h = r^2\dot{\theta}\boldsymbol{u}_h \longrightarrow \dot{\theta} = \frac{h}{r^2}, \tag{1.12}$$

in order to obtain the variation of θ as a function of the radius of the orbit. Then, calculating the eccentricity with Equation (1.11):

$$\boldsymbol{e} = \left(\frac{\dot{\theta}rh}{\mu} - 1\right)\boldsymbol{u}_r - \frac{\dot{r}h}{\mu}\boldsymbol{u}_\theta, \tag{1.13}$$

we can find a relation between the modulus of the eccentricity (e) and the energy of the orbit (ξ). Using Equations (1.7), (1.12) and (1.13) we obtain:

$$\xi = \frac{(e^2 - 1)\mu^2}{2h^2}, \tag{1.14}$$

being this expression the second relation between the first integrals defined at the beginning.

Equations (1.10) and (1.14) reduce the number of first integrals to five (seven conditions minus two relations), which leaves only one degree of freedom in the movement as the number of initial degrees of freedom is six and the number of first integrals is five. Thus, the complete dynamic of the particle can be defined by the use of just one parameter, being the other five constants. This is the basic concept behind the classical formulation.

1.1.2 Classical variables

The objective now is to define the classical variables of the problem. The most common variables used are the classical orbital elements, which have a clear physical and geometrical meaning that helps to understand the problem that we are treating.

First, as the movement is planar, we define the orientation of the orbital plane with respect of the inertial frame of reference. Two angles are required, the right ascension of the ascending node (Ω) and the inclination (i) (see Figure 1.1). The inclination is the angle between the angular momentum and the z axis, whilst the right ascension of the ascending node is the angle between

the passing of the particle over the equator (in the direction South-North) and the x inertial axis. Their mathematical expressions related to the angular momentum are:

$$\begin{aligned} \cos(i) &= \frac{\boldsymbol{h}\cdot\boldsymbol{u}_z}{\parallel \boldsymbol{h} \parallel}, \\ \cos(\Omega) &= \frac{(\boldsymbol{u}_z\times\boldsymbol{h})\cdot\boldsymbol{u}_x}{\parallel \boldsymbol{u}_z\times\boldsymbol{h} \parallel}, \end{aligned} \tag{1.15}$$

where $i \in [0,\pi)$ and $\Omega \in [0,2\pi)$. Thus, in order to obtain the precise value of the right ascension of the ascending node, we have to determine in which half of the space the angle is located.

Once the plane is fixed, the orientation inside it is required. As seen before, the eccentricity vector is constant and contained in the orbital plane thus, it provides the information on the orientation of the orbit in the plane. That way, the argument of perigee (ω) is introduced as the angle between the eccentricity (with direction $\boldsymbol{u}_e$) and $\boldsymbol{u}_n = \boldsymbol{u}_z \times \boldsymbol{u}_h$ (see Figure 1.1):

$$\cos(\omega) = \frac{(\boldsymbol{u}_z\times\boldsymbol{h})\cdot\boldsymbol{e}}{\parallel \boldsymbol{u}_z\times\boldsymbol{h} \parallel e}, \tag{1.16}$$

where $\omega \in [0,2\pi)$ and thus the determination of the half of the space in which the angle is located is required.

These parameters (Ω, i and ω) are fixed angles that orientate the orbit in space but they do not provide information about the energy of the trajectory or the position of the particle. The position of the particle can be related with the angle, in the orbital plane, between the position and the eccentricity. Let the true anomaly ν be that angle, which is defined as:

$$\cos(\nu) = \frac{\boldsymbol{r}\cdot\boldsymbol{e}}{re}, \tag{1.17}$$

and using Equations (1.9) and (1.12), we obtain:

$$r = \frac{p}{1+e\cos(\nu)}, \tag{1.18}$$

where $p = h^2/\mu$ is the semilatus rectum of the orbit. This expression provides the information of the curve that the particle describes in its movement. Substituting in Equation (1.18) $r^2 = x_p^2 + y_p^2$ and $x_p = r\cos(\nu)$, where x_p and y_p are the coordinates of the satellite in the perifocal frame of reference defined by the directions $(\boldsymbol{u}_e, \boldsymbol{u}_p = (\boldsymbol{u}_h \times \boldsymbol{u}_e), \boldsymbol{u}_h)$, the following equation is derived:

$$(1-e^2)x_p^2 + y_p^2 + 2epx_p - p^2 = 0, \tag{1.19}$$

which is the expression of a conic curve in Cartesian coordinates, where one of the focus of the conic is positioned in the center of the frame of reference.

As the orbit is a conic, the eccentricity e is used in order to define the shape of the conic and the semi-major axis a to establish its size. Using basic geometry, the semi-major axis can be calculated using the periapsis (r_{per}) and apoapsis (r_{apo}) of the orbit:

$$a = \frac{r_{per}+r_{apo}}{2} = \frac{p}{2}\left(\frac{1}{1+e}+\frac{1}{1-e}\right) = \frac{p}{1-e^2}. \tag{1.20}$$

The objective now is to associate the semi-major axis with the energy of the system. In order to do that, we perform the derivative of the radius:

$$\dot{r} = \frac{p}{(1 + e\cos(\nu))^2} e\sin(\nu)\dot{\nu}, \tag{1.21}$$

where we can realize that the derivative is zero when the particle is in the periapsis or the apoapsis of the orbit ($\sin(\nu) = 0$). Using this property and Equation(1.11), we conclude that the square of the velocity in these points is:

$$\| \dot{\boldsymbol{r}} \|^2 = \frac{h^2}{r^2}, \tag{1.22}$$

and applying the expression for the mechanical energy, Equation (1.7), in the periapsis of the orbit, we obtain:

$$\xi = \frac{1}{2}\frac{h^2}{p^2}(1+e)^2 - \frac{\mu}{p}(1+e) = -\frac{1}{2}\mu\frac{(1-e^2)}{p} = -\frac{\mu}{2a}, \tag{1.23}$$

and thus, the size of the orbit (the semi-major axis) has been related to the energy of the system.

Thus, all six classical elements have been defined: the semi-major axis a, the eccentricity e, the inclination i, the right ascension of the ascending node Ω, the argument of perigee ω and the true anomaly ν. These orbital elements present some singularities. Examples of that are circular, equatorial and parabolic orbits, where complementary variables have to be defined.

1.1.3 Elliptic movement

As the aim of this work is the study of satellite constellations, we only deal with elliptic orbits, which are the only ones that shows a periodic behavior. This implies that the semi-major axis of the orbit is positive and the mechanical energy of the system is negative.

Let E be the eccentric anomaly, which is the angle between the direction of the eccentricity vector and the position of the particle from the center of the ellipse. Applying the Pythagoras' theorem:

$$r^2 = a^2(1-e^2)\sin^2(E) + (ae - a\cos(E))^2, \tag{1.24}$$

and working with the expression, a relation between the radius and the eccentric anomaly can be obtained:

$$r = a(1 - e\cos(E)). \tag{1.25}$$

Then, as the semi-major axis and the eccentricity are constant, the derivative of Equation (1.25) is calculated:

$$\dot{r} = ae\sin(E)\dot{E}. \tag{1.26}$$

From Equations (1.11) and (1.7), the square of the modulus of the velocity can be computed and matched between both equations:

$$\dot{r}^2 + \left(\frac{h}{r}\right)^2 = \frac{2\mu}{r} - \frac{\mu}{a}, \tag{1.27}$$

obtaining the value of $\dot{r}$ by the application of the semilatus rectum and Equation (1.20):

$$\dot{r}^2 = \frac{\mu}{a}\left(\frac{2}{r} - 1 - \frac{(1-e^2)}{r^2}\right). \tag{1.28}$$

Using Equations (1.25), (1.26) and (1.28), a differential equation on E is achieved:

$$\sqrt{\frac{\mu}{a^3}} = (1 - e\cos(E))\dot{E}, \tag{1.29}$$

which can be integrated, obtaining the evolution of the eccentric anomaly over time:

$$M = E - e\sin(E) = \sqrt{\frac{\mu}{a^3}}\Delta t. \tag{1.30}$$

where Equation (1.30) is the Kepler's equation for elliptic orbits and M is the mean anomaly, a variable that has a linear evolution with respect time. Moreover, related to the derivative of M, we define the mean motion n as the rate of change of M:

$$n = \sqrt{\frac{\mu}{a^3}}, \tag{1.31}$$

which is a constant value in the unperturbed problem. Kepler's equation is the basic expression that provides the first order approximation of the dynamic of the particle along its movement.

From Equation (1.30) we can derive the period of the orbit, which is the time that the particle requires to return to the same initial position. Using the mean anomaly as the parameter of movement, the time that it takes to move from $M = 0$ to $M = 2\pi$ is:

$$T = 2\pi\sqrt{\frac{a^3}{\mu}}, \tag{1.32}$$

where T is the period of the orbit. As it can be seen, it only depends on the semi-major axis of the orbit (which is equivalent to the energy of the orbit) and the primary body of the problem (due to the gravitational constant of the Earth μ).

Kepler's formulation allows to perform the first order design and study of an orbit. However, in order to improve the accuracy of the model used, orbital perturbations must be included. This makes the problem more complex, but it also provides a better prediction on the problem studied.

1.2 Perturbation theory

Keplerian formulation is ideal, where it considers the bodies as points with no size subjected to just the gravitational force existing between them. Although simple, this model is very useful, as it provides the first order approximation to the real problem. To be more precise, and for objects orbiting the Earth, the biggest perturbation is provoked by the non spherical shape of the Earth J_2, and this term is three orders of magnitude lower than the keplerian term.

However, the keplerian formulation does not predict with enough accuracy the positions and velocities of objects orbiting the Earth. Note that, experiencing small accelerations due to perturbations does not mean negligible effects. In fact, as time passes, these small perturbations can have a big impact on the long term dynamics of satellites. These are the reason why more elaborated models are required in order to improve the accuracy of the predictions generated.

Orbital perturbations can have very different origins and nature. Examples of that are the ones provoked by the Earth, the Sun, the cosmic radiation or the general relativity. However, for satellites orbiting in a near to Earth environment, the most relevant orbital perturbations are:

- The Earth gravitational potential: it is generated by a non uniform distribution of the mass of the Earth. Its greatest effect is the J_2 perturbation, which is related to the non spherical shape of the Earth (in particular its oblateness). The effect of this perturbation decreases with the distance of satellites to the Earth surface.
- The Sun and Moon as third bodies: other massive bodies such as the Sun or the Moon modify the trajectories of satellites. This perturbation is bigger the farther the satellite is from Earth.
- The atmospheric drag: although the atmospheric pressure in space environments is extremely low, its effect can be important as satellites move at high speed related to the atmosphere. The importance of this perturbation increases drastically when in very low orbits.
- The solar radiation pressure (SRP): the Sun generates radiation that in contact with the surfaces of satellites, produces an acceleration on them. The intensity of this effect is nearly independent from the distance to the Earth.
- The albedo: it is the sum of two effects, the thermal radiation that the Earth produces for being hotter than deep space, and the reflexion of the Sun radiation in the Earth surface. This effect increases the closer satellites are to the Earth surface.

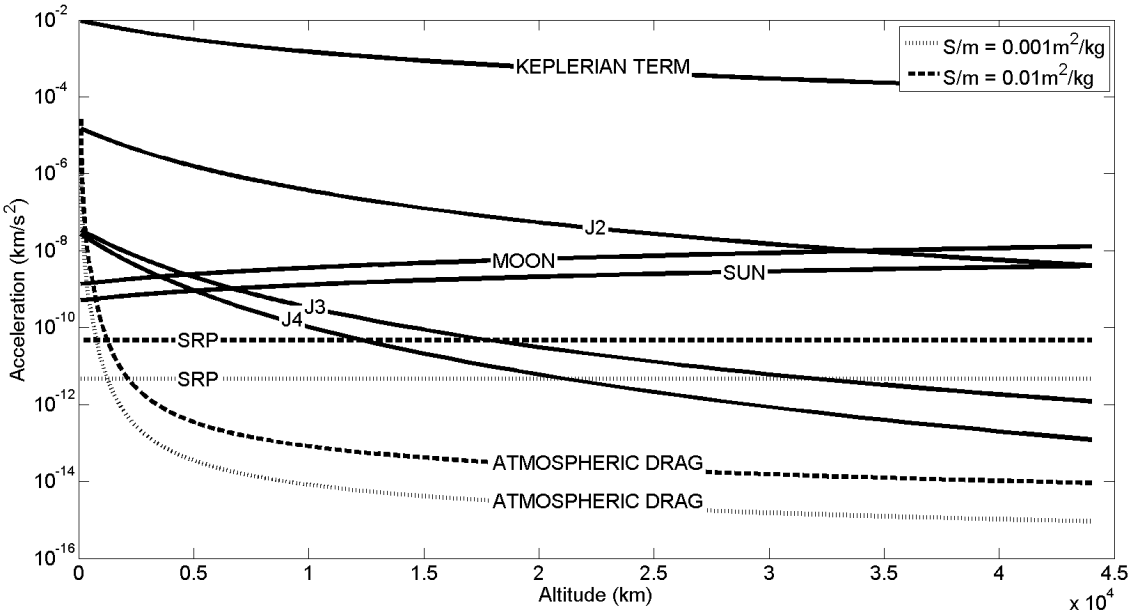

Figure 1.2: Orders of magnitude (in logarithmic scale) of orbital perturbations with the altitude of the orbits.

In order to show the importance of each perturbation, we create a force model consisting on the gravitational potential of the Earth [29] up to 4th order zonal terms (J_2, J_3, J_4), the Sun and Moon as disturbing third bodies [30], the solar radiation pressure [31] and the atmospheric drag (Harris-Priester [32, 33] model). The results of computing the acceleration (in logarithmic scale) provoked

by each perturbation with respect of the altitude are presented in Figure 1.2. There, it can be clearly seen that the primary term, the keplerian problem, is three orders of magnitude bigger than the most important of the orbital perturbations, the J_2. Moreover, as the acceleration that the satellites suffer due to the solar radiation pressure and the atmospheric drag depends on the ratio incident surface S with mass m, two different values have been included, $S/m = 0.001m^2/kg$ and $S/m = 0.01m^2/kg$, which represent the typical design boundary of common satellites.

On the other hand, and related to the effects that these perturbations generate in the orbital variables in study, two different kind of variations can be defined, the secular variations and the periodic variations [34], which are represented schematically in Figure 1.3. In that respect, the secular effect is the mean variation that the variables suffer over time, while, on the other hand, the periodic variations (also known as variations of long and short period) are related to the periodic behavior of the variables around the mean secular variation of the variable.

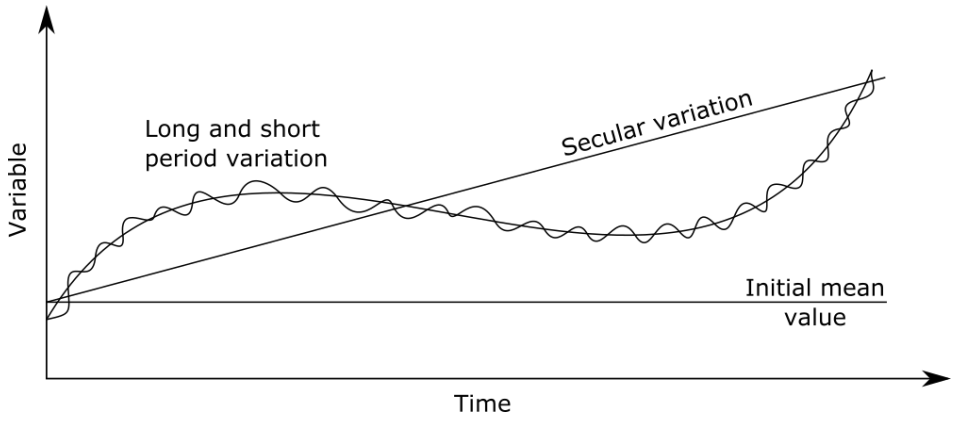

Figure 1.3: Secular, long and short effects of the orbital perturbation.

Once orbital perturbations are described, it is time to introduce the perturbation theory. The perturbation theory consist of the definition of the problem as the sum of two components: the keplerian problem and the effects of perturbations. That way, the acceleration of a particle can be represented as:

$$\ddot{\boldsymbol{r}} = -\mu\frac{\boldsymbol{r}}{r^3} + \boldsymbol{\gamma}, \tag{1.33}$$

where $\boldsymbol{\gamma}$ is the resultant acceleration provoked by orbital perturbations. There are many methodologies to deal with perturbations, being the most common ones, Lagrange planetary equations and Gauss planetary equations.

Lagrange planetary equations are used with conservative perturbations such as the effect of the non uniform gravitational potential of the Earth. In order to use them, we first have to express the Hamiltonian of the system ($\mathcal{H}$) as a function of the time t:

$$\mathcal{H} = -\frac{\mu}{2a} - R(a,\, e,\, i,\, \omega,\, \Omega,\, M,\, t), \tag{1.34}$$

where R is the resultant of the generalized potential of the disturbing forces affecting the problem, expressed by means of the classical elements. That way, it is possible to express the derivatives of

the orbital elements using Lagrange planetary equations:

$$\begin{aligned}
\frac{da}{dt} &= \frac{2}{na}\frac{\partial R}{\partial M}, \\
\frac{de}{dt} &= \frac{1-e^2}{na^2e}\frac{\partial R}{\partial M} - \frac{\sqrt{1-e^2}}{na^2e}\frac{\partial R}{\partial \omega}, \\
\frac{di}{dt} &= \frac{\cos i}{na^2\sqrt{1-e^2}\sin i}\frac{\partial R}{\partial M} - \frac{1}{na^2\sqrt{1-e^2}\sin i}\frac{\partial R}{\partial \Omega}, \\
\frac{d\omega}{dt} &= \frac{\sqrt{1-e^2}}{na^2e}\frac{\partial R}{\partial e} - \frac{\cos i}{na^2\sqrt{1-e^2}\sin i}\frac{\partial R}{\partial i}, \\
\frac{d\Omega}{dt} &= \frac{1}{na^2\sqrt{1-e^2}\sin i}\frac{\partial R}{\partial i}, \\
\frac{dM}{dt} &= n - \frac{2}{na}\frac{\partial R}{\partial a} - \frac{1-e^2}{na^2e}\frac{\partial R}{\partial e}.
\end{aligned} \tag{1.35}$$

However, in many situations, it is of interest the study of the problem with just the J_2 perturbation included, since it is the most important perturbation in many applications. In those cases, Lagrange planetary equations can be used in order to analytically obtain the secular variation of the orbital elements. In particular, the disturbing potential generated by J_2 can be expressed as [30]:

$$R = -\frac{3\mu J_2}{2r}\left(\frac{R_\oplus}{r}\right)^2\left(\sin^2(i)\sin^2(\omega+\nu) - \frac{1}{3}\right), \tag{1.36}$$

where $R_\oplus$ is the Equatorial radius of the Earth and $J_2 = 0.001082$ is the value of the second zonal harmonic coefficient. This potential can be averaged for one orbital revolution, in order to remove the periodic effects of the perturbation, and expressed by means of the classical elements [35]:

$$R_{avg} = -\frac{\mu J_2}{a}\left(\frac{R_\oplus}{a}\right)^2\left(\frac{3}{4}\sin^2(i) - \frac{1}{2}\right)\left(\frac{1}{(1-e^2)^{3/2}}\right), \tag{1.37}$$

and then, by applying Lagrange planetary equations to this averaged potential, the secular variations of the classical elements are obtained:

$$\begin{aligned}
\dot{a}_{sec} &= 0, \\
\dot{e}_{sec} &= 0, \\
\dot{i}_{sec} &= 0, \\
\dot{\omega}_{sec} &= \frac{3}{4}J_2\left(\frac{R_\oplus}{a(1-e^2)}\right)^2 n\left(4 - 5\sin^2(i)\right), \\
\dot{\Omega}_{sec} &= -\frac{3}{2}J_2\left(\frac{R_\oplus}{a(1-e^2)}\right)^2 n\cos(i), \\
\dot{M}_{sec} &= \sqrt{\frac{\mu}{a^3}}\left[1 + \frac{3}{4}J_2\left(\frac{R_\oplus}{a(1-e^2)}\right)^2\left(2 - 3\sin^2(i)\right)\sqrt{1-e^2}\right],
\end{aligned} \tag{1.38}$$

where $\dot{a}_{sec}$, $\dot{e}_{sec}$, $\dot{i}_{sec}$, $\dot{\omega}_{sec}$ $\dot{\Omega}_{sec}$ and $\dot{M}_{sec}$ are the secular variations of the orbital parameters under J_2 perturbation. Equation (1.38) represents the second order approximation to the problem and are extensively used in orbit design. Moreover, it is important to note that when $sin^2(i) = 4/5$,

the secular variation of the argument of perigee is equal to $\dot{\omega}_{sec} = 0$, and thus, orbits do not rotate during their dynamic (a property of great importance in many missions). The inclination that allows this result is called the critical inclination and has an approximated value of $i = 63.43^o$.

On the other hand, when perturbations are non conservative, Gauss planetary equations are used to compute the variation of the orbital parameters. This set of equations require to express the perturbing accelerations in the orbital reference system $(\boldsymbol{u}_r, \boldsymbol{u}_\theta, \boldsymbol{u}_h)$ where the origin of the reference system is centered in the satellite of study. Let γ_r, γ_θ and γ_h be the projection of the resultant acceleration in the former reference system. Then, the evolution of the orbital parameters over time can be calculated using the following expressions [35]:

$$\begin{aligned}
\dot{a} &= \frac{2a^2}{h}\left(e\sin(\nu)\gamma_r + \frac{p}{r}\gamma_\theta\right), \\
\dot{e} &= \frac{1}{h}\left(p\sin(\nu)\gamma_r + \left((p+r)\cos(\nu) + re\right)\gamma_\theta\right), \\
\dot{i} &= \frac{r}{h}\cos(\omega+\nu)\gamma_h, \\
\dot{\Omega} &= \frac{r}{h}\frac{\sin(\omega+\nu)}{\sin(i)}\gamma_h, \\
\dot{\omega} &= \frac{1}{eh}\left(-p\cos(\nu)\gamma_r + (p+r)\sin(\nu)\gamma_\theta\right) + \frac{r}{h}\frac{\sin(\omega+\nu)}{\tan(i)}\gamma_h, \\
\dot{M} &= n + \frac{\sqrt{1-e^2}}{eh}\left(\left(p\cos(\nu) - 2re\right)\gamma_r - (p+r)\sin(\nu)\gamma_\theta\right).
\end{aligned} \tag{1.39}$$

That way, the set of expressions shown in Equations (1.35) and (1.39) allow to obtain the instantaneous values of the orbital parameters over time for a dynamic under orbital perturbations.

Sections 1.1 and 1.2 are a summary of the basic orbital mechanics. In the next pages, we introduce the concept of satellite constellation, focusing on the Lattice Flower Constellation Theory. Moreover, we introduce the theory of necklaces for the case of 2D Lattice Flower Constellations as well as Burnside's Lemma.

1.3 The Flower Constellation Theory

Satellite constellations are groups of satellites that work cooperatively in order to achieve a common task or mission, and allow to optimize the performance of the system, reducing the costs of the mission. However, the study of several satellites at the same time, and more importantly, the relations that appear in the internal structure of the constellation, increases the complexity of the problem to solve, but also expands the possibilities in the design.

Satellite constellation design is a complex process that require in general a high number of iterations and the necessity of specific studies for each particular mission. This situation is worsen by the lack of established models for the generation and study of constellations. However, in the last decades, several satellite constellation design methodologies have appeared such as Walker Constellations [3] for circular orbits or the design of Draim [4] for elliptic orbits. In 2004, the Flower Constellation Theory [5, 6, 7] was presented, including in its formulation circular and elliptic orbits and containing

the former designs of Walker and Draim. The theory was later improved by the 2D Lattice [8] and 3D Lattice [9] theories which simplified the formulation and made the configuration independent of any reference frame. In particular, if observed from a rotating frame of reference, the orbits of Flower Constellations acquire a shape that reminds the petals of a flower. That is the reason why Flower Constellations take their name.

The most important property of Flower Constellations (and more specifically Lattice Flower Constellations) is that the distributions generated present a high number of symmetries, which makes this design methodology very interesting for many applications, especially global coverage and global positioning.

1.3.1 2D Lattice Flower Constellations

A 2D Lattice Flower Constellation [8] (2D-LFC) is described by nine parameters: three integers and six continuous parameters. The first three parameters are the number of inertial orbits (N_o), the number of satellites per orbit (N_{so}) and the configuration number (N_c), which is a parameter that satisfies $N_c \in [0, N_o - 1]$ and governs the phasing of the constellation. In particular, the location of the satellites in a 2D-LFC corresponds to a lattice in the (Ω, M)-space [12], that is, a space generated in the orbital variables right ascension of the ascending node Ω and mean anomaly M of all the satellites of the constellation in a given instant. The (Ω, M)-space can be also regarded as a 2D torus (both axes, Ω and M, are modulo 2π) where the points represented coincide with the solutions of the following system of equations:

$$\begin{pmatrix} N_o & 0 \\ N_c & N_{so} \end{pmatrix} \begin{pmatrix} \Delta\Omega_{ij} \\ \Delta M_{ij} \end{pmatrix} = 2\pi \begin{pmatrix} i-1 \\ j-1 \end{pmatrix}, \tag{1.40}$$

where $i = 1, \cdots, N_o$, $j = 1, \cdots, N_{so}$, and $N_c \in [0, N_o - 1]$, and $\Delta\Omega_{ij}$ and ΔM_{ij} represent the satellite distribution in the right ascension of the ascending node and the mean anomaly with respect to a reference satellite. Indexes (i, j) represent the j-th satellite on the i-th orbital plane. Note that this system of equations is derived from the Hermite Normal Form of the lattice, which is the minimum representation of a lattice in a 2D distribution [8].

On the other hand, the other six parameters are the semi-major axis (a), the eccentricity (e), the inclination (i) and the argument of perigee (ω) (which are the same for all the satellites of the constellation), and the longitude of the ascending node and the initial mean anomaly of the first satellite of the constellation, that is, Ω_{11} and M_{11} (and which define a reference for the constellation).

As an example of this kind of design, we choose a constellation made of 15 satellites that are distributed in 5 inertial orbits ($N_o = 5$), each one containing 3 satellites of the constellation ($N_{so} = 3$). Moreover, the constellation has semi-major axis $a = 14419,944\ km$, inclination $i = 63.435^o$, eccentricity $e = 0$, configuration number $N_c = 3$ and, without losing generality, we position the reference satellite in $\Omega_{11} = 0$ and $M_{11} = 0$.

The representation of the lattice of this distribution in the (Ω, M)-space can be seen in Figure 1.4. A (Ω, M)-space is a graphical representation of the constellation where each filled circle represents a satellite of the configuration. In the example shown, two properties can be observed. First, the configuration number performs a shift with the right ascension of the ascending node in the

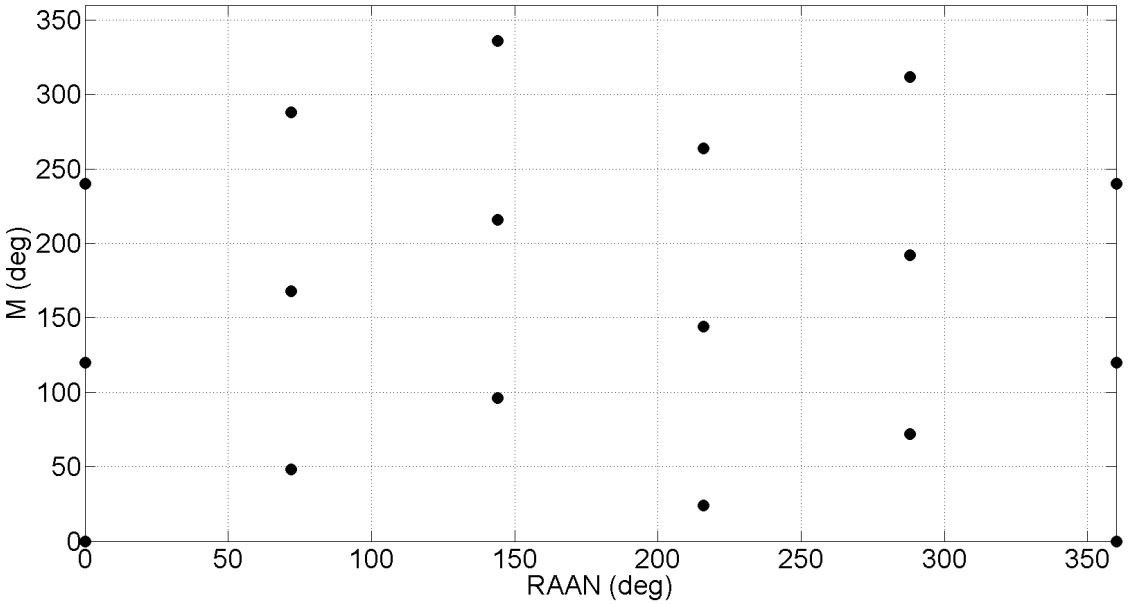

Figure 1.4: Representation of the initial positions of the satellites in the (Ω, M)-space.

distribution of satellites with respect the first orbit (where $\Omega = 0$). Second, the distribution is congruent in Ω and M, which means that the distribution is the same no matter the satellite selected as the reference of the constellation. In fact, both properties are representing a 2D torus in a 3D space as it can be seen in Figure 1.5. Moreover, this two properties are very important, as they provide the symmetric behavior to Lattice Flower Constellations.

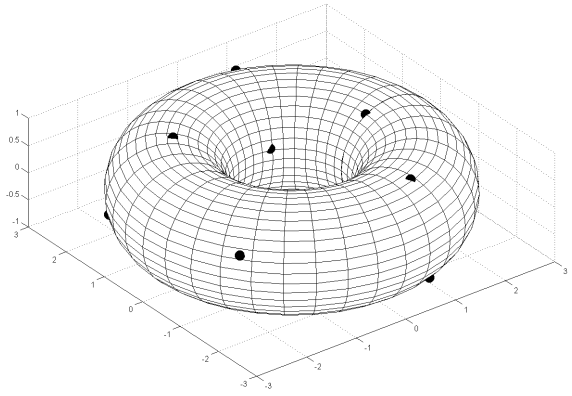

Figure 1.5: Representation of the initial positions of the satellites in the (Ω, M)-torus.

On the other hand, in Figure 1.6, the initial distribution of the constellation in the ECI (Earth Centered Inertial) frame of reference is presented. As it can be seen, the satellites form three pentagons in the polar view in the initial instant. The interesting property of this constellation is that this three pentagons are maintained during the motion of the constellation, creating a rigid structure.

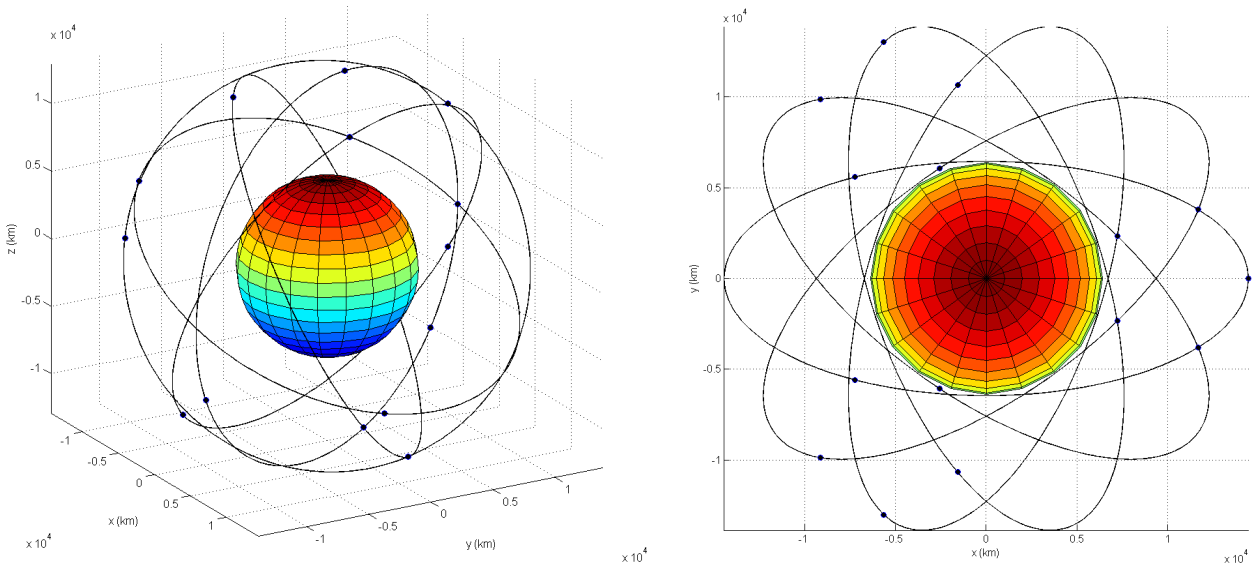

Figure 1.6: Initial distribution of the constellation in the ECI frame of reference.

1.3.2 3D Lattice Flower Constellations

The 3D Lattice Flower Constellation Theory is a satellite constellation design methodology in which satellites are distributed in several inertial orbits, where each satellite has a different value of its mean anomaly, argument of perigee and right ascension of the ascending node. Furthermore, the satellites of the constellation have the same semi-major axis, eccentricity and inclination. That way, we provide an additional degree of freedom to orbit design compared to the 2D formulation, the argument of perigee. Moreover, as in the case of 2D Lattice Flower constellations, the distributions present symmetric configurations in their lattices that are maintained over time.

Following Ref. [9], a 3D Lattice Flower Constellation can be described by the use of the Hermite Normal Form. In this case, the Hermite Normal Form is composed by six integers, three in the diagonal of the matrix and the other three in the inferior part of the matrix. The integers in the diagonal are the number of orbital planes of the constellation (N_o), the number of different argument of perigees in each orbital plane (N_w), and the number of satellites in each orbit (N_{so}). The other three parameters are configuration numbers ($N_{c_1}, N_{c_2}, N_{c_3}$) defined as follows: $N_{c_1} \in [0, N_o - 1]$, $N_{c_2} \in [0, N_w - 1]$ and $N_{c_3} \in [0, N_o - 1]$.

The expression that summarizes the distribution of the satellites in a 3D Lattice Flower Constellation is:

$$\begin{pmatrix} N_o & 0 & 0 \\ N_{c_3} & N_w & 0 \\ N_{c_1} & N_{c_2} & N_{so} \end{pmatrix} \begin{pmatrix} \Delta\Omega_{ijk} \\ \Delta\omega_{ijk} \\ \Delta M_{ijk} \end{pmatrix} = 2\pi \begin{pmatrix} i-1 \\ k-1 \\ j-1 \end{pmatrix}; \tag{1.41}$$

where $\Delta\Omega_{ijk}$ is the distribution in the right ascension of the ascending node of the constellation, $\Delta\omega_{ijk}$ is the distribution of the argument of perigee, and ΔM_{ijk} is the distribution of the mean anomaly with respect to a reference satellite of the constellation with parameters Ω_{111}, ω_{111} and

M_{111}. Moreover, the sub-indexes $i = 1, \cdots, N_o$; $j = 1, \cdots, N_{so}$; and $k = 1, \cdots, N_w$, represent the position of a satellite in the orbital plane i, with the argument of perigee k and the mean anomaly j. Note also that the values of Ω_{ijk}, ω_{ijk} and M_{ijk} represent three angles and thus are defined in the range $[0, 2\pi]$ (and thus, they show a modular behavior).

The distribution shown in Equation (1.41) can be represented as a set of points that are situated over the surface of a three dimensional torus in a four dimensional space (a representation that is non practical from a graphical point of view). However, the same distribution can also be represented by three different two dimensional tori in a three dimensional space.

As an example of that, a constellation is created with parameters: $N_o = 5$, $N_w = 3$, $N_{so} = 3$, $N_{c_1} = 3$, $N_{c_2} = 2$ and $N_{c_3} = 4$, which generates the following Hermite Normal Form using Equation (1.41):

$$\begin{pmatrix} 5 & 0 & 0 \\ 4 & 3 & 0 \\ 3 & 2 & 3 \end{pmatrix} \begin{pmatrix} \Delta\Omega_{ijk} \\ \Delta\omega_{ijk} \\ \Delta M_{ijk} \end{pmatrix} = 2\pi \begin{pmatrix} i-1 \\ k-1 \\ j-1 \end{pmatrix}; \tag{1.42}$$

where the constellation is made by $N_o N_w N_{so} = 45$ satellites. The tori representation of this constellation can be seen in Figure 1.7, where each point is represented by two coordinates, a polar longitude (toroidal direction), and the angle between the perpendicular to the torus surface in the point and the horizontal plane (poloidal direction). It is important to note that the figure represents all the satellites of the constellation, and as such, the points only show the different values of each variable in the constellation. That leads to $N_o N_\omega N_{so} = 45$ different combinations in the first and second tori, and $N_\omega N_{so} = 9$ in the third one, since all the configuration numbers $(N_{c_1}, N_{c_2}, N_{c_3})$ are different to zero, and N_o and N_{so} are co-primes. On the other hand, the figure clearly shows that the points are situated generating closed lines in the tori, the lattice of the constellation.

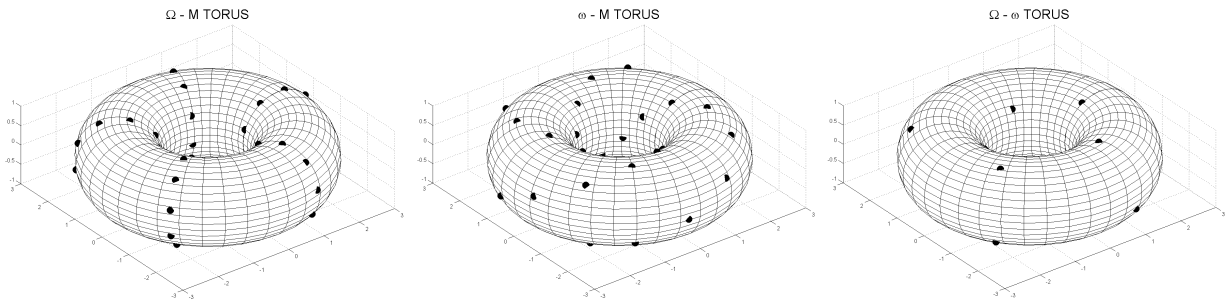

Figure 1.7: Graphical representation of the initial positions of the satellites of the constellation in three different torus.

Another useful representation of this distribution can be seen in Figure 1.8, where the (Ω, ω, M)-space for this particular configuration is shown. As it can be seen on this representation, the satellites are distributed in several planes in this space and these planes are not parallel with respect to the axis. This is caused by the configuration numbers (N_{c_1}, N_{c_2} and N_{c_3}) which produce this effect in the distribution. As it will be seen later, this property has deep implications in the development of the necklace theory, and the definition of congruence in systems where necklaces are introduced in a distribution.

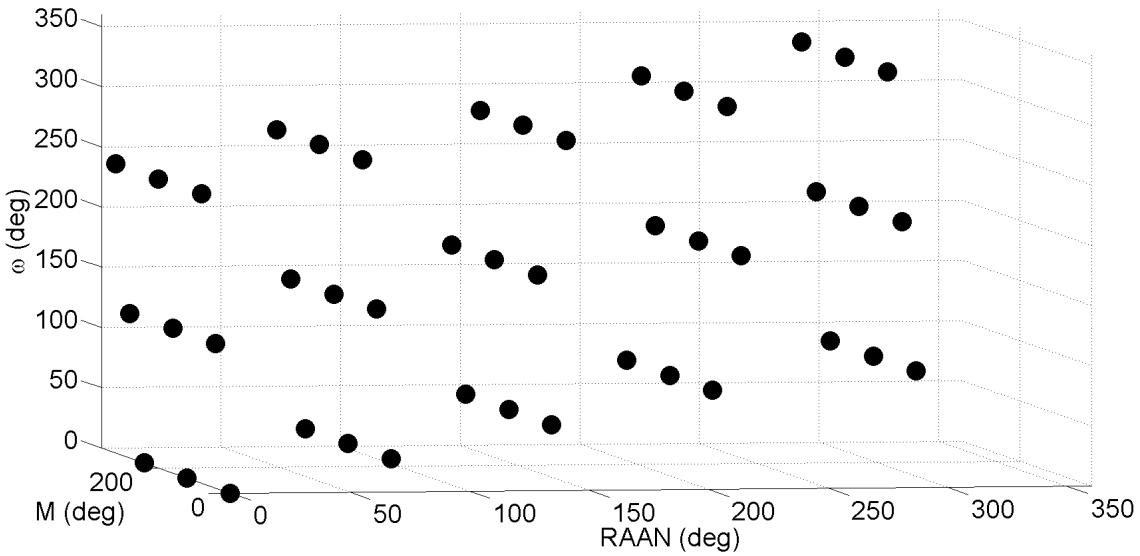

Figure 1.8: Graphical representation of the initial positions of the satellites of the constellation in the (Ω, ω, M)-space.

Using the distribution shown in the example, we build a constellation with orbital parameters $a = 11522,451\ km$, $e = 0.25$ and $i = 63.435^o$. Figure 1.9 shows the inertial distribution of this constellation in an isometric view (left) and a polar view (right). Note that from the polar view, it is possible to see some of the symmetries that appear in the distribution (for example the ones that are generated with respect to the plane $y = 0$).

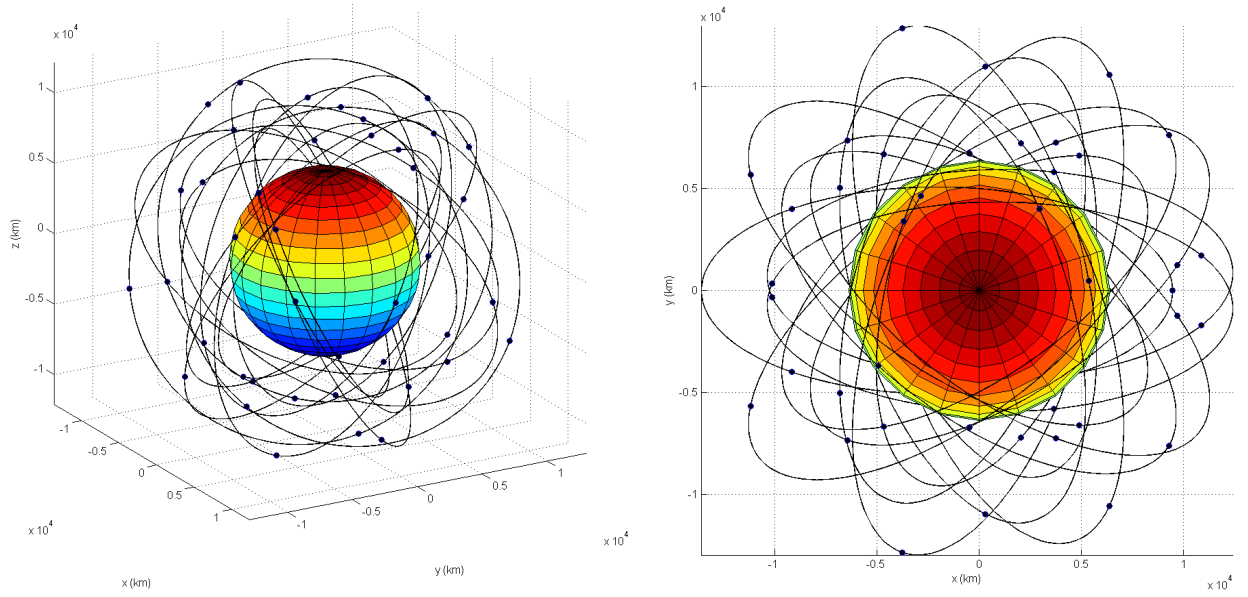

Figure 1.9: Initial distribution of the constellation in the ECI frame of reference.

1.4 2D Lattice Flower Constellations using Necklaces

The theories of 2D and 3D Lattice Flower Constellations always generate symmetric configurations. However, provided a set of satellites, the number of possible different configurations is limited by the possible combinations between the integer parameters that constitute the Hermite Normal Form, and thus, bigger constellations generate a larger number of possible configurations. In order to solve this issue and allow more possible configurations in small constellations, the concept of necklaces was introduced for the 2D Lattice Flower Constellations [17, 36].

1.4.1 Definition of a Necklace

A necklace is a subset of points selected from a set of n available positions that present modular arithmetic, that is, location 1 in the available positions is the same as location $n+1$. They are represented by the subset $\mathcal{G} \subseteq \mathbb{Z}_n = \{1, ..., n\}$.

As an example, if we have a configuration in which four positions are available, a necklace consisting in three points can be created as seen in Figure 1.10. In the figure, we have occupied three positions (the colored circles) form an available set of four positions, forming a necklace that is represented as $\mathcal{G} = \{1, 2, 4\} \subseteq \mathbb{Z}_4$.

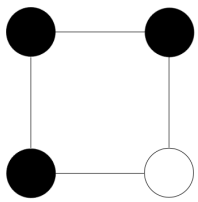

Figure 1.10: Example of necklace.

However, this is not the only representation that corresponds to this particular necklace. To be more precise, all the distributions that are obtained from a rotation of the whole configuration are considered identical. That is, two necklaces ($\mathcal{G}_1$ and $\mathcal{G}_2$) are considered to be equivalent, that is, an equivalence relation $\cong$, if they fulfill the following expression:

$$\mathcal{G}_1 \cong \mathcal{G}_2 \iff \exists s : \mathcal{G}_1 = \mathcal{G}_2 + s \mod (n), \tag{1.43}$$

where s is an integer that belongs to the group $\mathbb{Z}_n$. Taking as an example the necklace from Figure 1.10 and varying the parameter s, all these configurations can be obtained:

$$\mathcal{G} = \{1, 2, 4\} \cong \{1, 2, 3\} \cong \{2, 3, 4\} \cong \{1, 3, 4\}\,; \tag{1.44}$$

which correspond to the graphical representation shown in Figure 1.11. As it can be seen, the difference between them is just a rotation in the circular loop, not changing the distribution in the process.

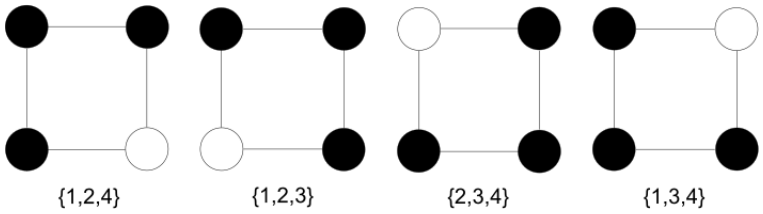

Figure 1.11: Identical necklaces.

1.4.1.1 Symmetry of a Necklace

The symmetry of a necklace is a parameter that provides information on how uniform the necklace distribution is [37, 38]. This is done by counting the minimum number of times that the configuration can be rotated in the available positions in order to obtain the same necklace in the modular arithmetic.

Let $K(n)$ be the set of equivalence classes of necklaces modulo the relation defined by $\cong$:

$$K(n) = \{\text{necklaces} \subseteq \mathbb{Z}_n\}/\cong, \tag{1.45}$$

and let $\mathcal{G}$ be a necklace such that $\mathcal{G} \subseteq \mathbb{Z}_n$. The symmetry of a necklace ($Sym(\mathcal{G})$) is defined as the smallest value of $r \in \mathbb{Z}_n$ such that $\mathcal{G} + r = \mathcal{G}$ in $\mathbb{Z}_n$:

$$Sym(\mathcal{G}) = \min\{1 \leq r \leq n : \mathcal{G} + r = \mathcal{G} \qquad \text{in} \quad \mathbb{Z}_n\}. \tag{1.46}$$

This means that r is the smallest value that the configuration has to be rotated in order to obtain the same initial configuration. In other words, if $\mathcal{G}_1 \cong \mathcal{G}_2$, then $Sym(\mathcal{G}_1) = Sym(\mathcal{G}_2)$ and thus, the symmetry can be defined over an equivalence class:

$$\begin{aligned} \overline{Sym}: \quad K(n) &\longrightarrow \mathbb{N} \\ \overline{\mathcal{G}} &\longmapsto \overline{Sym(\mathcal{G})}. \end{aligned} \tag{1.47}$$

Equivalent classes defined in this manner can be also regarded as the orbits that different symmetries of a necklace (seen as an action) generate in the group of possible combinations of elements taken from the available positions.

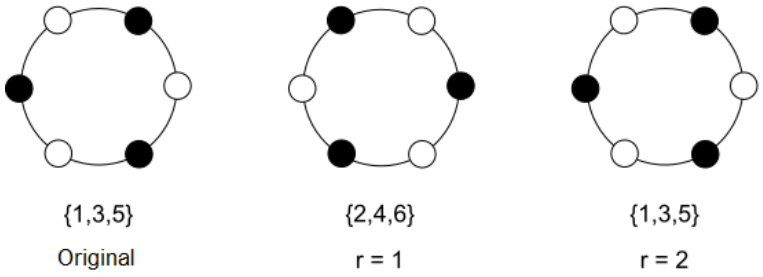

Figure 1.12: Symmetry of a necklace.

As an example of this concept, let assume that a configuration with six available positions is generated ($n = 6$), where a necklace $\mathcal{G} = \{1, 3, 5\} \subseteq \mathbb{Z}_6$ is defined. The representation of this example can be seen in Figure 1.12.

For this particular case, $Sym(\mathcal{G}) = 2$ because $\{1, 3, 5\} \equiv \{3, 5, 7\} \mod (6)$. Note that, in this example, although $\{2, 4, 6\}$ is an equivalent necklace with respect to $\mathcal{G}$, as defined in Equation (1.43), it does not fulfill the definition of symmetry of a necklace.

1.4.1.2 The Necklace problem

The necklace problem is a combinatorial problem that studies the number of different arrangements of n elements in a circular loop that can be generated assuming that each element comes in one of k different colors. In this definition, two arrangements are considered to be equivalent if they only differ by a rotation inside the loop (see Equation (1.43)). The number of different arrangements is given by the application of Burnside's counting theorem, which, applied to this particular case, can be summarized by the following formula[39]:

$$N_k(n) = \frac{1}{n} \sum_{d|n} \varphi(d) k^{n/d}, \tag{1.48}$$

where the sum is taken over all the divisors d of n, and $\varphi(d)$ is called the Euler's totient function of d, an arithmetic function that counts the number of positive integers less than or equal to d that are coprime with d. It is important to note that the number of different arrangements of pearls provided by Equation (1.48) is also representing the number of equivalent classes (that is, orbits) defined by the group and actions considered.

The case of study is a simplification of the general necklace problem, since only two different states for each position are possible, the first one having the position occupied, and the second, the case in which it is not. Thus, for this particular case, the number of colors is $k = 2$.

However, the question of why using a representation in which the positions are distributed in a circular loop still remains. 2D Lattice Flower Constellations generate a distribution related to a reference satellite, which means that we are interested in the relative positions of the satellites ($\Delta\Omega_{ij}$ and ΔM_{ij}), and not the absolute positions. In fact, having two configurations with shifted positions in M only means that the same constellation is observed at a different time, while a shifting in Ω represents a rotation of the full constellation. Both shifting movements generate the same structure, and thus, there is no point in considering all combinations of parameters. Moreover, $\Delta\Omega_{ij}$ and ΔM_{ij} have modular arithmetic nature, which translates into the representation as a circular loop in the necklace.

1.4.2 Admissible pairs

Let $\mathcal{G}$ be a necklace generated in the variable mean anomaly. We know from Equation (1.40) that the values of the mean anomaly depend on the values of the right ascension of the ascending node. Thus, we define $k \in \{1, \ldots, Sym(\mathcal{G}) - 1\}$ as the shifting parameter of the necklace, which is an constant integer that represents the additional movement required by the necklace each time that we change the position in the variable $\Delta\Omega$ in order to obtain a symmetric configuration.

Expanding Equation (1.40) and computing the variation of the mean anomaly between two consecutive values of the right ascension of the ascending node, we obtain the ΔM-Shifting, which

is defined as:

$$\Delta M = \frac{2\pi}{N_{so}} k - \frac{2\pi}{N_{so}} \frac{N_c}{N_o}, \tag{1.49}$$

where k is the shifting parameter. Moreover, imposing that the value of the mean anomaly is invariant under the addition of $N_o \Delta M$, we can obtain the relation that must be fulfilled by all admissible pairs:

$$Sym(\mathcal{G}) \mid kN_o - N_c, \tag{1.50}$$

which reads $Sym(\mathcal{G})$ divides $kN_o - N_c$. Equation (1.50) provides all possible admissible pairs given the values of the symmetry of the necklace $Sym(\mathcal{G})$, the number of orbits N_o and the configuration number N_c.

As an example, let $\mathcal{G} = \{1, 2\}$ be a necklace in the mean anomaly where the number of available positions $N_{so} = 4$. From the definition of symmetry of the necklace (Equation (1.46)), we obtain $Sym(\mathcal{G}) = 4$. In addition, the number of orbits is $N_o = 6$ and the configuration number is $N_c = 2$. Thus, initially, we have a distribution as shown in Figure 1.13, where the circles represent available positions and the filled circles are the position of the necklace in the first orbit. Now, we have to find the possible values of k that allow us to obtain the same configuration when $\Delta\Omega = 2\pi$ following Equation (1.40).

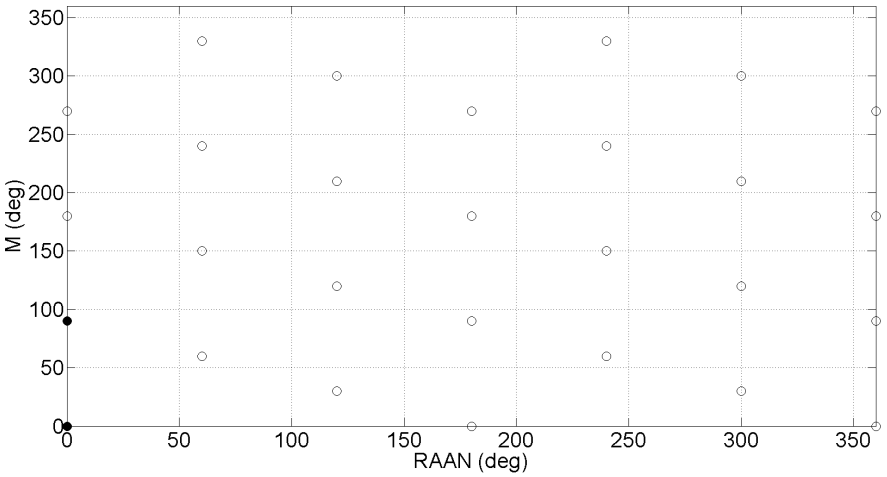

Figure 1.13: Available positions and initial necklace in the first orbit.

Using Equation (1.50) applied to the values of the example:

$$4 \mid 6k - 2, \tag{1.51}$$

where we can obtain the two values of the sifting parameter $k = \{1, 3\}$ that fulfills that expression. The representation of both configurations can be observed in Figure 1.14. As it can be seen, both distributions are completely different and maintain the properties of symmetry that we were looking for.

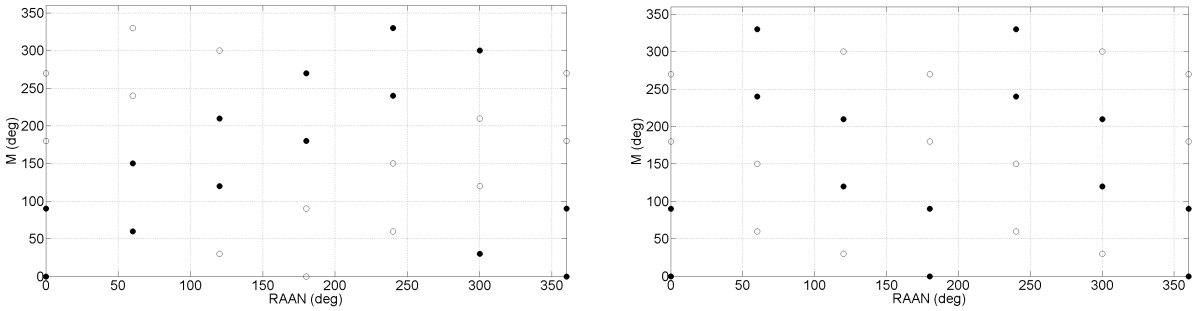

Figure 1.14: Admissible configurations.

1.5 Burnside's Lemma

Since we introduce some counting theorems that rely of Burnside's Lemma in this work, we have included a summary of it in this introductory chapter. This is done also for completeness, presenting in the same document all the concepts and formulation used in this work.

Let G be a group, and let $+$ be an action of this group over a set X, that is, an application defined as:

$$\begin{array}{rccc} + : & G \times X & \longrightarrow & X \\ & (g, x) & \longmapsto & g + x, \end{array} \tag{1.52}$$

such that:

$$\left.\begin{array}{rcl} g_1 + (g_2 + x) & = & (g_1 + g_2) + x \\ 1_G + x & = & x \end{array}\right\} \quad \forall\, g_1, g_2 \in G,\ x \in X \tag{1.53}$$

In addition, let an orbit ($\text{orbit}(x)$) be the set of elements that can be obtained from x by the application of the action ($+$), in other words:

$$\text{orbit}(x) = \{g + x \mid g \in G\} \subseteq X; \tag{1.54}$$

and let the fix of g ($\text{Fix}(g)$) be the elements of X that are invariant under the multiplication by g, that is:

$$\text{Fix}(g) = \{x \in X \mid g + x = x\}. \tag{1.55}$$

The action partitions the set X into orbits, since if $y = g + x$, then $\text{orbit}(y)$=$\text{orbit}(x)$. Thus, the number of orbits induced by the action $+$ is given by the Burnside's Lemma:

$$\frac{1}{|G|} \sum_{g \in G} |\text{Fix}(g)|, \tag{1.56}$$

where we denote $|Y|$ to the number of elements of the set Y.

With Burnside's Lemma we finish this introductory chapter, where the basic background of the research presented in this work is shown. In the next chapters the most relevant results from the research done are presented, including examples of application of the new concepts and methodologies introduced.

Chapter 2

2D Necklace Flower Constellations

In a Lattice Flower Constellation, the number of possible configurations that the theory provides is proportional to the number of satellites in the constellation, and thus, it imposes a great limitation in the design of constellations composed by a small number of satellites. In order to solve this issue, the concept of necklace was introduced for the 2D Lattice formulation [17], where the condition for maintaining the uniformity and symmetries of the configurations was presented. However, necklaces were not included directly in the formulation of the constellation and its computation was difficult to handle in a computer. This resulted in the impossibility to automatize the computation of the different configurations and the requirement to calculate all the available positions instead of just the real locations of the satellites. Thus, a new design framework was required to solve these difficulties.

In this chapter we introduce the formulation of the 2D Necklace Flower Constellations. This design framework constitutes the generalization of the methodology presented in 2D Lattice Flower Constellations using necklaces [17, 18] and includes in its definition all the former 2D lattice configurations. As it will be seen, 2D Lattice Flower Constellations are defined as a subset of solutions from the 2D Necklace Flower Constellations, where the satellites occupy all the available positions.

2D Necklace Flower Constellations are based on the idea of defining a fictitious constellation that is bigger than the one we want to obtain. Then, the necklace theory is applied in order to obtained the subsets of the positions generated that maintain the properties of uniformity and symmetry in the configuration. One of the most important advantages of this formulation is that during the process, it is no longer required to generate all the fictitious constellation, since the formulation allows to obtain the configuration of the real satellites directly. Moreover, this methodology of design also allows to study the sequence of launches for constellation building (for instance, being the final constellation the fictitious constellation of this problem), as well as the evaluation of possible reconfigurations available in case of failure of some satellites of the distribution.

In addition, three counting theorems are included, which allow to know beforehand the number of configurations obtained using this theory for the cases of fixed fictitious constellation, fixed symmetries of the configuration, and fixed number of satellites. This formulation is able to not only define the symmetries, but also to provide a methodology to easily define constellations, which will be used in future work for optimization, station-keeping [16], constellation reconfiguration [20] and launching schedule studies for satellites of a constellation.

2.1 2D Necklace Flower Constellation

We begin the Necklace Flower Constellation Theory with the case of a 2D Lattice. This is chosen in order to introduce in a clear way the new formulation that is carried out during the Necklace Flower Constellation Theory, as well as to serve as a common link between old and new formulations. In addition, this new formulation allows to have a better control in the design, since the necklace definition is performed directly in the formulation.

A 2D lattice can be generated in the same way as shown in Equation (1.40):

$$\begin{pmatrix} L_\Omega & 0 \\ L_{M\Omega} & L_M \end{pmatrix} \begin{pmatrix} \Delta\Omega_{ij} \\ \Delta M_{ij} \end{pmatrix} = 2\pi \begin{pmatrix} i-1 \\ j-1 \end{pmatrix}, \tag{2.1}$$

where we denote L_Ω to the number of orbital planes, L_M to the number of satellites per orbit and $L_{M\Omega}$ to the combination number between the right ascension of the ascending node and the mean anomaly. Moreover, Equation (2.1) can be expanded in order to obtain the distribution as a function of the integers $i \in \{1, \dots, L_\Omega\}$ and $j \in \{1, \dots, L_M\}$:

$$\begin{aligned} \Delta\Omega_{ij} &= \frac{2\pi}{L_\Omega}(i-1), \\ \Delta M_{ij} &= \frac{2\pi}{L_M}(j-1) - \frac{2\pi}{L_M}\frac{L_{M\Omega}}{L_\Omega}(i-1), \end{aligned} \tag{2.2}$$

where this equation corresponds to a complete configuration. Now, instead of considering all the admissible locations, we select a set of satellites that maintain the properties of uniformity and symmetry of the former configuration, that is, the same distribution can be observed with independence on the orbital plane chosen. In order to do that, we define a necklace in the mean anomaly $\mathcal{G}_M$ as a subset of $\mathbb{Z}_{L_M}$ of cardinality N_M which contains the positions occupied by the necklace (and that also corresponds to the number of real satellites per orbit). A necklace is a subset $\mathcal{G}_M$ of the set of admissible locations:

$$\mathcal{G}_M \subseteq \{1, \dots, L_M\}, \tag{2.3}$$

such that $|\mathcal{G}_M| = N_M$ is the number of elements of the necklace $\mathcal{G}_M$. On the other hand, and in order to simplify the notation used, we assume that:

$$\mathcal{G}_M = \{\mathcal{G}_M(1), \dots, \mathcal{G}_M(j^*), \dots, \mathcal{G}_M(N_M)\}, \tag{2.4}$$

with

$$1 \leq \mathcal{G}_M(1) < \cdots < \mathcal{G}_M(j^*) < \cdots < \mathcal{G}_M(N_M) \leq L_M, \tag{2.5}$$

where the index j^* names each element of the necklace $\mathcal{G}_M$ and it is represented by an integer modulo N_M, that is, $j^* + N_M$ is the same index as j^*. This allows to interpret necklaces as injective functions:

$$\begin{aligned} \mathcal{G}_M : \quad \mathbb{Z}_{N_M} &\longrightarrow \mathbb{Z}_{L_M} \\ j^* &\longmapsto \mathcal{G}_M(j^*). \end{aligned} \tag{2.6}$$

For this reason, it makes sense to refer to $\mathcal{G}_M(j^*)$, where the integer parameter $j^* \in \{1, \ldots, N_M\}$ represents the movement inside the necklace defined. In addition, and for simplicity of notation, we denote $\text{mod}(a, b) = a \mod (b)$. Thus, due to the modular arithmetic inside the necklace:

$$\mathcal{G}_M(j^*) = \mathcal{G}_M(\text{mod}(j^* + N_M, N_M)), \tag{2.7}$$

which corresponds to a complete loop in the available positions in the mean anomaly. It is important to note that this rotation is equivalent to a movement in the admissible locations defined by:

$$j = j + L_M \mod (L_M), \tag{2.8}$$

as both represent the same movement of the necklace, one using the parametrization of the necklace and the other using the parametrization of the fictitious constellation.

On the other hand, we require a parameter (the shifting parameter) that is able to modify the mean anomaly with respect to the change in the right ascension of the ascending node. Let $S_{M\Omega} \in \mathbb{Z}$ be that parameter. Thus, it is possible to define an application (T1) between the positions in the necklace necklace and the overall available positions:

$$\begin{array}{rccc} \text{T1}: & (\mathbb{Z}_{L_\Omega} \times \mathbb{Z}_{N_M}) & \longrightarrow & (\mathbb{Z}_{L_\Omega} \times \mathbb{Z}_{L_M}) \\ & (i, j^*) & \longmapsto & (i, j), \end{array} \tag{2.9}$$

where the integer j is described as:

$$j = \mathcal{G}_M(j^*) + S_{M\Omega}(i-1). \tag{2.10}$$

In order to agree with the formulation introduced in Equation (2.1), one unit is subtracted from the previous expression leading to:

$$j - 1 = \mathcal{G}_M(j^*) - 1 + S_{M\Omega}(i-1). \tag{2.11}$$

However, there is a modular behavior between the necklace and the available positions in the mean anomaly. Using the definition of symmetry of a necklace provided by Equation (1.46):

$$\mathcal{G}_M = \mathcal{G}_M + Sym(\mathcal{G}_M) \quad \text{in } \mathbb{Z}_{L_M}, \tag{2.12}$$

and thus, the movement in j is described as:

$$j - 1 = \text{mod}\left(\mathcal{G}_M(j^*) - 1 + S_{M\Omega}(i-1),\ Sym(\mathcal{G}_M)\right). \tag{2.13}$$

Introducing this expression in the original distribution shown in Equation (2.2), we obtain:

$$\begin{aligned} \Delta\Omega_{ij^*} &= \frac{2\pi}{L_\Omega}(i-1), \\ \Delta M_{ij^*} &= \frac{2\pi}{L_M}\left(\text{mod}\left(\mathcal{G}_M(j^*) - 1 + S_{M\Omega}(i-1),\ Sym(\mathcal{G}_M)\right)\right) - \frac{2\pi}{L_M}\frac{L_{M\Omega}}{L_\Omega}(i-1), \end{aligned} \tag{2.14}$$

which describes all possible movements that the necklace $\mathcal{G}_M$ can perform in the space generated. Using this formulation, i represents the movement of the necklace in the right ascension of the ascending node while j^* defines the positions inside the necklace. One important thing to notice

is that, although the shifting parameter $S_{M\Omega}$ can present any integer value, we only consider $S_{M\Omega} \in \{0, \ldots, Sym(\mathcal{G}_M) - 1\}$, since other values generate equivalent configurations due to the arithmetic nature of the problem in $Sym(\mathcal{G}_M)$.

Now, we impose the condition of symmetry, that is, a complete rotation in either variable, the right ascension of the ascending node or the mean anomaly, provides the same initial configuration. This definition is equivalent to:

$$\begin{aligned} \text{Rotation in } M\text{:} & \left\{ \begin{array}{ll} \Delta\Omega_{ij^*} & = \Delta\Omega_{i(j^*+N_M)}, \\ \Delta M_{ij^*} & = \Delta M_{i(j^*+N_M)}, \end{array} \right\} \\ \text{Rotation in } \Omega\text{:} & \left\{ \begin{array}{ll} \Delta\Omega_{ij^*} & = \Delta\Omega_{(i+L_\Omega)j^*}, \\ \Delta M_{ij^*} & = \Delta M_{(i+L_\Omega)j^*}, \end{array} \right\} \end{aligned} \tag{2.15}$$

where all relations must be fulfilled at the same time. From the first rotation in M, there is no effect on the right ascension of the ascending node:

$$\frac{2\pi}{L_\Omega}(i-1) = \frac{2\pi}{L_\Omega}(i-1), \tag{2.16}$$

while focusing on the mean anomaly, it must satisfy that:

$$\begin{aligned} &\mathrm{mod}\left(\mathcal{G}_M(j^*) - 1 + S_{M\Omega}(i-1),\ Sym(\mathcal{G}_M)\right) = \\ &= \mathrm{mod}\left(\mathcal{G}_M(\mathrm{mod}(j^* + N_M, N_M)) - 1 + S_{M\Omega}(i-1),\ Sym(\mathcal{G}_M)\right). \end{aligned} \tag{2.17}$$

This relation is achieved without imposing further conditions since $\mathcal{G}_M(j^*) = \mathcal{G}_M(\mathrm{mod}(j^* + N_M, N_M))$ (see also Equation (3.6)). On the other hand, in the rotation of the right ascension of the ascending node, the first relation is automatically achieved:

$$\frac{2\pi}{L_\Omega}(i-1) = \frac{2\pi}{L_\Omega}(L_\Omega + i - 1) \mod (L_\Omega), \tag{2.18}$$

while the second relation is not. Imposing the condition:

$$\frac{L_M}{2\pi}\Delta M_{(i+L_\Omega)j^*} = \frac{L_M}{2\pi}\Delta M_{ij^*}, \tag{2.19}$$

provides the following expression:

$$\begin{aligned} &\mathrm{mod}\left(\mathcal{G}_M(j^*) - 1 + S_{M\Omega}(L_\Omega + i - 1),\ Sym(\mathcal{G}_M)\right) - \frac{L_{M\Omega}}{L_\Omega}(L_\Omega + i - 1) = \\ &= \mathrm{mod}\left(\mathcal{G}_M(j^*) - 1 + S_{M\Omega}(i-1),\ Sym(\mathcal{G}_M)\right) - \frac{L_{M\Omega}}{L_\Omega}(i-1). \end{aligned} \tag{2.20}$$

Then, by the properties of modular arithmetics, there exists $A \in \mathbb{Z}$ such that the former expression can be transformed into:

$$\mathcal{G}_M(j^*) - 1 + S_{M\Omega}(i-1) + ASym(\mathcal{G}_M) = \mathcal{G}_M(j^*) - 1 + S_{M\Omega}(L_\Omega + i - 1) - L_{M\Omega}, \tag{2.21}$$

and finally, the terms that are equal in both sides of the equation can be simplified, providing the expression:

$$ASym(\mathcal{G}_M) = S_{M\Omega}L_\Omega - L_{M\Omega}, \tag{2.22}$$

which relates the shifting parameter ($S_{M\Omega}$) with both the necklace ($\mathcal{G}_M$) and the fictitious orbit (L_Ω and $L_{M\Omega}$). Equation (2.22) can also be represented as:

$$Sym(\mathcal{G}_M) \mid S_{M\Omega}L_\Omega - L_{M\Omega}, \tag{2.23}$$

which reads, $Sym(\mathcal{G}_M)$ divides $(S_{M\Omega}L_\Omega - L_{M\Omega})$ and constitutes a Diophantine equation that is also subjected to modular arithmetic. It is important to note that Equation (2.23) is equivalent to Equation (1.50). However, the new formulation allows to show an alternative proof to the relation proposed in [17] as well as present a methodology that can be used for optimization since only the real positions of the satellites of the constellation have to be computed.

The combination of Equations (2.14) and (2.23) allows to compute all possible symmetric configurations for a particular necklace $\mathcal{G}_M$ and a fictitious expanded constellation. In the following sections, an example of application is shown and then, the number of possible configurations that the 2D Necklace Flower Constellations can provide is studied.

2.1.1 Example of application

As an example of a 2D Necklace Flower Constellation, we design a constellation made of 14 satellites in circular orbits $e = 0$, with semi-major axis $a = 14420\ km$ and inclination $i = 63.435^o$. The satellites are distributed in seven inertial orbits ($L_\Omega = 7$), which means that there are two satellites per orbit ($N_M = 2$). The number of possible configurations that we can obtain using the Lattice Flower Constellation Theory in this case is given by the possible values of the combination number $N_c = \{0, \ldots, 6\}$, which is seven different distributions. However, the Necklace Flower Constellation Theory can be used to increase this number of possibilities.

Let $L_M = 20$ be the number of available positions in the mean anomaly that are defined in order to create a fictitious constellation composed by $L_\Omega L_M = 140$ satellites. In this fictitious constellation we look for the configurations with $N_M = 2$ that are symmetric in the sense of Equation (2.15). That way, we obtain 70 different distributions, ten times the former number of possible constellations.

In order to describe a simple example, we select only the distributions where $\mathcal{G}_M = \{1, 2\} \subseteq \mathbb{Z}_{20}$ and $L_{M\Omega} = 6$ from the set obtained. This implies that the symmetry of the necklace is $Sym(\mathcal{G}_M) = 20$, since $\{1, 2\} = \{1, 2\} + 20 \mod (20)$. Then, using Equation (2.23):

$$Sym(\mathcal{G}_M) \mid S_{M\Omega}L_\Omega - L_{M\Omega} \quad \Rightarrow \quad 20 \mid 7S_{M\Omega} - 6, \tag{2.24}$$

which leads to $S_{M\Omega} = 18$. Figure 2.1 shows the distribution of the constellation in the (Ω, M)-space, where, without losing generalization, we have chosen $\Omega_{11} = M_{11} = 0$ as the initial position of the reference satellite of the constellation. As it can be seen, the distribution when $\Omega = 0$ and when $\Omega = 2\pi$ is the same, and thus, the properties of symmetry of the constellation are maintained from the original lattice in L_Ω and L_M.

On the other hand, in Figure 2.2, the (Ω, M)-torus representation of the constellation is shown. There, it can be observed clearer how the satellites are positioned following two closed lines (as $N_M = 2$) around the surface of the torus, not having any satellite outside this configuration.

Finally, Figure 2.3 shows the inertial orbits of the constellation from an isometric view (left) and a polar view (right). This constellation presents two curious properties. First, all the satellites of

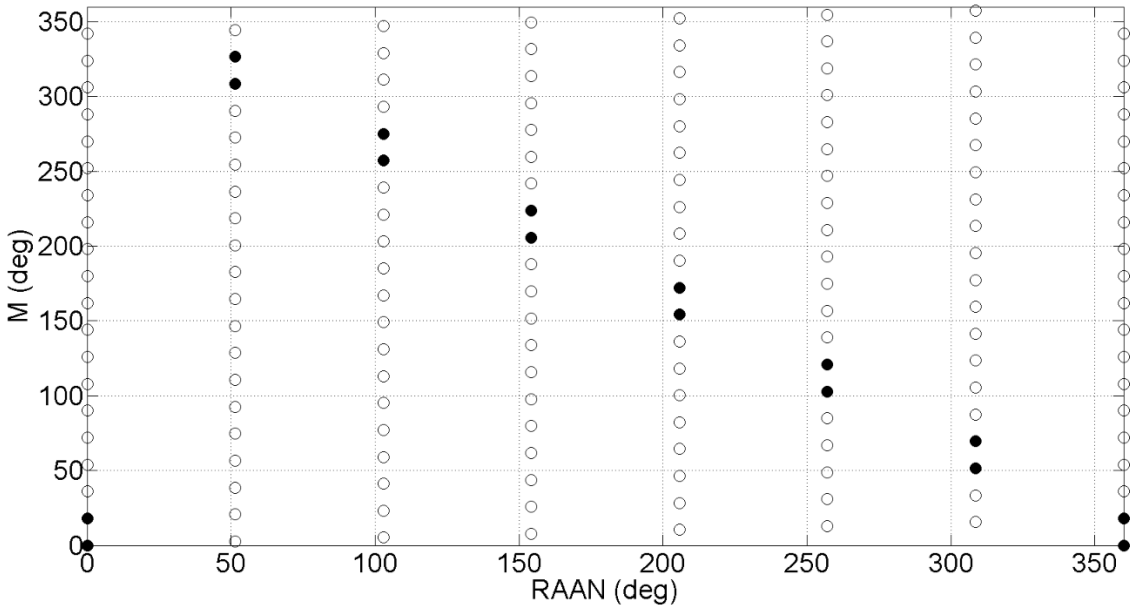

Figure 2.1: Representation of the initial positions of the satellites in the (Ω, M)-space.

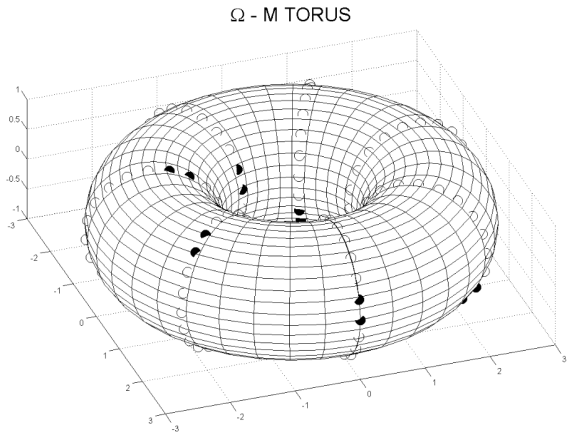

Figure 2.2: Representation of the initial positions of the satellites in the (Ω, M)-torus.

the constellation are always positioned in an interval of Earth longitudes smaller than 90^o. This means, that they fly as a formation over the same regions of the Earth. Second, from the polar view, we observe that the constellation generates two heptagons of satellites that are bounded. In fact, during the motion of the constellation, these heptagons are maintained, from a polar perspective, creating a rigid structure that is rotating with no collisions between both structures.

As it can be seen, using this new formulation (see Equations (2.14) and (2.23)), we can expand the searching space as much as required without having to compute all available positions in the fictitious constellation generated. This allows to considerably reduce the amount of computations required, as only the real positions are calculated, a property that will be used in the future in optimization problems using this new design methodology.

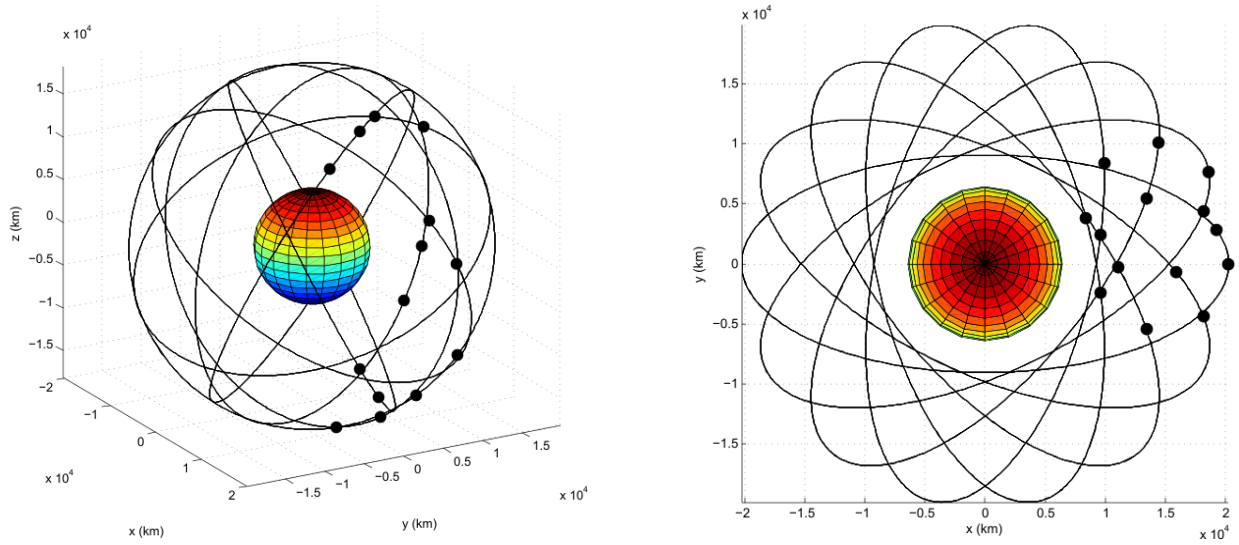

Figure 2.3: Initial distribution of the constellation in the ECI frame of reference.

2.2 Number of symmetric configurations in a 2D Necklace Flower Constellation

During this section, we deal with the computation of the number of configurations that the Necklace Flower Constellation Theory provides. In that respect, we consider three cases of interest which have different applications.

2.2.1 Fixing the necklace $\mathcal{G}_M$ and the Hermite Normal Form

In this case we focus on the study of the number of possibilities given a necklace $\mathcal{G}_M$ and the complete Hermite Normal Form for the fictitious constellation. By doing this, the available positions are fixed (they cannot shift), and thus, this methodology provides the number of symmetric configurations that follow a particular distribution given by the Hermite Normal Form. This is equivalent to compute the number of possible values that the shifting parameter $S_{M\Omega}$ can present in Equation (2.23).

Theorem 1. *Given a necklace in the mean anomaly $\mathcal{G}_M$ and a fixed Hermite Normal Form, there exists symmetric distributions in the constellation if and only if* $\gcd(Sym(\mathcal{G}_M), L_\Omega) \mid L_{M\Omega}$*, being the number of different configurations in that case:*

$$\gcd(Sym(\mathcal{G}_M), L_\Omega). \tag{2.25}$$

Proof. Equation (2.22) can be written as:

$$ASym(\mathcal{G}_M) + L_\Omega S_{M\Omega} = L_{M\Omega}, \tag{2.26}$$

where A is a unknown integer. If we select A and $S_{M\Omega}$ as the variables of study, the expression becomes a linear Diophantine equation where, by the use of Bézout's identity, we can conclude that there exist solution if and only if:

$$\gcd(Sym(\mathcal{G}_M), L_\Omega) \mid L_{M\Omega}. \tag{2.27}$$

In the case the former expression is fulfilled, there are an infinite number of solutions of Equation (2.26) that have the form:

$$\begin{aligned} (S_{M\Omega})_\lambda &= (S_{M\Omega})_0 + \lambda\Delta l, \quad \text{with} \quad \Delta l = \frac{Sym(\mathcal{G}_M)}{\gcd(Sym(\mathcal{G}_M), L_\Omega)}, \\ (A)_\lambda &= (A)_0 - \lambda\frac{L_\Omega}{\gcd(Sym(\mathcal{G}_M), L_\Omega)}, \end{aligned} \tag{2.28}$$

where $(S_{M\Omega})_0$ and $(A)_0$ is a known pair of solutions, and λ is an integer number.

However, the variables and parameters from Equation (2.26) have some constraints due to the modular nature of the problem, in particular:

$$\begin{aligned} Sym(\mathcal{G}_M) &\in \{1, \ldots, L_M\}, \\ S_{M\Omega} &\in \{0, \ldots, Sym(\mathcal{G}_M) - 1\}, \\ L_{M\Omega} &\in \{0, \ldots, L_\Omega - 1\}, \end{aligned} \tag{2.29}$$

and thus, there are a finite number of different solutions to this problem. From the second boundary, we can derive that the difference between the maximum and the minimum value of $S_{M\Omega}$ is, at most, $\Delta S_{M\Omega} = (Sym(\mathcal{G}_M) - 1)$. Now, we are interested to know the number of different values of λ that allows Equation (2.28) to be inside this constraints. Thus, we first count the number of integer sections of length Δl that lay in the interval $\Delta S_{M\Omega}$, that is:

$$\begin{aligned} \left\lfloor \frac{\Delta S_{M\Omega}}{\Delta l} \right\rfloor &= \left\lfloor \frac{(Sym(\mathcal{G}_M) - 1)\gcd(Sym(\mathcal{G}_M), L_\Omega)}{Sym(\mathcal{G}_M)} \right\rfloor = \\ &= \left\lfloor \gcd(Sym(\mathcal{G}_M), L_\Omega) - \frac{\gcd(Sym(\mathcal{G}_M), L_\Omega)}{Sym(\mathcal{G}_M)} \right\rfloor, \end{aligned} \tag{2.30}$$

where $\lfloor x \rfloor$ is the round down integer of x.

It is elemental that $\gcd(Sym(\mathcal{G}_M), L_\Omega)$ is an integer, so Equation (2.30) can be expressed as:

$$\gcd(Sym(\mathcal{G}_M), L_\Omega) - \left\lceil \frac{\gcd(Sym(\mathcal{G}_M), L_\Omega)}{Sym(\mathcal{G}_M)} \right\rceil, \tag{2.31}$$

where $\lceil x \rceil$ is the round up integer of x. On the other hand, we know that $\gcd(Sym(\mathcal{G}_M), L_\Omega) \in [1, Sym(\mathcal{G}_M)]$ by the definition of greatest common divisor, thus:

$$\frac{\gcd(Sym(\mathcal{G}_M), L_\Omega)}{Sym(\mathcal{G}_M)} \in (0, 1], \tag{2.32}$$

and applying this result we derive that the number of intervals is:

$$\gcd(Sym(\mathcal{G}_M), L_\Omega) - 1. \tag{2.33}$$

Finally, the number of intervals defines a set of different elements inside the interval $\Delta S_{M\Omega}$ equal to the number of intervals plus one. Consequently, the number of different values that $(S_{M\Omega})_\lambda$ can take is:

$$\gcd(Sym(\mathcal{G}_M), L_\Omega), \tag{2.34}$$

which is the number of solutions of Equation (2.26) provided that the number of orbital planes L_Ω, the combination number $L_{M\Omega}$, and the symmetry of the necklace $Sym(\mathcal{G}_M)$ are fixed. Note that this number of solutions only applies if the condition of existence of solution provided by Equation (2.27) is achieved.

□

2.2.2 Fixing the necklace $\mathcal{G}_M$, L_Ω and L_M

On the other hand, in this second case, we fix the necklace $\mathcal{G}_M$ and the size of the extended space, that is, the parameters L_Ω and L_M from the Hermite Normal Form. This provides the information of how many different distributions can be created with a given set of satellites (through the parameter $Sym(\mathcal{G}_M)$). This problem is equivalent to compute the amount of pairs $\{S_{M\Omega}, L_{M\Omega}\}$ that are solution of Equation (2.23).

Theorem 2. *Given a necklace in the mean anomaly $\mathcal{G}_M$ and a size of the fictitious constellation (L_Ω and L_M), the number of different symmetric constellation configurations is L_Ω.*

Proof. Equation (2.22) can be reordered as:

$$L_\Omega S_{M\Omega} - 1 L_{M\Omega} = ASym(\mathcal{G}_M), \tag{2.35}$$

where the parameters have the constraints shown in Equation (2.29). In this expression, we consider $S_{M\Omega}$ and $L_{M\Omega}$ the variables of the problem, and thus, the equation has solution only and only if:

$$\gcd(L_\Omega, 1) \mid ASym(\mathcal{G}_M), \tag{2.36}$$

which is always true as $\gcd(L_\Omega, 1) = 1$ and $ASym(\mathcal{G}_M)$ is an integer value. This provides an important result: given a symmetry of the necklace $Sym(\mathcal{G}_M)$, and a number of orbital planes L_Ω, there is always at least one solution to the equation. The objective now is to compute the number of solutions that this result represents.

Equation (2.35) is a linear Diophantine equation whose solutions are provided by the following relation:

$$\begin{aligned} (S_{M\Omega})_\lambda &= (S_{M\Omega})_0 + \lambda, \\ (L_{M\Omega})_\lambda &= (L_{M\Omega})_0 - \lambda L_\Omega, \end{aligned} \tag{2.37}$$

where $(S_{M\Omega})_0$ and $(L_{M\Omega})_0$ are a pair of possible solutions of Equation (2.35) and λ is an integer. From Equation (2.37), we can derive that there is only one solution for a fixed $ASym(\mathcal{G}_M)$, since $L_{M\Omega} \in \{0, \ldots, L_\Omega - 1\}$. Thus, the number of possible solutions is provided by the number of different equations in the form of Equation (2.37) (which is equivalent to the number of possible values of the integer A).

From Equation (2.35), the maximum and minimum values of $ASym(\mathcal{G}_M)$ can be obtained:

$$\begin{aligned} \min\left(ASym(\mathcal{G}_M)\right) &= -(L_\Omega - 1), \\ \max\left(ASym(\mathcal{G}_M)\right) &= (Sym(\mathcal{G}_M) - 1)L_\Omega. \end{aligned} \tag{2.38}$$

Then, we derive the maximum variation of the parameter $ASym(\mathcal{G}_M)$:

$$\Delta\left(ASym(\mathcal{G}_M)\right) = \max\left(ASym(\mathcal{G}_M)\right) - \min\left(ASym(\mathcal{G}_M)\right) = L_\Omega Sym(\mathcal{G}_M) - 1. \tag{2.39}$$

Moreover, $Sym(\mathcal{G}_M)$ is constant in this variation, thus:

$$\Delta\left(ASym(\mathcal{G}_M)\right) = \Delta ASym(\mathcal{G}_M), \tag{2.40}$$

where we can conclude that the admissible values of A lay in an interval of amplitude:

$$\Delta A = L_\Omega - \frac{1}{Sym(\mathcal{G}_M)}. \tag{2.41}$$

Now, we are interested in the number of complete intervals of amplitude 1 that are inside ΔA (remember that A is an integer number), since this number plus one defines the number of possible values of A. The number of complete intervals is:

$$\lfloor \Delta A \rfloor = \left\lfloor L_\Omega - \frac{1}{Sym(\mathcal{G}_M)} \right\rfloor = L_\Omega - \left\lceil \frac{1}{Sym(\mathcal{G}_M)} \right\rceil. \tag{2.42}$$

Moreover, since $\lceil Sym(\mathcal{G}_M)^{-1} \rceil \in (0, 1]$, the number of complete intervals is $(L_\Omega - 1)$, which define L_Ω different values that the parameter A can take in Equation (2.37). The different values of A are providing the number of possible different equations that we can obtain from Equation (2.37). Furthermore, we already know that each equation has only one solution. Thus, the total number of solutions of Equation (2.37) is L_Ω.

□

One important thing to notice is that the number of solutions provided by Theorem 5 requires to set a particular symmetry of the necklace $Sym(\mathcal{G}_M)$. If the symmetry of the necklace is not fixed, and instead only the size of the fictitious constellation is fixed, that is, L_Ω and L_M, we have to use the Burnside's counting theorem applied to this particular case in addition to the methodology presented in this section. That way, the number of possible solutions that a fictitious constellation distributed in L_Ω orbital planes, with L_M available positions in each orbit is:

$$\frac{L_\Omega}{L_M} \sum_{d|L_M} \varphi(d) 2^{L_M/d}, \tag{2.43}$$

where the sum is taken over all the divisors d of L_M, and $\varphi(d)$ is the Euler's totient function of d. Equation (2.43) represents a combinatorial problem where the number of possible combinations of necklaces is given by Burnside's counting theorem while the number of pairs $\{L_{M\Omega}, S_{M\Omega}\}$ are given by Theorem 5. This combination can be freely performed since the number of pairs $\{L_{M\Omega}, S_{M\Omega}\}$ does not depend on the symmetry of the necklace (the only parameter that is changing in Burnside's counting theorem).

2.2.3 Fixing N_M, L_Ω and L_M

This case is an interesting variation of the previous counting methodology, where now, the real satellites per orbit, that is, $N_M = |\mathcal{G}_M|$, is fixed instead of the necklace. Thus, it provides information on the number of possibilities of design that are available with a set of satellites and a size of a fictitious constellation. It is important to note that, in this case, the sizes of both the real and the fictitious constellations are fixed.

Theorem 3. *Given a number of satellites per orbit N_M, and a size of fictitious constellation (L_Ω and L_M), the number of different symmetric constellation configurations is:*

$$\frac{L_\Omega}{L_M} \sum_{\substack{g=1 \\ g|L_M \\ \frac{L_M}{g}|N_M}}^{L_M} |Fix(g)|\,, \tag{2.44}$$

where $Fix(g)$ is the number of elements contained in the Fix of a given symmetry g, and can be computed using the following recursive function:

$$|Fix(g)| = \frac{L_M}{g}\left[\binom{g}{\frac{N_M}{L_M}g} - \sum_{\substack{g'=1 \\ g'|g \\ \frac{L_M}{g'}|N_M}}^{g-1} \frac{g'}{L_M}\left|Fix(g')\right|\right]. \tag{2.45}$$

Proof. The process followed in this case is based on applying Burnside's Lemma to count the number of different solutions. In order to use it, we require to set first a particular symmetry of a necklace and compute the Fix in the space of all possible configurations under that symmetry. Second, we remove the configurations that were considered in other symmetries before. Third, the number of orbits for a particular symmetry is computed using Burnside's Lemma. And finally, the total number of solutions is obtained as a sum of all the possible symmetries.

Let $+\,\mathbb{Z}_{L_M}$ be the possible actions that are considered in this problem, which correspond to the possible different rotations that a necklace $\mathcal{G}_M$ can perform in the modulo $\mathbb{Z}_{L_M}$. In addition, $G = \mathbb{Z}_{L_M}$ is the group of possible actions that can apply to any necklace defined in L_M available positions. That way, the map ϕ can be defined as:

$$\begin{aligned} \phi: \quad G \times X &\longrightarrow X \\ (g, x) &\longmapsto x + g \mod (L_M). \end{aligned} \tag{2.46}$$

The objective is to apply the Burnside's Lemma to this application, and thus, we have to compute $|\mathrm{Fix}(g)|$ (see Equation (1.56)). The Fix of a given action is the set of elements that remain unaltered under the application of that action. In that respect, from the definition of symmetry of a necklace (see Equation (1.46)), we know that the only possible values of $g \in G$ that have elements in the $\mathrm{Fix}(X)$ are the ones that presents symmetries, that is, when an element fulfills $g = Sym(\mathcal{G}_M)$. This means that only the values such that $g|L_M$ and $\frac{L_M}{g}|N_M$ contribute to the elements of the Fix.

First, we focus in a particular value of symmetry of the necklace $g = Sym(\mathcal{G}_M)$ and its Fix (Fix(g)). As there exists symmetry in the necklace, the configuration can be regarded as a pattern comprised of g available positions that is repeated L_M/g times in the L_M available positions. In this pattern, there must be $N_M g/L_M$ elements from the necklace since all the patterns must have the same number of elements. Thus, the number of possible combinations that exists in a pattern of size g ($PC(g)$) is:

$$PC(g) = \binom{g}{\frac{N_M}{L_M}g}. \tag{2.47}$$

On the other hand, each pattern can rotate L_M/g possible times in the L_M available positions while maintaining the same configuration (due to the symmetry that we are imposing). Thus, the number of combinations of N_M elements in L_M available positions that present a given symmetry g is:

$$\frac{L_M}{g}PC(g) = \frac{L_M}{g}\binom{g}{\frac{N_M}{L_M}g}. \tag{2.48}$$

However, this counting also includes some elements that belong to other symmetries, and thus, they must be removed from this set of combinations in order to avoid duplicities in the counting process. For instance, if $L_M = 4$ and $N_M = 2$ and we consider $g = 4$ as the symmetry in study, the number of combinations that we compute with Equation (2.47) include combinations of elements that also present symmetry of $g = 2$: $\{1, 3\}$ and $\{2, 4\}$; and thus, we could count them twice if we are not careful in the counting process. In order to avoid these cases, we only consider g as the smallest symmetry that a combination of elements can present.

From the definition of Fix, we know that the number of possible combinations of N_M elements with a particular symmetry g is the $|\text{Fix}(g)|$ itself. In addition, the possible combinations of elements must have been generated based on patters of size g (as in Equation (2.47)). Thus, the number of different patterns that exist for a particular symmetry g' is:

$$PC(g') = \frac{g'}{L_M}\left|\text{Fix}(g')\right|. \tag{2.49}$$

Then, we can remove from the counting process, of the different pattern generators with symmetry g, all the elements that belong to a different symmetry such that $g' < g$:

$$PC(g) = \binom{g}{\frac{N_M}{L_M}g} - \sum_{\substack{g'=1 \\ g'|g \\ \frac{L_M}{g'}|N_M}}^{g-1} \frac{g'}{L_M}\left|\text{Fix}(g')\right|, \tag{2.50}$$

where the sum is performed in all the symmetries g' such that $g'|g$ and $\frac{L_M}{g'}|N_M$ since g' must also fulfill the conditions for symmetry.

Once the number of pattern combinations is computed, the $|\text{Fix}(g)|$ can be obtained using Equation (2.50), leading to:

$$|\text{Fix}(g)| = \frac{L_M}{g}\left[\binom{g}{\frac{N_M}{L_M}g} - \sum_{\substack{g'=1 \\ g'|g \\ \frac{L_M}{g'}|N_M}}^{g-1} \frac{g'}{L_M}\left|\text{Fix}(g')\right|\right], \tag{2.51}$$

which is a recursive function that can be easily computed. Equation (2.51) allows to obtain the number of different necklaces under a given symmetry g. This is done by the direct application of Burnside's Lemma (Equation (1.56)), where $G = \mathbb{Z}_{L_M}$ as pointed out before. That way, we can derive Corollary 1.

Corollary 1. *The number of different necklaces with a given symmetry g that can be obtained with N_M elements taken from L_M available positions is:*

$$\frac{1}{g}\left[\binom{g}{\frac{N_M}{L_M}g} - \sum_{\substack{g'=1 \\ g'|g \\ \frac{L_M}{g'}|N_M}}^{g-1} \frac{g'}{L_M}\left|Fix(g')\right|\right]. \tag{2.52}$$

where $|Fix(g')|$ is provided by Equation (2.51).

In addition, if we fix the necklace, we obtain the same conditions as in Theorem 2, which implies that the number of possible different configurations that each necklace can provide is L_Ω. Thus, and for a given symmetry g, the number of possible configurations is:

$$\frac{L_\Omega}{g}\left[\binom{g}{\frac{N_M}{L_M}g} - \sum_{\substack{g'=1 \\ g'|g \\ \frac{L_M}{g'}|N_M}}^{g-1} \frac{g'}{L_M}\left|\text{Fix}(g')\right|\right]. \tag{2.53}$$

Finally, since we already know the number of possible configurations that each symmetry can provide, we can sum all the contributions from the different symmetries to obtain the total number of configurations of a 2D Necklace Flower Constellation:

$$\sum_{\substack{g=1 \\ g|L_M \\ \frac{L_M}{g}|N_M}}^{L_M} \frac{L_\Omega}{g}\left[\binom{g}{\frac{N_M}{L_M}g} - \sum_{\substack{g'=1 \\ g'|g \\ \frac{L_M}{g'}|N_M}}^{g-1} \frac{g'}{L_M}\left|\text{Fix}(g')\right|\right], \tag{2.54}$$

which can be rewritten as:

$$\frac{L_\Omega}{L_M} \sum_{\substack{g=1 \\ g|L_M \\ \frac{L_M}{g}|N_M}}^{L_M} |\mathrm{Fix}(g)|\,, \tag{2.55}$$

where $|\mathrm{Fix}(g)|$ is provided by Equation (2.51).

□

The set of equations given by Theorem 3 are the general expressions to calculate the number of possible combinations that the 2D Necklace Flower Constellation methodology provides for a given number of satellites and a given size of the fictitious constellation. It also allows to fix the cost of the mission (the number of satellites and their general distribution), while providing information of the design possibilities available before starting the computation. That way, it is possible to decrease or increase the size of the fictitious constellation to adapt the number of possibilities to the memory and time available.

2.3 Generalizing into a double necklace

In Section 2.1 a necklace in the mean anomaly was introduced and then in Section 2.2 the number of possible configurations was assessed. In this section we introduce the formulation for a double necklace in the satellite distribution. This means that two necklaces are generated, one in the mean anomaly $\mathcal{G}_M$ and the other in the right ascension of the ascending node $\mathcal{G}_\Omega$.

Let N_Ω and L_Ω be the real and fictitious number of orbital planes in which the constellation is distributed. That way, the necklace in the right ascension of the ascending node can be defined as the subset:

$$\mathcal{G}_\Omega \subseteq \{1, \ldots, L_\Omega\}, \tag{2.56}$$

such that $|\mathcal{G}_\Omega| = N_\Omega$. In addition we define the index i^* as the parameter of distribution inside the necklace $\mathcal{G}_\Omega$. That way:

$$\mathcal{G}_\Omega(i^*) = \mathcal{G}_\Omega(\mathrm{mod}(i^* + N_\Omega, N_\Omega)), \tag{2.57}$$

which is equivalent to:

$$i = \mathrm{mod}(i + L_\Omega, L_\Omega). \tag{2.58}$$

Now, an application between i and i^* can be defined using the necklace $\mathcal{G}_\Omega$:

$$i = \mathcal{G}_\Omega(i^*), \tag{2.59}$$

and introducing this expression into Equation (2.14), we obtain:

$$\begin{aligned} \Delta\Omega_{i^*j^*} &= \frac{2\pi}{L_\Omega}\left(\mathcal{G}_\Omega(i^*) - 1\right), \\ \Delta M_{i^*j^*} &= \frac{2\pi}{L_M}\left(\mathrm{mod}\left(\mathcal{G}_M(j^*) - 1 + S_{M\Omega}(\mathcal{G}_\Omega(i^*) - 1),\ Sym(\mathcal{G}_M)\right)\right) - \\ &- \frac{2\pi}{L_M}\frac{L_{M\Omega}}{L_\Omega}\left(\mathcal{G}_\Omega(i^*) - 1\right), \end{aligned} \tag{2.60}$$

which is the general expression that allows to generate all the possible configurations when two necklaces are included. On the other hand the symmetric configurations of this formulation are still given by Equation (2.23) since the rotations in this new necklace does not modify the behavior of the system.

One important thing to notice is that this formulation represents the removal of complete orbital planes from the original configuration given by Equation (2.14). This means that, unless the necklace $\mathcal{G}_\Omega$ presents a symmetry, the configuration will lose the property of having an uniform distribution no matter the orbital plane observed. However, the resultant configuration still presents a structure related to the original distribution.

2.4 Generation of all the configurations

In this section, we present a general scheme in order to generate all the possible constellation configurations that the 2D Necklace theory can provide. In that respect, Figure 2.4 shows the summary of the process.

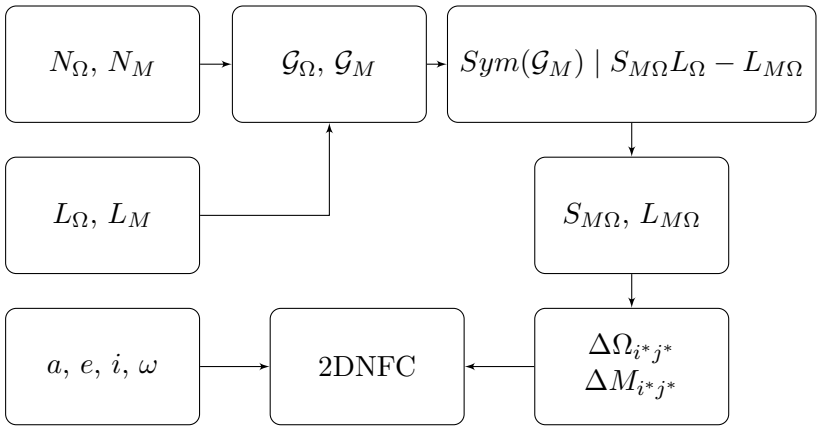

Figure 2.4: Flowchart of the 2D Necklace Flower Constellation generation process

First, the general classic elements for the whole constellation are defined, namely, the semi-major axis a, the eccentricity e, the inclination i and the argument of perigee ω. Second, the sizes of the real and fictitious constellations are set (N_Ω, N_M for the real and L_Ω, L_M for the expanded distributions). Then, using these sizes, all the possible necklaces are generated using a generation algorithm [40, 41]. With the results obtained, we apply Equation (2.23) to generate the shifting parameters $S_{M\Omega}$ and the configuration numbers $L_{M\Omega}$ that correspond to each combination of necklaces. Finally, the distribution in the right ascension of the ascending node ($\Delta\Omega_{i^*j^*}$) and in the mean anomaly ($\Delta M_{i^*j^*}$) is computed, and thus, in combination with the classical elements already defined, the configuration of the whole 2D Necklace Flower Constellation is defined.

This process can be parallelized in the generation of necklaces, the solution of the Diophantine equation and the generation of the distributions, allowing to generate and study a large number of configurations in a small amount of time. On the other hand, as the number of parameters required

to define a constellation is very low, it is easy to store in memory all the possible combinations for later study in other applications.

2.5 Conclusion

This chapter presents a new methodology of satellite constellation design, the 2D Necklace Flower Constellations. This methodology allows to overcome the limitation on the number of possibilities of design that the original 2D Lattice Flower Constellations presented while maintaining the number of satellites of the configuration. This is achieved by an expansion of the configuration into a fictitious constellation in which a set of satellites that maintain the properties of uniformity and symmetry are selected. Other applications of this design framework are the definition of the sequence of launches for large constellations, the study of possible reconfiguration strategies of a given constellation with very little fuel consumption, or the assessment of the effect of failure in satellites of the configuration.

Compared to previous formulations, the main advantage of 2D Necklace Flower Constellations is that it introduces the concept of necklaces directly into its formulation, which allows to have closed expressions of the distributions that a constellation can present. This is especially interesting for design since it provides more control in the process, and for optimization techniques, since it is possible to generate any configuration that the theory can provide in a fast and easy procedure.

In addition, three counting theorems are presented, which allow to predict the number of possible combinations that the 2D Necklace Flower Constellations theory can provide. The first covers the number of constellation configurations where a particular distribution is fixed. The second theorem provides the information of the number of possibilities that a particular symmetry generates in the design methodology. On the other hand, the third theorem allows to compute the total number of configurations that a set of satellites can provide for a particular size of fictitious constellation.

Finally, it is important to notice that the number of possibilities obtained using this methodology depends on the size of the fictitious constellation, and thus, it can be increased as much as required. This property is very interesting from a design point of view, since it allows to optimize the methodology to the computational resources available.

Chapter 3

3D Necklace Flower Constellations

We continue the development of the Necklace Flower Constellation theory with the generalization of the 3D Lattice Flower Constellations theory. This is done by an expansion of the configuration space of the 3D Lattice Flower Constellations consisting on generating a fictitious constellation with more satellites than the real constellation sought. 3D Necklace Flower Constellations constitutes a generalization of the 2D and 3D Lattice Flower Constellations, and contains as a subset, all the former Lattice Flower Constellations. This includes the 2D and 3D Lattice Flower Constellations as well as the 2D Necklace Flower Constellations.

The formulation developed for the 3D Necklace Flower Constellations allows to include the concept of necklace in any of the variables of distribution of a 3D Lattice Flower Constellation, that is, the right ascension of the ascending node, the argument of perigee and the mean anomaly. This allows to expand the possibilities of design, not limiting the generation of necklaces to the mean anomaly as done in previous works [17, 18]. Moreover, as all the former Lattice and Necklace Flower Constellations, all the constellations generated preserve the properties of uniformity and symmetry, which are of importance for many space missions, such as global positioning, telecommunications or Earth observation.

This chapter is organized as follows. First, a new methodology is introduced that includes necklaces directly into the formulation of the distribution in a 3D Lattice Flower Constellation. This provides a clearer formulation and moreover, allows a faster computation of the real constellation, since only the real positions of the satellites are calculated. Second, the expansion of the searching space is introduced, which allows to generate as many different possibilities in design as required. This two properties are especially interesting in optimization problems, where the time spent and the design possibilities are controlled using the size of the fictitious constellation. Third, the conditions to generate distributions that maintain the properties of symmetry and uniformity of the configuration (characteristic of the Lattice Flower Constellations) are presented. This allows to create structures in the constellation that are maintained during its movement. Finally, an example of application of this new formulation is presented, where the possibilities that this new methodology can provide in the design of satellite constellations are shown.

3.1 The 3D Necklace Flower Constellations Theory

As it can be seen in Equation (1.41), a 3D Lattice Flower Constellation can be described by the use of the Hermite Normal Form. The Hermite Normal Form is composed by six integers, three in the diagonal of the matrix and the other three in the lower triangular part of the matrix. The integers in the diagonal are the number of orbital planes of the constellation (L_Ω), the number of different argument of perigees in each orbital plane (L_ω), and the number of satellites in each orbit (L_M). The other three parameters are the configuration numbers ($L_{M\Omega}, L_{M\omega}, L_{\omega\Omega}$) defined as follows: $L_{M\Omega} \in [0, L_\Omega - 1]$, $L_{M\omega} \in [0, L_w - 1]$ and $L_{\omega\Omega} \in [0, L_\Omega - 1]$. The expression that summarizes the distribution of the satellites in a 3D Lattice Flower Constellation is:

$$\begin{bmatrix} L_\Omega & 0 & 0 \\ L_{\omega\Omega} & L_\omega & 0 \\ L_{M\Omega} & L_{M\omega} & L_M \end{bmatrix} \begin{pmatrix} \Delta\Omega_{ijk} \\ \Delta\omega_{ijk} \\ \Delta M_{ijk} \end{pmatrix} = 2\pi \begin{pmatrix} i-1 \\ k-1 \\ j-1 \end{pmatrix}; \tag{3.1}$$

where $\Delta\Omega_{ijk}$ is the distribution in the right ascension of the ascending node of the constellation, $\Delta\omega_{ijk}$ is the distribution of the argument of perigee, and ΔM_{ijk} is the initial distribution of the mean anomaly with respect a reference satellite of the constellation with orbital elements $\{\Omega_{000}, \omega_{000}, M_{000}\}$. Moreover, the list (i, j, k) represents the position of a satellite in the orbital plane $i \in [1, L_\Omega]$, with the argument of perigee $k \in [1, L_\omega]$ and the mean anomaly $j \in [1, L_M]$. Note also that the values of Ω_{ijk}, ω_{ijk} and M_{ijk} represent three angles and thus, they are defined in the range $[0, 2\pi]$.

Equation (3.1) defines the distribution of a 3D Lattice Flower Constellation. This distribution has the particularity of presenting a symmetric configuration in the lattice of the constellation with respect to all its variables, the right ascension of the ascending node, the argument of perigee and the mean anomaly. The objective now is to introduce the concept of necklaces in the formulation, but preserving the symmetries of the initial configuration.

In order to introduce the necklaces, Equation (3.1) must be expanded:

$$\begin{aligned} \Delta\Omega_{ijk} &= \frac{2\pi}{L_\Omega}(i-1), \\ \Delta\omega_{ijk} &= \frac{2\pi}{L_\omega}(k-1) - \frac{2\pi}{L_\omega}\frac{L_{\omega\Omega}}{L_\Omega}(i-1), \\ \Delta M_{ijk} &= \frac{2\pi}{L_M}(j-1) - \frac{2\pi}{L_M}\frac{L_{M\omega}}{L_\omega}(k-1) - \frac{2\pi}{L_M}\left(\frac{L_{M\Omega}}{L_\Omega} - \frac{L_{M\omega}}{L_\omega}\frac{L_{\omega\Omega}}{L_\Omega}\right)(i-1), \end{aligned} \tag{3.2}$$

where this configuration corresponds to a fictitious constellation that is used to define the available positions in which the real satellites of the constellation are located.

From Equation (3.2), it can be observed that the value of $\Delta\omega_{ijk}$ is different for $i = 1$ and $i = L_\Omega + 1$, and thus, moving in $i \in [1, L_\Omega + 1]$ does not close the configuration in the torus for a particular value of k. This means that in general $\Delta\omega_{ijk} \neq \Delta\omega_{(i+L_\Omega)jk}$. In the 3D Lattice formulation this has no effect since all the positions are filled and consequently, the configuration is complete. However, with the use of necklaces, this effect has to be taken into account in order to generate symmetric configurations. The same consideration has to be made in the expression of the mean anomaly.

In that sense, a complete rotation in the right ascension of the ascending node or the argument of perigee does not generate in general the same value on the mean anomaly since $\Delta M_{ijk} \neq \Delta M_{(i+L_\Omega)jk}$ and $\Delta M_{ijk} \neq \Delta M_{ij(k+L_\omega)}$.

Two different necklaces can be defined in a 3D Lattice Flower Constellation, one in the mean anomaly, and the other in the argument of perigee. It is possible to generate necklaces in the right ascension of the ascending node with the 3D Lattice Flower Constellation configuration. However this is equivalent to generate the distribution and keeping just the orbital planes that we are interested in. For this reason, we do not consider this case, since the use of necklaces is trivial in these kind of configurations.

Let $\mathcal{G}_M$ be a necklace defined in the mean anomaly with a number of elements equal to $N_M = |\mathcal{G}_M|$ and such that $\mathcal{G}_M \subseteq \mathbb{Z}_{L_M}$. This represents N_M satellites taken from a set of L_M available positions defined in a particular orbit. The necklace in the mean anomaly $\mathcal{G}_M$ is represented as a vector of dimension N_M:

$$\mathcal{G}_M = (\mathcal{G}_M(1), \cdots, \mathcal{G}_M(j^*), \cdots, \mathcal{G}_M(N_M)), \tag{3.3}$$

with

$$1 \leq \mathcal{G}_M(1) \leq \cdots \leq \mathcal{G}_M(j^*) \leq \cdots \leq \mathcal{G}_M(N_M) \leq L_M, \tag{3.4}$$

and where the index j^* represents an integer modulo N_M, that is, $j^* + N_M$ is the same index as j^*. This allows to define an application (T1) that points to the positions occupied by the necklace from the available positions:

$$\begin{array}{rccc} \text{T1}: & \mathbb{Z}_{N_M} & \longrightarrow & \mathbb{Z}_{L_M} \\ & j^* & \longmapsto & \mathcal{G}_M(j^*). \end{array} \tag{3.5}$$

Thus, it makes sense to refer to $\mathcal{G}_M(j^*)$, where the integer parameter $j^* \in \{1, \cdots, N_M\}$ represents the position inside the necklace defined. In addition, and for simplicity of notation, we denote $\text{mod}(a, b) = a \mod (b)$. Thus, due to the modular arithmetic inside the necklace:

$$\mathcal{G}_M(j^*) = \mathcal{G}_M(\text{mod}(j^* + N_M, N_M)), \tag{3.6}$$

which corresponds to a complete loop in the available positions in the mean anomaly. It is important to note that this rotation is equivalent to a movement in the admissible locations defined by:

$$j = j + L_M \mod (L_M), \tag{3.7}$$

as both represent the same movement of the necklace, one using the parametrization of the necklace and the other using the parametrization of the fictitious constellation.

On the other hand, let $\mathcal{G}_\omega$ be a necklace defined in the argument of perigee with a number of elements equal to $N_\omega = |\mathcal{G}_\omega|$, the number of real orbits per plane and a number of available positions equal to L_ω, which correspond to the size of the space of this variable in the fictitious constellation. This necklace is defined as a vector in the same way as $\mathcal{G}_M$:

$$\mathcal{G}_\omega = (\mathcal{G}_\omega(1), \cdots, \mathcal{G}_\omega(k^*), \cdots, \mathcal{G}_\omega(N_\omega)), \tag{3.8}$$

with

$$1 \leq \mathcal{G}_\omega(1) \leq \cdots \leq \mathcal{G}_\omega(k^*) \leq \cdots \leq \mathcal{G}_M(N_\omega) \leq L_\omega, \tag{3.9}$$

where the index k^* is an integer modulo N_ω. This allows to define an application (T2) that points to the positions occupied by the necklace from the available positions:

$$\begin{array}{rccl} \text{T2}: & \mathbb{Z}_{N_\omega} & \longrightarrow & \mathbb{Z}_{L_\omega} \\ & k^* & \longmapsto & \mathcal{G}_\omega(k^*), \end{array} \tag{3.10}$$

which is used to refer to $\mathcal{G}_\omega(k^*)$, where the integer parameter $k^* \in \{1, \cdots, N_\omega\}$ represents the movement inside the necklace defined. Moreover, the necklace represents a ring of integers, thus, there exist a modular arithmetic inside the necklace:

$$\mathcal{G}_\omega(k^*) = \mathcal{G}_\omega(\text{mod}(k^* + N_\omega, N_\omega)), \tag{3.11}$$

which is equivalent to a complete loop in the available positions in the argument of perigee:

$$k = k + L_\omega \mod (L_\omega), \tag{3.12}$$

as both are two formulations for the same movement, one using the parametrization of the necklace and the other using the parametrization of the fictitious constellation.

Now, an application (T3) has to be defined which relates the distribution indexes (i, j^*, k^*) from the necklace, with the indexes of the available positions (i, j, k):

$$\begin{array}{rccl} \text{T3}: & \mathbb{Z}_{L_\Omega} \times \mathbb{Z}_{N_M} \times \mathbb{Z}_{N_\omega} & \longrightarrow & \mathbb{Z}_{L_\Omega} \times \mathbb{Z}_{L_M} \times \mathbb{Z}_{L_\omega} \\ & (i, j^*, k^*) & \longmapsto & (i, j, k), \end{array} \tag{3.13}$$

where the effects of the possible movement with respect to the right ascension of the ascending node and the argument of perigee are introduced in the formulation by the use of the three shifting parameters, $S_{\omega\Omega}$ the shifting parameter that relates the argument of perigee with the right ascension of the ascending node, $S_{M\Omega}$ the shifting parameter that relates the mean anomaly and the right ascension of the ascending node, and $S_{M\omega}$ the shifting parameter that relates the mean anomaly and the argument of perigee. That way, the possible movements of the integers k and j are described respectively by:

$$\begin{array}{rcl} k & = & \mathcal{G}_\omega(k^*) + S_{\omega\Omega}(i-1), \\ j & = & \mathcal{G}_M(j^*) + S_{M\omega}(k-1) + S_{M\Omega}(i-1). \end{array} \tag{3.14}$$

We now subtract one unit of each expression to relate to the original formulation provided by Equation (3.2), obtaining:

$$\begin{array}{rcl} k-1 & = & \mathcal{G}_\omega(k^*) - 1 + S_{\omega\Omega}(i-1), \\ j-1 & = & \mathcal{G}_M(j^*) - 1 + S_{M\omega}(k-1) + S_{M\Omega}(i-1). \end{array} \tag{3.15}$$

Both expressions present modular arithmetic with respect to the symmetries of their necklaces, thus:

$$\begin{array}{rcl} k-1 & = & \mathcal{G}_\omega(k^*) - 1 + S_{\omega\Omega}(i-1) \mod Sym(\mathcal{G}_\omega), \\ j-1 & = & \mathcal{G}_M(j^*) - 1 + S_{M\omega}(k-1) + S_{M\Omega}(i-1) \mod Sym(\mathcal{G}_M). \end{array} \tag{3.16}$$

However, j depends on k, and we require a dependency over k^*, consequently, a substitution of k is performed in the second expression, leading to:

$$\begin{aligned} j-1 &= \mathcal{G}_M(j^*) - 1 + S_{M\omega}\text{mod}\left(\mathcal{G}_\omega(k^*) - 1 + S_{\omega\Omega}(i-1), Sym(\mathcal{G}_\omega)\right) + \\ &+ S_{M\Omega}(i-1) \mod Sym(\mathcal{G}_M), \end{aligned} \tag{3.17}$$

where it can be seen that the movement in j depends also on the necklace in the argument of perigee.

Once the distribution over each index is performed, we introduce Equations (3.16) and (3.17) into Equation (3.2), resulting in:

$$\begin{aligned} \Delta\Omega_{ij^*k^*} &= \frac{2\pi}{L_\Omega}(i-1), \\ \Delta\omega_{ij^*k^*} &= \frac{2\pi}{L_\omega}\left[\text{mod}\left(\mathcal{G}_\omega(k^*) - 1 + S_{\omega\Omega}(i-1), Sym(\mathcal{G}_\omega)\right) - \frac{L_{\omega\Omega}}{L_\Omega}(i-1)\right], \\ \Delta M_{ij^*k^*} &= \frac{2\pi}{L_M}\Bigg[\text{mod}\Big(\mathcal{G}_M(j^*) - 1 + S_{M\omega}\text{mod}\big(\mathcal{G}_\omega(k^*) - 1 + \\ &+ S_{\omega\Omega}(i-1), Sym(\mathcal{G}_\omega)\big) + S_{M\Omega}(i-1), Sym(\mathcal{G}_M)\Big) - \\ &- \frac{L_{M\omega}}{L_\omega}\text{mod}\left(\mathcal{G}_\omega(k^*) - 1 + S_{\omega\Omega}(i-1), Sym(\mathcal{G}_\omega)\right) - \\ &- \left(\frac{L_{M\Omega}}{L_\Omega} - \frac{L_{M\omega}}{L_\omega}\frac{L_{\omega\Omega}}{L_\Omega}\right)(i-1)\Bigg], \end{aligned} \tag{3.18}$$

which describes the possible movements of the two necklaces defined ($\mathcal{G}_M$ and $\mathcal{G}_\omega$) inside the distribution created in the fictitious constellation.

Equation (3.18) allows, not only to make the distribution of the satellites in the lattice, but also to find all symmetric configurations using the necklace theory. Note that, in the expression for $\Delta M_{ij^*k^*}$, the necklace in the argument of perigee appears, which means that properties in this necklace are affecting the distribution of the constellation in the mean anomaly. This effect is also seen in the conditions for the shifting parameters of the configuration as it will be seen later.

One important thing to notice regarding Equation (3.18) is that, since the shifting parameters ($S_{\omega\Omega}, S_{M\omega}, S_{M\Omega}$) are subjected to a modular arithmetic in the symmetry of the necklaces, duplicities can appear if no boundaries are defined. In that sense, and in order to avoid these duplicities in the formulation, we impose:

$$\begin{aligned} S_{\omega\Omega} &\in [0, Sym(\mathcal{G}_\omega) - 1], \\ S_{M\omega} &\in [0, Sym(\mathcal{G}_M) - 1], \\ S_{M\Omega} &\in [0, Sym(\mathcal{G}_M) - 1], \end{aligned} \tag{3.19}$$

to the shifting parameters. That way, we can assure that all combinations of parameters generate different constellation configurations, while we are still able to create all the different distributions that this formulation can provide.

3.1.1 Symmetry in the 3D Lattice Flower Constellations

In this section we impose the conditions of symmetry to the constellation configurations that can be obtained using Equation (3.18). That way, a relation between the distribution and the shifting parameters is obtained, which allows to define all the possible symmetric configurations that can be generated inside a given fictitious constellation.

3.1.1.1 Symmetry with respect to the mean anomaly

The conditions for symmetry in the three variables when a complete rotation in the mean anomaly is performed are:

$$\begin{aligned} \Delta\Omega_{ij^*k^*} &= \Delta\Omega_{i(j^*+N_M)k^*}, \\ \Delta\omega_{ij^*k^*} &= \Delta\omega_{i(j^*+N_M)k^*}, \\ \Delta M_{ij^*k^*} &= \Delta M_{i(j^*+N_M)k^*}, \end{aligned} \tag{3.20}$$

where all expressions are automatically fulfilled as $\Delta\Omega_{ij^*k^*}$ and $\Delta\omega_{ij^*k^*}$ do not depend on the movement of the mean anomaly whilst $\Delta M_{ij^*k^*}$ is also achieved due to the modular arithmetic nature of the problem seen in Equation (3.6).

3.1.1.2 Symmetry with respect to the argument of perigee

In order to have symmetry in the argument of perigee, the configuration of the constellation has to fulfill the following conditions:

$$\begin{aligned} \Delta\Omega_{ij^*k^*} &= \Delta\Omega_{ij(k^*+N_\omega)}, \\ \Delta\omega_{ij^*k^*} &= \Delta\omega_{ij^*(k^*+N_\omega)}, \\ \Delta M_{ij^*k^*} &= \Delta M_{ij^*(k^*+N_\omega)}, \end{aligned} \tag{3.21}$$

where the first equation is always true as it does not depend on the movement in the argument of perigee. On the other hand, the other two equations depend on k^* and, as such, they have to be studied.

Taking the condition in $\Delta\omega_{ij^*k^*}$, and from the equivalences in the definition between Equations (3.11) and (3.12), we can conclude that the operation $k^* + N_\omega$ is equivalent to a full rotation in the argument of perigee, that is:

$$\Delta\omega_{ij^*k^*} + 2\pi = \Delta\omega_{ij^*(k^*+N_\omega)}, \tag{3.22}$$

which applied to the expression of the argument of perigee, leads to:

$$\begin{aligned} &\frac{2\pi}{L_\omega}\left[\mathrm{mod}\left(\mathcal{G}_\omega(k^*) - 1 + S_{\omega\Omega}(i-1), Sym(\mathcal{G}_\omega)\right) - \frac{L_{\omega\Omega}}{L_\Omega}(i-1)\right] + 2\pi = \\ = \ &\frac{2\pi}{L_\omega}\left[\mathrm{mod}\left(\mathcal{G}_\omega(k^*+N_\omega) - 1 + S_{\omega\Omega}(i-1), Sym(\mathcal{G}_\omega)\right) - \frac{L_{\omega\Omega}}{L_\Omega}(i-1)\right], \end{aligned} \tag{3.23}$$

from where a relation between the two modular operators can be established:

$$\begin{aligned} & \mathrm{mod}\left(\mathcal{G}_\omega(k^*+N_\omega)-1+S_{\omega\Omega}(i-1), Sym(\mathcal{G}_\omega)\right) - \\ - \quad & \mathrm{mod}\left(\mathcal{G}_\omega(k^*)-1+S_{\omega\Omega}(i-1), Sym(\mathcal{G}_\omega)\right) = L_\omega, \end{aligned} \tag{3.24}$$

where this equation will be used later in order to impose the condition of symmetry in the mean anomaly with respect to the argument of perigee.

On the other hand, regarding the condition in $\Delta M_{ij^*k^*}$ from the system of Equations (3.21), and using Equation (3.18), the following expression can be derived:

$$\begin{aligned} & \frac{2\pi}{L_M}\Bigg[\mathrm{mod}\Big(\mathcal{G}_M(j^*)-1+S_{M\omega}\mathrm{mod}\big(\mathcal{G}_\omega(k^*)-1+ \\ + \quad & S_{\omega\Omega}(i-1), Sym(\mathcal{G}_\omega)\big)+S_{M\Omega}(i-1), Sym(\mathcal{G}_M)\Big) - \\ - \quad & \frac{L_{M\omega}}{L_\omega}\mathrm{mod}\left(\mathcal{G}_\omega(k^*)-1+S_{\omega\Omega}(i-1), Sym(\mathcal{G}_\omega)\right) - \\ - \quad & \left(\frac{L_{M\Omega}}{L_\Omega}-\frac{L_{M\omega}}{L_\omega}\frac{L_{\omega\Omega}}{L_\Omega}\right)(i-1)\Bigg] = \\ = \quad & \frac{2\pi}{L_M}\Bigg[\mathrm{mod}\Big(\mathcal{G}_M(j^*)-1+S_{M\omega}\mathrm{mod}\big(\mathcal{G}_\omega(k^*+N_\omega)-1+ \\ + \quad & S_{\omega\Omega}(i-1), Sym(\mathcal{G}_\omega)\big)+S_{M\Omega}(i-1), Sym(\mathcal{G}_M)\Big) - \\ - \quad & \frac{L_{M\omega}}{L_\omega}\mathrm{mod}\left(\mathcal{G}_\omega(k^*+N_\omega)-1+S_{\omega\Omega}(i-1), Sym(\mathcal{G}_\omega)\right) - \\ - \quad & \left(\frac{L_{M\Omega}}{L_\Omega}-\frac{L_{M\omega}}{L_\omega}\frac{L_{\omega\Omega}}{L_\Omega}\right)(i-1)\Bigg]; \end{aligned} \tag{3.25}$$

which can be simplified to:

$$\begin{aligned} & \mathrm{mod}\Big(\mathcal{G}_M(j^*)-1+S_{M\omega}\mathrm{mod}\left(\mathcal{G}_\omega(k^*)-1+S_{\omega\Omega}(i-1), Sym(\mathcal{G}_\omega)\right)+ \\ + \quad & S_{M\Omega}(i-1), Sym(\mathcal{G}_M)\Big) - \frac{L_{M\omega}}{L_\omega}\mathrm{mod}\left(\mathcal{G}_\omega(k^*)-1+S_{\omega\Omega}(i-1), Sym(\mathcal{G}_\omega)\right) = \\ = \quad & \mathrm{mod}\Big(\mathcal{G}_M(j^*)-1+S_{M\omega}\mathrm{mod}\left(\mathcal{G}_\omega(k^*+N_\omega)-1+S_{\omega\Omega}(i-1), Sym(\mathcal{G}_\omega)\right)+ \\ + \quad & S_{M\Omega}(i-1), Sym(\mathcal{G}_M)\Big) - \frac{L_{M\omega}}{L_\omega}\mathrm{mod}\left(\mathcal{G}_\omega(k^*+N_\omega)-1+S_{\omega\Omega}(i-1), Sym(\mathcal{G}_\omega)\right). \end{aligned} \tag{3.26}$$

Moreover, expanding the modular arithmetic in $Sym(\mathcal{G}_M)$ and using Equation (3.24) leads to:

$$A Sym(\mathcal{G}_M) = S_{M\omega}L_\omega - L_{M\omega}; \tag{3.27}$$

where A is an unknown integer number. This equation can be also represented with the following expression:

$$Sym(\mathcal{G}_M) \mid S_{M\omega}L_\omega - L_{M\omega}, \tag{3.28}$$

which reads, $Sym(\mathcal{G}_M)$ divides $(S_{M\omega}L_\omega - L_{M\omega})$.

Equation (3.28) is the first condition for the shifting parameters of the configuration. As it can be seen, it depends on the symmetry of the necklace, and some elements from the Hermite Normal

Form. Note that the shifting parameter of the mean anomaly with respect to the argument of perigee ($S_{M\omega}$) depends on the number of fictitious orbits per orbital plane and not the real number, a property that increases the number of possibilities in the configuration.

3.1.1.3 Symmetry with respect to the right ascension of the ascending node

The conditions of symmetry that we have to impose with respect to the right ascension of the ascending node are the following:

$$\begin{aligned} \Delta\Omega_{ij^*k^*} &= \Delta\Omega_{(i+L_\Omega)j^*k^*}, \\ \Delta\omega_{ij^*k^*} &= \Delta\omega_{(i+L_\Omega)j^*k^*}, \\ \Delta M_{ij^*k^*} &= \Delta M_{(i+L_\Omega)j^*k^*}. \end{aligned} \tag{3.29}$$

where each one of these conditions is treated separately.

The condition in the right ascension of the ascending node is automatically fulfilled as:

$$\Delta\Omega_{ij^*k^*} = \frac{2\pi}{L_\Omega}(i-1) = \frac{2\pi}{L_\Omega}(i-1) + 2\pi \mod (2\pi), \tag{3.30}$$

which is independent of any of the shifting parameters of the problem.

From the condition in the argument of perigee:

$$\frac{L_\omega}{2\pi}\Delta\omega_{ij^*k^*} = \frac{L_\omega}{2\pi}\Delta\omega_{(i+L_\Omega)j^*k^*}, \tag{3.31}$$

that can be used to obtain the following expression:

$$\begin{aligned} & \mod(\mathcal{G}_\omega(k^*) - 1 + S_{\omega\Omega}(i-1), Sym(\mathcal{G}_\omega)) - \frac{L_{\omega\Omega}}{L_\Omega}(i-1) = \\ = \ & \mod(\mathcal{G}_\omega(k^*) - 1 + S_{\omega\Omega}(i-1) + S_{\omega\Omega}L_\Omega, Sym(\mathcal{G}_\omega)) - \frac{L_{\omega\Omega}}{L_\Omega}(i-1) - L_{\omega\Omega}, \end{aligned} \tag{3.32}$$

which can be simplified, leading to:

$$\begin{aligned} & \mod(\mathcal{G}_\omega(k^*) - 1 + S_{\omega\Omega}(i-1) + S_{\omega\Omega}L_\Omega, Sym(\mathcal{G}_\omega)) - \\ - \ & \mod(\mathcal{G}_\omega(k^*) - 1 + S_{\omega\Omega}(i-1), Sym(\mathcal{G}_\omega)) = L_{\omega\Omega}, \end{aligned} \tag{3.33}$$

where Equation (3.33) is used later to solve the symmetries in the mean anomaly.

Expanding now the modular arithmetic in $Sym(\mathcal{G}_\omega)$ from Equation (3.33) and simplifying, we obtain:

$$BSym(\mathcal{G}_\omega) = S_{\omega\Omega}L_\Omega - L_{\omega\Omega}; \tag{3.34}$$

where B is an unknown integer. This expression is equivalent to:

$$Sym(\mathcal{G}_\omega) \mid S_{\omega\Omega}L_\Omega - L_{\omega\Omega}. \tag{3.35}$$

Equation (3.35) is the second condition for the shifting parameters. As it can be observed, it relates the shifting of the argument of perigee with respect to the right ascension of the ascending node

$S_{\omega\Omega}$, with the symmetries of the necklace in the argument of perigee $Sym(\mathcal{G}_\omega)$ and some elements of the Hermite Normal Form (L_Ω and $L_{\omega\Omega}$).

Once the problem of symmetry in the argument of perigee is solved, we impose the condition of symmetry in the mean anomaly by the use of its condition from Equation (3.29):

$$\frac{L_M}{2\pi}\Delta M_{ij^*k^*} = \frac{L_M}{2\pi}\Delta M_{(i+L_\Omega)j^*k^*}, \tag{3.36}$$

from where we can derive:

$$\begin{aligned}
& \mathrm{mod}\Big(\mathcal{G}_M(j^*) - 1 + S_{M\omega}\mathrm{mod}\left(\mathcal{G}_\omega(k^*) - 1 + S_{\omega\Omega}(i-1), Sym(\mathcal{G}_\omega)\right) + S_{M\Omega}(i-1), Sym(\mathcal{G}_M)\Big) - \\
- \quad & \frac{L_{M\omega}}{L_\omega}\mathrm{mod}\left(\mathcal{G}_\omega(k^*) - 1 + S_{\omega\Omega}(i-1), Sym(\mathcal{G}_\omega)\right) - \left(\frac{L_{M\Omega}}{L_\Omega} - \frac{L_{M\omega}}{L_\omega}\frac{L_{\omega\Omega}}{L_\Omega}\right)(i-1) = \\
= \quad & \mathrm{mod}\Big(\mathcal{G}_M(j^*) - 1 + S_{M\omega}\mathrm{mod}\left(\mathcal{G}_\omega(k^*) - 1 + S_{\omega\Omega}(i-1) + S_{\omega\Omega}L_\Omega, Sym(\mathcal{G}_\omega)\right) + \\
+ \quad & S_{M\Omega}(i-1) + S_{M\Omega}L_\Omega, Sym(\mathcal{G}_M)\Big) - \frac{L_{M\omega}}{L_\omega}\mathrm{mod}\left(\mathcal{G}_\omega(k^*) - 1 + S_{\omega\Omega}(i-1) + S_{\omega\Omega}L_\Omega, Sym(\mathcal{G}_\omega)\right) - \\
- \quad & \left(\frac{L_{M\Omega}}{L_\Omega} - \frac{L_{M\omega}}{L_\omega}\frac{L_{\omega\Omega}}{L_\Omega}\right)(i-1) - \left(L_{M\Omega} - \frac{L_{M\omega}L_{\omega\Omega}}{L_\omega}\right),
\end{aligned} \tag{3.37}$$

which, using Equation (3.33) can be simplified into:

$$\begin{aligned}
& \mathrm{mod}\Big(\mathcal{G}_M(j^*) - 1 + S_{M\omega}\mathrm{mod}\left(\mathcal{G}_\omega(k^*) - 1 + S_{\omega\Omega}(i-1) + \right. \\
+ \quad & \left. S_{\omega\Omega}L_\Omega, Sym(\mathcal{G}_\omega)\right) + S_{M\Omega}(i-1) + S_{M\Omega}L_\Omega, Sym(\mathcal{G}_M)\Big) - \\
- \quad & \mathrm{mod}\Big(\mathcal{G}_M(j^*) - 1 + S_{M\omega}\mathrm{mod}\left(\mathcal{G}_\omega(k^*) - 1 + S_{\omega\Omega}(i-1), Sym(\mathcal{G}_\omega)\right) + \\
+ \quad & S_{M\Omega}(i-1), Sym(\mathcal{G}_M)\Big) = L_{M\Omega}.
\end{aligned} \tag{3.38}$$

Now, we expand the modular arithmetic in $Sym(\mathcal{G}_\omega)$ and apply again the relation from Equation (3.33) in order to obtain:

$$CSym(\mathcal{G}_M) = S_{M\Omega}L_\Omega - \left(L_{M\Omega} - S_{M\omega}L_{\omega\Omega}\right), \tag{3.39}$$

where C is an unknown integer. The former expression can be also written as:

$$Sym(\mathcal{G}_M) \mid S_{M\Omega}L_\Omega - \left(L_{M\Omega} - S_{M\omega}L_{\omega\Omega}\right). \tag{3.40}$$

Equation (3.40) is the third condition for the shifting parameters. As we can see, this relation has a particularity, $S_{M\Omega}$ depends also on other shifting parameter, $S_{M\omega}$ which generates a logical order in the generation of the shifting parameters.

3.1.1.4 Symmetric configurations

In this subsection the formulation of the theory is summarized in order to present all the methodology in a more compact and clear way. All possible distributions of a particular necklace $\mathcal{G}$ can be described by the set of expressions:

$$\begin{aligned}
\Delta\Omega_{ij^*k^*} &= \frac{2\pi}{L_\Omega}(i-1), \\
\Delta\omega_{ij^*k^*} &= \frac{2\pi}{L_\omega}\left[\mathrm{mod}\left(\mathcal{G}_\omega(k^*)-1+S_{\omega\Omega}(i-1), Sym(\mathcal{G}_\omega)\right)-\frac{L_{\omega\Omega}}{L_\Omega}(i-1)\right], \\
\Delta M_{ij^*k^*} &= \frac{2\pi}{L_M}\Bigg[\mathrm{mod}\Big(\mathcal{G}_M(j^*)-1+S_{M\omega}\mathrm{mod}\big(\mathcal{G}_\omega(k^*)-1+ \\
&+ S_{\omega\Omega}(i-1), Sym(\mathcal{G}_\omega)\big)+S_{M\Omega}(i-1), Sym(\mathcal{G}_M)\Big)- \\
&- \frac{L_{M\omega}}{L_\omega}\mathrm{mod}\left(\mathcal{G}_\omega(k^*)-1+S_{\omega\Omega}(i-1), Sym(\mathcal{G}_\omega)\right)- \\
&- \left(\frac{L_{M\Omega}}{L_\Omega}-\frac{L_{M\omega}}{L_\omega}\frac{L_{\omega\Omega}}{L_\Omega}\right)(i-1)\Bigg],
\end{aligned} \tag{3.41}$$

where the values of the shifting parameters $S_{\omega\Omega}$, $S_{M\omega}$ and $S_{M\omega}$ have to fulfill the following relations in order to obtain symmetric configurations:

$$\begin{aligned}
Sym(\mathcal{G}_\omega) \mid S_{\omega\Omega}L_\Omega - L_{\omega\Omega}, \\
Sym(\mathcal{G}_M) \mid S_{M\omega}L_\omega - L_{M\omega}, \\
Sym(\mathcal{G}_M) \mid S_{M\Omega}L_\Omega - (L_{M\Omega} - S_{M\omega}L_{\omega\Omega}).
\end{aligned} \tag{3.42}$$

As it can be seen, the set of Equations (3.41) and (3.42) leads to the 3D Lattice Flower Constellations distributions if no necklace is defined, and to the 2D Lattice Flower Constellations [9] if additionally, no distribution is performed in the argument of perigee. Regarding the 2D Lattice Flower Constellations using necklaces [17], the shifting parameter in the mean anomaly was defined as:

$$Sym(\mathcal{G}) \mid S_{M\Omega}L_\Omega - N_c, \tag{3.43}$$

where $\mathcal{G}$ is a necklace in the mean anomaly and N_c is the configuration number for the 2D Lattice Flower Constellations which corresponds to the $L_{M\Omega}$ parameter in the 3D Lattice Flower Constellations. This relation is equivalent to the last condition in Equation (3.42) when the argument of perigee is not a variable of the configuration, thus, the 3D Necklace Flower Constellations also includes the 2D Lattice Flower Constellations using necklaces.

Therefore, Equations (3.41) and (3.42) constitute the generalization of the necklace theory for the 3D Lattice Flower Constellations, which include all the former Lattice Flower Constellations: 2D Lattice Flower Constellations, 2D Lattice Flower Constellations using necklaces, 3D Lattice Flower Constellations and now 3D Lattice Flower Constellations using necklaces.

In the next section a detailed example is presented in order to show, in a clear manner, the methodology to generate 3D Necklace Flower Constellations.

3.1.2 Example of application

For this example, we assume that a constellation made of 42 satellites is chosen. Let suppose that the constellation is required to be built in 7 orbital planes, thus, $L_\Omega = 7$, and each plane contains two orbits, that is, the number of real orbits per plane is $N_\omega = 2$. Moreover, the number of real satellites per orbit is $N_M = 3$.

Now, an expansion of the search space is done, choosing a fictitious constellation with parameters $L_\omega = 6$ and $L_M = 9$. This means that we are generating two different necklaces, one in the argument of perigee and the other in the mean anomaly. Moreover, as it can be seen, the available positions both in mean anomaly and in the argument of perigee have been trebled, being just the ninth part of all available real positions of satellites in the constellation.

Applying the 3D Necklace Flower Constellations to these parameters, we obtain $|\mathcal{G}_M| = 10$ different necklaces in the mean anomaly and $|\mathcal{G}_\omega| = 3$ in the argument of perigee [19, 40, 41], generating a total of $|\mathcal{G}_M||\mathcal{G}_\omega|L_\Omega^2 L_\omega = 8820$ different symmetrical configurations (compared to the $L_\Omega^2 N_\omega = 98$ configurations obtained using just the 3D Lattice Flower Constellations theory due to the boundaries in the configuration numbers). Note that the number of configurations using necklaces can be increased even further by expanding the fictitious constellation or generating other fictitious constellations.

As there are too many configurations to analyze, we choose, without losing generality, $L_{M\Omega} = 4$, $L_{M\omega} = 3$ and $L_{\omega\Omega} = 6$ as combination numbers of the constellation, and $G_M = \{1, 4, 7\}$ and $G_\omega = \{1, 4\}$ as the necklaces in the mean anomaly and the argument of perigee respectively. Applying the definition of symmetry of a necklace from Equation (1.46), these results are obtained: $Sym(\mathcal{G}_M) = 3$ and $Sym(\mathcal{G}_\omega) = 3$.

With these parameters, we can use Equation (3.35) to obtain the shifting of the argument of perigee with respect to the right ascension of the ascending node:

$$Sym(\mathcal{G}_\omega) \mid S_{\omega\Omega}L_\Omega - L_{\omega\Omega} \quad \Rightarrow \quad 3 \mid 7S_{\omega\Omega} - 6, \tag{3.44}$$

which leads to $S_{\omega\Omega} = 0$. On the other hand, the shifting parameter of the mean anomaly with respect to the argument of perigee can be computed using Equation (3.28):

$$Sym(\mathcal{G}_M) \mid S_{M\omega}L_\omega - L_{M\omega} \quad \Rightarrow \quad 3 \mid 6S_{M\omega} - 3, \tag{3.45}$$

which has three solutions, $S_{M\omega} = 0, 1, 2$. Now, with this result, we apply Equation (3.40) to obtain the shifting parameter of the mean anomaly with respect the right ascension of the ascending node:

$$Sym(\mathcal{G}_M) \mid S_{M\Omega}L_\Omega - (L_{M\Omega} - S_{M\omega}L_{\omega\Omega}) \quad \Rightarrow \quad 3 \mid 7S_{M\Omega} - (4 - 6S_{M\omega}), \tag{3.46}$$

which is $S_{M\Omega} = 1$ no matter the value of $S_{M\omega} = 0, 1, 2$ used. Note that in other examples, different values of $S_{M\omega}$ require different $S_{M\Omega}$.

As it can be seen, three configurations can be generated due to the multiple solutions of $S_{M\omega}$. In particular, we choose $S_{\omega\Omega} = 0$, $S_{M\omega} = 2$ and $S_{M\Omega} = 1$ as the selected configuration. The lattice obtained from this configuration can be seen in Figure 3.1 where the (Ω, ω, M)-space of the distribution selected is shown. The circles represent available positions while the colored ones are the real satellites of the configuration.

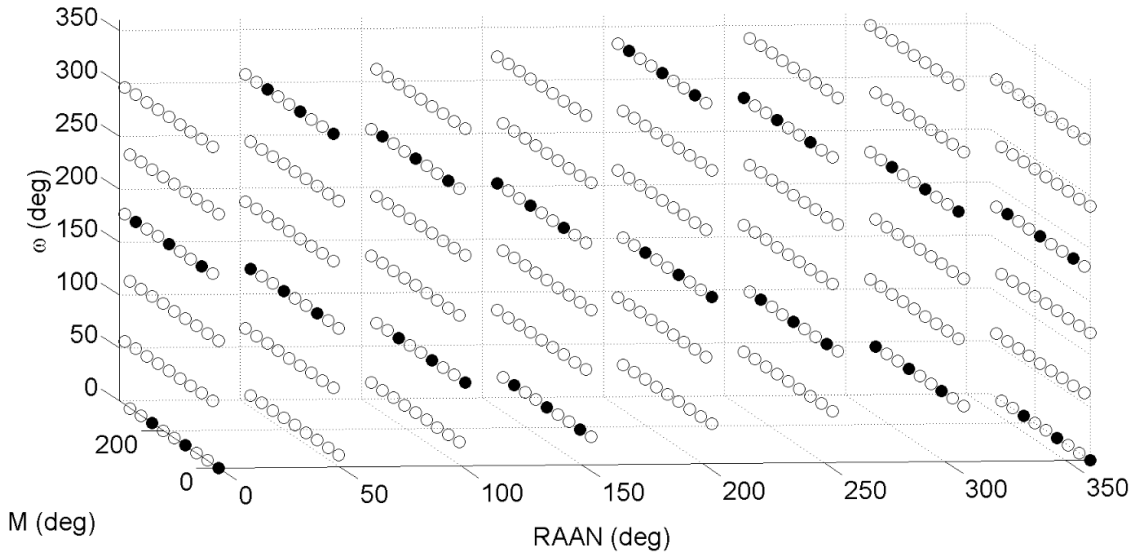

Figure 3.1: (Ω, ω, M)-space representation of the constellation.

Moreover, it is interesting to study the representation of this lattice using tori. This can be observed in Figure 3.2 where the three tori that define the distribution are shown. As it can be seen from Figure 3.1 and Figure 3.2, the distribution is symmetrical in all three orbital parameters: the right ascension of the ascending node, the argument of perigee and the mean anomaly.

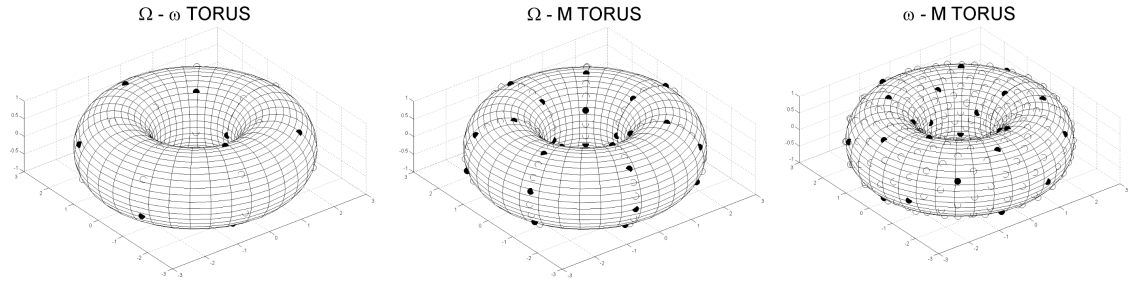

Figure 3.2: Tori representation of the constellation distribution.

Now, this configuration is applied to a satellite constellation. Without losing generality, we choose an eccentricity of $e = 0.3$, an inclination equal to the critical inclination $i = 63.43^o$ and a semi-major axis equal to $a = 12,770\,km$. With these orbital parameters, an inertial configuration as shown in Figure 3.3 is obtained.

This constellation is just an example of the possibilities that the application of necklaces into the 3D lattice flower constellations theory can bring. As it has been said, the number of possibilities can be increased indefinitely, being the only constraint the computational power available.

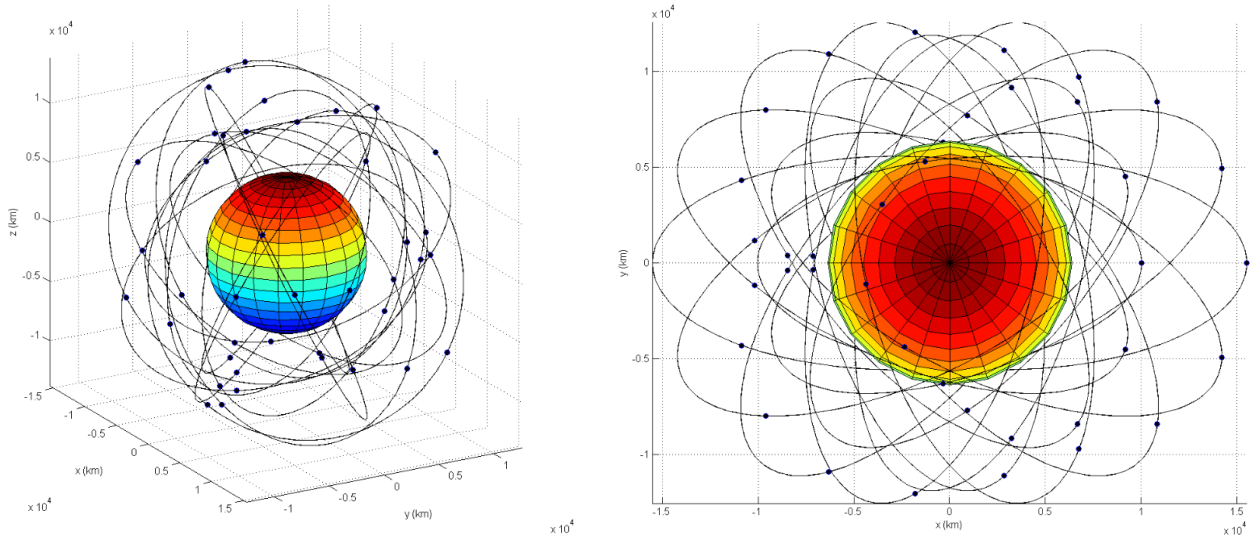

Figure 3.3: Inertial orbits of the constellation.

3.2 Conclusions

3D Lattice Flower Constellations is a powerful tool that allows the generation of constellations with symmetric configurations and minimum parametrization. The distribution obtained with this methodology is fixed to certain positions which is a constraint in the number of possible configurations that the theory can generate.

This chapter introduces the concept of necklaces in the formulation of 3D Lattice Flower Constellations, increasing the number of possible symmetric configurations, being the only limitation the computational power available. This is achieved by an expansion of the searching space of the constellation and applying the necklace to fit the configuration again to the one sought. Moreover, all the configurations obtained by this methodology maintain the properties of the former Lattice Flower Constellations, presenting symmetry in the lattice of the right ascension of the ascending node, the argument of perigee and the mean anomaly of all the satellites in the constellation.

In addition, this new design framework can be used to introduce non uniformities in the distribution while maintaining a structure in the configuration. This is done by defining necklaces adapted to the mission requirements, which provides a powerful tool during the initial constellation design process. Other applications of this methodology include the study of constellation reconfiguration problems, the assessment of satellite failure in a distribution, or the definition of the launching schedule for a constellation made of a large number of satellites.

Furthermore, the 3D Necklace Flower Constellations includes all the former Lattice Flower Constellation designs, being as such, a generalization of the Lattice Flower Constellation theory. This means that the 3D Necklace Flower Constellation theory is able to generate all former configurations (2D, 3D Lattice Flower Constellations and 2D Lattice Flower Constellations using necklaces), and create new distributions using the necklace theory.

Finally, it is important to note that the expansion of the search space can be increased as much as desired, providing more possibilities of design as the size of the fictitious constellation becomes larger. Moreover, as it will be seen in the next chapters, this expansion can also be done in an n-dimensional Lattice, instead of just a 2D or a 3D Lattice, which increases the number of possibilities of design.

Chapter 4

4D Necklace Flower Constellations

Previous 2D and 3D Necklace Flower Constellations were able to perform uniform distributions in the mean anomaly, the right ascension of the ascending node and the argument of perigee, maintaining the rest of the orbital parameters constant in the distribution. This leads to constellations that maintain a fixed structure in their movement and whose satellites share the same period of repetition. However, the ability to distribute satellites uniformly when they present different semi-major axes was still remaining.

This chapter aims to generalize the concepts of lattices and necklaces for a 4D distribution of satellites. In that respect, we introduce as the new variable of design the semi-major axis of the satellites. This allows to bound satellites from very different orbits to create a structure that is continuously changing. However, as it will be seen during this chapter, the constellation still presents internal structures with subsets of satellites that relates to former 2D and 3D distributions. That way, 4D Necklace Flower Constellations can be regarded as a bounding of different Flower Constellations.

In addition, and in order to maintain the configuration over time, a methodology to design these constellations under the J_2 perturbation is introduced. As it will be seen, this effect requires to modify all orbit parameters for every satellite of the constellation. Thus, it is not possible to include a 5D or greater Lattice theory in satellite constellation design, which makes 4D Necklace Flower Constellations the greatest generalization of this constellation theory.

In this chapter we proceed as follows. First, the 4D Lattice Flower Constellation theory is introduced, a further generalization of the 2D and 3D Lattice Flower Constellations where the new variable of design is the semi-major axis of the orbits, and a four by four Hermite Normal Form is used. Second, the effects of the J_2 perturbation are included in the design in order to maintain the structure of the constellation over longer periods of time. Third, the concept of necklace is applied to this kind of design, allowing to expand the search space of possible configurations.

4.1 4D Lattice Flower Constellations

The generation of a 4D Lattice has deeper implications in the formulation compared with the evolution from the 2D Lattice to the 3D Lattice Flower Constellations where the argument of perigee was included in the design. The reason for that lays in two properties. First, the semi-major axis

(a) does not have a modular nature unlike the angles mean anomaly (M), argument of perigee (ω) and right ascension of the ascending node (Ω). This means that the definition of the lattice must be done in a completely different manner. Second, we are seeking constellation structures that are maintained over time, thus, we require that the configuration as a constellation presents periodicity. This new kind of distribution provokes that the structure of the constellation is changing continuously. Nevertheless, over its movement, the constellation maintains the characteristic symmetries of a Lattice Flower Constellation and presents a period of repetition for the whole structure.

In order to generate a lattice in a 4D space, we require four variables. Let $\{V^a, V^\Omega, V^\omega, V^M\}$ be the distribution variables of a lattice where V^a is related to the variation of the semi-major axis, V^Ω is related to the right ascension of the ascending node, V^ω is related to the argument of perigee, and V^M is related to the initial mean anomaly of a satellite of the constellation. It is important to note that $\{V^a, V^\Omega, V^\omega, V^M\}$ do not represent the actual variation of the semi-major axis, the right ascension of the ascending node, the argument of perigee or the initial mean anomaly, instead, this variables define a set of values for each variable that are used in order to generate the distribution of the constellation. In particular, and without losing generality, we define the distribution variables $\{V^a, V^\Omega, V^\omega, V^M\}$ in the range $[0, 1]$. In case other sizes of these variables are required, the resultant space can be modified by terms of an homotopy.

Therefore, a four dimensional lattice can be created using the Hermite Normal Form and a set of distribution parameters $\{r, i, k, j\}$, each one associated with a different dimension of the space. That way, the 4D lattice is defined as:

$$\begin{pmatrix} L_a & 0 & 0 & 0 \\ L_{\Omega a} & L_\Omega & 0 & 0 \\ L_{\omega a} & L_{\omega\Omega} & L_\omega & 0 \\ L_{Ma} & L_{M\Omega} & L_{M\omega} & L_M \end{pmatrix} \begin{pmatrix} V^a_{ijkr} \\ V^\Omega_{ijkr} \\ V^\omega_{ijkr} \\ V^M_{ijkr} \end{pmatrix} = \begin{pmatrix} r \\ i \\ k \\ j \end{pmatrix}; \tag{4.1}$$

where in order to ease notation, we denote L_a to the number of different semi-major axes, L_Ω to the number of orbital planes with the same semi-major axis, L_ω to the number of orbits per plane with the same semi-major axis, and L_M to the number of satellites per orbit. Moreover, and in order to avoid duplicities in the constellation definition, we define the parameters of distribution as $r = \{1, \ldots, L_a\}$, $i = \{1, \ldots, L_\Omega\}$, $k = \{1, \ldots, L_\omega\}$ and $j = \{1, \ldots, L_M\}$ which name each satellite of the constellation. On the other hand, the configuration numbers have these constraints: $L_{\Omega a} \in \{0, \ldots, L_a - 1\}$, $L_{\omega a} \in \{0, \ldots, L_a - 1\}$, $L_{\omega\Omega} \in \{0, \ldots, L_\Omega - 1\}$, $L_{Ma} \in \{0, \ldots, L_a - 1\}$, $L_{M\Omega} \in \{0, \ldots, L_\Omega - 1\}$ and $L_{M\omega} \in \{0, \ldots, L_\omega - 1\}$, for the same reason.

However, as opposed to what happens 2D and 3D Lattice Flower Constellations, Equation (4.1) cannot be used directly to generate the variables of the satellites of the constellation since the semi-major axis does not present modular arithmetic naturally and, in general, it is not constraint in value. Thus, we have to proceed with a 4D lattice in a slightly different manner.

By expanding (4.1), the values of the distribution variables can be obtained:

$$\begin{aligned}
V^a_{ijkr} &= \frac{1}{L_a}r, \\
V^\Omega_{ijkr} &= \frac{1}{L_\Omega}i - \frac{L_{\Omega a}}{L_a L_\Omega}r, \\
V^\omega_{ijkr} &= \frac{1}{L_\omega}k - \frac{L_{\omega\Omega}}{L_\omega L_\Omega}i - \frac{1}{L_\omega}\left(\frac{L_{\omega a}}{L_a} - \frac{L_{\omega\Omega}}{L_\Omega}\frac{L_{\Omega a}}{L_a}\right)r, \\
V^M_{ijkr} &= \frac{1}{L_M}j - \frac{L_{M\omega}}{L_M L_\omega}k - \frac{1}{L_M}\left(\frac{L_{M\Omega}}{L_\Omega} - \frac{L_{M\omega}}{L_\omega}\frac{L_{\omega\Omega}}{L_\Omega}\right)i - \\
&- \frac{1}{L_M}\left(\frac{L_{Ma}}{L_a} - \frac{L_{M\Omega}}{L_\Omega}\frac{L_{\Omega a}}{L_a} - \frac{L_{M\omega}}{L_\omega}\left(\frac{L_{\omega a}}{L_a} - \frac{L_{\Omega a}}{L_a}\frac{L_{\omega\Omega}}{L_\Omega}\right)\right)r,
\end{aligned} \tag{4.2}$$

where, as said before, the distribution variables are subjected to modular arithmetic (modulo 1). Thus, Equation (4.2) can be rewritten as:

$$\begin{aligned}
V^a_{ijkr} &= \mathrm{mod}\left[\frac{1}{L_a}r, 1\right], \\
V^\Omega_{ijkr} &= \mathrm{mod}\left[\frac{1}{L_\Omega}\left(i - \frac{L_{\Omega a}}{L_a}r\right), 1\right], \\
V^\omega_{ijkr} &= \mathrm{mod}\left[\frac{1}{L_\omega}\left(k - \frac{L_{\omega\Omega}}{L_\omega}i - \left(\frac{L_{\omega a}}{L_a} - \frac{L_{\omega\Omega}}{L_\Omega}\frac{L_{\Omega a}}{L_a}\right)r\right), 1\right], \\
V^M_{ijkr} &= \mathrm{mod}\left[\frac{1}{L_M}\left(j - \frac{L_{M\omega}}{L_\omega}k - \left(\frac{L_{M\Omega}}{L_\Omega} - \frac{L_{M\omega}}{L_\omega}\frac{L_{\omega\Omega}}{L_\Omega}\right)i - \right.\right. \\
&- \left.\left.\left(\frac{L_{Ma}}{L_a} - \frac{L_{M\Omega}}{L_\Omega}\frac{L_{\Omega a}}{L_a} - \frac{L_{M\omega}}{L_\omega}\left(\frac{L_{\omega a}}{L_a} - \frac{L_{\Omega a}}{L_a}\frac{L_{\omega\Omega}}{L_\Omega}\right)\right)r\right), 1\right],
\end{aligned} \tag{4.3}$$

where, in order to simplify notation, we denote $\mathrm{mod}[a, b]$ to the value of a under modulo b. Now, we aim to obtain a set of distribution variables based on integer numbers. In order to do that, we multiply the first expression from Equation (4.3) by L_a, the second by $L_a L_\Omega$, the third by $L_a L_\Omega L_\omega$, and the fourth by $L_a L_\Omega L_{\omega M}$, leading to the following set of equations:

$$\begin{aligned}
L_a V^a_{ijkr} &= \mathrm{mod}\left[r, L_a\right], \\
L_\Omega L_a V^\Omega_{ijkr} &= \mathrm{mod}\left[L_a i - L_{\Omega a} r, L_\Omega L_a\right], \\
L_\omega L_\Omega L_a V^\omega_{ijkr} &= \mathrm{mod}\left[L_\Omega L_a k - L_{\omega\Omega} L_a i - \left(L_{\omega a} L_\Omega - L_{\omega\Omega} L_{\Omega a}\right) r, L_\omega L_\Omega L_a\right], \\
L_M L_\omega L_\Omega L_a V^M_{ijkr} &= \mathrm{mod}\left[L_\omega L_\Omega L_a j - L_{M\omega} L_\Omega L_a k - \left(L_{M\Omega} L_\omega L_a - L_{M\omega} L_{\omega\Omega} L_a\right) i - \right. \\
&- \left. \left(L_{Ma} L_\omega L_\Omega - L_{M\Omega} L_{\Omega a} L_\omega - L_{M\omega}\left(L_{\omega a} L_\Omega - L_{\Omega a} L_{\omega\Omega}\right)\right) r, L_M L_\omega L_\Omega L_a\right].
\end{aligned} \tag{4.4}$$

Then, we define a new set of variables $\{\mathcal{N}^a, \mathcal{N}^\Omega, \mathcal{N}^\omega, \mathcal{N}^M\}$ which relate to the original through these expressions:

$$\begin{aligned}
\mathcal{N}^a_{ijkr} &= L_a V^a_{ijkr}, \\
\mathcal{N}^\Omega_{ijkr} &= L_\Omega L_a V^\Omega_{ijkr}, \\
\mathcal{N}^\omega_{ijkr} &= L_\omega L_\Omega L_a V^\omega_{ijkr}, \\
\mathcal{N}^M_{ijkr} &= L_M L_\omega L_\Omega L_a V^M_{ijkr},
\end{aligned} \tag{4.5}$$

and introduced in Equation (4.4), we obtain:

$$\begin{aligned}
\mathcal{N}^a_{ijkr} &= \mathrm{mod}\left[r, L_a\right], \\
\mathcal{N}^\Omega_{ijkr} &= \mathrm{mod}\left[L_a i - L_{\Omega a} r, L_\Omega L_a\right], \\
\mathcal{N}^\omega_{ijkr} &= \mathrm{mod}\left[L_\Omega L_a k - L_{\omega\Omega} L_a i - \left(L_{\omega a} L_\Omega - L_{\omega\Omega} L_{\Omega a}\right) r, L_\omega L_\Omega L_a\right], \\
\mathcal{N}^M_{ijkr} &= \mathrm{mod}\left[L_\omega L_\Omega L_a j - L_{M\omega} L_\Omega L_a k - \left(L_{M\Omega} L_\omega L_a - L_{M\omega} L_{\omega\Omega} L_a\right) i - \right. \\
&- \left. \left(L_{Ma} L_\omega L_\Omega - L_{M\Omega} L_{\Omega a} L_\omega - L_{M\omega}\left(L_{\omega a} L_\Omega - L_{\Omega a} L_{\omega\Omega}\right)\right) r, L_M L_\omega L_\Omega L_a\right], \qquad (4.6)
\end{aligned}$$

where it is easy to derive that $\{\mathcal{N}^a, \mathcal{N}^\Omega, \mathcal{N}^\omega, \mathcal{N}^M\}$ are integer numbers since there are the result of sums and multiplications of integer numbers. We can also derive that these new distribution variables can only present the values shown in the following expressions:

$$\begin{aligned}
\mathcal{N}^a &\in \{1, \ldots, L_a\}, \\
\mathcal{N}^\Omega &\in \{1, \ldots, L_\Omega L_a\}, \\
\mathcal{N}^\omega &\in \{1, \ldots, L_\omega L_\Omega L_a\}, \\
\mathcal{N}^M &\in \{1, \ldots, L_M L_\omega L_\Omega L_a\}, \qquad (4.7)
\end{aligned}$$

which define a set of possible values for each different dimension of the space. This means that we can define given values of the semi-major axis, the right ascension of the ascending node, the argument of perigee, and the initial mean anomaly for the satellites of the constellation to share. For instance, let $L_a L_\Omega = 4$ be the number of different positions in the right ascension of the ascending node, that is, the number of different orbital planes of the constellation. If we relate $\mathcal{N}^\Omega = \{1, 2, 3, 4\}$ to $\Omega_1 = 0^o$, $\Omega_2 = 30^o$, $\Omega_3 = 90^o$ and $\Omega_4 = 180^o$ respectively, we are setting the possible orbital planes in which the satellites of the constellation will be positioned.

4.1.1 Setting the values of the semi-major axes of the constellation

Although the methodology presented in the 4D Lattice Flower Constellations allows to generate any kind of distribution, in most applications it is interesting that the structure of the constellation present some periodic properties, and thus, some constraints must be imposed in the semi-major axis in order to obtain that characteristic.

Let N_p be the number of complete orbits that a satellite requires in order to complete a closed track in a given frame of reference, and let N_d be the number of complete rotations that the frame of reference performs during this time. For instance, if the selected frame of reference is the Earth Fixed (ECEF), N_p and N_d correspond to the number of orbit revolutions and the number of days that a satellite requires to repeat its ground-track. In that respect, it is worth noticing that even if an orbit does not repeat its ground-track in the Earth Fixed, it is possible to find another rotating frame of reference in which it is. Thus, we can define a period of repetition for the whole structure defined as:

$$T_c = N_p T = N_d T_d, \qquad (4.8)$$

where T is the orbital period of each satellite and T_d is the rotating period of the reference frame.

Then, since we want all the satellites to generate a structure that is repeated, we impose that T_c is shared by all the satellites in the constellation. This means that, in general, all the satellites will repeat their motion in N_d revolutions of the rotating frame of reference, while, on the other hand, the number of orbit revolutions that each satellite will require depends on each individual satellite (due to different values of their semi-major axis). Thus, we are free to select the different values of N_p for the constellation, taking into account that N_p must be an integer number.

4.1.2 Introducing the $J2$ perturbation in the formulation

The former formulation considers a keplerian movement where the satellites are only subjected to the main term of the gravitational potential of the primary body. However, for satellites orbiting the Earth, it is very interesting to include the oblateness effect of the Earth (J_2 of the gravitational potential) in the design process of the constellation due to the important effects that this perturbation provokes. In particular, it produces a shifting of the orbital planes and also rotates the orbits inside their plane. This causes the destruction of the initial design of the constellation in very short periods of time, shorter the closer the satellite is to the Earth. For these reasons, we include in the constellation design the effects of the J_2 perturbation.

The secular variations of the classical elements for a satellite orbiting the Earth under the J_2 perturbation are:

$$\begin{aligned}
&\dot{a}_{sec} = 0; \qquad n = \sqrt{\frac{\mu}{a^3}}\left[1 + \frac{3}{4}J_2\left(\frac{R_\oplus}{a(1-e^2)}\right)^2\left(2 - 3\sin^2(i)\right)\sqrt{1-e^2}\right];\\
&\dot{e}_{sec} = 0; \qquad \dot{\omega}_{sec} = \frac{3}{4}J_2\left(\frac{R_\oplus}{a(1-e^2)}\right)^2 n\left(5\cos^2(i) - 1\right);\\
&\dot{i}_{sec} = 0; \qquad \dot{\Omega}_{sec} = -\frac{3}{2}J_2\left(\frac{R_\oplus}{a(1-e^2)}\right)^2 n\cos(i);
\end{aligned} \tag{4.9}$$

where μ and $R_\oplus$ are the gravitational constant and the equatorial radius of the Earth respectively, and n is the mean motion of the satellite. Thus, there are three secular variables that change over time: the right ascension of the ascending node, the argument of perigee and the mean motion. In order to maintain the configuration as a constellation, we require that all the orbital planes shift at the same speed ($\dot{\Omega}_{sec} = \dot{\Omega}_{sec0}$), that the rotations in the orbital plane are performed at the same speed ($\dot{\omega}_{sec} = \dot{\omega}_{sec0}$), and that the period of the orbits is congruent with the repetition period of the whole structure (T_c must be the same for all the satellites of the constellations), that is, there exists a time period when the constellation repeats its dynamic. We denote $\dot{\Omega}_{sec0}$ and $\dot{\omega}_{sec0}$ to the constellation reference for the secular variations of the right ascension of the ascending node and the argument of perigee. On the other hand, and for a given satellite of the constellation, there exists a relation between the different periods:

$$T_c = N_p\frac{2\pi}{n} = N_d T_d. \tag{4.10}$$

Thus, using Equation (4.9) and the former constraints, we obtain:

$$\begin{aligned}\frac{2\pi}{T_d}\frac{N_p}{N_d} &= \sqrt{\frac{\mu}{a^3}}\left[1+\frac{3}{4}J_2\left(\frac{R_\oplus}{a(1-e^2)}\right)^2\left(2-3\sin^2(i)\right)\sqrt{1-e^2}\right],\\ \dot{\omega}_{sec0} &= \frac{3}{4}J_2\left(\frac{R_\oplus}{a(1-e^2)}\right)^2\frac{2\pi}{T_d}\frac{N_p}{N_d}\left(5\cos^2(i)-1\right),\\ \dot{\Omega}_{sec0} &= -\frac{3}{2}J_2\left(\frac{R_\oplus}{a(1-e^2)}\right)^2\frac{2\pi}{T_d}\frac{N_p}{N_d}\cos(i),\end{aligned} \tag{4.11}$$

which is a system of three nonlinear equations with three unknowns (the semi-major axis, the inclination and the eccentricity) for each different value of $\mathcal{N}^a$. From the expressions of $\dot{\omega}_{sec0}$ and $\dot{\Omega}_{sec0}$, we can derive that:

$$\cos(i) = \frac{-\dot{\omega}_{sec0} \pm \sqrt{\dot{\omega}_{sec0}^2 + 5\dot{\Omega}_{sec0}^2}}{5\dot{\Omega}_{sec0}}, \tag{4.12}$$

which means that all the satellites in the constellation have the same inclination (the one of the reference orbit), since $\dot{\omega}_{sec0}$ and $\dot{\Omega}_{sec0}$ are common for the constellation. On the other hand, from the expression in $\dot{\Omega}_{sec0}$ we obtain a relation between the semi-major axis and the eccentricity of the orbit:

$$1-e^2 = \frac{R_\oplus}{a}\sqrt{-\frac{3}{2}\frac{J_2}{\dot{\Omega}_{sec0}}\frac{2\pi}{T_d}\frac{N_p}{N_d}\cos(i)}, \tag{4.13}$$

and we introduce it in the expression of the mean motion, obtaining a nonlinear equation in the semi-major axis:

$$a^{\frac{3}{2}} = \frac{T_d}{2\pi}\frac{N_d}{N_p}\sqrt{\mu}\left[1-\frac{\dot{\Omega}_{sec0}}{4\pi}\frac{T_d N_d}{N_p}\frac{2-3\sin^2(i)}{\cos(i)}\sqrt{\frac{R_\oplus}{a}\sqrt{-\frac{3}{2}\frac{J_2}{\dot{\Omega}_{sec0}}\frac{2\pi}{T_d}\frac{N_p}{N_d}\cos(i)}}\right], \tag{4.14}$$

from where the value of the semi-major axis can be obtained numerically, and then, the value of the eccentricity using Equation (4.13).

This means that all satellites of the constellation that share the same value of $\mathcal{N}^a$ present the same values of semi-major axis, inclination and eccentricity. This is effectively generating a 3D Lattice Flower Constellation inside the 4D configuration. Thus, a 4D Lattice Flower Constellation can also be regarded as a set of 3D Lattice Flower Constellations that present a given relation in their motions provided by Equation (4.8).

Finally, it is important to note that under additional perturbations, the satellites of the constellation will require of orbital maneuvers in order to maintain the configuration defined [22, 16]. This is more important in a 4D Lattice Flower Constellation since the inclination, eccentricity and semi-major axis are in general different for the satellites in the constellation.

4.1.3 Example of application

As an example of application, we consider a constellation made of 54 satellites. This constellation is distributed in 2 different semi-major axes ($L_a = 2$), three orbital planes per each semi-major axis

($L_\Omega = 3$), three orbits per orbital plane and given semi-major axis ($L_\omega = 3$) and three satellites per orbit $L_M = 3$. This defines the size of the constellation and the number of possibilities of design (provided by the different values of the combination numbers). In addition, the satellites of the constellation present the repeating ground-track property, generating a repetition in the dynamic of the constellation each three days ($N_d = 3$).

First, the inclination of the constellation is the critical inclination $i = 63.43^o$, while $e = 0.1$ is the reference eccentricity. The two different values of the semi-major axis and eccentricity are defined in such a way that the two subsets of satellites (each related to a different semi-major axis) perform $N_p = \{8, 6\}$ orbital revolutions respectively in three days and that they maintain the conditions provided by Equation (4.11). This leads to two semi-major axes: 21926 km and 26561 km, and two eccentricities: 0.1 and 0.5406 respectively. On the other hand, we impose that the distribution in the right ascension of the ascending node, the argument of perigee and the mean anomaly follows a uniform distribution, and thus:

$$\Omega_{ijkr} = 2\pi \frac{\mathcal{N}^{\Omega}_{ijkr}}{L_a L_\Omega}; \qquad \omega_{ijkr} = 2\pi \frac{\mathcal{N}^{\omega}_{ijkr}}{L_a L_\Omega L_\omega}; \qquad M_{ijkr} = 2\pi \frac{\mathcal{N}^{M}_{ijkr}}{L_a L_\Omega L_\omega L_M}. \tag{4.15}$$

Then, we select the values of the combination numbers L_{ij}, in particular: $L_{21} = 0$, $L_{32} = 2$, $L_{31} = 1$, $L_{43} = 0$, $L_{42} = 2$ and $L_{41} = 1$; and generate the distribution using Equation (4.6). This configuration can be seen in Figure 4.1, where a tori representation has been selected since it is the most clear manner to represent a 4D space with modular arithmetic. In the figure, all the filled circles represent the projection of the variables of the satellites of the constellation in the tori, thus, each tori contains a different number of points due to the superposition of variables during the projection. Furthermore, it can be observed that all the satellites in the distribution are positioned following closed lines in the tori, which is the graphical representation of the symmetry (or congruence) of the configuration.

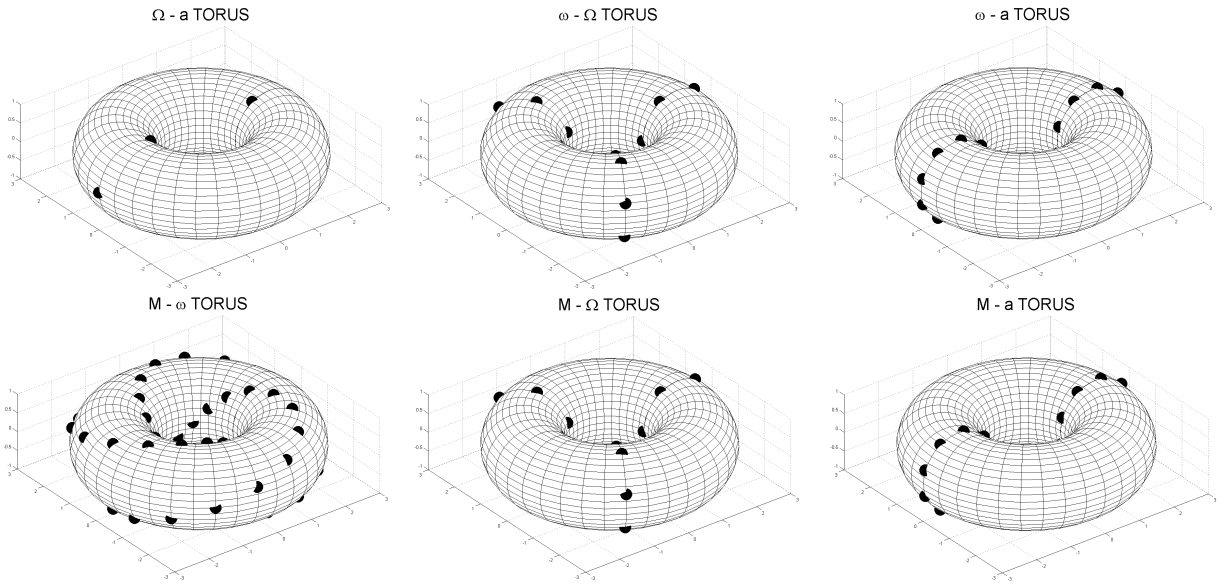

Figure 4.1: Tori representation of the 4D Lattice Flower Constellation.

On the other hand, the initial inertial distribution of the constellation can be observed in Figure 4.2. The most important property of 4D Lattice Flower Constellations, compared to 2D and 3D Lattice Flower Constellations, is that the structure of the constellation is changing continuously due to the dynamic of the system. However, several structures appear in the constellation, some of them are periodic (due to the different semi-major axes) and others are fixed (as in the 2D and 3D Lattice Flower Constellations).

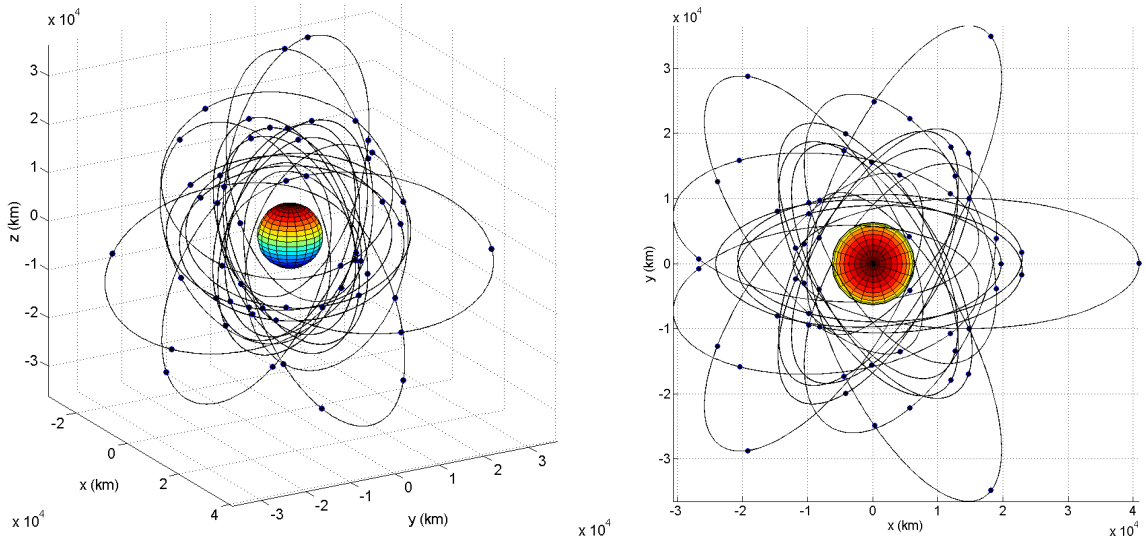

Figure 4.2: Isometric (left) and polar (right) views of the 4D Lattice Flower Constellation.

4.2 4D Necklace Flower Constellations

Once the 4D Lattice Flower Constellation design is introduced, it is time to generalize the theory with the concept of necklaces. A necklace is a subset of elements taken from a set of available positions. In the case of study, the available positions are generated by the definition of a fictitious constellation that has a larger number of satellites than the one that is required to be designed. On the other hand, the elements chosen from these available positions are the real satellites of the constellation. In that respect, we are interested in introducing necklaces in the distribution in such a way that the resultant configurations maintain the properties of uniformity and symmetry from the original theory.

In a 4D Lattice configuration, we can introduce four different necklaces, one per variable in the lattice. However, creating a necklace in the top most variable, that is $\mathcal{N}^a$, is equivalent to remove all the orbits with certain values of the semi-major axis, and thus, it is trivial from a mathematical point of view as well as by using the theory of 4D Lattice Flower Constellations presented in this work. For that reason and in order to simplify the formulation, we only consider necklaces generated in the other three variables.

Let $\mathcal{G}_\Omega$, $\mathcal{G}_\omega$ and $\mathcal{G}_M$ be a set of necklaces defined in the variables considered in the distribution, in particular, the right ascension of the ascending node, the argument of perigee and the mean

anomaly respectively. A necklace $\mathcal{G}$ is a subset of elements taken from a set of available positions presented in each dimension, that is:

$$\begin{aligned} \mathcal{G}_\Omega &\subseteq \{1,\dots,L_\Omega\}, \\ \mathcal{G}_\omega &\subseteq \{1,\dots,L_\omega\}, \\ \mathcal{G}_M &\subseteq \{1,\dots,L_M\}, \end{aligned} \tag{4.16}$$

such that $|\mathcal{G}_\Omega| = N_\Omega$ is the number of elements in the necklace $\mathcal{G}_\Omega$, $|\mathcal{G}_\omega| = N_\omega$ are the number of elements in $\mathcal{G}_\omega$, and $|\mathcal{G}_M| = N_M$ are the number of elements in $\mathcal{G}_M$. In addition, and in order to simplify the notation used, we assume that:

$$\begin{aligned} \mathcal{G}_\Omega &= \{\mathcal{G}_\Omega(1),\dots,\mathcal{G}_\Omega(i^*),\dots,\mathcal{G}_\Omega(N_\Omega)\}, \\ \mathcal{G}_\omega &= \{\mathcal{G}_\omega(1),\dots,\mathcal{G}_\omega(k^*),\dots,\mathcal{G}_\omega(N_\omega)\}, \\ \mathcal{G}_M &= \{\mathcal{G}_M(1),\dots,\mathcal{G}_M(j^*),\dots,\mathcal{G}_M(N_M)\}, \end{aligned} \tag{4.17}$$

with:

$$\begin{aligned} 1 \le \mathcal{G}_\Omega(1) < \cdots < \mathcal{G}_\Omega(i^*) < \cdots < \mathcal{G}_\Omega(N_\Omega) \le L_\Omega, \\ 1 \le \mathcal{G}_\omega(1) < \cdots < \mathcal{G}_\omega(k^*) < \cdots < \mathcal{G}_\omega(N_\omega) \le L_\omega, \\ 1 \le \mathcal{G}_M(1) < \cdots < \mathcal{G}_M(j^*) < \cdots < \mathcal{G}_M(N_M) \le L_M, \end{aligned} \tag{4.18}$$

where the indexes i^*, k^* and j^* name each element of their respective necklaces $\mathcal{G}_\Omega$, $\mathcal{G}_\omega$ and $\mathcal{G}_M$. This allows to interpret necklaces as injective functions between the elements of the necklace and the available positions in the space:

$$\begin{aligned} \mathcal{G}: \quad \mathbb{Z}_{L_a} \times \mathbb{Z}_{N_\Omega} \times \mathbb{Z}_{N_\omega} \times \mathbb{Z}_{N_M} &\longrightarrow \mathbb{Z}_{L_a} \times \mathbb{Z}_{L_\Omega} \times \mathbb{Z}_{L_\omega} \times \mathbb{Z}_{L_M} \\ (r, i^*, k^*, j^*) &\longmapsto (r, \mathcal{G}_\Omega(i^*), \mathcal{G}_\omega(k^*), \mathcal{G}_M(j^*)). \end{aligned} \tag{4.19}$$

Thus, it makes sense to refer to $\mathcal{G}$, where the integer parameters $i^* \in \{1,\dots,N_\Omega\}$, $k^* \in \{1,\dots,N_\omega\}$ and $j^* \in \{1,\dots,N_M\}$ represent the different elements inside the necklaces defined. In addition, we define the shifting parameters $S_{\Omega r}$, $S_{\omega r}$, $S_{\omega\Omega}$, S_{Mr}, $S_{M\Omega}$ and $S_{M\omega}$ as degrees of freedom that the necklaces present relative to the movement in other dimensions. Thus, the relation between the positions in the fictitious constellation and the ones in the necklaces is provided by:

$$\begin{aligned} i &= \mathcal{G}_\Omega(i^*) + S_{\Omega r} r, \\ k &= \mathcal{G}_\omega(k^*) + S_{\omega r} r + S_{\omega\Omega} i, \\ j &= \mathcal{G}_M(j^*) + S_{Mr} r + S_{M\Omega} i + S_{M\omega} k. \end{aligned} \tag{4.20}$$

However, necklaces also present an internal structure that alters slightly the modular arithmetic inside them, since there are some rotations that allows to obtain the same distribution and not just a complete rotation of the configuration. We define symmetry of a necklace ($Sym(\mathcal{G})$) to the minimum rotation that must be performed in a necklace in order to obtain the same configuration[19, 20, 37]. In other words:

$$Sym(\mathcal{G}) = \min\{1 \le r \le n : \mathcal{G} + r \equiv \mathcal{G}\}. \tag{4.21}$$

Thus, introducing the concept of symmetry of the necklace in Equation (4.20), we obtain:

$$\begin{aligned} i &= \mod[\mathcal{G}_\Omega(i^*) + S_{\Omega r} r, Sym(\mathcal{G}_\Omega)], \\ k &= \mod[\mathcal{G}_\omega(k^*) + S_{\omega r} r + S_{\omega\Omega} i, Sym(\mathcal{G}_\omega)], \\ j &= \mod[\mathcal{G}_M(j^*) + S_{Mr} r + S_{M\Omega} i + S_{M\omega} k, Sym(\mathcal{G}_M)]. \end{aligned} \tag{4.22}$$

It is important to note that since the shifting parameters are subjected to the modular arithmetic of their respective necklaces, we can impose the following constraints in order to avoid duplicities in the formulation:

$$\begin{aligned} S_{\Omega r} &\in \{0,\dots,Sym(\mathcal{G}_\Omega)-1\},\\ S_{\omega r}, S_{\omega\Omega} &\in \{0,\dots,Sym(\mathcal{G}_\omega)-1\},\\ S_{Mr}, S_{M\Omega}, S_{M\omega} &\in \{0,\dots,Sym(\mathcal{G}_M)-1\}. \end{aligned} \tag{4.23}$$

On the other hand, the expressions of the distribution parameters i and k from Equation (4.22) can be substituted in the equations of j and k, obtaining:

$$\begin{aligned} i &= \mathrm{mod}\left[\mathcal{G}_\Omega(i^*)+S_{\Omega r}r, Sym(\mathcal{G}_\Omega)\right],\\ k &= \mathrm{mod}\left[\mathcal{G}_\omega(k^*)+S_{\omega r}r+S_{\omega\Omega}\mathrm{mod}\left[\mathcal{G}_\Omega(i^*)+S_{\Omega r}r, Sym(\mathcal{G}_\Omega)\right], Sym(\mathcal{G}_\omega)\right],\\ j &= \mathrm{mod}\left[\mathcal{G}_M(j^*)+S_{Mr}r+S_{M\Omega}\mathrm{mod}\left[\mathcal{G}_\Omega(i^*)+S_{\Omega r}r, Sym(\mathcal{G}_\Omega)\right]+\right.\\ &+ \left. S_{M\omega}\mathrm{mod}\left[\mathcal{G}_\omega(k^*)+S_{\omega r}r+\right.\right.\\ &+ \left.\left. S_{\omega\Omega}\mathrm{mod}\left[\mathcal{G}_\Omega(i^*)+S_{\Omega r}r, Sym(\mathcal{G}_\Omega)\right], Sym(\mathcal{G}_\omega)\right], Sym(\mathcal{G}_M)\right], \end{aligned} \tag{4.24}$$

which can be introduced in the original lattice of the distribution given by Equation (4.6), leading to the following expression of the lattice including necklaces in its formulation:

$$\begin{aligned} \mathcal{N}^a_{i^*j^*k^*r} &= \mathrm{mod}\left[r, L_a\right],\\ \mathcal{N}^\Omega_{i^*j^*k^*r} &= \mathrm{mod}\left[L_a\mathrm{mod}\left[\mathcal{G}_\Omega(i^*)+S_{\Omega r}r, Sym(\mathcal{G}_\Omega)\right]-L_{\Omega a}r, L_\Omega L_a\right],\\ \mathcal{N}^\omega_{i^*j^*k^*r} &= \mathrm{mod}\left[L_\Omega L_a\mathrm{mod}\left[\mathcal{G}_\omega(k^*)+S_{\omega r}r+S_{\omega\Omega}\mathrm{mod}\left[\mathcal{G}_\Omega(i^*)+\right.\right.\right.\\ &+ \left.\left.\left. S_{\Omega r}r, Sym(\mathcal{G}_\Omega)\right], Sym(\mathcal{G}_\omega)\right]-L_{\omega\Omega}L_a\mathrm{mod}\left[\mathcal{G}_\Omega(i^*)+\right.\\ &+ \left. S_{\Omega r}r, Sym(\mathcal{G}_\Omega)\right]-\left(L_{\omega a}L_\Omega-L_{\omega\Omega}L_{\Omega a}\right)r, L_\omega L_\Omega L_a\right],\\ \mathcal{N}^M_{i^*j^*k^*r} &= \mathrm{mod}\left[L_\omega L_\Omega L_a\mathrm{mod}\left[\mathcal{G}_M(j^*)+S_{Mr}r+S_{M\Omega}\mathrm{mod}\left[\mathcal{G}_\Omega(i^*)+\right.\right.\right.\\ &+ \left.\left.\left. S_{\Omega r}r, Sym(\mathcal{G}_\Omega)\right]+S_{M\omega}\mathrm{mod}\left[\mathcal{G}_\omega(k^*)+S_{\omega r}r+\right.\right.\\ &+ \left.\left. S_{\omega\Omega}\mathrm{mod}\left[\mathcal{G}_\Omega(i^*)+S_{\Omega r}r, Sym(\mathcal{G}_\Omega)\right], Sym(\mathcal{G}_\omega)\right], Sym(\mathcal{G}_M)\right]-\\ &- L_{M\omega}L_\Omega L_a\mathrm{mod}\left[\mathcal{G}_\omega(k^*)+S_{\omega r}r+S_{\omega\Omega}\mathrm{mod}\left[\mathcal{G}_\Omega(i^*)+\right.\right.\\ &+ \left.\left. S_{\Omega r}r, Sym(\mathcal{G}_\Omega)\right], Sym(\mathcal{G}_\omega)\right]-\\ &- \left(L_{M\Omega}L_\omega L_a-L_{M\omega}L_{\omega\Omega}L_a\right)\mathrm{mod}\left[\mathcal{G}_\Omega(i^*)+S_{\Omega r}r, Sym(\mathcal{G}_\Omega)\right]-\\ &- \left(L_{Ma}L_\omega L_\Omega-L_{M\Omega}L_{\Omega a}L_\omega-\right.\\ &- \left. L_{M\omega}\left(L_{\omega a}L_\Omega-L_{\Omega a}L_{\omega\Omega}\right)\right)r, L_M L_\omega L_\Omega L_a\right]. \end{aligned} \tag{4.25}$$

Equation (4.25) allows to define any lattice configuration based on fixed necklaces that performs uniform distributions in a given space. However, since the space considered is also subjected to modular arithmetic, we are specially interested in the configurations where a complete rotation in the available positions in any dimension generates the same configuration, that is, the structure generated is independent of rotations in the distribution variables. This implies that each satellite of the constellation observes an equivalent configuration with respect to the rest of the satellites of the constellation. In addition, this condition allows to define constellations that maintain the original properties of uniformity and symmetry from the original Lattice Flower Constellations.

Mathematically, the condition of symmetry must be fulfilled in every variable under the rotation of any dimension, that is:

$$\begin{aligned}
\left(\mathcal{N}^a_{i^*j^*k^*(r+L_a)}, \mathcal{N}^\Omega_{i^*j^*k^*(r+L_a)}, \mathcal{N}^\omega_{i^*j^*k^*(r+L_a)}, \mathcal{N}^M_{i^*j^*k^*(r+L_a)}\right) = \\
= \left(\mathcal{N}^a_{i^*j^*k^*r}, \mathcal{N}^\Omega_{i^*j^*k^*r}, \mathcal{N}^\omega_{i^*j^*k^*r}, \mathcal{N}^M_{i^*j^*k^*r}\right), \\
\left(\mathcal{N}^a_{(i^*+N_\Omega)j^*k^*r}, \mathcal{N}^\Omega_{(i^*+N_\Omega)j^*k^*r}, \mathcal{N}^\omega_{(i^*+N_\Omega)j^*k^*r}, \mathcal{N}^M_{(i^*+N_\Omega)j^*k^*r}\right) = \\
= \left(\mathcal{N}^a_{i^*j^*k^*r}, \mathcal{N}^\Omega_{i^*j^*k^*r}, \mathcal{N}^\omega_{i^*j^*k^*r}, \mathcal{N}^M_{i^*j^*k^*r}\right), \\
\left(\mathcal{N}^a_{i^*j^*(k^*+N_\omega)r}, \mathcal{N}^\Omega_{i^*j^*(k^*+N_\omega)r}, \mathcal{N}^\omega_{i^*j^*(k^*+N_\omega)r}, \mathcal{N}^M_{i^*j^*(k^*+N_\omega)r}\right) = \\
= \left(\mathcal{N}^a_{i^*j^*k^*r}, \mathcal{N}^\Omega_{i^*j^*k^*r}, \mathcal{N}^\omega_{i^*j^*k^*r}, \mathcal{N}^M_{i^*j^*k^*r}\right), \\
\left(\mathcal{N}^a_{i^*(j^*+N_M)k^*r}, \mathcal{N}^\Omega_{i^*(j^*+N_M)k^*r}, \mathcal{N}^\omega_{i^*(j^*+N_M)k^*r}, \mathcal{N}^M_{i^*(j^*+N_M)k^*r}\right) = \\
= \left(\mathcal{N}^a_{i^*j^*k^*r}, \mathcal{N}^\Omega_{i^*j^*k^*r}, \mathcal{N}^\omega_{i^*j^*k^*r}, \mathcal{N}^M_{i^*j^*k^*r}\right),
\end{aligned} \tag{4.26}$$

for a complete rotation in the right ascension of the ascending node, the argument of perigee and the mean anomaly respectively. Note that a complete rotation in the set of available positions in one variable is equivalent to a complete rotation in the elements inside the necklaces.

Then, by applying the conditions from Equation (4.26) to the distribution given by Equation (4.25), we obtain the following relations (see References [19, 20, 21] and Chapters 2 and 3 for a more detailed insight on this process):

$$\begin{aligned}
Sym(\mathcal{G}_\Omega) &\mid S_{\Omega r}L_r - L_{\Omega r}, \\
Sym(\mathcal{G}_\omega) &\mid S_{\omega\Omega}L_\Omega - L_{\omega\Omega}, \\
Sym(\mathcal{G}_\omega) &\mid S_{\omega r}L_r - \left(L_{\omega r} - S_{\omega\Omega}L_{\Omega r}\right), \\
Sym(\mathcal{G}_M) &\mid S_{M\omega}L_\omega - L_{M\omega}, \\
Sym(\mathcal{G}_M) &\mid S_{M\Omega}L_\Omega - \left(L_{M\Omega} - S_{M\omega}L_{\omega\Omega}\right), \\
Sym(\mathcal{G}_M) &\mid S_{Mr}L_r - \left(L_{Mr} - S_{M\Omega}L_{\Omega r} - S_{M\omega}L_{\omega r}\right),
\end{aligned} \tag{4.27}$$

which represent the constraints that the shifting parameters have to fulfill in order to obtain symmetric configurations.

It is important to note that both the variables and the shifting parameters present a hierarchy (clearly seen in Equations (4.25) and (4.27)), where a variable higher in the hierarchy is able to influence a higher number of variables while having a lower number of dependencies with the rest of variables. For instance, a variation in the semi-major axis of a satellite (the variable in the top most position of the hierarchy) modify the distribution of any other variable, while, on the other hand, a variation in the mean anomaly (the lowest variable in the hierarchy) does not influence the others. Thus, by using this property it is possible to alter the constellation distribution by just performing a change in the order of the hierarchy presented in this manuscript. In that regard, we selected the hierarchy $a > \Omega > \omega > M$ to decrease the number of different orbits, and thus, the number of launches to build the constellation in orbit.

4.2.1 Example of application

In order to maintain the example as simple as possible, we take as the fictitious constellation, the configuration presented in Section 4.1.3, where now, instead of occupying all the available positions generated in that distribution, a necklace is introduced. In particular, we only introduce one necklace in the mean anomaly corresponding to $\mathcal{G}_M = \{1\}$, which means that only one satellite in each orbit is selected ($N_M = 1$). This could represent, for example, an incomplete constellation that is being built in orbit, where, in order to provide functionality to the constellation, we are interested that all the orbits are occupied by at least one satellite while still requiring a distribution as uniform as possible.

Since the constellation has a complete configuration in the right ascension of the ascending node and the argument of perigee, their respective necklaces are $\mathcal{G}_\omega = \{1, 2, 3\}$ and $\mathcal{G}_\omega = \{1, 2, 3\}$. Then using Equation (4.21) we derive that the symmetry of the necklaces are $Sym(\mathcal{G}_M) = 3$, . Moreover, from the application of the first condition from Equation (4.27) we obtain:

$$1|2S_{\Omega r} - 0, \tag{4.28}$$

where $S_{\Omega r} = 0$ in order to fulfill the expression; from the second condition:

$$1|3S_{\omega\Omega} - 2, \tag{4.29}$$

$S_{\omega\Omega} = 0$; from the third condition:

$$1|2S_{\omega r} - (1 - 0)\,, \tag{4.30}$$

$S_{\omega r} = 0$; and from the fourth condition:

$$3|3S_{M\omega} - 0, \tag{4.31}$$

$S_{M\omega} = 0, 1, 2$. This means that we have three possible values of the shifting parameter. However, if we apply the fifth condition:

$$3|3S_{M\Omega} - (2 - 2S_{M\omega})\,, \tag{4.32}$$

we can derive that there exist solution if and only if $S_{M\omega} = 1$. In that case $S_{M\Omega} = 0, 1, 2$. Finally, from the sixth condition:

$$3|2S_{Mr} - (1 - 0 - 1)\,, \tag{4.33}$$

$S_{Mr} = 0$ no matter the value of $S_{M\Omega}$ used. Thus, we have no constraint to select the value of $S_{M\Omega}$ from $S_{M\Omega} = 0, 1, 2$. For the purpose of this example, we take $S_{M\Omega} = 2$ as the shifting parameter for the constellation.

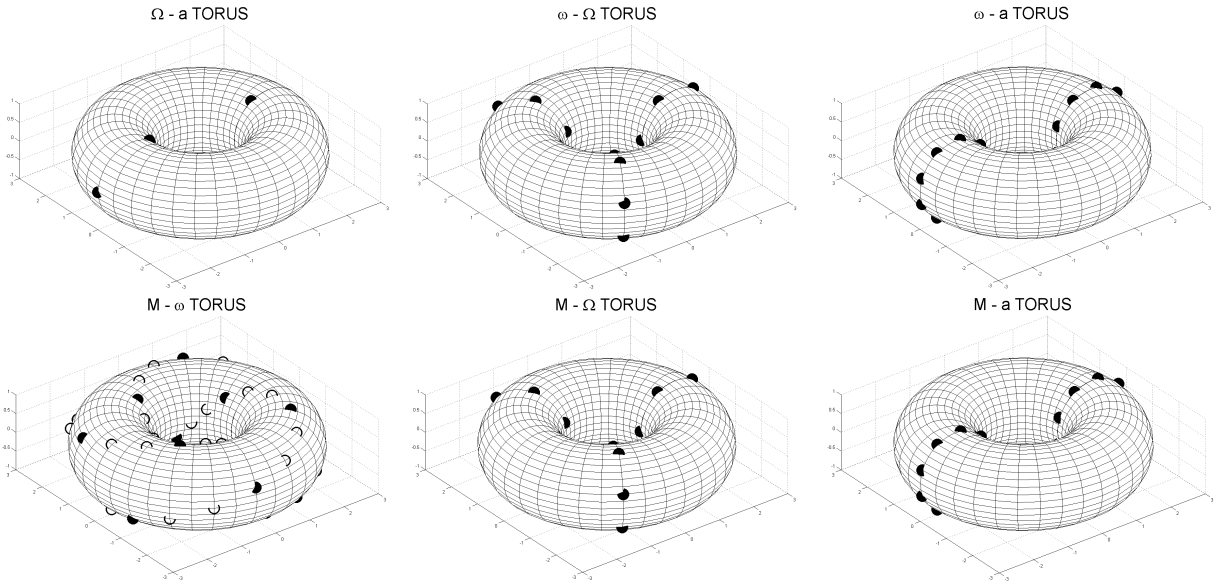

Figure 4.3: Tori representation of the 4D Necklace Flower Constellation.

Figure 4.3 shows the tori representation of the constellation where the satellites are represented with filled circles and the available positions with emptied circumferences. In this figure, it can be observed that all the tori are identical to Figure 4.1 except for the $M - \omega$ torus where the effects of the necklace can be observed. As it can be seen in that torus, the property of symmetry is maintained (the distribution is still congruent), presenting a uniform configuration in the available positions. Moreover, it is worth noting that although the effect of the necklace are only observed in the $M - \omega$ torus, the tori in $M - \Omega$ and $M - r$ are also being affected. However, due to the fact that this representation is just a projection of a 4D space, the holes in the configurations are covered by other satellites of the distribution.

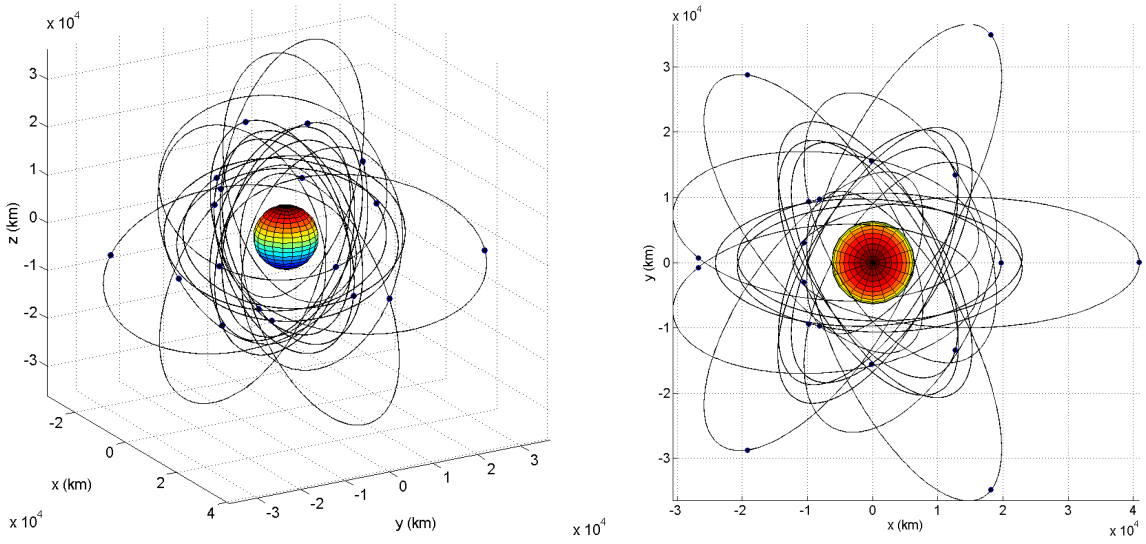

Figure 4.4: Isometric (left) and polar (right) views of the 4D Necklace Flower Constellation.

The inertial distribution of the constellation can be seen in Figure 4.4. Compared with Figure 4.2 it can be observed that the inertial orbits in both constellations are the same, having the constellation in this example only one satellite in each orbit. In addition, from the polar view of Figure 4.4 we can see that there is a symmetry in the $x - z$ plane in this projection, which is a property that has been maintained from the original distribution of Figure 4.2

4.3 4D Necklace Flower Constellations as a generalization of all possible Lattice Flower Constellations

4D Necklace Flower Constellations contains as a subset all the former Lattice and Necklace Flower Constellations, namely, the 2D Lattice Flower Constellations, the 3D Lattice Flower Constellations, the 2D Necklace Flower Constellations and the 3D Necklace Flower Constellations. From Equations (4.25) and (4.27), if we impose that $L_a = 1$, we obtain a 3D Necklace Flower Constellation. If, in addition, we impose $L_\omega = 1$, 2D Necklace Flower Constellations are generated. Finally, if we impose that all the necklaces occupy all the available positions, the symmetries of all necklaces are equal to one and all the shifting parameters are zero, thus, leading to their Lattice Flower Constellations counterparts.

Moreover, since the formulation now is not constraint by uniform distributions (since we can define the positions in each dimension freely) the 4D Necklace Flower Constellation methodology provides a larger number of possibilities of design. The ability to define such non uniform distributions is also possible using necklaces properly, however, being able to define the positions that are more interesting directly simplifies the constellation design process and simplifies the possibilities of design.

4.4 Conclusion

This chapter introduces the 4D Lattice and Necklace Flower Constellations as new frameworks in satellite constellation design. In that respect, these 4D methodologies allow to expand the possibilities of design of the former 2D and 3D Lattice Flower Constellations. This is done by introducing a new variable of distribution, the semi-major axis, and modifying the manner in which the possible configurations are defined, which allows more freedom in the design.

The most important characteristic of 4D Lattice and Necklace Flower Constellations is that the general structure of the constellation is continuously changing, presenting a period of repetition during its dynamic. Nevertheless, inside this configuration, there are substructures that can be appreciated, which correspond to internal 2D and 3D Necklace Flower Constellations. This provides a tool to bound several Lattice Flower Constellations.

The present chapter also introduces necklaces in the formulation, which allows to generate a fictitious constellation, that has more satellites than the constellation that we want to design, and select from it a subset of satellites in such a way that the properties of uniformity and symmetry are maintained in the configuration. This allows to increase the number of possibilities in design, as they are proportional to the number of satellites in the fictitious constellation generated. With

this technique, constellations with a small number of satellites can provide the same number of possibilities in design that constellations composed by a bigger number of satellites.

Finally, the effects of the J_2 perturbation are considered with the final purpose of maintaining the initial design configuration for longer periods of time. We include the effects of the J_2 perturbation by a modification in the mean values of the eccentricity and semi-major axis of the orbits of each satellite so that the compatibility condition in the rotating frame of reference is maintained under this perturbation. Following that procedure, it is possible to maintain not only the configuration, but also the symmetries of the constellation, requiring a fewer amount of fuel in order to perform the relative station keeping of the constellation.

Chapter 5

n-Dimensional congruent lattices using necklaces

The formulation to generate uniform distributions of satellites in several variables was introduced in the 2D, 3D and 4D Necklace Flower Constellations chapters. However, as we pointed out, 4D Necklace Flower Constellations is the greatest generalization that the theory can provide for satellite constellation design. However, the necklace methodology introduced in these designs can be applied to any problem that relates with uniform distribution of elements in a given space. For this reason, the generalization of the necklace lattice theory for n dimensions is introduced in this chapter.

Necklaces in n-dimensional lattices provides a powerful tool to generate uniform distributions in a modular space of any dimension, maintaining the properties of uniformity, symmetry and congruence in the resultant configurations. In addition, the theory presented in this chapter represents the generalization of the methodology introduced in the 2D, 3D and 4D Necklace Flower Constellations, making the formulation more compact and robust. In that respect, this chapter deals also with the problem of existence and uniqueness of the configurations obtained, providing the set of constraints that the parameters of the distribution must fulfill in order to avoid duplicities in the formulation.

In addition, some counting theorems are introduced that allow to count the number of different possibilities in design that this theory can provide under different conditions. As such, it represents a generalization of the theorems presented in the 2D Necklace Flower Constellations.

This chapter contains two different parts. In the first part, we introduce the definition of congruent lattice and study its properties. This allows to generate uniform lattices in a n-dimensional modular space. Second, the concept of necklace is introduced in the formulation, providing a methodology to select subsets of elements from the original congruent lattice, while maintaining the congruence property in the selection.

5.1 n-Dimensional congruent lattice distribution

The objective of this section is to generate a uniform distribution of points in a n-dimensional space that is subjected to modular arithmetic. This implies three important consequences. First, due to the modular arithmetic affecting the n-dimensional space, such space can be regarded as a $(n-1)$-dimensional torus in a n-dimensional space. Second, since points cannot be split, there

are an integer number of them that are distributed in the space considered. Third, the locations of these points are defined using coordinates in the space, which means that, in order to locate a point, n real numbers are required, being n the number of dimensions of the space. Thus, a relation between a set of integers and the real space must be defined, that is, a lattice.

Let n be the number of dimensions of a space where a congruent lattice is required to be generated. The lattice is defined as an application between $\mathbb{Z}^n$ and $\mathbb{R}^n$:

$$\begin{array}{rccc} \mathrm{T1}: & \mathbb{Z}^n & \longrightarrow & \mathbb{R}^n \\ & \boldsymbol{k} & \longmapsto & \boldsymbol{V} \end{array}, \tag{5.1}$$

where $\boldsymbol{k}$ names each point of the distribution, and $\boldsymbol{V}$ locates it in the space considered, that is, it is the set of coordinates of each point of the distribution. In particular, k_i represents the position number of the point in the dimension $i \in \mathbb{Z}_n$, while V_i is the distribution variable considered to range between $[0, 1]$ due to the modular arithmetic of the space. Note that spaces with other sizes can be obtained by an homotopy of the space studied.

Let $i = 1, \ldots, n$ be an integer parameter that names each of the dimensions of the space, where $\{V_i \in \boldsymbol{V} \mid V_i \in [0, 1]\}$ is the distribution variable in the dimension i of the space, and $\{k_i \in \boldsymbol{k} \mid k_i \in \mathbb{Z}\}$ is the distribution parameter on each dimension. In addition, let L_{ii} be the number of different values of V_i provided that $\{k_j \mid j \neq i\}$ are fixed, in other words, L_{ii} is the number of available positions in the dimension i. This means that, since k_i names a particular position in the space, only L_{ii} different values of k_i generate different configurations.

Definition 1. Two lattice configurations are equivalent if they represent the same points in the space. This means that the set of points defined by $\{\boldsymbol{V}(\boldsymbol{k})\}$ is the same as $\{\boldsymbol{V}^*(\boldsymbol{k}^*)\}$, where $\{\boldsymbol{V}(\boldsymbol{k})\}$ and $\{\boldsymbol{V}^*(\boldsymbol{k}^*)\}$ are two different distribution. This definition is represented as:

$$\{\boldsymbol{V}^*(\boldsymbol{k}^*)\} = \{\boldsymbol{V}(\boldsymbol{k})\}. \tag{5.2}$$

However, an in order to simplify notation, we refer to two equivalent configurations as:

$$\boldsymbol{V}^*(\boldsymbol{k}^*) \cong \boldsymbol{V}(\boldsymbol{k}), \tag{5.3}$$

for the whole distribution, or:

$$V_i^*(\boldsymbol{k}^*) \cong V_i(\boldsymbol{k}), \tag{5.4}$$

with $i \in \{1, \ldots, n\}$, for each particular dimension of the configuration.

Definition 2. A congruent lattice $\boldsymbol{V}(\boldsymbol{k})$ is defined as a lattice where:

$$\begin{aligned} & V_i(\{1, \ldots, k_{m-1}, k_m, k_{m+1}, \ldots, k_n\}) \cong \\ \cong \; & V_i(\{1, \ldots, k_{m-1}, k_m + L_{mm}, k_{m+1}, \ldots, k_n\}) \quad \forall\, i, m \in \{1, 2, \ldots, n\}, \end{aligned} \tag{5.5}$$

which means that a complete rotation in one of the dimensions of the space of configuration generates an equivalent distribution. In that respect, it is worth noticing that even if two distributions are equivalent, each point can be defined with a different combination of the values of $\boldsymbol{k}$. In addition, and in order to ease the notation, from now on we will refer to this condition as:

$$V_i(k_m) \cong V_i(k_m + L_{mm}). \tag{5.6}$$

Theorem 4. *Given a Hermite Normal Form L_{ij} of size $n \times n$, a congruent lattice in a n-dimensional space can be described as:*

$$V_i = mod\left[\frac{1}{L_{ii}}\left(k_i - \sum_{j=1}^{i-1}(L_{ij}V_j)\right), 1\right], \tag{5.7}$$

where $mod(a, b)$ is the modulo in base b of a, and L_{ij} are the elements of the Hermite Normal Form associated with the distribution.

Proof. A lattice between $\mathbb{Z}^n$ and $\mathbb{R}^n$ can be defined as an isomorphism:

$$\begin{array}{rccc} \text{T2}: & \mathbb{Z}^n & \longrightarrow & \mathbb{R}^n \\ & \{\alpha_1, \ldots, \alpha_i, \ldots, \alpha_n\} & \longmapsto & \{V_1, \ldots, V_i, \ldots, V_n\} \end{array}, \tag{5.8}$$

which, in general, can be represented by a system of n independent equations:

$$\begin{pmatrix} P_{1,1} & P_{1,2} & \cdots & P_{1,n} \\ P_{2,1} & P_{2,2} & \cdots & P_{2,n} \\ \vdots & \vdots & \ddots & \vdots \\ P_{n,1} & P_{n,2} & \cdots & P_{n,n} \end{pmatrix} \begin{pmatrix} V_1 \\ V_2 \\ \vdots \\ V_n \end{pmatrix} = \begin{pmatrix} \alpha_1 \\ \alpha_2 \\ \vdots \\ \alpha_n \end{pmatrix}, \tag{5.9}$$

where $P_{i,j}$ are a set of integers, and the values of V_i can be obtained by an inversion of the matrix (since it is non singular). However, Equation (5.9) can produce the same distributions with different combinations of the values of $P_{i,j}$ and α_i. For this reason, the Hermite Normal Form [42] is introduced in order to avoid these duplicities in the formulation.

By performing row operations in Equation (5.9), the Hermite Normal Form of the system is obtained [43], that is, a system expressed by a lower triangular matrix:

$$\begin{pmatrix} L_{1,1} & 0 & 0 & \cdots & 0 \\ L_{2,1} & L_{2,2} & 0 & \cdots & 0 \\ \vdots & \vdots & \ddots & \ddots & \vdots \\ L_{n-1,1} & L_{n-1,2} & \cdots & L_{n-1,n-1} & 0 \\ L_{n,1} & L_{n,2} & \cdots & \cdots & L_{n,n} \end{pmatrix} \begin{pmatrix} V_1 \\ V_2 \\ \vdots \\ V_{n-1} \\ V_n \end{pmatrix} = \begin{pmatrix} k_1 \\ k_2 \\ \vdots \\ k_{n-1} \\ k_n \end{pmatrix}, \tag{5.10}$$

where due to the process of row operations, $L_{ij} \in \mathbb{Z}$ and $k_i \in \mathbb{Z}$ are obtained as a linear combination of the former parameters P_{ij} and α_i respectively. Equation (5.10) can be also expressed in matrix notation as:

$$\sum_{j=1}^{i} L_{ij}V_j = k_i, \tag{5.11}$$

and from this equation, an expression for V_i can be obtained:

$$V_i = \frac{1}{L_{ii}}\left(k_i - \sum_{j=1}^{i-1} L_{ij}V_j\right), \tag{5.12}$$

which defines a lattice in the space studied. However, Equation (5.12) does not fulfill, in general, the conditions for a congruence lattice as it is explained in Definition 2. In particular, using Equation (5.12), and applying the condition for congruence lattice:

$$V_i(k_m) \cong V_i(k_m + L_{mm}), \tag{5.13}$$

three different cases can be observed:

- If $m > i$ the congruency is fulfilled automatically since V_i only depends on terms of k_j such that $j \leq i$.
- If $m = i$, we have to impose that:

$$V_i(k_i) \cong V_i(k_i + L_{ii}) \quad \forall\, i \in \{1, 2, \ldots, n\}, \tag{5.14}$$

which leads to:

$$\frac{1}{L_{ii}} \left(k_i - \sum_{j=1}^{i-1} L_{ij} V_j \right) = \frac{1}{L_{ii}} \left(k_i + L_{ii} - \sum_{j=1}^{i-1} L_{ij} V_j \right), \tag{5.15}$$

where, both sides of the equation are identical only if $L_{ii} = 0$. However, that would mean that there are no available positions in any dimension, and thus, no lattice would be generated. That is the reason why another property of the space has to be considered. In particular, if the modular arithmetic of the space is introduced in Equation (5.12) by limiting the number of different available positions in a dimension:

$$V_i = \frac{1}{L_{ii}} \mathrm{mod} \left(k_i - \sum_{j=1}^{i-1} L_{ij} V_j, L_{ii} \right), \tag{5.16}$$

then, the condition of congruence lattice is achieved if:

$$k_i = k_i + L_{ii} \mod (L_{ii}). \tag{5.17}$$

This leads to the first boundary of the distribution parameters:

Corollary 2. *In order to avoid duplicities in the formulation and to obtain a congruent distribution, $k_i \in \mathbb{Z}_{L_{ii}}$ and there exist an intrinsic modular arithmetic in the distribution parameters such that:*

$$k_i = k_i + L_{ii} \mod (L_{ii}). \tag{5.18}$$

- If $m < i$, the resulting condition becomes:

$$\frac{1}{L_{ii}} \left(k_i - \sum_{j=1}^{i-1} L_{ij} V_j(k_m) \right) = \frac{1}{L_{ii}} \left(k_i - \sum_{j=1}^{i-1} L_{ij} V_j(k_m + L_{mm}) \right), \tag{5.19}$$

which is equivalent to the congruence lattice condition since:

$$V_j(k_m) = V_j(k_m + L_{mm}) \quad \forall\, j, m \in \{1, 2, \ldots, n\}, \tag{5.20}$$

as presented in Corollary 2.

That way, using Equation (5.16), it is possible to fulfill the congruence condition for all the dimensions of the lattice. Moreover, by introducing the term L_{ii} inside the modular operator, the following expression is obtained:

$$V_i = \mathrm{mod}\left[\frac{1}{L_{ii}}\left(k_i - \sum_{j=1}^{i-1} L_{ij}V_j\right), 1\right]. \tag{5.21}$$

This means that the point with distribution parameters $k_i = L_{ii}\ \forall\, i \in \mathbb{Z}^n$ is located in the center of the coordinate system of the space, serving as a reference for the distribution.

□

It is important to note that having included the modular arithmetic in L_{ii}, the terms L_{ii} represent the number of different positions in V_i provided that $\{k_j \mid j \neq i\}$ are fixed, while $\{L_{ij} \mid i \neq j\}$ are the configuration numbers, a set of integers that modify the distribution of the lattice.

Once the lattice is defined in Theorem 4, a boundary of the parameters is established in order to avoid duplicities in the formulation. Two sets of boundaries are generated, the first related with the parameter distribution k_i, and the second related to the possible values of the Hermite Normal Form L_{ij}.

Theorem 5. *The set of distribution parameters k_i is bounded in order to avoid duplicities in the formulation of a congruent lattice. In particular:*

$$k_i \in \{1, 2, \ldots, L_{ii}\} \tag{5.22}$$

Proof. Let $\boldsymbol{k}$ be a vector containing the distribution parameters where the position m is occupied by $k_m \in \mathbb{Z}$, and let $\boldsymbol{k}^*$ be the same vector but with the position m occupied by the parameter $k_m^* \in \mathbb{Z}$ instead of k_m. Let suppose that both distributions are equivalent in the dimension m, then, using Equation (5.21), a relation between both distribution parameters is obtained:

$$\mathrm{mod}\left[\frac{1}{L_{mm}}\left(k_m - \sum_{j=1}^{m-1} L_{mj}V_j\right), 1\right] = \mathrm{mod}\left[\frac{1}{L_{mm}}\left(k_m^* - \sum_{j=1}^{m-1} L_{mj}V_j\right), 1\right]. \tag{5.23}$$

which can be expanded, leading to:

$$\frac{1}{L_{mm}}\left(k_m - \sum_{j=1}^{m-1} L_{mj}V_j\right) + A = \frac{1}{L_{mm}}\left(k_m^* - \sum_{j=1}^{m-1} L_{mj}V_j\right), \tag{5.24}$$

where A is an unknown integer. Then, performing some operations in the former expression, the following relation is obtained:

$$k_m + AL_{mm} = k_m^*, \tag{5.25}$$

and thus, if k_m is defined in the ring of integers $\mathbb{Z}_{L_{mm}} = \{1, 2, \ldots, L_{mm}\}$, k_m^* can range all $\mathbb{Z}$. On the other hand, the lattices generated in the rest of the dimensions are equivalent due to the congruence lattice condition (Corollary 2). Consequently, all possible configurations are equivalent to the ones defined by $k_m \in \{1, 2, \ldots, L_{mm}\}$.

□

Theorem 6. *The set of configuration numbers L_{ij} must be constraint in order to avoid duplicities in the formulation of a congruent lattice. In particular:*

$$L_{ij} \in \{0, 1, \ldots, L_{jj} - 1\}. \tag{5.26}$$

In addition, the relation between two equivalent distributions L and L^* is given by:

$$L^*_{ij} = L_{ij} + \sum_{p=j}^{i-1} A_p L_{pj}, \tag{5.27}$$

where A_p are a set of integer numbers that are used to perform row operations in the Hermite Normal Form.

Proof. From the properties of the Hermite Normal Forms [42], an $n \times n$ integral matrix is in Hermite Normal Form if the matrix is lower triangular (or upper triangular), the elements of the diagonal are positive, and the elements of a column are bounded by $L_{ij} \in [0, L_{jj} - 1]$. If these conditions are met, we can conclude that the matrix is in its Hermite Normal Form and in addition, we can assure that the representation of the system is unique. This means that all the equivalent congruent lattice configurations can be generated performing row operations in this Hermite Normal Form (which is unique).

Let i an arbitrary row in which we want to modify the configuration numbers L_{ij} in such a way that the resultant distribution is equivalent to the original. In order to obtain the new combination numbers, we perform row operations such that the matrix is still triangular and the diagonal remains unaltered since the diagonal defines the number of elements in each dimension (see Theorem 5). That way, the formulation of the congruent lattice, defined in this work, is maintained no matter the distribution presented.

Let L and L^* be two equivalent distributions. Thus, each element of the matrix L^* can be expressed by means of the elements of L. In particular, the general term of the matrix can be written as:

$$L^*_{ij} = L_{ij} + \sum_{p=1}^{n} A_p L_{pj}, \tag{5.28}$$

where A_p are a set of integer numbers that are used to perform the row operations and n is the number of dimensions of the distribution. Since we want the matrix that defines each distribution to be triangular, and with a given set of values in the diagonal, we have to limit the sum to certain rows. In particular:

$$L^*_{ij} = L_{ij} + \sum_{p=j}^{i-1} A_p L_{pj}, \tag{5.29}$$

We can rewrite the former expression into:

$$L^*_{ij} = L_{ij} + \sum_{p=j+1}^{i-1} A_p L_{pj} + A_j L_{jj}, \tag{5.30}$$

which represents the general expression to obtain all the equivalent distributions of a given configuration. From Equation (5.30) and since we can impose the parameters A_j to present any integer value, we can transform the expression into:

$$L^*_{ij} = L_{ij} + \sum_{p=j+1}^{i-1} A_p L_{pj} \mod (L_{jj}), \tag{5.31}$$

where it is easy to observe that any distribution can be defined by an equivalent set of parameters that follow this boundary:

$$L^*_{ij} \in \{0, 1, \ldots, L_{jj} - 1\}, \tag{5.32}$$

That way, we prove the boundaries of the configuration numbers ($L_{ij} \in \{0, 1, \ldots, L_{jj} - 1\}$) and also the relations between two equivalent configurations given by this theory. □

5.1.1 Number of possible configurations

Once the lattice and the distribution is completely defined, it is time to calculate the number of different configurations that can be obtained under the assumption that the number of elements in each dimension i (L_{ii}) is already known.

Theorem 7. *Given a lattice distribution defined by:*

$$V_i = mod \left[\frac{1}{L_{ii}} \left(k_i - \sum_{j=1}^{i-1} (L_{ij} V_j) \right), 1 \right], \tag{5.33}$$

and for a fixed number of elements distributed in each dimension i (L_{ii}), the number of different configurations provided by this lattice configuration is:

$$\prod_{i=1}^{n} \prod_{j=1}^{n-i} L_{ii} \tag{5.34}$$

where n is the number of dimensions of the problem.

Proof. Since the number of elements in each dimension is fixed L_{ii}, the only parameters that can modify the distribution are the combination numbers L_{ij} which have the particularity that $i \neq j$. Additionally, from Theorem 6, we now that the values of L_{ij} are constraint in order to obtain different configurations. Thus, in the dimension i there are:

$$\prod_{j=1}^{i-1} L_{jj} \tag{5.35}$$

possible combinations of the combination numbers. Then, for the complete Hermite Normal From, we have:

$$\prod_{i=1}^{n} \prod_{j=1}^{i-1} L_{jj} \tag{5.36}$$

different configurations of the lattice. The former expression can be rearranged into:

$$\left(\prod_{j=1}^{n-1} L_{jj}\right)\left(\prod_{j=1}^{n-2} L_{jj}\right)\cdots\left(\prod_{j=1}^{n-(n-1)} L_{jj}\right) = L_{11}^{(n-1)} L_{22}^{(n-2)} \cdots L_{(n-1)(n-1)}^{(1)}, \tag{5.37}$$

or in a more compact notation:

$$\prod_{i=1}^{n} L_{ii}^{(n-i)} = \prod_{i=1}^{n}\prod_{j=1}^{n-i} L_{ii}. \tag{5.38}$$

which is the number of different possible configurations in a congruent lattice in a space of n dimensions.

□

5.2 n-Dimensional congruent necklace distributions

The objective now is to generate a configuration space using a congruent lattice as described in Equation (5.7) and then select a subset of available positions in such a way that the property of congruence in the distribution is maintained. In order to do that, we first introduce the concept of necklace and some of its basic properties.

Definition 3. A necklace is a subset of elements taken from a set of available positions that present modular arithmetic. It is represented as:

$$\mathcal{G} \subseteq \mathbb{Z}_m, \tag{5.39}$$

where m is the number of available positions considered.

Definition 4. Two necklaces ($\mathcal{G}_1$ and $\mathcal{G}_2$) are identical ($\equiv$) if they select the same subset of elements from the available positions:

$$\mathcal{G}_1 \equiv \mathcal{G}_2 \Longleftrightarrow \{\mathcal{G}_1\} = \{\mathcal{G}_2\}. \tag{5.40}$$

Definition 5. Two necklaces ($\mathcal{G}_1$ and $\mathcal{G}_2$) are considered to be equivalent, that is, there exists an equivalence relation $\cong$ between them, if they fulfill the following expression:

$$\mathcal{G}_1 \cong \mathcal{G}_2 \Longleftrightarrow \exists\, s : \mathcal{G}_1 \equiv \mathcal{G}_2 + s \mod (m), \tag{5.41}$$

where s is an integer that belongs to $\mathbb{Z}_m$.

It is important to note the differences between identical and equivalent necklaces. In that regard, a necklace whose elements are reordered but they occupy the same available positions define an identical necklace. On the other hand, a necklace that performs a rotation in the available positions generate an equivalent necklace. In addition, it is easy to derive that two necklaces that are identical, are also equivalent (as seen in Definition 5 if $s \mid m$). However, there are other cases where a rotation generates an identical necklace. For that reason, we introduce the concept of symmetry of the necklace.

Definition 6. Symmetry of the necklace is the minimum number of positions that a necklace has to rotate in order to obtain an identical necklace. The symmetry of a given necklace $\mathcal{G}$ is represented by $Sym(\mathcal{G})$ and its mathematical expression is provided by the following equation:

$$Sym(\mathcal{G}) = \min\{1 \leq r \leq n : \mathcal{G} + r \equiv \mathcal{G}\}. \tag{5.42}$$

This means that given a necklace $\mathcal{G}$ and applying a rotation of $\{s : Sym(\mathcal{G}) \mid s\}$ generates an identical necklace (see Definition 4) which is also equivalent to $\mathcal{G}$ (see Definition 5). In addition, this implies that the maximum number of rotations that we can apply to the necklace $\mathcal{G}$ without generating an identical necklace is $(Sym(\mathcal{G}) - 1)$. This allows us to define the shifting parameter, whose objective is the definition of all the possible different movements that a necklace can perform in its available positions.

Definition 7. The shifting parameter S is the minimum representation of any rotation that a necklace can perform in its available positions. As a consequence of the definition of Symmetry of the necklace and the modular arithmetic of the problem, the shifting parameter is constrained such that:

$$S \in \{0, 1, ..., (Sym(\mathcal{G}) - 1)\}. \tag{5.43}$$

With the definitions and properties of the necklace already defined, it is now possible to find all the different movements that each necklace introduced in the lattice is able to perform in order to maintain the property of congruence in the lattice. As before, we are very interested in avoiding duplicities in the formulation both for counting purposes as for efficiency in the study.

Let $\mathcal{G}_i$ be a necklace defined in the dimension i of the space, where $\mathcal{G}_i$ is represented as a vector of dimension N_i which contains the information of the positions occupied from the available positions. Note that N_i also corresponds to the number of different elements in the dimension i provided that $\{k_j \mid j \neq i\}$ are fixed. That is, the necklace $\mathcal{G}_i$ is a subset from the set of available locations in $\mathbb{Z}_{L_{ii}}$:

$$\mathcal{G}_i \subseteq \{1, \ldots, L_{ii}\}, \tag{5.44}$$

such that $|\mathcal{G}_i| = N_i$ is the number of elements of the necklace $\mathcal{G}_i$. On the other hand, and in order to simplify the notation used, we assume that:

$$\mathcal{G}_i = \{\mathcal{G}_i(1), \ldots, \mathcal{G}_M(k_i^*), \ldots, \mathcal{G}_i(N_i)\}, \tag{5.45}$$

with

$$1 \leq \mathcal{G}_i(1) \leq \cdots \leq \mathcal{G}_i(k_i^*) \leq \cdots \leq \mathcal{G}_i(N_i) \leq L_{ii}, \tag{5.46}$$

and where the index $k_i^* \in \{1, \ldots, N_i\}$ is an integer modulo N_i, that is, $k_i^* + N_i$ is the same index as k_i^*, that points to each element inside the necklace. This allows to define an application $(\mathcal{G}_i)$ that defines the positions that the necklace occupies in the available positions:

$$\begin{array}{rccc} \mathcal{G}_i: & \mathbb{Z}_{N_i} & \longrightarrow & \mathbb{Z}_{L_{ii}} \\ & k_i^* & \longmapsto & \mathcal{G}_i(k_i^*). \end{array} \tag{5.47}$$

For this reason, it makes sense to refer to $\mathcal{G}_i(k_i^*)$. Thus, due to the modular arithmetic inside the necklace:

$$\mathcal{G}_i(k_i^*) = \mathcal{G}_i(\text{mod}(k_i^* + N_i, N_i)), \tag{5.48}$$

which corresponds to a complete rotation in the available positions in dimension i. It is important to note that this rotation is equivalent to a movement in the admissible locations defined by Corollary 2:

$$k_i = k_i + L_{ii} \mod (L_{ii}), \tag{5.49}$$

as both represent the same movement of the necklace, one using the parametrization of the necklace and the other using the parametrization of the available positions. In addition, by applying the definition of symmetry of the necklace (Definition 6), the former equation can be defined in terms of the symmetry of the necklace in the dimension i ($Sym(\mathcal{G}_i)$) and the necklace $\mathcal{G}_i$:

$$\mathcal{G}_i \equiv \mathcal{G}_i + ASym(\mathcal{G}_i), \tag{5.50}$$

where A is an unknown integer. Thus, the following corollary can be derived:

Corollary 3. *The modular arithmetic governing the rotations in the set of available positions subjected to a given necklace is:*

$$\mathcal{G}_i = \mathcal{G}_i + Sym(\mathcal{G}_i) \mod (Sym(\mathcal{G}_i)). \tag{5.51}$$

It is important to note that since a complete rotation over the available positions generates an identical distribution, L_{ii} must be a multiple of $Sym\,(\mathcal{G})$ due to the fact that $Sym\,(\mathcal{G})$ is the minimum rotation to generate an identical necklace. This implies that $Sym\,(\mathcal{G}) \mid L_{ii}$.

On the other hand, we define a set of movements for each necklace in its dimension in order to provide a methodology in the formulation to shift the necklaces over the available positions respect the movement performed in other dimensions. Let the shifting matrix S be a lower triangular matrix of size $n \times n$, made entirely of integer elements, where the term $S_{ij} \in \mathbb{Z}$ is the shifting parameter (see Definition 7) that relates the movement of the necklace $\mathcal{G}_i$ with the movement performed in the dimension j. This means that the movement of the necklace $\mathcal{G}_i$ is only affected by the movement of necklaces G_j located in dimensions where $j < i$ (as was previously the case with the variables V_i and the distribution parameters k_i).

Theorem 8. *A necklace defined lattice in a n-dimensional modular space can be generated by the following expression:*

$$\begin{aligned} \sum_{j=1}^{i} L_{ij} V_j &= k_i; \\ k_i &= mod\left[\mathcal{G}_i(k_i^*) + \sum_{j=1}^{i-1} S_{ij} k_j, Sym\,(\mathcal{G}_i)\right], \end{aligned} \tag{5.52}$$

where $\mathcal{G}_i$ is the necklace in the dimension i, k_i^* is the distribution parameter inside the necklace and S_{ij} is the shifting parameter of the necklace $\mathcal{G}_i$ with respect to the dimension j.

Proof. An application between the available locations k_i and the necklace elements $\mathcal{G}_i(k_i^*)$ can be defined as done in Equation (5.47):

$$\begin{aligned} \text{T3}: \quad (\mathbb{Z}_{N_1} \times \mathbb{Z}_{N_2} \times \cdots \times \mathbb{Z}_{N_n}) &\longrightarrow (\mathbb{Z}_{L_{11}} \times \mathbb{Z}_{L_{22}} \times \cdots \times \mathbb{Z}_{L_{nn}}) \\ (k_1^*, k_2^*, \ldots, k_n^*) &\longmapsto (k_1, k_2, \ldots, k_n), \end{aligned} \tag{5.53}$$

where the relation between the distribution parameters in the available positions k_i, and the elements of the necklace is described as:

$$k_i = \mathcal{G}_i(k_i^*) + \sum_{j=1}^{i-1} S_{ij} k_j, \tag{5.54}$$

being $\mathcal{G}_i(k_i^*)$ the term that provides the information about the structure of the necklace in the dimension, while the term $\sum_{j=1}^{i-1} S_{ij} k_j$ represents all the possible dependences between the necklace $\mathcal{G}_i$ with the movement of the configuration in other dimensions. However, and due to the existence of symmetries in the necklace, there are movements that generate identical configurations. Thus, using Corollary 3:

$$k_i = \text{mod}\left(\mathcal{G}_i(k_i^*) + \sum_{j=1}^{i-1} S_{ij} k_j, Sym(\mathcal{G}_i)\right), \tag{5.55}$$

which avoids the duplicities of configurations for different sets of shifting parameters.

Now, we introduce Equation (5.55) into the initial lattice defined in Equation (5.11), obtaining:

$$\begin{aligned} \sum_{j=1}^{i} L_{ij} V_j &= k_i; \\ k_i &= \text{mod}\left[\mathcal{G}_i(k_i^*) + \sum_{j=1}^{i-1} S_{ij} k_j, Sym\left(\mathcal{G}_i\right)\right]. \end{aligned} \tag{5.56}$$

Note that the former expression is a recursive function in the different dimensions of the space in study due to the fact that both L_{ij} and S_{ij} are zero when $j > i$.

□

Theorem 9. *The shifting parameters that allow the lattice defined by:*

$$\begin{aligned} \sum_{j=1}^{i} L_{ij} V_j &= k_i; \\ k_i &= mod\left[\mathcal{G}_i(k_i^*) + \sum_{j=1}^{i-1} S_{ij} k_j, Sym\left(\mathcal{G}_i\right)\right], \end{aligned} \tag{5.57}$$

to be congruent must fulfill the following relation:

$$Sym(\mathcal{G}_i) \left| S_{ij} L_{jj} - \left(L_{ij} - \sum_{q=j+1}^{i-1} S_{iq} L_{qj}\right)\right. . \tag{5.58}$$

Proof. In order to derive the theorem, we focus on a particular dimension i where we apply the congruence condition seen in Definition 2:

$$V_i(k_j) \cong V_i(k_j + L_{jj}) \quad \forall\, i, j \in \{1, 2, \ldots, n\}, \tag{5.59}$$

where we assume that a complete rotation of the configuration is performed in the dimension j while the other dimensions remain unrotated. This means that in addition to the congruence condition:

$$V_i(k_j) = V_i(k_j + L_{jj}) \quad \forall\, i \neq j, \tag{5.60}$$

since only the dimension i is subjected to a movement.

Studying the lattice presented in Equation (5.52) we can observe three different cases, the case in which $j > i$, the case $j = i$ and the case $j < i$. For all the cases of study we consider:

$$\begin{aligned} \sum_{p=1}^{i} L_{ip} V_p(k_j) &= k_i(k_j) \\ k_i(k_j) &= \mathcal{G}_i(k_i^*) + \sum_{p=1}^{i-1} S_{ip} k_p(k_j) + A_i Sym\left(\mathcal{G}_i\right), \end{aligned} \tag{5.61}$$

as the original lattice before the complete rotation in the dimension j, where $V_p(k_j)$ and $k_p(k_j)$ represent the variable and the distribution parameters of the original configuration and A_i is an unknown integer. On the other hand:

$$\begin{aligned} \sum_{p=1}^{i} L_{ip} V_p(k_j + L_{jj}) &= k_i(k_j + L_{jj}) \\ k_i(k_j + L_{jj}) &= \mathcal{G}_i(k_i^*) + \sum_{p=1}^{i-1} S_{ip} k_p(k_j + L_{jj}) + B_i Sym\left(\mathcal{G}_i\right), \end{aligned} \tag{5.62}$$

is the lattice after the complete rotation in the dimension j, where $V_q(k_j + L_{jj})$ represents the variable in the dimension q affected by a complete rotation performed in the dimension j and $k_p(k_j + L_{jj})$ is the modified distribution parameter k_p after the rotation. Finally B_i is an unknown integer generated due to the modular arithmetic of the problem.

- If $j > i$, the rotation in the dimension j does not affect k_i since:

$$\sum_{p=1}^{i} L_{ip} V_p(k_j + L_{jj}) - \sum_{p=1}^{i} L_{ip} V_p(k_j) = \sum_{p=1}^{i} L_{ip} \left[V_p(k_j + L_{jj}) - V_p(k_j)\right] = 0, \tag{5.63}$$

  which implies that:

$$k_p(k_j + L_{jj}) = k_p(k_j) \quad \forall\, p < j. \tag{5.64}$$

  Regarding the second expression of the lattice, we compare the original and the rotated configuration, obtaining:

$$0 = \sum_{p=1}^{i-1} S_{ip} \left[k_p(k_j + L_{jj}) - k_p(k_j)\right] + (B_i - A_i) Sym\left(\mathcal{G}_i\right) \tag{5.65}$$

  which means that no constraint has to be imposed in the shifting parameters for the fulfillment of the congruent condition.

- If $j = i$, the difference between both lattices is:

$$\sum_{p=1}^{j} L_{jp} \left[V_p(k_j + L_{jj}) - V_p(k_j) \right] = L_{jj}, \tag{5.66}$$

since $L_{jj} = k_j(k_j + L_{jj}) - k_j(k_j)$ (a complete rotation in this dimension). In addition, the former equation can be rearranged into:

$$L_{jj} \left[V_j(k_j + L_{jj}) - V_j(k_j) \right] + \sum_{p=1}^{j-1} L_{jp} \left[V_p(k_j + L_{jj}) - V_p(k_j) \right] = L_{jj}, \tag{5.67}$$

and using Equation (5.60), we obtain:

$$V_j(k_j + L_{jj}) - V_j(k_j) = 1 \tag{5.68}$$

that represents the complete rotation in the dimension i. It is clear that since the variables V_i are subjected to a modulo 1 arithmetic, $V_i(k_i + L_{ii}) \cong V_i(k_i)$. However, this result affects other dimensions as it is shown later.

On the other hand, from the differences between the second terms of the lattice of the original and rotated configurations:

$$L_{jj} = \sum_{p=1}^{j-1} S_{jp} \left[k_p(k_j + L_{jj}) - k_p(k_j) \right] + (B_j - A_j) Sym\left(\mathcal{G}_j\right), \tag{5.69}$$

where applying the condition presented in Equation (5.64) we derive that:

$$L_{jj} = (B_j - A_j) Sym\left(\mathcal{G}_j\right), \tag{5.70}$$

and thus, no additional constraint must be imposed since $Sym\left(\mathcal{G}_j\right) \mid L_{jj}$.

- If $j < i$, the difference between both lattices is:

$$\sum_{q=1}^{i} L_{iq} V_q(k_j + L_{jj}) - \sum_{q=1}^{i} L_{iq} V_q(k_j) = k_i(k_j + L_{jj}) - k_i(k_j), \tag{5.71}$$

which is equal to:

$$\sum_{q=1}^{i} L_{iq} \left[V_q(k_j + L_{jj}) - V_q(k_j) \right] = k_i(k_j + L_{jj}) - k_i(k_j), \tag{5.72}$$

and rearranged it leads to:

$$\begin{aligned} &\sum_{q=1}^{j-1} L_{iq} \left[V_q(k_j + L_{jj}) - V_q(k_j) \right] + L_{ij} \left[V_j(k_j + L_{jj}) - V_j(k_j) \right] + \\ + &\sum_{q=j+1}^{i} L_{iq} \left[V_q(k_j + L_{jj}) - V_q(k_j) \right] = k_i(k_j + L_{jj}) - k_i(k_j), \end{aligned} \tag{5.73}$$

which can be simplified using Equations (5.60) and (5.68), obtaining:

$$L_{ij} = k_i(k_j + L_{jj}) - k_i(k_j). \tag{5.74}$$

On the other hand, from the differences in the second term of the lattice of both configurations:

$$k_i(k_j + L_{jj}) - k_i(k_j) = \sum_{p=1}^{i-1} S_{ip} \left[k_p(k_j + L_{jj}) - k_p(k_j)\right] + (B_j - A_j) Sym\left(\mathcal{G}_j\right), \tag{5.75}$$

where using Equation (5.74) and (5.64) leads to:

$$L_{ij} = \sum_{p=j}^{i-1} S_{ip} \left[k_p(k_j + L_{jj}) - k_p(k_j)\right] + (B_j - A_j) Sym\left(\mathcal{G}_j\right). \tag{5.76}$$

In addition, the former expression can be rearranged into:

$$\begin{aligned} L_{ij} &= S_{ij} \left[k_j(k_j + L_{jj}) - k_j(k_j)\right] + \\ &+ \sum_{p=j+1}^{i-1} S_{ip} \left[k_p(k_j + L_{jj}) - k_p(k_j)\right] + (B_j - A_j) Sym\left(\mathcal{G}_j\right), \end{aligned} \tag{5.77}$$

where:

$$k_j(k_j + L_{jj}) - k_j(k_j) = L_{jj}, \tag{5.78}$$

representing the complete rotation in the dimension j, while:

$$k_p(k_j + L_{jj}) - k_p(k_j) = L_{pj} \tag{5.79}$$

as seen in Equation (5.74). Thus, Equation (5.77) can be written as:

$$L_{ij} = S_{ij} L_{jj} + \sum_{p=j+1}^{i-1} S_{ip} L_{pj} + (B_j - A_j) Sym\left(\mathcal{G}_j\right), \tag{5.80}$$

or, in a more compact manner:

$$Sym(\mathcal{G}_i) \left| S_{ij} L_{jj} - \left(L_{ij} - \sum_{q=j+1}^{i-1} S_{iq} L_{qj} \right) \right., \tag{5.81}$$

which is an expression that relates the values of the shifting parameters with respect to elements of the Hermite Normal Form and other shifting parameters. Note that the expression is a recursive function.

Thus, and as seen from the three cases studied, the only constraint that affects the shifting parameters is:

$$Sym(\mathcal{G}_i) \left| S_{ij} L_{jj} - \left(L_{ij} - \sum_{q=j+1}^{i-1} S_{iq} L_{qj} \right) \right.. \tag{5.82}$$

□

5.2.1 Number of possible configurations

In this section we deal with the problem of counting the number of different configurations that the n-dimensional congruent lattices using necklaces can generate. In that respect, we consider three different cases of study:

- Fixing the set of necklaces $\mathcal{G}_i$ for all $i \in \{1, \ldots, n\}$, and the Hermite Normal Form.
- Fixing the set of necklaces $\mathcal{G}_i$ and L_{ii} for all $i \in \{1, \ldots, n\}$.
- Fixing the sizes of the necklaces $N_i = |\mathcal{G}_i|$ and L_{ii} for all $i \in \{1, \ldots, n\}$.

However, first we need to determine the number of different necklaces of a given size that can be generated in a given dimension. Let L be a set of available positions in a given dimension where we select a necklace $\mathcal{G}$ comprised of N elements taken from the available positions. In other words $\mathcal{G} \subseteq \{1, \ldots, L\}$ where $|\mathcal{G}| = N$.

Theorem 10. *The number of different necklaces under the equivalence relation $\cong$ and that are comprised by N elements taken from L available positions is:*

$$\sum_{\substack{g=1 \\ g|L \\ \frac{L}{g}|N}}^{L} \frac{1}{g} \left[\binom{g}{\frac{N}{L}g} - \sum_{\substack{g'=1 \\ g'|g \\ \frac{L}{g'}|N}}^{g-1} \frac{g'}{L} \left| Fix(g') \right| \right]. \tag{5.83}$$

where $g = Sym(\mathcal{G})$ are the possible symmetries in the problem considered and $|Fix(g')|$ is the number of elements contained in the Fix of g, and which is provided by:

$$|Fix(g)| = \frac{L}{g} \left[\binom{g}{\frac{N}{L}g} - \sum_{\substack{g'=1 \\ g'|g \\ \frac{L}{g'}|N}}^{g-1} \frac{g'}{L} \left| Fix(g') \right| \right], \tag{5.84}$$

Proof. Let $+\,\mathbb{Z}_L$ be the possible different actions that can be applied to a given necklace, and which correspond to the possible different rotations that a necklace $\mathcal{G}$ can perform in the available positions $\mathbb{Z}_L$. In addition, let $G = \mathbb{Z}_L$ be the group containing the possible actions that can apply to any necklace defined in L available positions. That way, we can define a map ϕ as:

$$\begin{array}{rccl} \phi: & G \times X & \longrightarrow & X \\ & (g, x) & \longmapsto & x + g \mod (L). \end{array} \tag{5.85}$$

The objective is to apply the Burnside's Lemma to this application. Therefore, we have to compute $|\mathrm{Fix}(g)|$. The Fix of a given action is the set of elements that remain unaltered under the application of that action. In that respect, from the definition of symmetry of a necklace (see Equation (5.42)), we know that the only possible values of $g \in G$ that have elements in the $\mathrm{Fix}(X)$ are the ones that

presents symmetries, that is, when an element fulfills $g = Sym(\mathcal{G})$. This means that only the values such that $g|L$ and $\frac{L}{g}|N$ contribute to the elements of the Fix.

First, we focus in a particular value of symmetry of the necklace $g = Sym(\mathcal{G})$ and its Fix (Fix(g)). Since there exists symmetry in the necklace, the configuration can be regarded as a pattern comprised of g available positions that is repeated L/g times in the L available positions. In this pattern, there must be Ng/L elements from the necklace since all the patterns must have the same number of elements. Thus, the number of possible combinations that exists in a pattern of size g ($PC(g)$) is:

$$PC(g) = \left(\begin{array}{c} g \\ \frac{N}{L}g \end{array} \right). \tag{5.86}$$

On the other hand, each pattern can rotate L/g possible times in the L available positions while maintaining the same configuration (due to the symmetry that we are imposing). Thus, the number of combinations of N elements in L available positions that present a given symmetry g is:

$$\frac{L}{g}PC(g) = \frac{L}{g}\left(\begin{array}{c} g \\ \frac{N}{L}g \end{array} \right). \tag{5.87}$$

However, this counting also includes some elements that belong to other symmetries (remember that from Definition 6 the symmetry of a necklace was defined as the minimum rotation in order to obtain an identical necklace), and thus, they must be removed from this set of combinations in order to avoid duplicities in the counting process. For instance, if $L = 6$ and $N = 3$ and we consider $g = 6$ as the symmetry in study, the number of combinations that we compute with Equation (5.86) include combinations of elements that also present symmetry of $g = 3$: $\{1, 4\}$, $\{2, 5\}$ and $\{3, 6\}$; and thus, we could count them twice if we are not careful in the counting process. In order to avoid these cases, we only consider g as the smallest symmetry that a combination of elements can present.

From the definition of Fix, we know that the number of possible combinations of N elements with a particular symmetry g is the $|\text{Fix}(g)|$ itself. In addition, the possible combinations of elements must have been generated based on patters of size g (as in Equation (5.86)). Thus, the number of different patterns that exists for a particular symmetry g' is:

$$PC(g') = \frac{g'}{L}\left|\text{Fix}(g')\right|. \tag{5.88}$$

Then, we can remove from the counting process, of the different pattern generators with symmetry g, all the elements that belong to a different symmetry such that $g' < g$:

$$PC(g) = \left(\begin{array}{c} g \\ \frac{N}{L}g \end{array} \right) - \sum_{\substack{g'=1 \\ g'|g \\ \frac{L}{g'}|N}}^{g-1} \frac{g'}{L}\left|\text{Fix}(g')\right|, \tag{5.89}$$

where the sum is performed in all the symmetries g' such that $g'|g$ and $\frac{L}{g}|N$ since g' must also fulfill the conditions for symmetry.

Once the number of pattern combinations is computed, the $|\text{Fix}(g)|$ can be obtained using Equation (5.89), leading to:

$$|\text{Fix}(g)| = \frac{L}{g}\left[\binom{g}{\frac{N}{L}g} - \sum_{\substack{g'=1 \\ g'|g \\ \frac{L}{g'}|N}}^{g-1} \frac{g'}{L}\left|\text{Fix}(g')\right|\right], \tag{5.90}$$

which is a recursive function that can be easily computed. Equation (5.90) allows to obtain the number of different necklaces under a given symmetry g. This is done by the direct application of Burnside's Lemma, where $G = \mathbb{Z}_L$ as pointed out before. That way, we can derive that the number of different necklaces is:

$$\frac{1}{L}\sum_{\substack{g=1 \\ g|L_M \\ \frac{L_M}{g}|N_M}}^{L_M} |\text{Fix}(g)|, \tag{5.91}$$

which using Equation (5.90) can be rewritten as:

$$\sum_{\substack{g=1 \\ g|L_M \\ \frac{L}{g}|N}}^{L_M} \frac{1}{g}\left[\binom{g}{\frac{N}{L}g} - \sum_{\substack{g'=1 \\ g'|g \\ \frac{L}{g'}|N}}^{g-1} \frac{g'}{L}\left|\text{Fix}(g')\right|\right]. \tag{5.92}$$

□

Once Theorem 10 is presented, it is now possible to introduce the counting theorems for congruent lattices using necklaces. Each condition studied and theorem is presented in a different subsection.

5.2.1.1 Fixing $\mathcal{G}_i$ for all $i \in \{1, \ldots, n\}$ and the Hermite Normal Form.

In this case we focus on the study of the number of possibilities given a set of necklaces $\mathcal{G}_i$ and the complete Hermite Normal Form of the fictitious constellation. By doing this, the available positions are fixed (they cannot shift), and thus, this methodology provides the number of congruent configurations that follow the particular distribution given by the Hermite Normal Form. This is equivalent to compute the number of possible values that the shifting parameters S_{ij} can present in Equation (5.58).

Theorem 11. *Given a set of necklaces $\mathcal{G}_i$ in each dimension of the space such that $i \in \{1, \ldots, n\}$, and a fixed Hermite Normal Form, there exist congruent configurations in the available distributions if and only if:*

$$\gcd(Sym(\mathcal{G}_i), L_{jj}) \left| \left(L_{ij} - \sum_{q=j+1}^{i-1} S_{ij} L_{qj}\right), \ \forall \{i, j : i > j\}, \right. \tag{5.93}$$

being the number of different configurations in that case:

$$\prod_{i=1}^{n}\prod_{j=1}^{i-1}\gcd(Sym(\mathcal{G}_i),L_{jj}), \tag{5.94}$$

Proof. Equation (5.58) can be expressed as:

$$ASym(\mathcal{G}_i)+L_{jj}S_{ij}=L_{ij}-\sum_{q=j+1}^{i-1}S_{ij}L_{qj}, \tag{5.95}$$

where A is a unknown integer. As it can be seen, Equation (5.95) can be regarded as a linear Diophantine equation where we select A and S_{ij} as the variables of study. By the use of Bézout's identity, we can conclude that there exist solution if and only if:

$$\gcd(Sym(\mathcal{G}_i),L_{jj})\left|L_{ij}-\sum_{q=j+1}^{i-1}S_{ij}L_{qj}\right.. \tag{5.96}$$

In the case the former expression is fulfilled, the solutions of Equation (5.95) have the form:

$$\begin{aligned}(S_{ij})_\lambda &= (S_{ij})_0+\lambda\Delta l, \quad \text{with} \quad \Delta l=\frac{Sym(\mathcal{G}_i)}{\gcd(Sym(\mathcal{G}_i),L_{jj})},\\ (A)_\lambda &= (A)_0-\lambda\frac{L_{jj}}{\gcd(Sym(\mathcal{G}_i),L_{jj})},\end{aligned} \tag{5.97}$$

where $(S_{ij})_0$ and $(A)_0$ is a known pair of solutions, and λ is an integer number.

However, the shifting parameters S_{ij} are constrained as seen in Definition 7, and thus, $S_{ij}\in\{0,\dots,Sym(\mathcal{G}_i)-1\}$. This means that the number of different values of S_{ij} that can be defined is provided by:

$$\begin{aligned}\left\lfloor\frac{Sym(\mathcal{G}_i)-1}{\Delta l}\right\rfloor+1 &= \left\lfloor\frac{(Sym(\mathcal{G}_i)-1)\gcd(Sym(\mathcal{G}_i),L_{jj})}{Sym(\mathcal{G}_i)}\right\rfloor+1=\\ &= \gcd(Sym(\mathcal{G}_i),L_{jj})-\left\lceil\frac{\gcd(Sym(\mathcal{G}_M),L_\Omega)}{Sym(\mathcal{G}_M)}\right\rceil+1=\\ &= \gcd(Sym(\mathcal{G}_i),L_{jj}).\end{aligned} \tag{5.98}$$

The condition provided by Equation (5.97) as well as the number of different values of S_{ij} given by Equation (5.98) must be fulfilled for all the dimensions of the space, thus, the condition for the existence of solution is:

$$gcd(Sym(\mathcal{G}_i),L_{jj})\left|\left(L_{ij}-\sum_{q=j+1}^{i-1}S_{ij}L_{qj}\right),\ \forall\{i,j:i>j\}\right., \tag{5.99}$$

while the total number of different configurations is given by all possible combinations of the shifting parameters S_{ij}. Therefore the number of different configurations is:

$$\prod_{i=1}^{n}\prod_{j=1}^{i-1}\gcd(Sym(\mathcal{G}_i),L_{jj}). \tag{5.100}$$

□

As it can be observed, if all the necklaces comprise all the available positions of their respective dimensions, we obtain that there exists congruent configurations always since $Sym(\mathcal{G}_i) = 1$ for any dimension. In addition, there is only one possible configuration due to the fact that:

$$\prod_{i=1}^{n}\prod_{j=1}^{i-1}\gcd(1, L_{jj}) = 1. \tag{5.101}$$

This is an expected result, since in a complete configuration, a given Hermite Normal Form can only generate one congruent lattice distribution.

5.2.1.2 Fixing $\mathcal{G}_i$ and L_{ii} for all $i \in \{1, \ldots, n\}$.

On the other hand, in this second case, we fix the necklace $\mathcal{G}_i$ and the number of available positions in each dimension, that is, the parameters L_{ii} from the Hermite Normal Form. This provides the information of how many different distributions can be created with a given set of patterns (through the parameter $Sym(\mathcal{G}_i)$). This problem is equivalent to compute the amount of pairs $\{S_{ij}, L_{ij}\}$ that are solution of Equation (5.58).

Theorem 12. *Given a set of necklaces $\mathcal{G}_i$ and a number of available positions in each dimension L_{ii}, the number of different congruent configurations that can be generated is:*

$$\prod_{i=1}^{n}\prod_{j=1}^{n-i} L_{ii}. \tag{5.102}$$

Proof. We first focus on a particular combination of dimension of study i and dimension in which rotations are considered. Then, by using Equation (5.58) we can present the relation between S_{ij} and L_{ij}:

$$L_{jj}S_{ij} - 1L_{ij} = ASym(\mathcal{G}_M) - \sum_{q=j+1}^{i-1} S_{iq}L_{qj}, \tag{5.103}$$

where the elements S_{iq} and L_{qj} with $q > j$ are supposed to be known since can be computed in other recursions of the equation. Equation (5.103) can be regarded as a Diophantine equation where S_{ij} and L_{ij} are its variables. Then, this Diophantine equation has solution if and only if:

$$\gcd(L_{jj}, 1) \left| ASym(\mathcal{G}_M) - \sum_{q=j+1}^{i-1} S_{iq}L_{qj} \right. \tag{5.104}$$

which is always true. Furthermore, the solutions generated are:

$$\begin{aligned} (S_{ij})_\lambda &= (S_{ij})_0 + \lambda, \\ (L_{ij})_\lambda &= (L_{ij})_0 + \lambda L_{jj}, \end{aligned} \tag{5.105}$$

where $(S_{ij})_0$ and $(L_{ij})_0$ are a pair of possible solutions of Equation (5.103) and λ is an integer. From Equation (5.105), we can deduce that there is only one solution for each particular value of

the integer A, since $L_{ij} \in \{0, \ldots, L_{jj} - 1\}$ and the the summation is assumed to be fixed in the equation. Thus, we are interested to know the number of the different values that A can present in the equation.

From Equation (5.103) and the different maximum and minimum constraints of L_{ij} and S_{ij} (see Theorem 6 and Definition 7), the maximum and minimum values of A that can be obtained are:

$$\begin{aligned} A_{min} &= \frac{1}{Sym(\mathcal{G}_i)} \left(\sum_{q=j+1}^{i-1} S_{iq} L_{qj} - (L_{jj} - 1) \right), \\ A_{max} &= \frac{1}{Sym(\mathcal{G}_i)} \left(\sum_{q=j+1}^{i-1} S_{iq} L_{qj} + L_{jj}(Sym(\mathcal{G}_i) - 1) \right), \end{aligned} \tag{5.106}$$

which define:

$$\lfloor A_{max} - A_{min} \rfloor + 1 = \left\lfloor \frac{L_{jj}(Sym(\mathcal{G}_i) - 1) + (L_{jj} - 1)}{Sym(\mathcal{G}_i)} \right\rfloor + 1 = L_{jj} \tag{5.107}$$

different possible values of A. This means that, there are L_{jj} different combinations for the pairs $\{L_{ij}, S_{ij}\}$. It is interesting to note that this is coincident with the number of possibilities that $L_{ij} \in \{0, \ldots, L_{jj} - 1\}$ presents.

Therefore, the number of different configurations that we can obtain under these conditions is:

$$\prod_{i=1}^{n} \prod_{j=1}^{n-i} L_{ii}, \tag{5.108}$$

which corresponds to the number of possible configurations of a complete congruent lattice (see Theorem 7).

□

Theorem 12 also leads to an important property when both the set of necklaces $\mathcal{G}_i$ and the number of available positions in each dimension L_{ii} is fixed: the number of possibilities only depends on the number of available positions, not in the necklace selected nor in the configuration numbers.

5.2.1.3 Fixing N_i and L_{ii} for all $i \in \{1, \ldots, n\}$.

This case is an interesting variation of the previous counting methodology, where now, instead of fixing the necklaces $\mathcal{G}_i$, the number of elements taken in each dimension is set, that is, $N_i = |\mathcal{G}_i|$. Thus, it provides information on the number of possibilities of distribution that are available with a given number of elements retrieved and a set of available positions in each dimension.

Theorem 13. *Let L_{ii} where $i \in \{1, \ldots, n\}$ be the number of available positions in each dimension i of a n-dimensional space, and let N_i be number of elements taken as a subset of the available positions. Then, the number of different congruent lattice configurations using necklaces that can be generated is:*

$$\prod_{i=1}^{n} L_{ii}^{(n-i)} \sum_{\substack{g=1 \\ g|L_{ii} \\ \frac{L_{ii}}{g}|N_i}}^{L_{ii}} \frac{1}{g} \left[\binom{g}{\frac{N_i}{L_{ii}}g} - \sum_{\substack{g'=1 \\ g'|g \\ \frac{L_{ii}}{g'}|N_i}}^{g-1} \frac{g'}{L_{ii}} \left| Fix(g') \right| \right], \tag{5.109}$$

where $|Fix(g')|$ for the dimension i is the number of elements contained in the Fix of g, and that can be computed as:

$$|Fix(g)| = \frac{L}{g} \left[\binom{g}{\frac{N}{L}g} - \sum_{\substack{g'=1 \\ g'|g \\ \frac{L}{g'}|N}}^{g-1} \frac{g'}{L} \left| Fix(g') \right| \right], \tag{5.110}$$

Proof. From Theorem 10 we know that in each dimension i, it is possible to generate:

$$\mathcal{P}_i = \sum_{\substack{g=1 \\ g|L_{ii} \\ \frac{L_{ii}}{g}|N_i}}^{L_{ii}} \frac{1}{g} \left[\binom{g}{\frac{N_i}{L_{ii}}g} - \sum_{\substack{g'=1 \\ g'|g \\ \frac{L_{ii}}{g'}|N_i}}^{g-1} \frac{g'}{L_{ii}} \left| \mathrm{Fix}(g') \right| \right], \tag{5.111}$$

different necklaces, where:

$$|\mathrm{Fix}(g)| = \frac{L_{ii}}{g} \left[\binom{g}{\frac{N_i}{L_{ii}}g} - \sum_{\substack{g'=1 \\ g'|g \\ \frac{L_{ii}}{g'}|N_i}}^{g-1} \frac{g'}{L_{ii}} \left| \mathrm{Fix}(g') \right| \right]. \tag{5.112}$$

This means that the total number of combinations of necklaces between the different dimensions is:

$$\prod_{i=1}^{n} \mathcal{P}_i. \tag{5.113}$$

In addition, once all the necklaces in the space are fixed, we can apply Theorem 12 in order to obtain the total number of different configurations by a combination of all the possibilities:

$$\prod_{i=1}^{n} \mathcal{P}_i \prod_{i=1}^{n} L_{ii}^{(n-i)}. \tag{5.114}$$

The former expression can be rearranged into:

$$\prod_{i=1}^{n} \mathcal{P}_i L_{ii}^{(n-i)}, \tag{5.115}$$

and using Equation (5.111) we obtain:

$$\prod_{i=1}^{n} L_{ii}^{(n-i)} \sum_{\substack{g=1 \\ g|L_{ii} \\ \frac{L_{ii}}{g}|N_i}}^{L_{ii}} \frac{1}{g} \left[\binom{g}{\frac{N_i}{L_{ii}} g} - \sum_{\substack{g'=1 \\ g'|g \\ \frac{L_{ii}}{g'}|N_i}}^{g-1} \frac{g'}{L_{ii}} \left| \mathrm{Fix}(g') \right| \right], \tag{5.116}$$

which shows the total number of configurations that are presented in the lattice under the considered conditions of fixed N_i and L_{ii}.

□

In addition, it is interesting to note that if $N_i = L_{ii}$ for all i, the number of configurations is the same as in the case of a complete lattice (as seen in Theorem 7). This result was expected due to the fact that the necklace theory is a generalization of the original lattice theory presented.

5.3 Alternative formulation

It is possible to generate a congruent lattice, and its generalization using necklaces, based on an entirely integer formulation. This includes the variables V_i which are real numbers in the original formulation.

We depart from Equation (5.11):

$$\sum_{j=1}^{i} L_{ij} V_j = k_i, \tag{5.117}$$

and multiply each expression by the integer $\prod_{p=1}^{i-1} L_{pp}$, obtaining:

$$\sum_{j=1}^{i} L_{ij} \prod_{p=1}^{i-1} L_{pp} V_j = k_i \prod_{p=1}^{i-1} L_{pp}, \tag{5.118}$$

which can be expressed in a different manner by simple operations in the summation:

$$L_{ii} \prod_{p=1}^{i-1} L_{pp} V_i + \sum_{j=1}^{i-1} L_{ij} \prod_{p=1}^{i-1} L_{pp} V_j = k_i \prod_{p=1}^{i-1} L_{pp}, \tag{5.119}$$

and by merging the product in the first term of the equation and rearranging the product of the second term we derive:

$$\prod_{p=1}^{i} L_{pp} V_i + \sum_{j=1}^{i-1} L_{ij} \prod_{m=j+1}^{i-1} L_{mm} \prod_{p=1}^{j} L_{pp} V_j = k_i \prod_{p=1}^{i-1} L_{pp}. \tag{5.120}$$

Now, a change in the distribution variable V_i is performed. Let $\mathcal{N}_i$ be the new set of variables that relate with the originals V_i through the following relation:

$$\mathcal{N}_i = \prod_{p=1}^{i} L_{pp} V_i. \tag{5.121}$$

which introduced in Equation (5.120) leads to:

$$\mathcal{N}_i + \sum_{j=1}^{i-1} L_{ij} N_j \prod_{m=j+1}^{i-1} L_{mm} = k_i \prod_{p=1}^{i-1} L_{pp}, \tag{5.122}$$

where we can obtain the value of the new variable by means of the distribution parameters k_i:

$$\mathcal{N}_i = k_i \prod_{p=1}^{i-1} L_{pp} - \sum_{j=1}^{i-1} L_{ij} N_j \prod_{m=j+1}^{i-1} L_{mm}. \tag{5.123}$$

As in the case of V_i, the former expression is constraint due to the modular arithmetic of the space. In particular, and since $\mathcal{N}_i = \prod_{p=1}^{i} L_{pp} V_i$, $\mathcal{N}_i \in \left[0, \prod_{p=1}^{i} L_{pp}\right]$:

$$\mathcal{N}_i = \mathrm{mod} \left[k_i \prod_{p=1}^{i-1} L_{pp} - \sum_{j=1}^{i-1} L_{ij} N_j \prod_{m=j+1}^{i-1} L_{mm}, \prod_{p=1}^{i} L_{pp} \right]. \tag{5.124}$$

One important thing to note is that $\mathcal{N}_i \in \mathbb{Z} \; \forall \, i$ since all the operations performed are products and sums of integer numbers.

Now, we introduce in the new formulation provided by Equation (5.124) into the necklace formulation given by Equation (5.52), which leads to:

$$\begin{aligned} \mathcal{N}_i + \sum_{j=1}^{i-1} L_{ij} N_j \prod_{m=j+1}^{i-1} L_{mm} &= k_i \prod_{p=1}^{i-1} L_{pp}; \\ k_i &= \mathrm{mod} \left[\mathcal{G}_i(k_i^*) + \sum_{j=1}^{i-1} S_{ij} k_j, Sym\left(\mathcal{G}_i\right) \right], \end{aligned} \tag{5.125}$$

where the congruent configurations correspond to the ones provided by Theorem 9. In that respect, note that the congruent relations provided by Equation (5.58) are independent on the definition of the variables used.

Equation (5.125) defines congruent lattices where the variables $\mathcal{N}_i$ present now integer numbers (note that they are sums and products of integers) that are defined in $\mathcal{N}_i \in \left[1, \ldots, \prod_{p=1}^{i} L_{pp}\right]$.

5.4 Conclusion

This chapter introduces the generalization to n-dimensions of the theory behind the 2D, 3D and 4D Necklace Flower Constellations. This methodology allows to generate all the congruent and uniform distributions in a n-dimensional space subjected to modular arithmetic. Moreover, the theory allows to select subsets of elements in such a way that the properties of uniformity and congruence are maintained in the resultant configuration.

On the other hand, the chapter introduces three sets of theorems. The first set provides the formulation to generate lattice and necklace congruent distributions in the space considered. The second set aims to determine the constraints that the distribution parameters must follow in order to avoid duplicities in the formulation. Finally, the third set consist of counting theorems which provide the number of different possibilities of design that this theory can generate.

This theory provides a deep mathematical foundation for the configurations presented in the Lattice and Necklace Flower Constellations, as well as in any other uniform congruent distribution in a modular n-dimensional space. In that respect, it complements the theory presented for Necklace Flower Constellations providing mathematical robustness to the whole methodology of design. As such, with this theory we close the Necklace Flower Constellations methodology.

Chapter 6

Ground-Track Constellations

The designs of Walker, Draim and the Lattice Flower Constellation Theory distribute the satellites in the inertial frame of reference, not providing any tool to control the distribution in the Earth Fixed frame of reference. As such, generating a constellation whose satellites share their ground-tracks becomes difficult. For this reason, we introduce the Ground-Track Constellations as a general constellation design methodology to generate constellations directly in the Earth Fixed frame of reference.

The proposed constellation design allows to generate a configuration in which a number of different relative trajectories is defined, each of these containing a number of satellites that present the same instantaneous relative trajectory over time. Moreover, in order to decrease the number of orbital launches to build the constellation, another constraint will be set: satellites from different relative trajectories have to share the same inertial orbit, allowing a decrease in the number of inertial orbits.

In addition, this methodology allows to include orbital perturbations in the initial design of the constellation. This process is possible since the greatest orbital perturbation in satellites orbiting the Earth is the Earth gravitational potential, which is a periodic perturbation from the Earth Fixed frame of reference. This allows to generate distributions that are resistant to these kind of perturbations, providing a powerful tool to define constellations independent of the orbital perturbations. This represents a great difference when comparing with other satellite constellation designs, where the effects of perturbations where including after the definition of the constellation. Furthermore, the distribution of these constellations is defined using the along track distances measured in time, which provides very interesting results and possibilities for design.

The time distribution methodology introduced is able to generate all kinds of satellite configurations including equally spaced in time distributions (as the Lattice Flower Constellations Theory does) but also formations of satellites. Examples of these are presented in this chapter for both keplerian formulation and perturbed models using the time distribution methodology introduced in this work.

This chapter is organized as follows. First, a keplerian formulation for the Ground-Track Constellations is introduced, where in order to make things easier, we have separated the design in three steps. In the first step, a constellation whose satellites belong to the same ground-track is presented. Later, in the second step, additional ground-tracks are included in the formulation, while in the third step, the condition for minimum number of inertial orbits is imposed in the design. Once the keplerian formulation is presented, an alternative design process is described which allows to define constellations under orbital perturbations. Examples of all the methodologies presented

in this chapter are included to show some of the possibilities that this design can provide.

6.1 Keplerian model for constellation design

In an unperturbed dynamic model, the classical orbital parameters (a, e, i, ω, Ω) are constant whilst the mean anomaly (M) varies through time. This property will be used to show in a clear way the analytical model behind the constellation design proposed in this chapter.

Along this section, three different constellation designs will be shown, each one expanding the possibilities of the former one with a new concept. First, a constellation design model in which satellites share the same relative trajectory with respect to a rotating reference frame will be presented. Second, this model will be expanded with the possibility of distribution of the satellites in several different relative trajectories. And finally, a constraint will be set in order to reduce the number of inertial orbits to a minimum. That way, the costs of building the constellation in orbit are considerably reduced.

All these constellation designs share the mean values of the semi-major axis, the eccentricity, the inclination and the argument of perigee. This is done in order to achieve the sharing of the relative trajectories.

One important thing to notice is that the definition of the relative trajectory done throughout this chapter can be established in whatever rotating frame of reference that rotates at a constant speed with respect to the inertial frame of reference, and thus, it does not have to be the one fixed with the movement of the Earth. This has two important implications. The first one is that the methodology can be used in constellations orbiting any celestial body. The second one is that even if the satellites rotate a particular celestial body, the definition of the constellation does not have to be made in the reference frame fixed to the central body, it can be made in other reference system, increasing the freedom in the design. However, in most applications, it is more practical the use of the ECEF (Earth Centered - Earth Fixed) frame of reference as it defines the constellation in a relative to Earth position, so during this chapter, it is assumed that the design of the constellation is done in the ECEF frame of reference.

6.1.1 Constellation design with a common relative trajectory

The objective of this design model is to generate a constellation whose satellites share the same relative trajectory over time. The first thing required to achieve this condition is to define that particular relative trajectory. It is worth noting that the relative trajectory is not required to be closed in the proposed methodology.

The position of a satellite along its trajectory in the perifocal frame of reference is:

$$\mathbf{x} = (r\cos f,\ r\sin f,\ 0)\,, \tag{6.1}$$

where r is the radius of the orbit in each instant of time:

$$r = \frac{a\left(1-e^2\right)}{1+e\cos f}, \tag{6.2}$$

and f is the true anomaly of the satellite.

These positions can be expressed in the inertial frame of reference (ECI: Earth Centered Inertial) using rotational matrices ($\mathcal{R}_3$ and $\mathcal{R}_1$):

$$\mathbf{x}|_{ECI} = \mathcal{R}_3(\Omega)\,\mathcal{R}_1(i)\,\mathcal{R}_3(\omega)\,\mathbf{x}, \tag{6.3}$$

and it can also be expressed in the ECEF (Earth Centered - Earth Fixed) frame of reference:

$$\mathbf{x}|_{ECEF} = \mathcal{R}_3(-\psi_{G0} - \omega_{\oplus} t)\,\mathbf{x}|_{ECI}, \tag{6.4}$$

where ψ_{G0} is the longitude of Greenwich at the time of reference $t = 0$ and $\omega_{\oplus}$ is the angular velocity of rotation of the Earth.

Thus, using Equations (6.1), (6.3) and (6.4), the position of a certain satellite is obtained in the ECEF frame of reference:

$$\mathbf{x}|_{ECEF} = \mathcal{R}_3(-\psi_{G0} - \omega_{\oplus} t)\,\mathcal{R}_3(\Omega)\,\mathcal{R}_1(i)\,\mathcal{R}_3(\omega) \begin{pmatrix} r\cos f \\ r\sin f \\ 0 \end{pmatrix}, \tag{6.5}$$

where combining the first two matrices, the following expression is obtained:

$$\mathbf{x}|_{ECEF} = \mathcal{R}_3(\Omega - \psi_{G0} - \omega_{\oplus} t)\,\mathcal{R}_1(i)\,\mathcal{R}_3(\omega) \begin{pmatrix} r\cos f \\ r\sin f \\ 0 \end{pmatrix}. \tag{6.6}$$

The aim now is to create a constellation of satellites whose trajectories in the ECEF frame of reference are the same. To be able to do that, the orbital elements a, e, i and ω must be equal for all the satellites of the constellation. Let a, e, i, ω, Ω_0 be the orbital parameters of the reference trajectory and let t_0 be the reference time of the constellation which is associated with a reference satellite of the constellation (which can be an actual satellite or a fictitious position). This reference trajectory (named $\mathbf{x_0}$) can be expressed in the relative frame of reference as:

$$\mathbf{x_0}|_{ECEF} = \mathcal{R}_3(\Omega_0 - \psi_{G0} - \omega_{\oplus} t)\,\mathcal{R}_1(i)\,\mathcal{R}_3(\omega) \begin{pmatrix} r\cos f \\ r\sin f \\ 0 \end{pmatrix}, \tag{6.7}$$

where r and f are a function of $\mathbf{t}$. This relative trajectory must be fulfilled by every satellite in the constellation, so it is fixed in the design of the constellation. If another point of this relative trajectory is considered, a satellite that shares the same relative trajectory can be obtained. If the value of t_0 is modified, this relative trajectory remains the same. Let t_1 be the changed value of t_0,

then, the right ascension of the ascending node suffers a variation of $\Delta\Omega = -\omega_{\oplus}(t_1 - t_0)$. Thus, the relative trajectory of the satellite ($\mathbf{x_1}$) when t_1 is considered is:

$$\mathbf{x_1}|_{ECEF} = \mathcal{R}_3\left(\Omega_0 - \psi_{G0} - \omega_{\oplus}(t_1 - t_0 + t)\right)\mathcal{R}_1\left(i\right)\mathcal{R}_3\left(\omega\right)\begin{pmatrix} r\cos f \\ r\sin f \\ 0 \end{pmatrix}, \tag{6.8}$$

where r and f are now a function of $(t_1 + t)$. From Equation (6.8) and using the inverse relation of Equation (6.4), the inertial orbit of this second satellite can be obtained through:

$$\mathbf{x_1}|_{ECI} = \mathcal{R}_3\left(\psi_{G0} + \omega_{\oplus}t\right)\mathbf{x_1}|_{ECEF}, \tag{6.9}$$

so the inertial orbit is:

$$\mathbf{x_1}|_{ECI} = \mathcal{R}_3\left(\Omega_0 - \omega_{\oplus}(t_1 - t_0)\right)\mathcal{R}_1\left(i\right)\mathcal{R}_3\left(\omega\right)\begin{pmatrix} r\cos f \\ r\sin f \\ 0 \end{pmatrix}. \tag{6.10}$$

In other words, let $\{a, e, i, \omega, \Omega_0, M_0\}$ and $\{a, e, i, \omega, \Omega_1, M_1\}$ be the classical orbital elements of two satellites where M_0 and M_1 are given for the initial time. We impose that both satellites lay in the same relative trajectory:

$$\mathbf{x_0}|_{ECEF}(t + (t_1 - t_0)) = \mathbf{x_1}|_{ECEF}(t) \quad \forall t \in \mathbb{R}, \tag{6.11}$$

where $t_1 - t_0$ is the time that satellite 0 requires to reach the same position of satellite 1 in the relative trajectory. Then, in the inertial frame of reference and following Equation (6.10), a relation between both right ascensions of the ascending nodes can be obtained:

$$\Omega_1 = \Omega_0 - \omega_{\oplus}(t_1 - t_0). \tag{6.12}$$

On the other hand, the mean anomaly of the reference satellite can be defined as:

$$M = n(t + t_0 - \tau), \tag{6.13}$$

where τ is the time of pass for the perigee, t_0 is the time of reference of the constellation and n is the mean motion of the satellite, which, for a keplerian movement is:

$$n = \sqrt{\frac{\mu}{a^3}}, \tag{6.14}$$

being μ the standard gravitational constant of the Earth. As all the inertial orbits are identical except for a rotation and a time of reference, we can define τ as the time of pass for the perigee of the leading satellite of the constellation, that is, satellite 0. It is important to notice that with this definition, τ becomes independent of the satellite of study. Thus, the mean anomaly of satellite 1 can be expressed as:

$$M_1 = n(t + t_1 - \tau), \tag{6.15}$$

where t_1 is the reference time of satellite 1. Then, a relation between both mean anomalies can be obtained:

$$M_1 = M_0 + n(t_1 - t_0). \tag{6.16}$$

As it can be seen, combining Equations (6.12) and (6.16), a function between M_1 and Ω_1 can be established:

$$M_1 = \left(M_0 + \frac{n}{\omega_\oplus}\Omega_0\right) - \frac{n}{\omega_\oplus}\Omega_1; \tag{6.17}$$

which represent a straight line ($M_1(\Omega_1)$ with a slope of $n/\omega_\oplus$) as it can be seen in the (Ω, M)-space [13] representation of the relative trajectory shown in Figure 6.1, where each vertical line represents the inertial orbit and the diagonal represents the relative trajectory of the satellite for a particular instant.

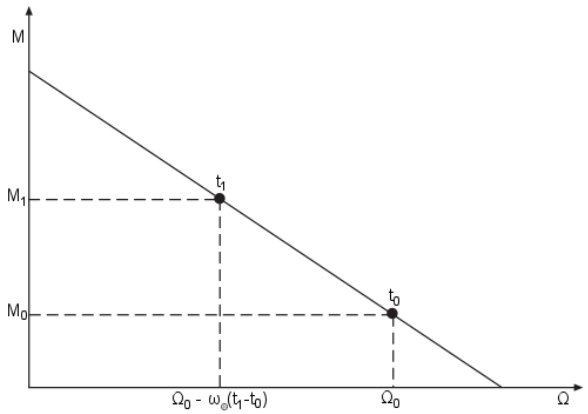

Figure 6.1: (Ω, M)-space representation of a relative trajectory.

If instead of only one satellite, a certain number of them are taken, it is possible to generate a constellation whose satellites share the same relative trajectory. Let t_q be the temporal positions in the relative trajectory (in the same sense as t_1 worked) and let N_{st} be the number of satellites in the relative trajectory, where $q \in [1, N_{st}]$ represent each particular satellite of the constellation. Then, for each q:

$$M_q = \left(M_0 + \frac{n}{\omega_\oplus}\Omega_0\right) - \frac{n}{\omega_\oplus}\Omega_q; \tag{6.18}$$

and the inertial orbits can be expressed as:

$$\mathbf{x_q}|_{ECI} = \mathcal{R}_3\left(\Omega_0 - \omega_\oplus(t_q - t_0)\right)\mathcal{R}_1\left(i\right)\mathcal{R}_3\left(\omega\right)\begin{pmatrix} r\cos f \\ r\sin f \\ 0 \end{pmatrix}. \tag{6.19}$$

As Equation (6.19) shows, the first matrix corresponds to a rotation in a modified right ascension of the ascending node for each satellite. Let Ω_q be the right ascension of the ascending node of the satellite q, then:

$$\Omega_q = \Omega_0 - \omega_\oplus(t_q - t_0). \tag{6.20}$$

Note that $(t_q - t_0)$ represents a distribution over time with respect to the reference trajectory defined in the beginning, and as such, it does not depend on the time (t) used in the propagation, that is, it remains constant. Moreover, t_q and $\omega_\oplus$ are also constant in time, so it can be concluded that Ω_q is fixed for each satellite of the constellation. On the other hand, the initial value of the true anomaly of each satellite of the constellation (f_q) only depends on t_q. Then, it is possible to generate the full constellation by the only use of the parameter of distribution t_q. Each inertial orbit of the constellation is obtained by:

$$\mathbf{x_q}|_{ECI} = \mathcal{R}_3\left(\Omega_0 - \omega_\oplus(t_q - t_0)\right)\mathcal{R}_1\left(i\right)\mathcal{R}_3\left(\omega\right)\begin{pmatrix} \frac{a\left(1-e^2\right)}{1+e\cos f_q}\cos f_q \\ \frac{a\left(1-e^2\right)}{1+e\cos f_q}\sin f_q \\ 0 \end{pmatrix}. \tag{6.21}$$

Equation (6.21) allows to design a distribution of satellites in which all have the same relative trajectory (and thus, they share the same ground-track). This distribution is done over time, with no constraints in the selection of the different values of t_q which is the parameter of distribution in the configuration.

A more compact representation of the distribution can be done combining Equations (6.18) and (6.20), which lead to:

$$\begin{aligned} \Omega_q &= \Omega_0 - \omega_\oplus(t_q - t_0); \\ M_q &= M_0 + n(t_q - t_0); \end{aligned} \tag{6.22}$$

where t_q is the parameter of distribution of the configuration, and Ω_0, t_0 and M_0 are the parameters related to the leading satellite.

6.1.1.1 Example of constellation defined in a single relative trajectory

As an example of application, a constellation consisting on five satellites is selected. The semi-major axis of the constellation is $a = 14420\,km$, the eccentricity is $e = 0.4$ and the inclination is $i = 63.435^o$. Suppose that a distribution of satellites is required in such a way that once the first satellite has observed a particular region, the rest of the satellites have to pass over the same region but with a delay of five minutes between them.

Without losing generality, let $\Omega_0 = 0$, $M_0 = 0$ and $t_0 = 0$ be the parameters of the leading satellite. Then, the time distribution of the constellation is defined by the following relation:

$$t_q = 300(q-1); \tag{6.23}$$

where $q \in [1, 5]$ defines the parameter of distribution for each particular satellite and 300 represents the delay in seconds between satellites. From Equation (6.22), the following distribution is obtained:

$$\begin{aligned} \Omega_q &= -\omega_\oplus t_q; \\ M_q &= n t_q; \end{aligned} \tag{6.24}$$

Table 6.1: Initial distribution of the constellation.

Element	Sat. 1	Sat. 2	Sat. 3	Sat. 4	Sat. 5
Ω_q (deg)	0.000	-1.2534	-2.5068	-3.7603	-5.0137
M_q (deg)	0.000	6.2671	12.5342	18.8013	25.0684

which leads to the configuration shown in Table 6.1.

Figure 6.2 shows the inertial and relative trajectories of the constellation. As it can be seen, the relative trajectory is common for all the satellites in the constellation whilst they have five different inertial orbits. One important property of this design is that, even if we decrease the distances between satellites, it is not possible for the satellites to collide because they are moving in the same relative trajectory which does not have self intersections.

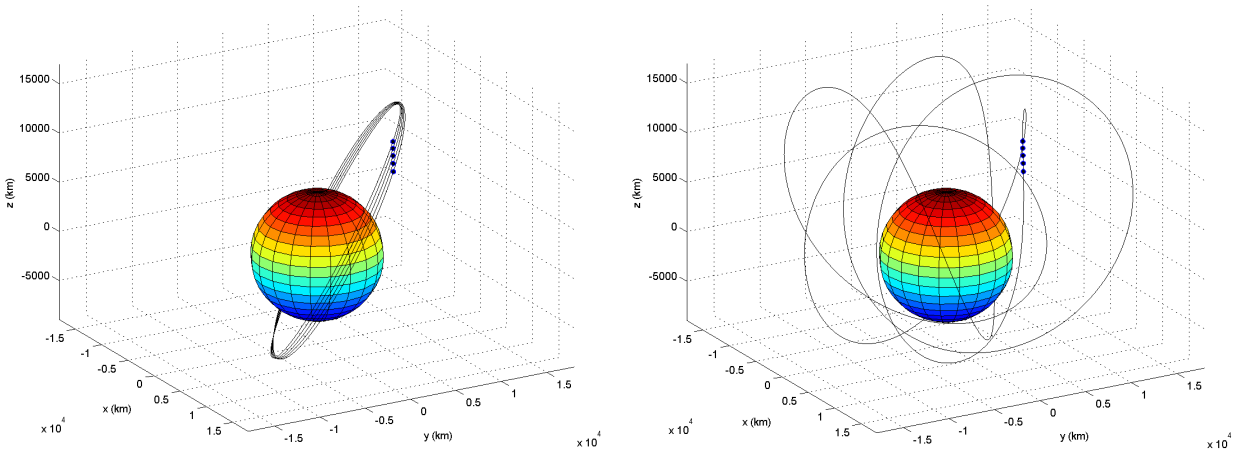

Figure 6.2: Inertial (left) and relative (right) trajectories of the constellation.

6.1.2 Constellation design with multiple relative trajectories

The objective now is to distribute the satellites in more than one relative trajectory. The methodology is similar to the previous one (see Section 6.1.1), but in this case, other degrees of freedom are added in the spacing of the relative trajectories in the ECEF frame of reference. Let N_t be the number of relative trajectories in which the constellation is distributed and let $k \in [1, N_t]$ be the parameter that names each one of this trajectories. Therefore, the total number of satellites in the constellation N_s is:

$$N_s = N_{st} N_t, \tag{6.25}$$

where N_{st} is the number of satellites in each relative trajectory.

Furthermore, the satellites named with the sub-index $k0$ are the leading satellites of each k relative trajectory, that is, the reference satellites that define the trajectories in the ECEF frame of reference. Moreover, the leading satellite, named with the sub-index 00, represents the reference origin of the

whole constellation. Thus, as seen before, the relative trajectories can be defined as:

$$\mathbf{x_{kq}}|_{ECEF} = \mathcal{R}_3(\sigma)\,\mathcal{R}_1(i)\,\mathcal{R}_3(\omega)\begin{pmatrix} r\cos f \\ r\sin f \\ 0 \end{pmatrix}, \tag{6.26}$$

where:

$$\sigma = \Omega_0 + \Delta\Omega_k - \psi_{G0} - \omega_\oplus(t_{kq} - t_0 + t), \tag{6.27}$$

$\Delta\Omega_k$ is the space distribution of the relative trajectories in the ECEF frame of reference and t_{kq} represents the distribution parameter of the constellation. Note that r and f are now functions of t_{kq}. The parameter t_{kq} distributes the satellites in a k relative trajectory and the q position in that relative trajectory. As it can be seen, two degrees of freedom control the distribution of the constellation: $\Delta\Omega_k$ and t_{kq}.

Transforming those coordinates to the ECI frame of reference, and naming f_{kq} the true anomaly of the satellite q of the k relative trajectory at the initial time, the following inertial orbits for each satellite of the constellation are obtained:

$$\mathbf{x_{kq}}|_{ECI} = \mathcal{R}_3(\Omega_{kq})\,\mathcal{R}_1(i)\,\mathcal{R}_3(\omega)\begin{pmatrix} \dfrac{a\left(1-e^2\right)}{1+e\cos f_{kq}}\cos f_{kq} \\ \dfrac{a\left(1-e^2\right)}{1+e\cos f_{kq}}\sin f_{kq} \\ 0 \end{pmatrix}, \tag{6.28}$$

where the right ascension of the ascending node of each satellite is:

$$\Omega_{kq} = \Omega_0 + \Delta\Omega_k - \omega_\oplus(t_{kq} - t_0), \tag{6.29}$$

which means that, in general, each satellite presents a different inertial orbit.

This distribution can also be represented in the $(\Omega,\ M)$-space. As done before:

$$\begin{aligned} \Omega_{kq} &= \Omega_0 + \Delta\Omega_k - \omega_\oplus(t_{kq} - t_0), \\ M_{kq} &= M_0 + n(t_{kq} - t_0), \end{aligned} \tag{6.30}$$

and the relation between Ω_{kq} and M_{kq} is:

$$M_{kq} = \left(M_0 + \frac{n}{\omega_\oplus}\Omega_0\right) + \frac{n}{\omega_\oplus}\Delta\Omega_k - \frac{n}{\omega_\oplus}\Omega_{kq}; \tag{6.31}$$

which is a distribution of points over a family of straight lines that have the same slope. Figure 6.3 shows a particular case of a satellite with respect to the reference trajectory (named 0). There, the satellite 11 ($k = 1, q = 1$) is located in the relative trajectory 1 which presents a rotation of $\Delta\Omega_1$ with respect to the reference trajectory.

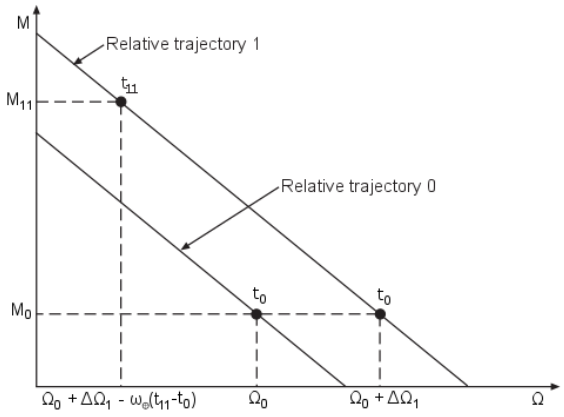

Figure 6.3: (Ω, M)-space representation of the configuration for multiple relative trajectories.

6.1.2.1 Example of constellation defined in various relative trajectories

As an example of this section, we present a sun synchronous constellation based on 15 satellites distributed in 3 relative trajectories and circular orbits. The constellation has an altitude of $880\,km$, and thus, $a = 7260\ km$ and $i = 98.95^o$. Now, we choose a distribution of the constellation such that the relative trajectories are equally spaced and the satellites in each orbital plane are equally spaced in time. That way, this distribution can be expressed as:

$$\begin{aligned} \Delta\Omega_k &= 2\pi\frac{k-1}{N_t}, \\ t_{kq} &= 2\pi\frac{q-1}{N_{st}}; \end{aligned} \tag{6.32}$$

where $N_t = 3$ is the number of relative trajectories and $N_{st} = 5$ is the number of satellites per relative trajectory. Using Equation (6.30) this initial distribution leads to the following configuration:

$$\begin{aligned} \Omega_{kq} &= 2\pi\frac{k-1}{N_t} - \frac{2\pi\omega_\oplus}{n}\frac{q-1}{N_{st}}, \\ M_{kq} &= 2\pi\frac{q-1}{N_{st}}, \end{aligned} \tag{6.33}$$

where $k \in [1, N_t]$ and $q \in [1, N_{st}]$. The distribution is shown in the (Ω, M)-space in Figure 6.4, where it can be observed how the satellites are positioned in three different lines that represent the relative trajectories of the constellation.

Figure 6.5 shows the inertial and relative trajectories of the constellation. As it can be seen, there are 15 different orbits, one for each satellite, however there are only three different relative trajectories (a solid line, a dashed line and a dotted line), which was the objective sought.

As it can be seen from Figures 6.4 and 6.5, this distribution generates too many different orbital planes, one per satellite, a fact that increases the expenses of building the constellation in orbit. Therefore, in the next subsection the constraint of minimum number of inertial orbits will be set in order to correct this situation.

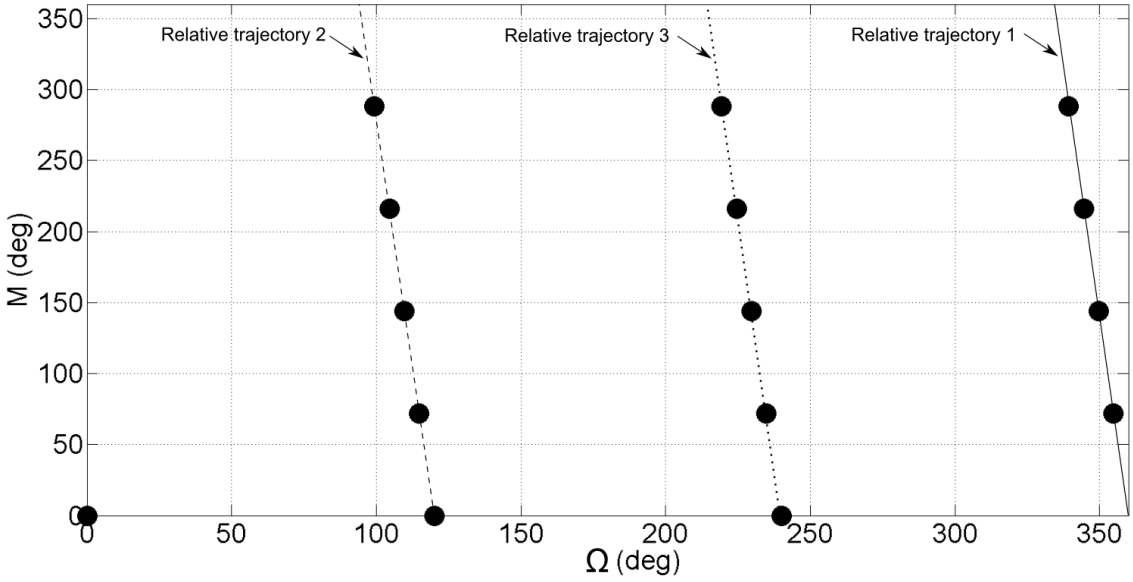

Figure 6.4: $(\Omega,\ M)$-space, where each point represents a satellite in the constellation.

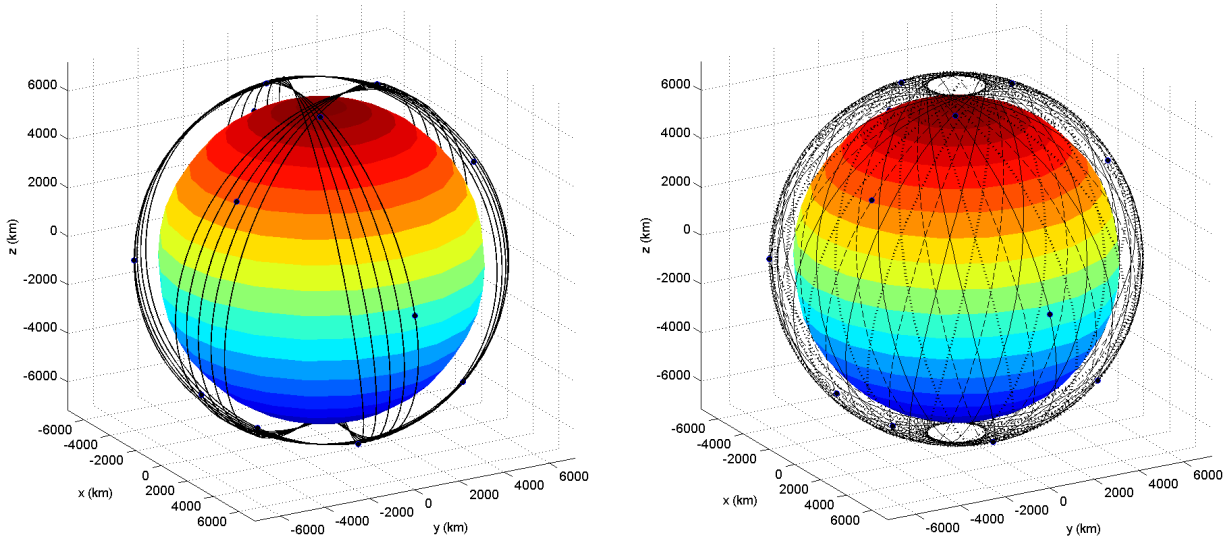

Figure 6.5: Inertial (left) and relative (right) trajectories of the constellation.

6.1.3 Constellation design with minimum number of inertial orbits

Once a distribution over different relative trajectories is done, it is interesting to impose the restriction that the constellation has to be built in the least number of inertial orbits due to costs reduction. As seen before, the procedure places the satellites in different relative trajectories. Nevertheless, there is no constraint with respect to the inertial frame of reference, and in fact, each Ω_{kq} is in general different. The aim now is to impose that the values of Ω_{kq} are shared between relative trajectories.

The parameter t_{kq} is a time distribution of the satellites in the constellation, but in reality, there exist two effects provoked by this parameter, the movement along the relative trajectory and the spacing of the inertial orbits. On the other hand, the spacing of the relative trajectories is controlled by the parameter $\Delta\Omega_k$. As we require to reduce the number of inertial orbits to a minimum, a relation between t_{kq} and $\Delta\Omega_k$ has to be found in order to achieve this condition. As t_{kq} is a distribution, we can separate it in two different parameters t_k and t_q such that:

$$t_{kq} = t_k + t_q, \tag{6.34}$$

where t_q is related to the distribution of satellites in the same relative trajectory as done in Section 6.1.1, and we want t_k to be related with the inertial orbits. In order to achieve that, we impose the right ascension of the ascending node to be independent of the parameter k, in the form of t_k or $\Delta\Omega_k$. That way, the number of inertial orbits only depends on t_q, which is related with the number of points per relative trajectory.

Thus, applying Equation (6.34) in Equation (6.29), we obtain:

$$\Omega_{kq} = \Omega_0 + \Delta\Omega_k - \omega_\oplus(t_k + t_q - t_0), \tag{6.35}$$

where it is possible to eliminate the dependence on k imposing:

$$t_k = \frac{\Delta\Omega_k}{\omega_\oplus}, \tag{6.36}$$

and thus, introducing this value for t_k in Equation (6.35) the following expression for the right ascension of the ascending node is obtained:

$$\Omega_{kq} = \Omega_0 - \omega_\oplus(t_q - t_0). \tag{6.37}$$

Note that now, Ω_{kq} does not depend on the terms in k, and as such, is the same for every satellite that shares the value of t_q, one for each relative trajectory. That leads to a distribution in which the satellites with the same q are distributed in the same inertial orbit whilst the satellites with the same k are distributed in the same relative trajectory (remember that f_{kq} is a function of $t_q + t_k$). Figure 6.6 shows how the distribution works in the ECEF and the ECI frames of reference for two generic relative trajectories.

The (Ω, M)-space representation can be defined as before:

$$\begin{aligned} \Omega_{kq} &= \Omega_0 - \omega_\oplus(t_q - t_0), \\ M_{kq} &= M_0 + n\left(\frac{\Delta\Omega_k}{\omega_\oplus} + t_q - t_0\right), \end{aligned} \tag{6.38}$$

obtaining the same expression as in Equation (6.31):

$$M_{kq} = \left(M_0 + \frac{n}{\omega_\oplus}\Omega_0\right) + \frac{n}{\omega_\oplus}\Delta\Omega_k - \frac{n}{\omega_\oplus}\Omega_{kq}. \tag{6.39}$$

The difference now is that the right ascension of the ascending node is shared by one satellite of each relative trajectory as seen in Figure 6.7. In fact this is a particular case of the one presented in Section 6.1.2.

Using the two time distributions t_q and t_k, it is possible to achieve the configuration desired with no constraints in the distribution, generating constellation configurations distributed in a reduced number of orbital planes.

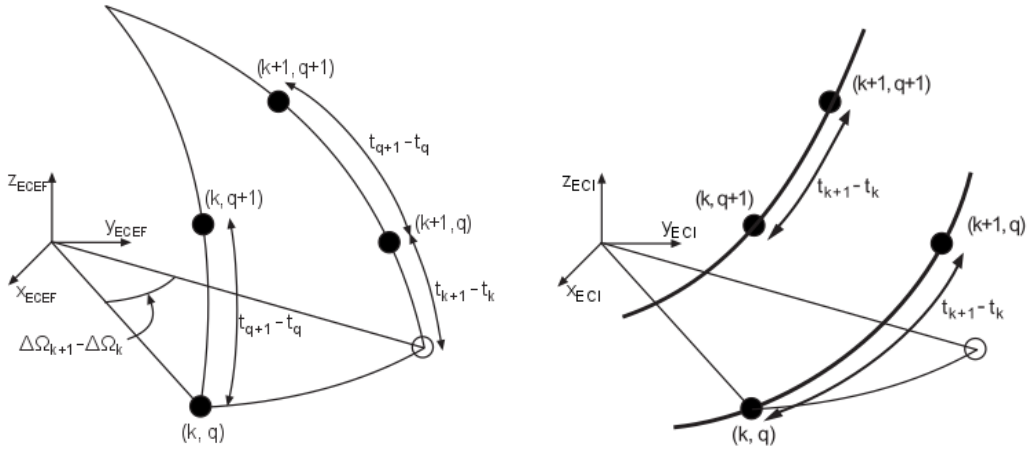

Figure 6.6: Constellation distribution in the ECEF (left) and ECI (right) frames of reference.

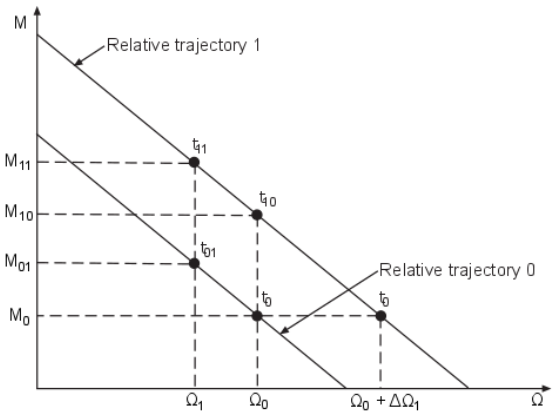

Figure 6.7: (Ω, M)-space representation of the configuration for minimum number of inertial orbits.

6.1.3.1 Example of constellation defined in various relative trajectories with minimum number of inertial orbits

As an example of application, a constellation of five satellites is chosen. This time we impose as a requirement of the mission that the satellites have to be distributed forming a "+" shape during their movement around the Earth. Let $a = 26562\,km$, $e = 0$ and $i = 50^o$ be the orbital parameters of the constellation, and let $\Omega_0 = 0$, $M_0 = 0$ and $t_0 = 0$ be the parameters of the leading satellite.

In order to design the constellation, three relative trajectories and three inertial orbits are required to be able to obtain that shape. So three different values of t_q (inertial orbits) and three different values of $\Delta\Omega_k$ (relative trajectories) must be taken. We define the first relative trajectory as the one that contains the central point of the "+" ($k = 1$), being the upper and lower points also contained in this relative trajectory (see Figure 6.8). On the other hand, the left and right points are contained in two different relative trajectories, $k = 2$ and $k = 3$ respectively. Moreover, the left and right points of the "+" are defined in the same inertial orbits as the upper and lower points, more precisely, the left and the upper points have the same inertial orbit $q = 2$, whilst the right and

lower point are contained in the same inertial orbit $q = 3$. The central point has its own inertial orbit $q = 1$.

If the delay between satellites in the same relative trajectory is taken as 10 minutes, the values of t_q can be defined as: $t_1 = 0\,s$, $t_2 = 600\,s$ and $t_3 = -600\,s$. Regarding the values of $\Delta\Omega_k$ and for the sake of simplicity, we choose $\Delta\Omega_1 = 0$, $\Delta\Omega_2 = -\omega_{\oplus} t_2$ and $\Delta\Omega_3 = -\omega_{\oplus} t_3$. With those parameters, the distribution of the constellation is shown in Table 6.2, where Sat. (k, q) represents the satellite contained in the inertial orbit q and the relative trajectory k.

Table 6.2: Initial distribution of the constellation.

Element	Sat. $(1,1)$	Sat. $(1,2)$	Sat. $(1,3)$	Sat. $(2,2)$	Sat. $(3,3)$
Ω_{kq} (deg)	0	-2.5068	2.5068	-2.5068	2.5068
M_{kq} (deg)	0	5.0137	-5.0137	0	0

Figure 6.8 shows the inertial orbits and relative trajectories of the constellation. As it can be seen, the constellation is built in three different inertial orbits and three relative trajectories generating the "+" shape that we were aiming for.

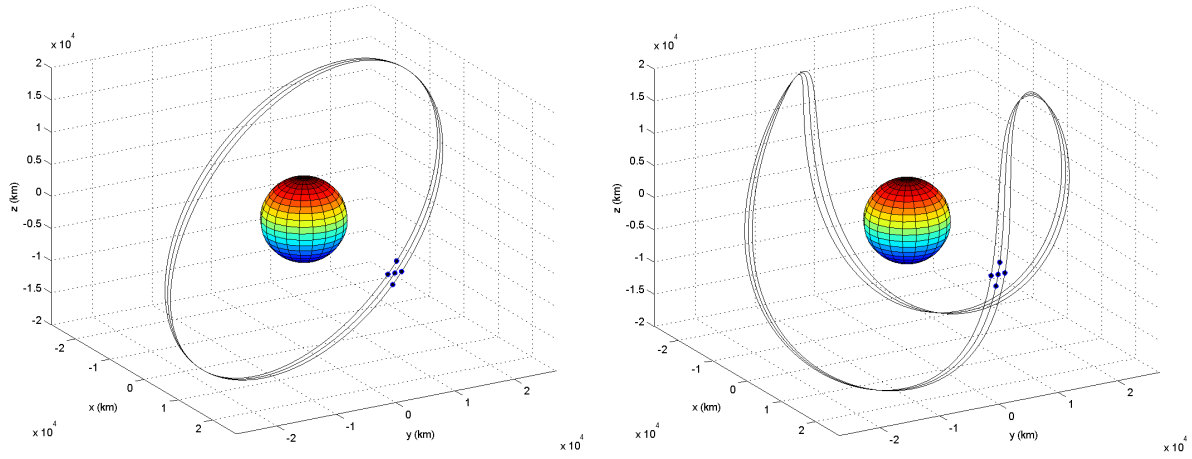

Figure 6.8: Inertial (left) and relative (right) trajectories of the constellation.

6.2 Perturbed model for constellation design

Previously, it has been seen how to generate the constellation design in a keplerian model. The objective now is to apply this methodology to the case of orbital perturbations. Orbital perturbations such as the gravitational potential of the Earth, the solar radiation pressure, the Sun and Moon as disturbing third bodies or the atmospheric drag, will destroy the keplerian configuration proposed in a short period of time, so other complementary model has to be developed to solve this problem. The perturbed model proposed in this chapter achieves the sharing of the relative trajectories despite of being the satellites subjected to certain known orbital perturbations.

This methodology can be applied with any kind of orbital propagators (analytical, semi-analytical or numerical) not having any constraint in that respect.

As done in the latter section, three different constellation designs will be presented, corresponding to the ones studied previously in the keplerian model. That way, a clearer exposition of the methodology is presented.

6.2.1 Constellation design with a common relative-trajectory

The objective is to generate a constellation whose satellites share the same relative trajectory despite of being subjected to several known orbital perturbations. Note that sharing the same relative trajectory does not mean that it has to be closed, in fact, the model is independent of this property.

The idea behind the perturbed model is to propagate first a reference satellite $\mathbf{x_0}$, which will be called the leading satellite, taking into account all the perturbations of the dynamical model chosen, and keeping the results of times, positions and velocities of the propagation in certain moments to generate the positions and velocities of the satellites of the constellation. The information that is kept correspond to the moments when:

$$t = t_q - t_0, \tag{6.40}$$

where t_0 is the reference time of the leading satellite, and t_q represents the parameter of distribution of each particular satellite. Moreover, using the nomenclature introduced in the keplerian model, $q \in [1, N_{st}]$.

Then, a transformation of these positions and velocities, given in the ECI frame of reference, will be performed in order to define the initial positions and velocities of the satellites of the constellation. Therefore, two transformations will be required: the first one to define the relative trajectory, and the second one to obtain the inertial orbits that have generated that relative trajectory and correspond to satellites of the constellation.

Let $\tilde{\mathbf{x}}_\mathbf{q}|_{ECI}$ and $\tilde{\mathbf{v}}_\mathbf{q}|_{ECI}$ be the positions and velocities of the leading satellite in the inertial frame of reference. The relative positions ($\mathbf{x_q}|_{ECEF}$) and velocities ($\mathbf{v_q}|_{ECEF}$) are obtained from the inertial ones by using the following expressions:

$$\begin{aligned} \mathbf{x_q}|_{ECEF} &= \mathcal{R}_3\left(-\psi_{G0} - \omega_\oplus (t_q - t_0)\right) \tilde{\mathbf{x}}_\mathbf{q}|_{ECI}, \\ \mathbf{v_q}|_{ECEF} &= \mathcal{R}_3\left(-\psi_{G0} - \omega_\oplus (t_q - t_0)\right) \tilde{\mathbf{v}}_\mathbf{q}|_{ECI} - \boldsymbol{\omega}_\oplus \times \mathbf{x_q}|_{ECEF}. \end{aligned} \tag{6.41}$$

However, the initial inertial positions $\mathbf{x_q}|_{ECI}$ and velocities $\mathbf{v_q}|_{ECI}$ are required in order to define the constellation, thus, the second transformation of frames of reference is needed:

$$\begin{aligned} \mathbf{x_q}|_{ECI} &= \mathcal{R}_3\left(\psi_{G0}\right) \mathbf{x_q}|_{ECEF}, \\ \mathbf{v_q}|_{ECI} &= \mathcal{R}_3\left(\psi_{G0}\right) \mathbf{v_q}|_{ECEF} + \boldsymbol{\omega}_\oplus \times \mathbf{x_q}|_{ECI}. \end{aligned} \tag{6.42}$$

One important thing to notice is that, having included the perturbations in the initial orbit propagation, all the satellites follow the same relative trajectory for the perturbations considered in the constellation design. Thus, the more realistic the orbital perturbation model is, the better the constellation will perform in the reality.

6.2.2 Constellation design with multiple relative trajectories

The next step in complexity in the design of a constellation is to include multiple relative trajectories in the configuration. The process is similar as before, but now, several leading satellites are required in order to define the different relative trajectories, one leading satellite for each relative trajectory. Furthermore, the distribution of the satellites is done using two parameters: the time distribution over the different relative trajectories t_{kq} and the angular distribution of the relative trajectories in the ECEF frame of reference $\Delta\Omega_k$.

As it has been said, each relative trajectory requires a leading satellite. Those satellites have the same values of a_0, e_0, i_0 and w_0, whilst the right ascension of the ascending node follows:

$$\Omega_{k0} = \Omega_0 + \Delta\Omega_k - \omega_\oplus \left(t_{k0} - t_0\right), \tag{6.43}$$

where Ω_{k0} are the right ascension of the ascending nodes of the leading satellites and each relative trajectory is named as $k \in [1, N_t]$. Moreover, each one can present a different reference with respect to the global reference time of the constellation t_0, that means that in general, each leading satellite define a time of reference for each relative trajectory t_{k0}.

Once the leading satellites are defined, each one of them is propagated for a time equal to at least the maximum value of $(t_{kq} - t_{k0})$, that is, the maximum distance in time between the leading satellite and the satellites in the constellation related to it. This generates a number of relative trajectories equal to N_t, the number of different relative trajectories of the constellation. As previously, the values of the positions and velocities of each relative trajectory for the moments when $(t = t_{kq} - t_0)$ are kept, which represent the distribution of the constellation, and two transformations are performed:

$$\begin{aligned}
&\mathbf{x_{kq}}|_{ECEF} = \mathcal{R}_3\left(-\psi_{G0} - \omega_\oplus(t_{kq} - t_0)\right)\tilde{\mathbf{x}}_{\mathbf{kq}}|_{ECI},\\
&\mathbf{v_{kq}}|_{ECEF} = \mathcal{R}_3\left(-\psi_{G0} - \omega_\oplus(t_{kq} - t_0)\right)\tilde{\mathbf{v}}_{\mathbf{kq}}|_{ECI} - \boldsymbol{\omega}_\oplus \times \mathbf{x_{kq}}|_{ECEF};\\
&\mathbf{x_{kq}}|_{ECI} = \mathcal{R}_3\left(\psi_{G0}\right)\mathbf{x_{kq}}|_{ECEF},\\
&\mathbf{v_{kq}}|_{ECI} = \mathcal{R}_3\left(\psi_{G0}\right)\mathbf{v_{kq}}|_{ECEF} + \boldsymbol{\omega}_\oplus \times \mathbf{x_{kq}}|_{ECI}.
\end{aligned} \tag{6.44}$$

The values of the inertial positions $\mathbf{x_{kq}}|_{ECI}$ and velocities $\mathbf{v_{kq}}|_{ECI}$ of each satellite determine the initial configuration of the constellation. This configuration distributes the constellation in N_t different relative trajectories and a number of inertial orbits equal to the number of satellites (in general). This is the same case as the one seen in Section 6.1.2 but for a non keplerian model. In that regard, having too many different orbital planes in the constellation increases the costs of the mission, therefore, it is required to include the constraint of minimum number of inertial orbits which is presented in the next section.

6.2.3 Constellation design with minimum number of inertial orbits

The latter configuration distributes the constellation in N_s different inertial orbits, which is a design decision that carries a lot of expenses to build the constellation in orbit. In order to solve that, and as done Section 6.1.3, the distribution parameter can be separated in two different distribution parameters t_k and t_q, where $t_{kq} = t_k + t_q$. Then, a relation can be established between t_k and Ω_k using Equation (6.36). However, the orbital perturbations make the right ascension of the

ascending node to shift and therefore, the configuration obtained from the keplerian procedure does not generate orbits in the same inertial planes.

In order to solve that, we introduce a modification in the distribution of t_k from Equation (6.36) that allows to include the effects of the shifting of the right ascension of the ascending node in the formulation. If we fix a frame of reference in the orbit, we observe that the Earth does not rotate at $\omega_\oplus$ due to the shifting in the right ascension of the ascending node. In this frame of reference, the Earth rotates respect to the orbit at $\omega_\oplus - \dot{\Omega}$, where $\dot{\Omega}$ is the derivative of the right ascension of the ascending node. Thus, applying this modification to Equation (6.36), we obtain:

$$t_k = \frac{\Delta\Omega_k}{\omega_\oplus - \dot{\Omega}_{k0}}, \tag{6.45}$$

where $\dot{\Omega}_{k0}$ is the derivative of the right ascension of the ascending node for the leading satellite of the relative trajectory k, which can be obtained using the secular value of the perturbation. The value of t_k is introduced in Equation (6.44) leading to a constellation based on N_s satellites distributed in N_t relative trajectories and N_{st} inertial orbits. All this design includes the orbital perturbations considered in the propagations that were made.

6.3 Constellation design based on equally spaced in time distributions

The aim of this section is to define a constellation distribution that is equally spaced in time, basing the design in the case of multiple relative trajectories and minimum number of inertial orbits. In order to do this kind of distribution, it is required to have a closed relative track, which defines a repeating cycle that allows to define the distribution.

Let a cycle be the time that a satellite requires to repeat its ground-track, and let T_c be the period of this cycle. In order to achieve the repeating ground-track property, the orbital parameters have to fulfill a relation with the rotation of the Earth, given by:

$$T_c = N_p T_\Omega = N_d T_{\Omega G}, \tag{6.46}$$

where N_p is the number of orbital revolutions to cycle repetition, N_d is the number of revolutions of the ECEF frame with respect the orbital plane to cycle repetition, T_Ω is the nodal period of the orbit and $T_{\Omega G}$ is the nodal period of Greenwich.

Let N_{st} be the number of satellites in each different relative trajectory, and let $q \in [1, N_{st}]$ be the integer that names each satellite of each relative trajectory of the constellation. In order to obtain an equally spaced in time distribution in each relative trajectory, we distribute the values of t_q over the period of the cycle T_c, where $t_q < T_c$, generating the following configuration:

$$t_q = (q-1)\frac{T_c}{N_{st}}. \tag{6.47}$$

Furthermore, let N_t be the number of different relative trajectories, and let $k \in [1, N_t]$ be the integer that names each different relative trajectory of the constellation. The right ascension of the

ascending nodes of the leading satellites of each relative trajectory are expressed as:

$$\Omega_k = \Omega_0 + (k-1)\frac{2\pi}{N_t}, \tag{6.48}$$

where:

$$\Delta\Omega_k = \Omega_k - \Omega_0 = (k-1)\frac{2\pi}{N_t}. \tag{6.49}$$

Note that the right ascension of the ascending node of the leading satellites is not shared in general with the rest of the satellites situated in the same relative trajectory (see Equation (6.20)).

Using Equation (6.45), the distribution of t_k is obtained:

$$t_k = \frac{(k-1)\frac{2\pi}{N_t}}{\omega_\oplus - \dot{\Omega}_{k0}}, \tag{6.50}$$

thus, the distribution of each satellite ($t_{kq} = t_k + t_q$) for an equally spaced in time configuration is:

$$t_{kq} = (q-1)\frac{T_c}{N_{st}} + (k-1)\frac{2\pi}{N_t\left(\omega_\oplus - \dot{\Omega}_{k0}\right)}. \tag{6.51}$$

One thing to notice is that due to the possible symmetries in the configuration, two conditions have to be assured by the designer. The first one is that the parameters N_d and N_p must be relatively primes in order to avoid duplicities in the formulation (for example $N_p = 2$ and $N_d = 3$ is equivalent to $N_p = 4$ and $N_d = 6$).

The second condition is related to avoiding the overlapping of satellites in the configuration. This may occur if the distribution is uniform with symmetries in time and space, a condition that appears when the parameters N_p and N_t are relatively primes between them. Let N_f be the maximum common divisor between N_p and N_t. Then, the distribution over space is:

$$\Omega_k = \Omega_0 + (k-1)\frac{2\pi}{N_t N_f}, \tag{6.52}$$

and therefore, the distribution over time is:

$$t_{kq} = (q-1)\frac{T_c}{N_{st}} + (k-1)\frac{2\pi}{N_t N_f\left(\omega_\oplus - \dot{\Omega}_{k0}\right)}, \tag{6.53}$$

where Equations (6.52) and (6.53) substitute Equations (6.48) and (6.51) in order to avoid the overlapping of satellites.

6.4 Examples of application

In this section, two examples of application are shown. In particular, a Medium Earth Orbit Constellation and a Low Earth Orbit Constellation are presented. In these designs, constellations

whose satellites are equally spaced in time are defined (see Section 6.3). Moreover, the satellites will present the repeating ground-track property and will be distributed in the least number of inertial orbits using the perturbed model (see Section 6.2.3).

During these examples the following perturbations have been taken into account: the gravitational potential of the Earth [29] up to 4th order terms (including tesserals), the Sun and Moon as disturbing third bodies [30], the solar radiation pressure [31] and the atmospheric drag (Harris-Priester [32, 33] model). In addition, it has been supposed that all the satellites are identical in each constellation.

6.4.1 Example of Medium Earth Orbit Constellation

First, it is supposed, as part of the mission requirements, that the parameters N_p, N_d, N_{st} and N_t are known, as well as the inclination and eccentricity of the orbits. Moreover, as a mission requirement, the pass of the constellation over a certain point of the Earth with coordinates in longitude and latitude (ψ_r, ϕ_r) is imposed, and we choose $f = \pi$ over that point to maximize the time of coverage of the constellation in these coordinates.

Table 6.3: Initial positions and velocities of the constellation.

Sat. (k,q)	x [km]	y [km]	z [km]	v_x [km/s]	v_y [km/s]	v_z [km/s]
1,1	29742.291	-453.883	26500.795	-1.171	1.358	1.337
1,2	154.758	9918.577	-8829.518	-4.072	-3.511	-4.013
1,3	-29744.259	452.557	26498.609	1.171	-1.358	1.338
1,4	-160.231	-9924.333	-8822.957	4.072	3.509	-4.016
2,1	16921.730	8809.410	31186.380	-2.343	1.135	-0.134
2,2	-14103.296	-21475.852	-5338.235	-0.094	-2.969	2.559
2,3	-16924.510	-8809.572	31186.600	2.343	-1.135	-0.134
2,4	14100.583	21472.679	-5342.417	0.094	2.970	2.559
3,1	-2593.920	13813.974	22164.558	-2.884	-0.004	-2.655
3,2	-9567.105	-32767.410	13084.071	1.093	-0.422	2.330
3,3	2590.853	-13813.672	22168.897	2.884	0.004	-2.654
3,4	9564.986	32767.859	13080.263	-1.093	0.422	2.330
4,1	-9918.577	154.758	-8829.518	3.511	-4.072	-4.013
4,2	-452.557	-29744.259	26498.609	1.358	1.171	1.338
4,3	9924.333	-160.231	-8822.957	-3.509	4.072	-4.016
4,4	451.231	29746.226	26496.423	-1.357	-1.171	1.338
5,1	21475.852	-14103.296	-5338.235	2.969	-0.094	2.559
5,2	8809.572	-16924.510	31186.600	1.135	2.343	-0.134
5,3	-21472.679	14100.583	-5342.418	-2.970	0.094	2.559
5,4	-8809.735	16927.289	31186.819	-1.135	-2.343	-0.134
6,1	32767.410	-9567.105	13084.071	0.422	1.093	2.330
6,2	13813.672	2590.854	22168.896	-0.004	2.884	-2.654
6,3	-32767.859	9564.986	13080.264	-0.422	-1.093	2.330
6,4	-13813.370	-2587.787	22173.233	0.004	-2.884	-2.653

On the other hand, we impose that the semi-major axis of all the satellites of the constellation present the repeating ground-track property. This condition is achieved by the use of osculating elements in the constellation for each satellite, having considered the orbital perturbations mentioned before. This is performed by the use of the numerical method presented in the following chapter.

Once the orbital parameters are established for one satellite, it is time to generate the initial configuration of a constellation with minimum number of inertial orbits, that is, the methodology presented in Section 6.2.3 is used. However, in order to do that, the constellation distribution must be chosen firstly. For the sake of simplicity, the value of t_0 is fixed as $t_0 = 0$ and Equations (6.47) and (6.53) are used in order to define the equally spaced in time configuration.

Using this equally spaced in time distribution, we apply it to a constellation consisting of 24 satellites and show the results. The constellation repeats its ground-track each two orbital revolutions ($N_p = 2$) and each day ($N_d = 1$). Furthermore, all satellites have an inclination of $i = 63.435^o$ and an eccentricity of $e = 0.5$. A high eccentricity orbit has been selected in order to show the possibilities of the constellation design model. The constellation is distributed in 6 different relative trajectories ($N_t = 6$) and 4 inertial orbits ($N_{st} = 4$), thus $N_s = N_t N_{st} = 24$.

Note that $N_t = 6$ and $N_p = 2$ have a maximum common divisor of $N_f = 2$, so, Equations (6.52) and (6.53) must be used to perform the distribution. As a further requirement, it has been imposed that one ground-track of the constellation passes over the city of Zaragoza (Spain) with coordinates ($\phi_r = 41.698169^o$ and $\psi_r = -0.874295^o$).

With these conditions, the constellation is designed following the perturbed model proposed in this work obtaining the initial positions and velocities shown in Table 6.3. These results are given in the inertial frame of reference and generate a constellation whose satellites are distributed in 4 different inertial orbits and 6 relative trajectories.

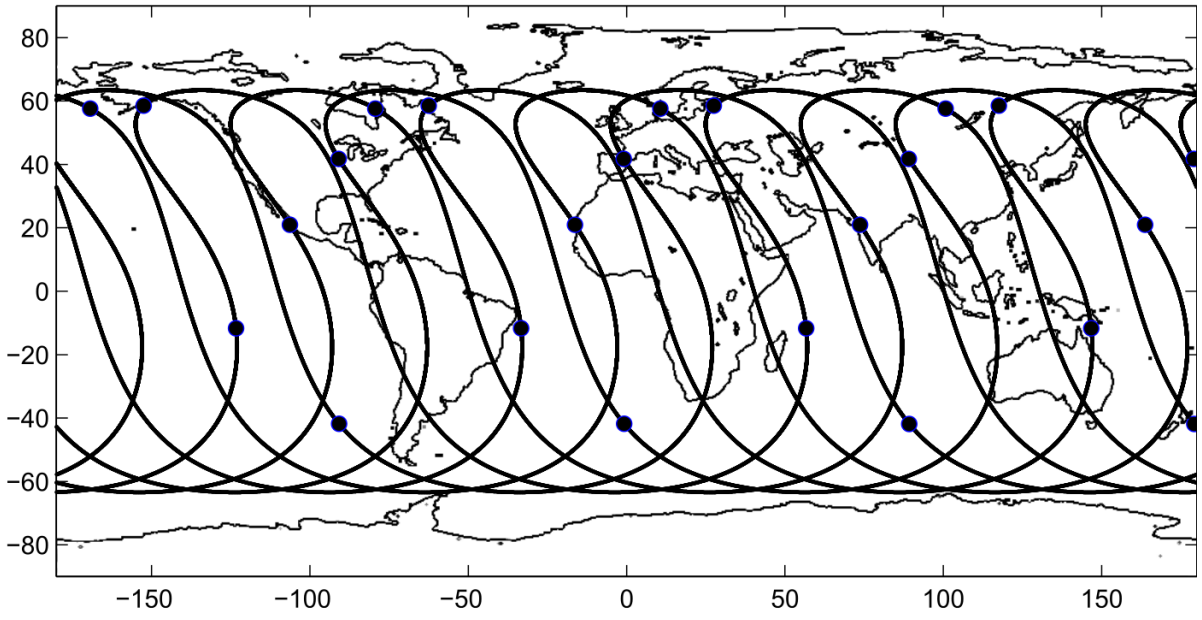

Figure 6.9: Ground-track of the constellation.

This configuration can be seen in Figure 6.9, where the ground-track of the whole constellation is presented. There, it can be observed that the constellation is distributed in 6 different ground-tracks, being them completely closed and shared by 4 satellites each.

Figure 6.10 shows the inertial (left) and relative (right) trajectories of all the satellites in the constellation. There, it can be seen how the constellation is distributed in only 4 different inertial orbits, and how the relative trajectory is shared by groups of satellites (4 for each relative trajectory). The figure allows also to see the possibilities that the definition of the constellation in the relative frame of reference brings, generalizing the orbits from a conic shape in the inertial frame of reference into a more diverse group of configurations in the relative frame of reference.

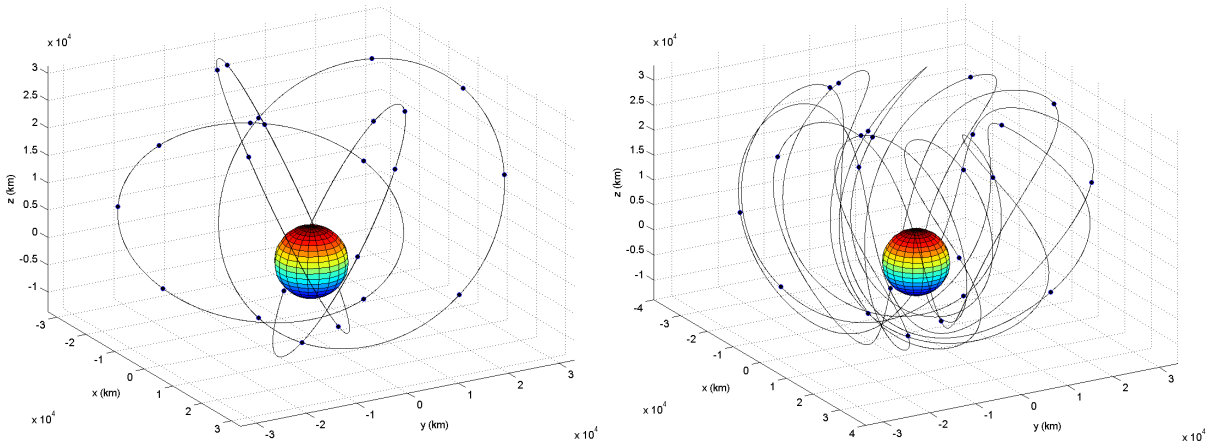

Figure 6.10: Inertial (left) and relative (right) trajectories of the constellation.

Finally, in Figure 6.11, the polar view of the constellation in the ECEF frame of reference can be observed. It can be concluded that the satellites are able to share their relative trajectories (4 satellites in each trajectory) despite of being subjected to orbital perturbations.

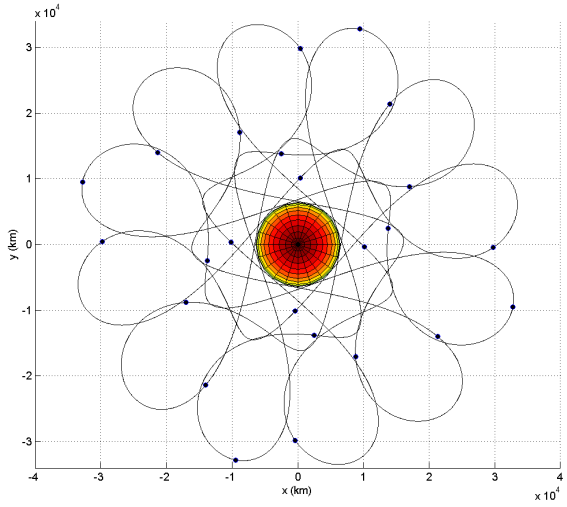

Figure 6.11: Polar view of the constellation in the ECEF frame of reference.

6.4.2 Example of Low Earth Orbit Constellation

For this second example, we choose a constellation composed by 16 satellites that has as main mission Earth observation. The constellation is distributed in circular orbits and in the same relative trajectory in the ECEF frame of reference using the uniform in time distribution seen in Section 6.3. As in the former example, the repeating ground-track property is imposed following the methodology explained for orbital perturbations. However, due to the nature of the mission, two new requirements are included, the sun-synchrony of the orbits and the ability to scan all the Earth surface in the minimum time considering a sensor with a field of view of 7.5^o that requires to work at $705 \pm 5\, km$ over the Earth surface.

With these conditions, we obtain a constellation whose satellites have $a = 7978.61\, km$, $e = 0$, $i = 98.21^o$ and that repeat a cycle of their ground-tracks in 233 orbital revolutions or 16 days. The initial positions and velocities of the satellites of the constellation can be seen in Table 6.4.

Table 6.4: Initial positions and velocities of the constellation.

Sat. (q)	x [km]	y [km]	z [km]	v_x [km/s]	v_y [km/s]	v_z [km/s]
1	5284.700	-80.647	4708.740	-4.921	-1.361	5.499
2	-3121.980	563.734	-6332.950	6.679	1.224	-3.175
3	453.969	-965.619	6999.826	-7.4332	-0.903	0.362
4	2247.912	1216.725	-6601.230	7.060	0.446	2.489
5	-4640.872	-1286.606	5197.538	-5.605	0.081	-4.976
6	6302.855	1158.491	-3006.073	3.312	-0.595	6.711
7	-7027.148	-856.836	358.524	-0.502	1.019	-7.412
8	6664.128	421.497	2352.191	-2.388	-1.290	6.999
9	-5310.014	73.102	-4688.967	4.897	1.361	-5.512
10	3123.734	-562.082	6330.047	-6.675	-1.228	3.188
11	-495.962	960.076	-6995.614	7.433	0.910	-0.397
12	-2237.058	-1217.700	6610.987	-7.061	-0.452	-2.467
13	4605.905	1287.042	-5217.115	5.636	-0.073	4.955
14	-6295.586	-1164.822	3040.536	-3.340	0.587	-6.686
15	7016.553	862.183	-387.252	0.538	-1.015	7.419
16	-6686.889	-433.575	-2302.522	2.337	1.286	-7.010

On the other hand, in Figure 6.12, the inertial orbits for the constellation in the initial time (left) and during a propagation of 16 days (right) are presented. As it can be seen, all the satellites of the constellation lay in the same inertial orbit that, due to the orbital perturbations considered, is modified during the time of propagation as seen clearly in the figure. Nevertheless, although the inertial orbits are greatly perturbed, we can observe in Figure 6.13 that the ground-track of the constellation for 16 days of propagation remains fixed for all the satellites of the constellation.

The property of ground-track repetition (or the sharing of the same relative trajectory) can be maintained over time without orbital maneuvers using the design methodology proposed in this work. However, due to the non periodic perturbations such as the atmospheric drag or the solar radiation pressure, the constellation will be modified and thus, orbital maneuvers will be required in the long term. One important thing to notice is that although in orbit maneuvers are always needed, the use of this methodology reduces the effects of orbital perturbations over the constellation

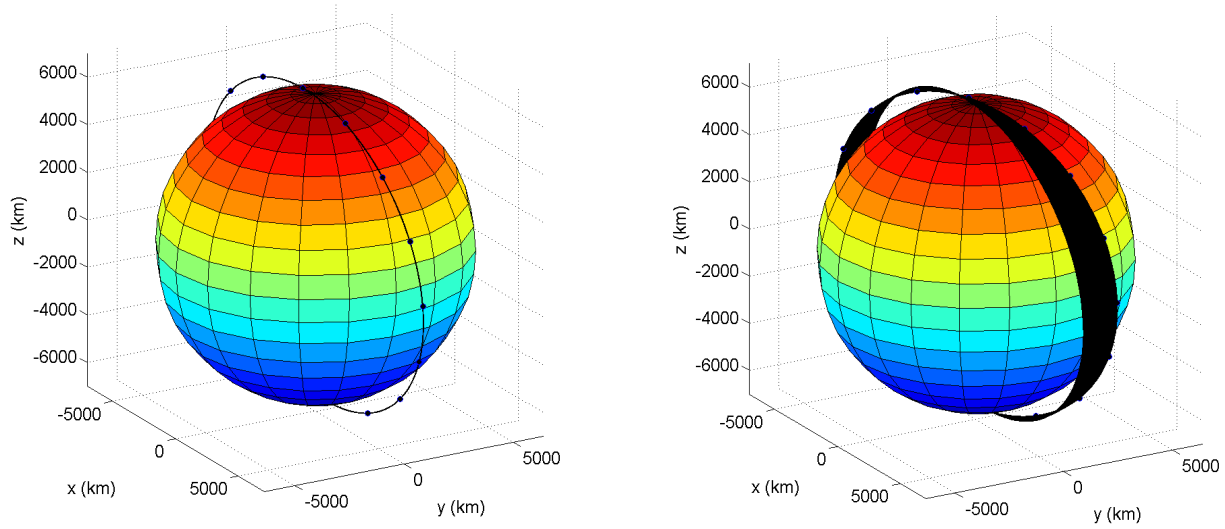

Figure 6.12: Inertial orbits of the constellation at a given time (left) and over 16 days of propagation (right).

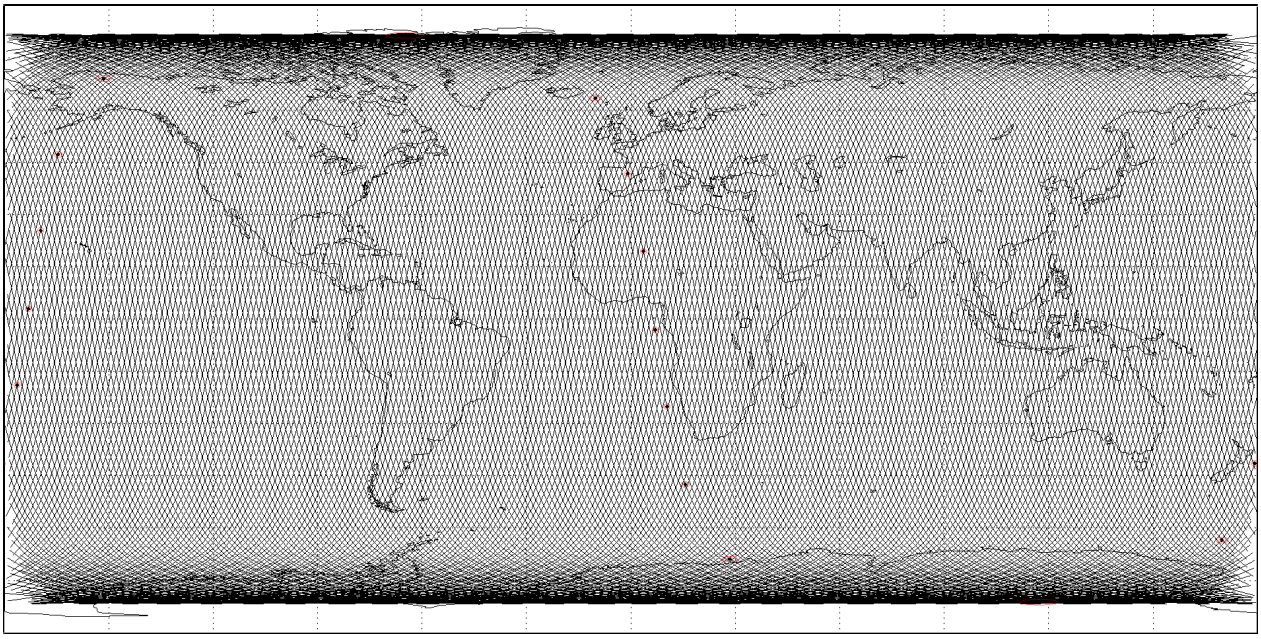

Figure 6.13: Coverage and ground-track of the constellation for 16 days of propagation.

(specially periodic perturbations such as the non-uniformity of the Earth gravitational field) and thus, this perturbed design model allows the reduction of the fuel required for the station-keeping of the constellation.

6.5 Conclusions

This chapter has shown a new design model to create constellations whose satellites share one or several relative trajectories using time as parameter of distribution in the configuration. This design allows to distribute satellites in several relative trajectories without no restrictions at all in their distribution, a property that can be used to configure missions in which the satellites have to pass consecutively over a certain point of the Earth's surface.

This design model opens a wide variety of possibilities in the configuration of satellite constellations, and it is able to handle any combination of orbital parameters, being the model applicable even with constellations based on high eccentricity orbits.

Furthermore, two different approaches have been presented for this design model, a keplerian model in which no orbital perturbation was considered, and a perturbed model that can handle orbital perturbations. These two methodologies represent the same idea, but each one has its own peculiarities and uses. Specifically, the perturbed model allows to include the orbital perturbations inside the design process, improving the results obtained.

Moreover, this constellation design model allows to include orbital properties to the basic design. In that respect, a semi-major axis correction has been applied to the two examples presented in this chapter in order to achieve the repeating ground-track property in the constellation despite of being the satellites subjected to certain known orbital perturbations. The ability to include other properties such as the sun-synchrony or the frozen character is also possible as it has been seen in the second example.

Finally the decrease on the number of inertial orbits to a minimum, represents a big design advantage, due to the fact that the reduction of inertial orbits allows to group satellites in their launches, therefore reducing the costs of the mission.

Chapter 7

On the definition of repeating ground-track constellations

Many satellite missions require to pass over the same points of the Earth surface periodically for different purposes. One of the most common examples is Earth observation satellites, but there are other uses, such as the ability to establish communications periodically with certain ground stations or the study of defined regions of the planet surface that require regional coverage.

All these applications are based on satellites that present a particular set of orbital elements related to a feature, the repeating ground-track property. This property can be easily modeled in a keplerian formulation with a closed solution. However, if orbital perturbations are considered, the problem increases greatly its complexity and transforms, what once was a simple formulation, into a problem that has no analytical solution.

As a result, several formulations have appeared over the years to solve this problem with different approaches. As an example, Mortari in his Flower Constellations [5] presented a repeating ground-track property formulation in which the effect produced by the oblateness of the Earth (J2 perturbation) was the only perturbation considered. Other example can be seen in Wagner's [44] work, where a numerical method based on a semi-major axis correction is used to achieve the repeating ground-track property.

In this chapter we introduce a new numerical method that improves the maintenance of the repeating ground-track property of a given satellite no matter the orbital configuration used. The idea behind this method is to include the perturbations in the design process [45, 15, 16] instead of trying to compensate the orbital perturbations by on orbit maneuvers. Thus, the methodology proposed is able to include the effects of orbital perturbations in its formulation, modifying the design value of the semi-major axis in order to define the reference orbit of a given satellite.

One important thing to notice is that orbital perturbations will eventually destroy the repeating ground-track property of a satellite no matter the orbit design. In particular, with just the J2 perturbation, the only orbits that maintain indefinitely its configuration are circular or critical inclination orbits, all others rotate in their orbital planes, modifying their initial ground-track in the process. This problem aggravates with the inclusion of other orbital perturbations.

Even so, the numerical method proposed in this chapter improves the maintenance of the repeating ground-track property of a given satellite over time compared to other analytical and numerical

methods. The methodology can be applied to any kind of orbital configuration, including retrograde and high eccentric orbits. Moreover, the work also includes the study of other orbital properties such as the sun-synchrony or the frozen conditions, which are very important requirements for some missions, specially Earth observation satellites. This provides a wider range of possible applications for this methodology.

After this numerical method is shown, a general methodology to impose the repeating ground track property to any constellation distribution under the effects of periodic orbital perturbations is presented. The design proposed is based on the Ground-Track Constellations [22, 23] (see Chapter 6), a design methodology that performs the definition of the constellation directly in the Earth Fixed frame of reference, unlike other satellite constellation designs such as Flower Constellations [8, 19, 9, 20], Walker Constellations [3] or Draim elliptic constellations [4] where this definition is done in the inertial frame of reference. This allows to perform a more natural definition of the constellation related to the Earth and to include the effects of orbital perturbations in the initial design of the constellation.

In addition, Ground-Track Constellations provide the possibility to use an alternative formulation for perturbed systems that allows to include the effect of the Earth gravitational potential in the definition of the constellation. That way, it is possible to combine the algorithm presented in this work for repeating ground-track orbits, with a satellite constellation design. Finally, this work presents a complete example where these methodologies are used together to define the reference orbits of a sun-synchronous repeating ground-track constellation.

7.1 On the definition of repeating ground-track orbits

Throughout this paper, the so called classical orbital elements are used, namely: a the semi-major axis, e the eccentricity, i the inclination, ω the argument of perigee, Ω the right ascension of the ascending node and M the mean anomaly. Other common parameters used are: $\omega_\oplus$ the angular velocity of the Earth, μ the Earth gravitational constant, $R_\oplus$ the Equatorial Earth radius and J_2 the second order term of the gravitational potential of the Earth.

In this section, and for the purpose of having a reference solution that is simple and clear, only the perturbation produced by the Earth oblateness (J_2) is considered. This limitation will be overcome afterwards with the addition of other orbital perturbations in the semi-major axis correction model introduced in this work.

Let a cycle be the time that a satellite requires to repeat its ground-track, being T_c the period of the cycle. In order to achieve the repeating ground-track property, the orbital parameters have to fulfill a compatibility relation with the rotation of the Earth given by:

$$T_c = N_p T_\Omega = N_d T_{\Omega G}, \tag{7.1}$$

where N_p is the number of orbital revolutions to cycle repetition, and N_d is the number of sidereal days to cycle repetition. Moreover, T_Ω is the nodal period of the orbit, that can be expressed as a function of the mean motion (n), the secular variation of the mean argument with respect from the mean motion ($\dot{M}_o$), and the secular variation of the argument of perigee ($\dot{\omega}$). In particular:

$$T_\Omega = \frac{2\pi}{\dot{M} + \dot{\omega}} = \frac{2\pi}{n + \dot{M}_o + \dot{\omega}}. \tag{7.2}$$

On the other hand $T_{\Omega G}$ is defined as the nodal period of Greenwich, whose value is given by the following expression:

$$T_{\Omega G} = \frac{2\pi}{\omega_\oplus - \dot{\Omega}}, \tag{7.3}$$

where the drifting of the orbital plane has been taken into account.

Using Equations (7.1), (7.2) and (7.3), the following expression can be obtained:

$$n + \dot{M}_o + \dot{\omega} = \frac{N_p}{N_d}\left(\omega_\oplus - \dot{\Omega}\right), \tag{7.4}$$

where the derivatives of the mean orbital elements, considering only the J_2 perturbation, are:

$$\begin{aligned}
n &= \sqrt{\frac{\mu}{a^3}};\\
\dot{M}_o &= \frac{3J_2 n R_\oplus^2}{4a^2\left(1-e^2\right)^2}\sqrt{1-e^2}\left(2-3\sin^2 i\right) = \frac{3J_2 n R_\oplus^2}{4a^2\left(1-e^2\right)^2}\sqrt{1-e^2}\left(3\cos^2 i - 1\right);\\
\dot{\omega} &= \frac{3J_2 n R_\oplus^2}{4a^2\left(1-e^2\right)^2}\left(4-5\sin^2 i\right) = \frac{3J_2 n R_\oplus^2}{4a^2\left(1-e^2\right)^2}\left(5\cos^2 i - 1\right);\\
\dot{\Omega} &= -\frac{3J_2 n R_\oplus^2}{2a^2\left(1-e^2\right)^2}\cos i.
\end{aligned} \tag{7.5}$$

If these derivatives are replaced in Equation (7.4), an expression as a function of the semi-major axis is obtained:

$$\begin{aligned}
&\sqrt{\frac{\mu}{a^3}}\left[1 + \frac{3J_2 R_\oplus^2}{4a^2\left(1-e^2\right)^2}\left[\left(2-3\sin^2 i\right)\sqrt{1-e^2} + 4 - 5\sin^2 i\right]\right] =\\
&\qquad = \frac{N_p}{N_d}\left(\omega_\oplus + \frac{3J_2\sqrt{\frac{\mu}{a^3}}R_\oplus^2}{2a^2\left(1-e^2\right)^2}\cos i\right),
\end{aligned} \tag{7.6}$$

and manipulating it, a polynomial in the semi-major axis can be derived:

$$\sqrt{\mu}\left[a^2 + \frac{3J_2 R_\oplus^2}{4\left(1-e^2\right)^2}\left[\left(2-3\sin^2 i\right)\sqrt{1-e^2} + 4 - 5\sin^2 i - 2\frac{N_p}{N_d}\cos i\right]\right] = \frac{N_p}{N_d}\omega_\oplus a^{7/2}. \tag{7.7}$$

In order to solve Equation (7.7) and to simplify the notation, k_1 and k_2 are defined as:

$$\begin{aligned}
k_1 &= \frac{N_d}{N_p}\frac{\sqrt{\mu}}{\omega_\oplus};\\
k_2 &= k_1\frac{3J_2 R_\oplus^2}{4\left(1-e^2\right)^2}\left[\left(2-3\sin^2 i\right)\sqrt{1-e^2} + 4 - 5\sin^2 i - 2\frac{N_p}{N_d}\cos i\right],
\end{aligned} \tag{7.8}$$

which are introduced in Equation (7.7) to obtain the following expression:

$$a^{7/2} - k_1 a^2 - k_2 = 0. \tag{7.9}$$

Equation (7.9) allows to find the value of the semi-major axis as a function of the rest of the orbital elements by just using a Newton-Raphson's method to find the roots of the function:

$$a_{j+1} = a_j - \frac{a_j^{7/2} - k_1 a_j^2 - k_2}{\frac{7}{2} a_j^{5/2} - 2k_1 a_j}, \tag{7.10}$$

where the stop condition of the method is given by $\mid a_{j+1} - a_j \mid < tol$, with tol being the desired accuracy. In order to initialize the method, the semi-major axis for the unperturbed case (a_0) is chosen as the initial value for the iteration:

$$\sqrt{\frac{a_0^3}{\mu}} N_p = \frac{N_d}{\omega_\oplus} \qquad \Longrightarrow \qquad a_0 = \left[\left(\frac{N_d}{N_p} \right)^2 \frac{\mu}{\omega_\oplus^2} \right]^{1/3}. \tag{7.11}$$

The previous procedure is a corrector algorithm that iteratively search the most accurate value of the semi-major axis, and which is equivalent to other classical approaches [5, 35]. However, this approach presents several problems in its usage. First, it only takes into account the J_2 perturbation. Second, the value obtained from those expressions is the mean semi-major axis, and not the instantaneous one. Therefore, in a certain position of the orbit, the precise semi-major axis is unknown. And third, the definition of the nodal period of the orbit (T_Ω), as seen in Equation (7.2), is not correct, as it performs an addition of a true angle (the argument of perigee) with a mean angle (the mean anomaly), which causes the introduction of an error in the process.

7.1.1 Example of ground-track drift with J_2 perturbation

An example of the implications of these assumptions is presented in this section. In particular, a circular orbit with critical inclination (that is $i = 63.43^o$) is selected. We also impose that the orbit has to repeat its ground-track each 14 orbital revolutions and each day (that is $N_p = 14$ and $N_d = 1$). Moreover, and in order to fix its position, a point of pass is fixed with coordinates $\phi_r = 41.698169^o N$ and $\psi_r = 0.874295^o W$ (Zaragoza, Spain). With this coordinates, it is possible to derive the rest of the orbital elements required to define the orbit.

Once the orbit has been completely defined, it is possible to calculate its ground-track during a day of propagation (note that the orbit has been defined to repeat its ground-track in one day). The computed ground-track can be seen in Figure 7.1 for the case of the algorithm presented in Equation (7.7). This figure shows clearly how the ground-track of the orbit does not close at all in the region above South-Western Europe (Iberian Peninsula), with a computed drift of -107.605 km/day, being the effect more noticeable the closer the satellite is to the Earth surface.

A much better approximation can be obtained by using the algorithm provided by Vallado [35] and a transformation from mean to osculating elements (like the ones devised by Deprit [24] or Brouwer [25, 46]). In particular, using this procedure and for the example provided, a drift of 0.007 km/day is computed. As it can be seen, the improvement is very significant. Thus, during this paper, we will use this methodology as the reference for performance comparisons. However, even by using this methodology, the ground-track of the orbit is not completely closed and the problem becomes mere severe as other terms of the Earth gravitational potential are considered. Thus, we introduce a new numerical methodology to overcome this problem and improve the accuracy.

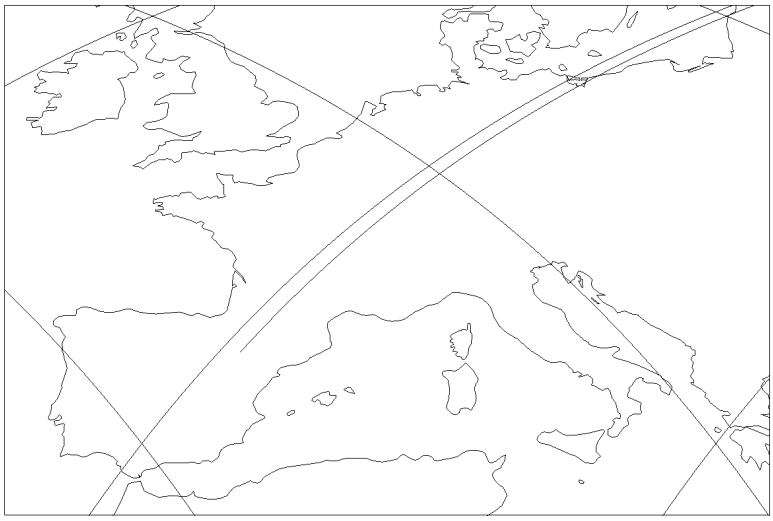

Figure 7.1: Ground-track of a circular orbit with $N_p = 14$, $N_d = 1$ and $i = 63.43^o$.

7.2 Reference orbit under the Earth gravitational potential

A numerical methodology has been developed to improve the repeating ground-track behavior of satellites subjected to orbital perturbations. The basis of the methodology is to correct the value of the semi-major axis obtained from the reference model (Vallado [35] and a transformation from mean to osculating elements) by adjusting the orbit of the satellite in the ECEF (Earth-Centered, Earth-Fixed) frame of reference. This correction is achieved by using a basic property in celestial mechanics: if the semi-major axis of an orbit increases, its period also increases, which makes the ground-track to drift towards the West, and vice versa. Therefore, the goal of the correction proposed is to find the value of the instantaneous semi-major axis that allows the closing of the ground-track in a period of time equal to a cycle, T_c.

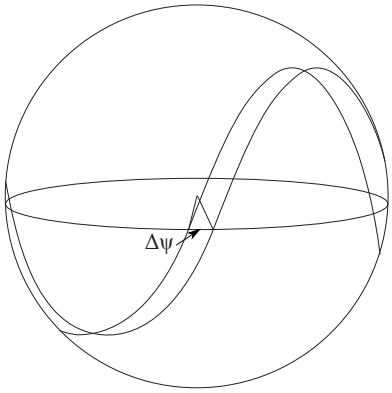

Figure 7.2: Deviation between two passings through the Earth Equator ($\Delta\psi$).

In order to do so, a series of propagations of the orbit of the satellite are performed. In particular, each propagation has to be done for a time of at least two cycles in order to assure that the satellite

is able to cross the Earth Equator at least $2N_p$ times in the same direction in the ECEF frame of reference. This propagation has two different objectives. The first one is to obtain the time that the satellite requires to complete a cycle (T_c), while the second aims to compute the deviation of the ground-track produced in that time in its passing through the Earth Equator in the ECEF frame of reference, named $\Delta\psi$ (see Figure 7.2).

Let a_0 be the semi-major axis obtained using the reference approach for a given combination of orbits and days to ground track repetition (N_p and N_d respectively). During the propagation, the resultant orbit produces a drift in the ground-track after the repetition cycle that is denoted as $\Delta\psi_0$. The value of $\Delta\psi_0$ is computed as the angle between the instantaneous angular momentums, projected upon the Earth Equator plane (in the ECEF frame of reference), of the satellite in its two passings through the Earth Equator.

On the other hand, let a be the value of the semi-major axis that makes the ground-track to close, that is, the nominal value of the semi-major axis that we want to compute. In addition, as it is the nominal value, we know by definition that the drift of its ground-track in a repeating cycle is zero. Thus, it is possible to express the ground-track drift of the satellite under consideration respect to this nominal orbit:

$$\Delta\psi_0 = \omega_\oplus \left(T_{c_0} - T_c\right) = \omega_\oplus \, N_p \, \left(T_0 - T\right), \tag{7.12}$$

where N_p is the repetition cycle, and T_0, T are the period of the orbits with semi-major axis a_0 and a respectively. If a strictly keplerian formulation is considered as a first approximation, the former equation can be expressed as:

$$\Delta\psi_0 = \omega_\oplus N_p \left(2\pi\sqrt{\frac{a_0^3}{\mu}} - 2\pi\sqrt{\frac{a^3}{\mu}}\right). \tag{7.13}$$

In addition, let $\overline{d\psi}$ be the mean variation of the ground-track drift of an orbit in the period of a repeating cycle, that is:

$$\overline{d\psi_0} = \frac{\Delta\psi_0}{T_c}. \tag{7.14}$$

where $\overline{d\psi_0}$ can be expressed by means of both values of the semi-major axis by using Equations (7.13) and (7.14):

$$\overline{d\psi_0} = \omega_\oplus \left(\sqrt{1 - \frac{a^3}{a_0^3}}\right). \tag{7.15}$$

Therefore, as a_0 and $\overline{d\psi_0}$ are already known, we can obtain the value of a as a function of the parameters of the former propagation. In particular:

$$a = a_0 \left(1 - \frac{\overline{d\psi_0}}{\omega_\oplus}\right)^{-2/3}. \tag{7.16}$$

The value provided by Equation (7.16) can be used as a first approximation to the solution. In fact, Equation (7.16) can be transformed into an interpolating formula:

$$a_i = a_{i-1} \left(1 - \frac{\overline{d\psi_{i-1}}}{\omega_\oplus}\right)^{-2/3}, \tag{7.17}$$

however, this iterative process can be improved significantly by the use of the secant method:

$$a_j = a_{(j-1)} - \overline{d\psi_{(j-1)}} \frac{\left(a_{(j-1)} - a_{(j-2)}\right)}{\left(\overline{d\psi_{(j-1)}} - \overline{d\psi_{(j-2)}}\right)}, \tag{7.18}$$

which is initialized with solutions provided by Equation (7.17).

The process shown above requires a number of propagations of the same satellite with different values of its semi-major axis (maintaining the rest of mean orbital parameters constant) until a value of a_j that fulfills the repeating ground-track property is obtained (condition $\overline{d\psi_j} < \epsilon$, where ϵ is the parameter that controls the precision of the numerical method).

This method can be applied no matter the orbit considered, including satellites with high eccentricity, low semi-major axis or retrograde orbits. Moreover, the methodology is not limited by the Earth gravitational model considered, being possible to include the effect of zonal and tesseral terms in the computation of the nominal orbit.

7.2.1 Example of semi-major axis perturbation

Now, an application of the methodology to the example shown in Section 7.1.1 is presented. Figure 7.1 showed how a low circular orbit with critical inclination and parameters $N_d = 1$ and $N_p = 14$ behaved using Equation (7.7), and how a simple transformation from mean to osculating elements improved the result. In here, the numerical semi-major axis correction introduced in this work is used. Figure 7.3 shows the results of the propagation of an orbit obtained through this methodology. As it can be seen, the corrected orbit is completely closed.

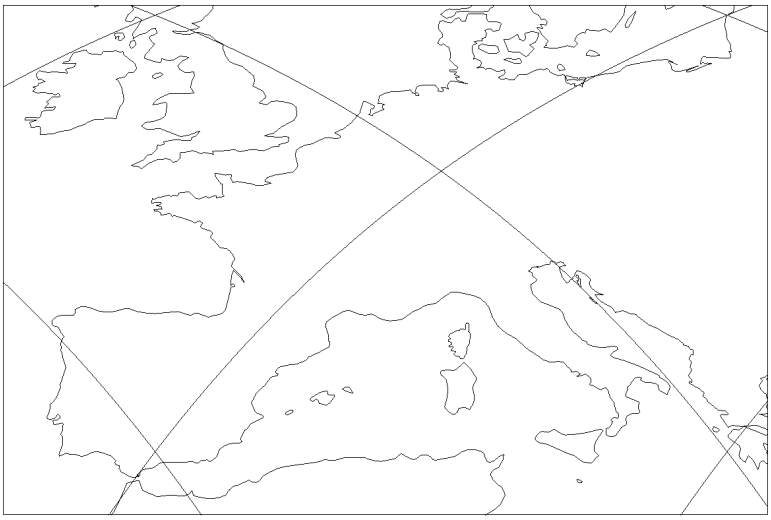

Figure 7.3: Ground-track of the semi-major axis corrected orbit with design parameters: $N_p = 14$, $N_d = 1$, $e = 0.0$ and $i = 63.43^o$.

However, and in order to have a quantitative parameter to study the repeating ground-track performance that presents each one of these orbits, the drift that the ground-track of an orbit

suffers over the Earth Equator per day is selected. This parameter is computed as explained in the previous section, and it is measured as the amount of kilometers that the ground-track drifts over the Earth Equator per day.

Table 7.1: Ground-track deviation in the equator and semi-major axis for the two methods under J_2 perturbation.

Methodology	Reference algorithm	a-correction's method
Drift [km/day]	0.007	$< 10^{-10}$
a [km]	7219.001	7219.000

Table 7.1 provides a comparison of the two methods to calculate the semi-major axis of the orbit. The table shows that using the reference model, a semi-major axis of 7219.001 km with a drift of 0.007 km/day is obtained (which represents a deviation towards the East). On the other hand, using the semi-major axis correction, a semi-major axis of 7219.000 km is obtained with a drift of less than 10^{-10} km/day. As it can be seen, the difference in the value of the semi-major axis is not too big (approximately 1 m), however, this difference is important to define the nominal orbit not only for the effect of the Earth gravitational potential, but also for the atmospheric drag. As we will see later, the difference between methodologies increases if more terms of the Earth potential are included.

Table 7.2: Ground-track deviation in the equator and semi-major axis for the two methods for a gravitational potential with terms up to 4th order (including tesseral terms).

Methodology	Reference algorithm	a-correction's method
Drift [km/day]	0.113	$< 10^{-10}$
a [km]	7219.001	7219.015

On the other hand, a similar study has been made considering a Earth gravitational model with terms up to the 4th order, including zonal and tesseral terms. The results of this computation are provided in Table 7.2. As it can be seen, the drift of the ground-track for the reference algorithm has increased to 0.113 km/day, while the proposed methodology maintains the accuracy.

Table 7.3: Initial position and velocity of the modified orbit in the ECI frame of reference.

Coordinates	x [km]	y [km]	z [km]	v_x [km/s]	v_y [km/s]	v_z [km/s]
Satellite	5391.764	4803.640	110.223	-2.286	2.413	6.647

The initial positions and velocities of the orbit in the ECI (Earth Centered Inertial) frame of reference are shown in Table 7.3. These orbital parameters have been obtained using the semi-major axis correction presented in this work and are the ones that allow the closing of the relative-track for the conditions considered.

7.2.2 Performance of the numerical method

In this section, we aim to show the improvements on the ground-track repetition that the semi-major axis correction proposed in this work is able to achieve. For that objective, we take into

consideration the orbital perturbations provoked by a 4 by 4 order Earth gravitational potential model [29] in order to show the performance of the method. Note that the semi-major axis that is able to achieve the repeating ground-track property is very dependent on the various parameters of the problem, more precisely, the reference point of pass in the Earth surface, the inclination, the eccentricity, the argument of perigee, the relation between N_p and N_d and the right ascension of the ascending node. For that reason and in order to simplify the results obtained, we will assume that the point of pass is 0^o N and 0^o W as coordinates, a perigee equal to $w = 90^o$, and a right ascension of the ascending node equal to 0^o. Fixing those parameters allows to generate a family of surfaces that only depends on the relation between N_p and N_d, the eccentricity, and the inclination.

Three examples are provided, a Low Earth Orbit (LEO), a Medium Earth Orbit (MEO), and a Geosynchronous Orbit (GSO). In each example the drift of the ground-track in the equator is presented for the case of the semi-major axis obtained from the reference algorithm (Vallado [35] and a transformation from mean to osculating elements). On the other hand, the drift obtained from the semi-major axis correction can be reduced as much as required, by increasing the number of iterations. Particularly, during the computation of these examples, a tolerance in the drift of $10^{-10}\,km$ is imposed, which is also the maximum drift obtained during the numerical tests in all the cases in study. On the other hand, and for the cases of study, the number of iterations that the algorithm required to find this precision was maintained below 5 iterations, using in most cases only 2 iterations. Now, the results for this examples are presented.

7.2.2.1 Low Earth Orbits

Figure 7.4 shows the ground-track drift in the equator of a set of Leo orbits with parameters $N_p = 15$ and $N_d = 1$ and for the case of the reference algorithm. As it can be seen, a maximum deviation of $6.34\,km/day$ in the ground-track is observed in the equator. It is important to note that the maximum drifts computed occur for orbits with an orbital plane near the equator. This is due to the effect of the zonal harmonics of Earth potential that are not considered in the reference algorithm. Moreover, we can compare these results with the ones obtained from the algorithm introduced in this article, where a maximum drift of $10^{-10}\,km$ per day is obtained. This shows the improvement that this algorithm presents. The results are presented up to eccentricity equal to 0.05 in order to avoid possible collisions of the satellite with the Earth surface at the altitudes considered. In the other examples, larger values of the eccentricity will be studied.

On the other hand, Figure 7.5 presents the effect of the correction performed in the mean semi-major axis of the orbits. As it can be seen, the correction varies from $-0.7\,km$ to $0.55\,km$. This variation can be regarded as very small, however, when defining a reference orbit for orbit control maintenance, these variations can be very appreciable. As an example of this, let a satellite at the altitude presented in the example be imposed to have a dead band of $1\,km$ under the atmospheric drag. This means that the mean semi-major axis of the satellite will vary typically in a range on the order of $10 - 100$ meters around the reference orbit, depending on the satellite physical properties and the solar activity. As it can be seen, this shows the importance of defining a reference orbit as precise as possible for the periodic orbital perturbations.

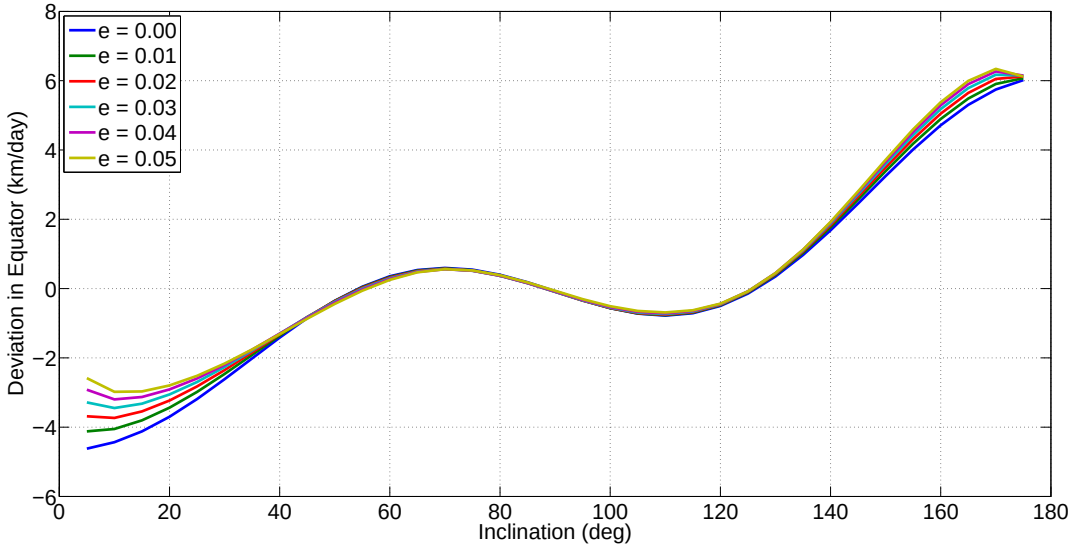

Figure 7.4: Ground-track drift for LEO orbits with parameters: $N_p = 15$, $N_d = 1$.

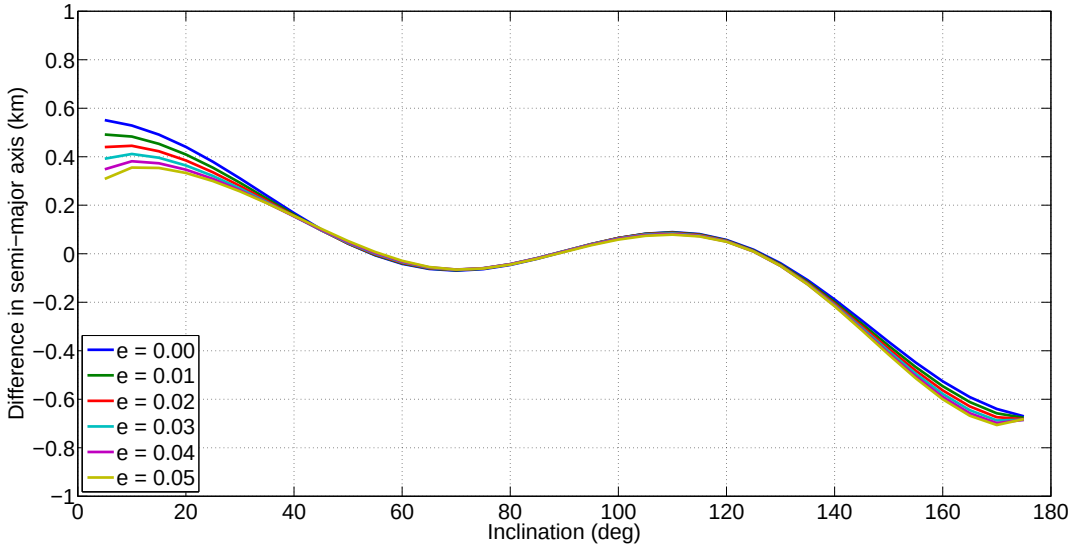

Figure 7.5: Difference in semi-major axis for LEO orbits with parameters: $N_p = 15$, $N_d = 1$.

7.2.2.2 Medium Earth Orbits

Now, the study for a set of MEO orbits with parameters $N_p = 3$ and $N_d = 1$ is presented. Figure 7.6 shows the ground-track drift in the equator that is obtained if the reference algorithm is used under a 4 by 4 Earth gravitational potential. As it can be seen, increasing the eccentricity of the orbits increases the drift up to 8 km/day if using the reference algorithm and for the cases of study. This effect is provoked by the approximations associated with the reference algorithm and the transformations from mean to osculating elements.

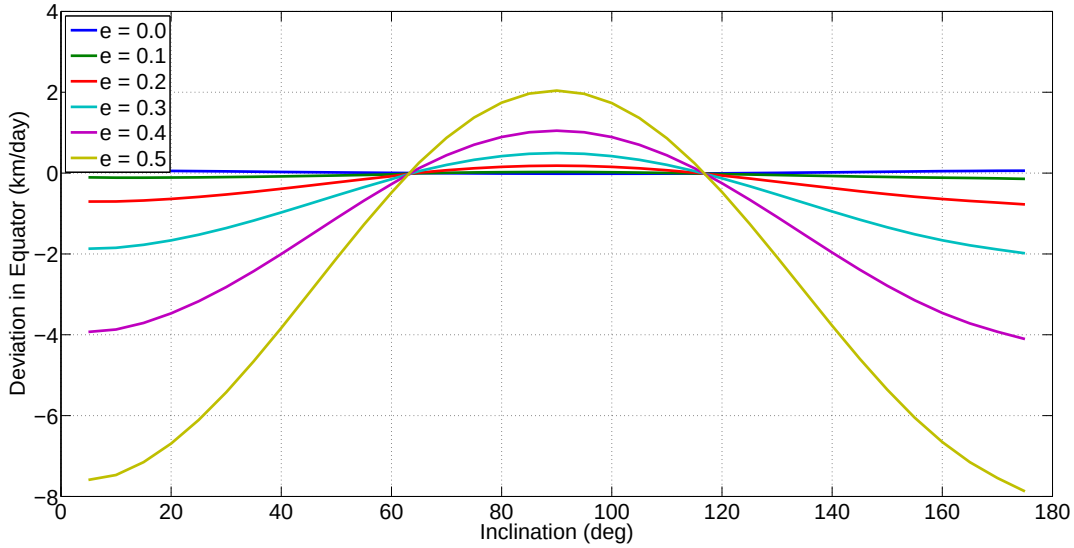

Figure 7.6: Ground-track drift for MEO orbits with parameters: $N_p = 3$, $N_d = 1$.

The difference in the semi-major axis obtained in both algorithms is presented in Figure 7.7. As it can be observed, even at this altitude, the difference in the semi-major axis is noticeable with a maximum variation of 2.65 km. On the other hand, if we focus in the same region of study as in the previous example, a reduction in the variation of the semi-major axis is obtained. This result is expected as the perturbation forces provoked by the Earth gravitational potential increase the closer the satellite is to the Earth.

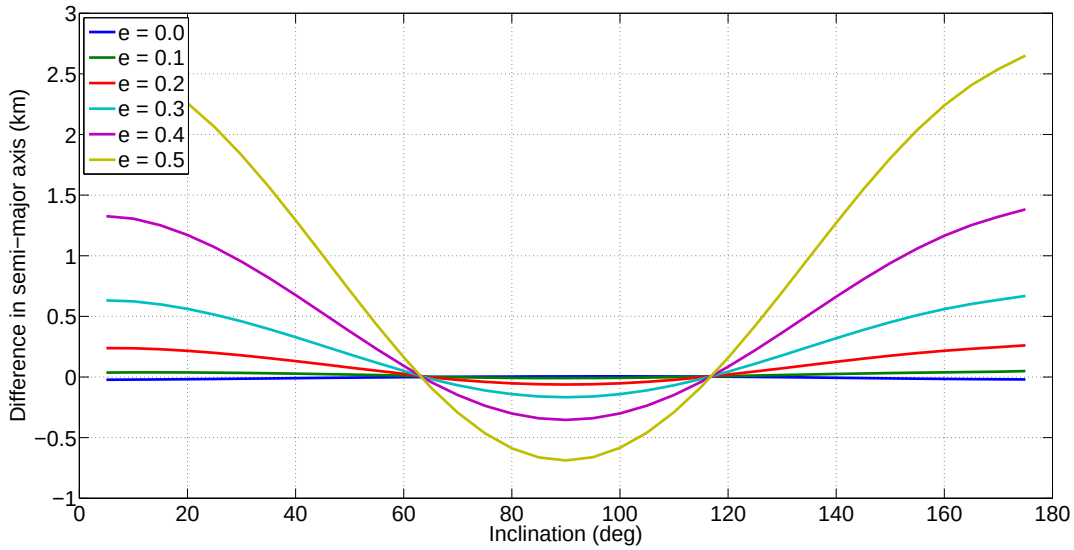

Figure 7.7: Difference in semi-major axis for MEO orbits with parameters: $N_p = 3$, $N_d = 1$.

7.2.2.3 Geo Synchronous Orbits

As a final example, we present the results of these algorithms for GSO orbits. In order to obtain this kind of configuration the satellites have to complete an orbit in one day, that is, $N_p = 1$ and $N_d = 1$. As before, the results for ground-track drift of the reference algorithm and its difference in semi-major axis with the methodology introduced in this work are presented in Figures 7.8 and 7.9 respectively.

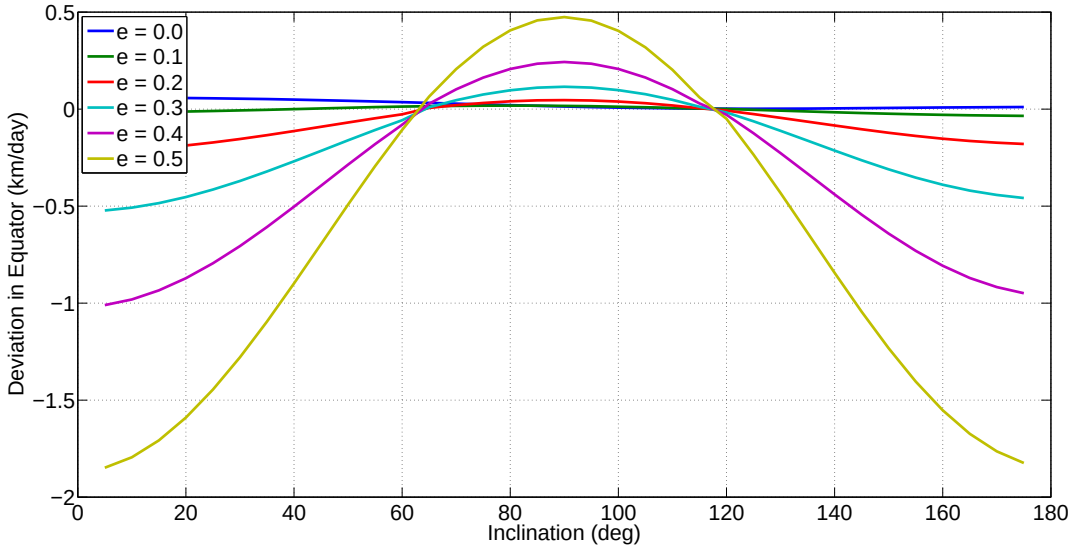

Figure 7.8: Ground-track drift for GSO orbits with parameters: $N_p = 1$, $N_d = 1$.

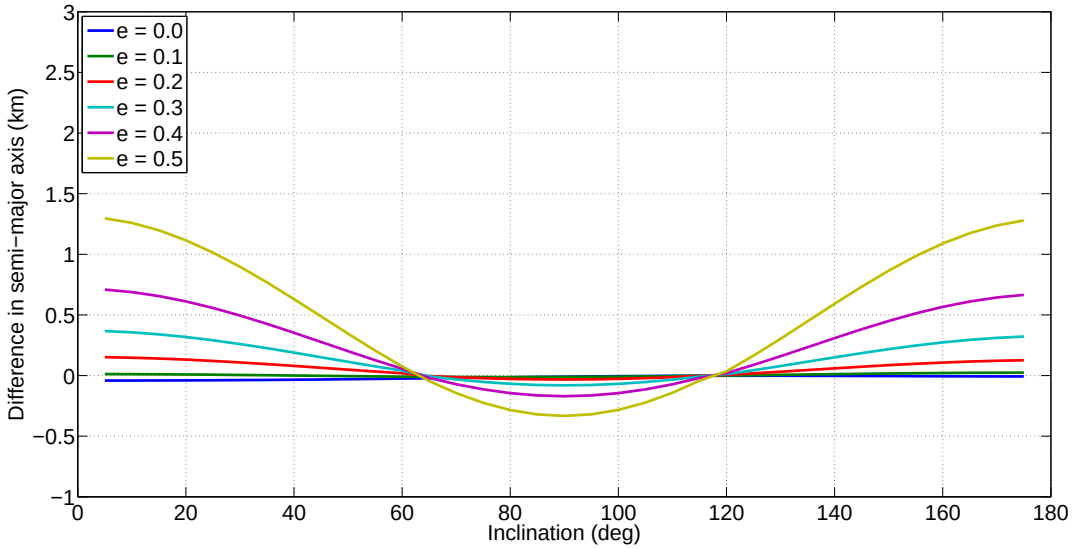

Figure 7.9: Difference in semi-major axis for GSO orbits with parameters: $N_p = 1$, $N_d = 1$.

As it can be seen, the drift computed for the reference algorithm is smaller than in the previous example. This is due to the fact that the satellites are farther from the Earth, and thus, the effect of

the Earth gravitational potential is reduced. However, we can still see notable differences between both algorithms as the eccentricity of the orbits increases.

7.2.3 Including other perturbations

It is possible to include other orbital perturbations such as the Sun and Moon as disturbing third bodies, the solar radiation pressure or the atmospheric drag in the correction of the reference semi-major axis of the orbit without any modification of the algorithm. However, as these perturbations are not periodic in the Earth Fixed frame of reference, the repeating ground-track property will be lost after several repeating cycles. This means that, as time passes, orbital maneuvers must be performed in order to maintain the orbit properties. For these reasons, the algorithm presented in this work is specially interesting when defining a reference orbit in mission design. That way, the semi-major axis correction allows to reduce the relative to Earth station-keeping of a satellite, as it can absorb the effects of conservative perturbations that are periodic, such as the Earth gravitational potential, including them in the initial design of the orbit.

7.2.4 Addition of other orbital properties

Most of the Earth observation satellites require, in addition to the repeating ground-track property, other orbital properties due to the nature of their missions. As an example of that, optical missions usually require to have near circular, frozen, sun-synchronous and near to Earth orbits. However, not all the missions are subjected to the same requirements and some conditions in the orbit can be relaxed. Other examples that require frozen or sun-synchronous orbits include radar missions or remote sensing.

Therefore, in addition to the repeating ground-track property, it is interesting to study the possibility to include the sun-synchrony and the frozen orbit conditions in the algorithm introduced in this work. This allows to include this properties (alongside with the Earth gravitational model) directly in the computation of the reference orbit of a mission.

7.2.4.1 Sun-Synchrony

Sun-synchrony is an interesting property that allows satellites to visit regions of the surface at the same solar time. This property has important advantages in Earth observation cameras as it maintains the conditions of lighting over the regions of study. The condition for sun-synchrony is:

$$\dot{\Omega}_{sec} = \frac{\omega_{\oplus}}{yr}, \tag{7.19}$$

where $\dot{\Omega}_{sec}$ is the secular variation of the right ascension of the ascending node and $yr = 365.25636042$ is the number of sidereal days contained in a year. Using Lagrange Planetary equations, a relation between Equation (7.19) and the orbital elements can be established through:

$$\dot{\Omega}_{sec} = -\frac{3}{2} J_2 \frac{R_{\oplus}^2 \sqrt{\mu}}{a^{7/2} \left(1 - e^2\right)^2} \cos i. \tag{7.20}$$

Equations (7.20) and (7.19) can be combined and related with the number of orbital revolutions to cycle repetition (N_p) and the number of sidereal days to cycle repetition (N_d) using Equation (7.11), obtaining:

$$\left(1-e^2\right)^2 = -\frac{3}{2} J_2\, yr\, R_\oplus^2 \left(\frac{N_p^7}{N_d^7}\frac{\omega_\oplus^4}{\mu^2}\right)^{1/3} \cos i. \tag{7.21}$$

However, Equation (7.21) is not defined for any combination of eccentricity, inclination and semi-major axis of the orbit. First of all, the eccentricity has an upper and a lower boundary. The upper boundary is related with the minimum altitude over the Earth surface; the perigee,

$$r_p = a\left(1-e\right), \tag{7.22}$$

and relating this equation with parameters N_p and N_d using Equation (7.11):

$$e_{max} = 1 - \left(\frac{N_p^2\omega_\oplus^2}{N_d^2\mu}\right)^{1/3} r_p. \tag{7.23}$$

On the other hand, the lower boundary is related with the existence of a real solution in Equation (7.21). That way,

$$e_{min} = \sqrt{1-\sqrt{\frac{3}{2} J_2\, yr\, R_\oplus^2 \left(\frac{N_p^7}{N_d^7}\frac{\omega_\oplus^4}{\mu^2}\right)^{1/3}}}. \tag{7.24}$$

Furthermore, Equations (7.23) and (7.24) relate with the minimum and maximum angle between the orbital plane and the equator:

$$\begin{aligned} \cos i_{max} &= -\frac{2}{3}\frac{\left(1-e_{min}^2\right)^2}{J_2\, yr\, R_\oplus}\left(\frac{N_d^7}{N_p^7}\frac{\mu^2}{\omega_\oplus^4}\right)^{1/3} \\ \cos i_{min} &= -\frac{2}{3}\frac{\left(1-e_{max}^2\right)^2}{J_2\, yr\, R_\oplus}\left(\frac{N_d^7}{N_p^7}\frac{\mu^2}{\omega_\oplus^4}\right)^{1/3}. \end{aligned} \tag{7.25}$$

Once the boundaries of the problem have been defined, it is time to include the sun-synchrony in the semi-major axis correction. In order to do that, it is required to modify the inclination and/or the eccentricity of the orbits as the same time that the semi-major axis of the orbit is modified in the algorithm in order to maintain the condition of sun-synchrony. In that respect, three possibilities can be considered: to modify the inclination in each step of the iteration (with a fixed eccentricity), to modify the eccentricity (with a fixed inclination), or to vary both variables in each iteration (if a frozen orbit is also required). Each approach has its advantages and disadvantages and it depends on the orbit requirements. More precisely, modifying the inclination implies calculating in each step the conditions of the orbit to pass over the point of reference, but it also assures the control over the eccentricity, a parameter that can be more critical depending on the mission. On the other hand, modifying the eccentricity requires less computation but the inclination is controlled by Equation (7.21). Finally, varying both variables allows a better control of the result at a cost

of more computational time and a more complex algorithm. However, this allows to obtain orbits which are sun-synchronous and Frozen, which is a property very interesting in many applications.

Regarding the algorithm, the semi-major axis correction is done as before, but with a slightly modification: each time that a semi-major axis is computed using Equation (7.18), a new value of either the inclination and/or the eccentricity is done (as has been defined before), which means that the next computed propagation calculated includes the modified values of semi-major axis, inclination and eccentricity. This process is maintained until the precision in the drift of the relative track is fulfilled, just in the same way as the semi-major axis correction was explained.

7.2.4.2 Frozen orbits

Frozen orbits are those whose eccentricity and argument of perigee do not suffer from secular variations in the evolution of the satellite movement. This condition is very interesting for optical missions, where this property allows to observe a given region from the same altitudes in each passing of the satellite. For a model in which only the J_2 effect is considered, there are only two possibilities to achieve that condition, having a circular orbit or having a critical inclination orbit. However, in this chapter, the J_3 effect will also be considered, as it includes more possible frozen solutions to the problem and allows to find more stable solutions.

Thus, considering the J_2 and J_3 perturbations, the secular derivatives of the eccentricity and the argument of perigee are:

$$\begin{aligned} \dot{e} &= -\frac{3}{2}\sqrt{\frac{\mu}{a^3}}\left(\frac{R_\oplus}{a}\right)^3 \frac{J_3}{\left(1-e^2\right)^2}\sin i\cos\omega\left(1-\frac{5}{4}\sin^2 i\right), \\ \dot{w} &= \left[\frac{3J_3}{\left(1-e^2\right)^2}\sqrt{\frac{\mu}{a^3}}\frac{R_\oplus^2}{a^2}\left(1-\frac{5}{4}\sin^2 i\right)\right]\left[1+\frac{J_3}{J_2}\frac{R_\oplus}{2a}\frac{\sin\omega}{1-e^2}\left(\frac{\sin^2 i-e^2\cos^2 i}{e\sin i}\right)\right]. \end{aligned} \quad (7.26)$$

Equation (7.26) has solutions when the inclination is zero or the critical inclination, and when the argument of perigee is either $\omega = \pi/2, 3\pi/2$, and this relation is fulfilled:

$$\left(1-e^2\right)e = -\frac{1}{2}\frac{J_3}{J_2}\frac{R_\oplus}{a}\frac{\sin^2 i-e^2\cos^2 i}{\sin i}\sin\omega, \quad (7.27)$$

which is a third degree equation in the eccentricity.

In order to get a repeating grand-track and frozen orbit, we follow a similar process to the one showed for the sun-synchrony property. First, the semi-major axis correction is performed, and for each new value of a_i obtained, the inclination and eccentricity of the orbit are also modified in order to achieve the frozen orbit (using one of the conditions presented).

7.2.4.3 Syn-synchronous and Frozen orbits

As it has been said previously, it is possible to include both conditions in an orbit. Using Equations (7.21) and (7.27), the values of the inclination and eccentricity for a given semi-major axis can be obtained. Thus, in each iteration, the values of the eccentricity and inclination are

updated with the new vale of the semi-major axis provided by the actual iteration. This allows to obtain the three properties (ground-track repetition, sun-synchrony and frozen) at the same time. It is important to note that by doing this, the number of iterations required by the algorithm slightly increases. However, and for the cases of study, the maximum number of iterations never overpassed the 8 iterations.

7.3 Repeating ground-track constellation design

One of the most interesting applications of the semi-major axis correction is satellite constellation design. That way, it is possible to combine the semi-major axis correction with the Ground-Track Constellations [22, 23] methodology of design, which is summarized below, to generate satellite configurations that can be preserved for long periods of time without orbital maneuvers.

The Ground-Track Constellations methodology is based on the idea of generating relative trajectories defined with orbital perturbations taken into account, and distributing the satellites along these relative trajectories. That way, the effects of orbital perturbations are introduced in the design of the constellation, allowing the maintenance of the configuration for longer periods of time.

The distribution of a Ground-Track Constellation follows this relation:

$$\begin{aligned} \Omega_{kq} &= \Omega_{00} - \omega_{\oplus}(t_q - t_0), \\ M_{kq} &= M_{00} + n\,(t_k + t_q - t_0)\,; \end{aligned} \tag{7.28}$$

where Ω_{00}, M_{00} and t_0 are the values of right ascension of the ascending node, mean anomaly and time respect to the Greenwich meridian for the reference satellite of the constellation. On the other hand, t_q and t_k represent the distribution based on time of the satellites along k different relative trajectories, and Ω_{kq} and M_{kq} names the right ascension of the ascending node and the mean anomaly of a satellite placed in the position q of the relative trajectory k.

As an example of this application, an equally spaced in time distribution is chosen. This configuration can be defined as:

$$\begin{aligned} t_k &= (k-1)\frac{2\pi}{N_t N_f \left(\omega_{\oplus} - \dot{\Omega}_{k0}\right)}, \\ t_q &= (q-1)\frac{T_c}{N_{st}}, \end{aligned} \tag{7.29}$$

where N_t is the number of relative-tracks, N_{st} the number of satellites per relative-track, $\dot{\Omega}_{k0}$ the secular variation of the right ascension of the ascending node of the reference satellite $k0$, and N_f the maximum common divisor between N_p and N_t ($N_f = gcd(N_p, N_t)$). In this distribution $k \in [1, N_t]$ and $q \in [1, N_{st}]$.

We impose as a requirement of the constellation that all satellites must have the repeating ground-track and the sun-synchronous properties, and thus, the semi-major axis correction presented in this work is applied. Moreover, each satellite presents a repeating ground-track cycle each 59 orbital revolutions ($N_p = 59$) and four days ($N_d = 4$). Regarding the satellite distribution, all satellites

present the same relative trajectory ($N_t = 1$) which means that this relative trajectory contains all four satellites ($N_{st} = 4$).

One important property of this constellation is that, although the satellites are distributed in only one relative trajectory, they are also contained in the same inertial orbit. This property can be achieved as the number of inertial orbits using this kind of distribution is equal to $N_{st}/gcd(N_{st}, N_d)$. That way, only one semi-major axis correction has to be done, as all the constellation is defined using the same relative trajectory obtained from the propagation of one reference satellite.

In the current example, the only perturbation considered is the gravitational potential of the Earth [29] up to 4th order terms (including tesserals). This perturbation has the particularity that it is periodic in the ECEF frame of reference, which allows to obtain a stable solution in this case. With this perturbation and the distribution defined in Equations (7.28) and (7.29), the initial positions and velocities can be computed. The initial state of the constellation is presented in Table 7.4 where the positions and velocities are defined in the ECI frame of reference.

Table 7.4: Initial positions and velocities of the constellation.

Sat. (k,q)	x [km]	y [km]	z [km]	v_x [km/s]	v_y [km/s]	v_z [km/s]
1,1	5239.796	-79.962	4668.731	-4.947	-1.324	5.529
1,2	4597.367	1234.183	-5157.908	5.634	-0.083	5.002
1,3	-5251.144	78.267	-4665.286	4.939	1.323	-5.527
1,4	-4609.440	-1235.011	5154.648	-5.625	0.084	-5.003

Figure 7.10 shows the ground-track of the constellation for a propagation of 4 days. As it can be seen, all four satellites share the same ground-track, which is closed, achieving the ground-track property for the whole constellation. This state has been achieved even with the perturbation provoked by the Earth gravitational potential, obtaining a repeating ground-track property that can be maintained for months (and for the perturbation considered) without orbital maneuvers.

On the other hand, Figure 7.11 represents the inertial orbits of the constellation. The image on the left shows the initial inertial orbit, whilst the image on the right presents the propagation of the constellation for a time equal to four days. As it can be observed, the inertial orbit plane has drifted due to the effect of the J_2 perturbation. Nevertheless, as it has been seen in Figure 7.10, the ground-track of the constellation remains unchanged despite the orbital perturbations considered, which shows the possibilities that the semi-major axis correction provides.

This configuration can be maintained indefinitely with only a periodic perturbation such as the Earth gravitational potential. However, if other orbital perturbations are considered, the ground-track and relative trajectories of the constellation will change over time, and thus, orbital maneuvers will be required to be applied to correct that situation. However, as the effects of the Earth gravitational potential are included in the original design, less fuel will be required to maintain the relative to Earth station-keeping.

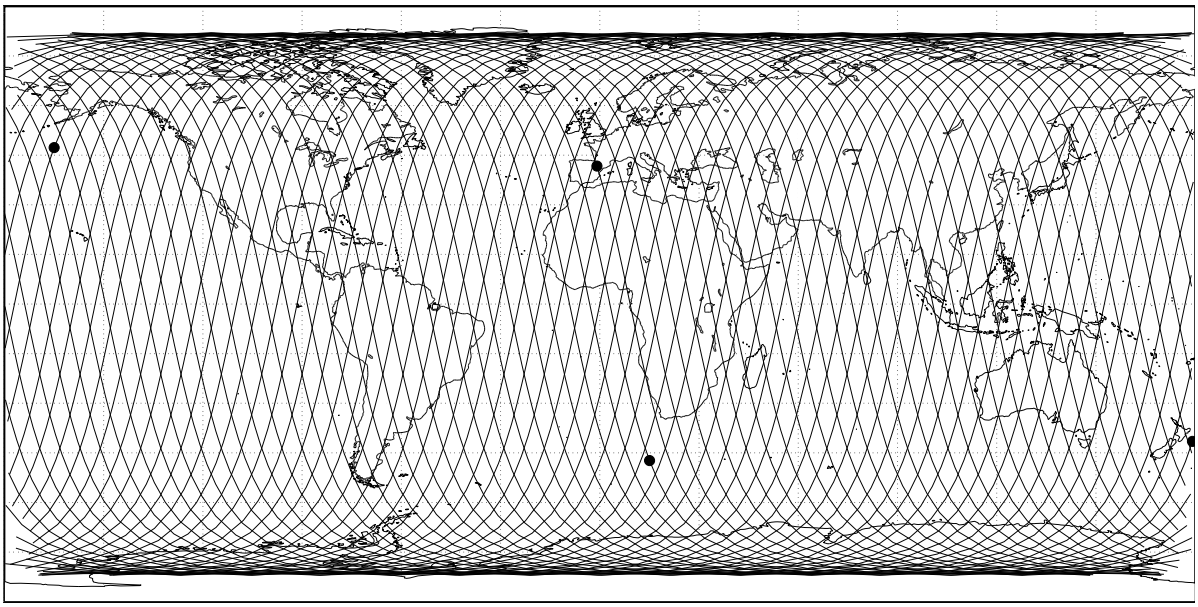

Figure 7.10: Ground-track of the constellation.

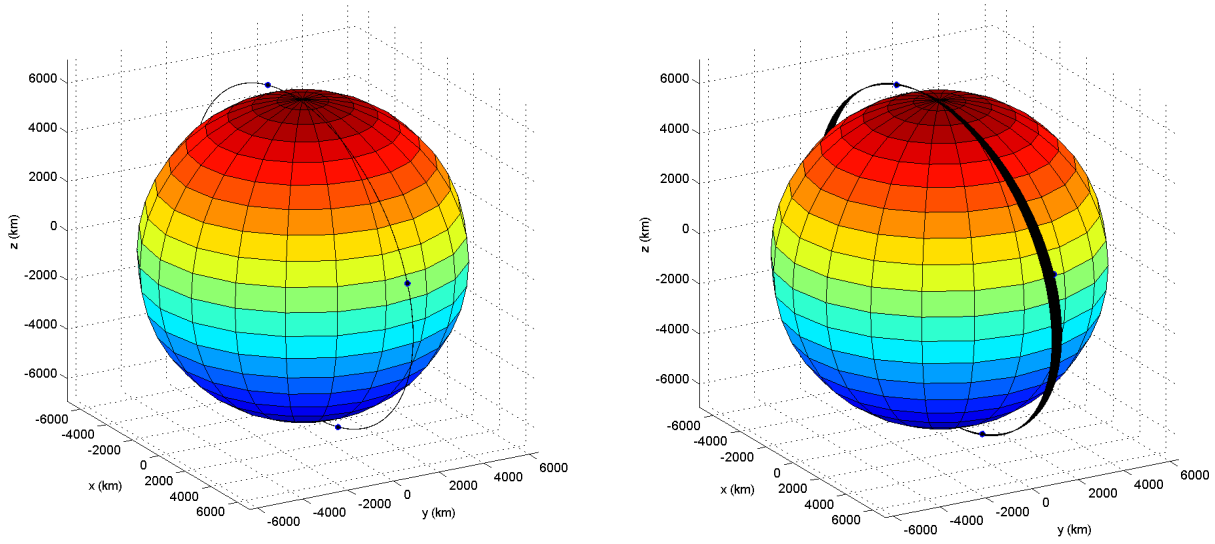

Figure 7.11: Initial (left) and 4 days propagation (right) of the inertial orbits of the constellation.

7.4 Conclusions

This chapter presents a new numerical method designed to obtain repeating ground-track orbits of a given satellite, taking into account orbital perturbations. This method is based on a semi-major axis correction that is performed in the orbit design and which includes the effects of all the perturbations considered in its formulation.

The advantages of this method is that it allows to improve the maintenance of the repeating ground-track property of a satellite despite of the orbital perturbations by just calculating a small number of orbit propagations. It has also applications on very different orbit designs, including retrograde or high elliptical orbits. Moreover, the method presented can be used with different perturbation models and propagators, being not restricted in that sense.

The most important property of the semi-major axis correction is that it allows to include periodic perturbations such as the Earth gravitational potential in the design of an orbit, which reduces the amount of fuel required to maintain the relative to Earth station-keeping. Other perturbations can be also included in the methodology improving the design obtained, however, due to the nature of non periodic and non conservative perturbations, the initial ground-tracks will be modified over time, and orbital maneuvers will be required to maintain the repeating ground-track property.

This numerical method has direct applications in different space missions, providing a wide variety of uses. This is improved with the addition of other orbital properties such as the sun-synchrony or the frozen condition. One of the most important applications of this methodology is Earth observation satellites that require the repeating ground-track property. With this technique, those missions can reduce the amount of fuel required to maintain their ground-tracks due to a decrease in the drift that their ground-track suffers over time compared with other methods. Other useful applications are communications, where the possibility of connecting satellites and ground segment in a periodic basis represents a repeating ground-track problem of great interest.

Another important application is satellite constellation design. In particular, the semi-major axis correction and the concept of designing a constellation in the ECEF frame of reference, can be combined to generate satellite constellations that take orbital perturbations into account in their design. This allows to maintain the configuration of the constellations for longer periods of time without using orbital maneuvers.

Chapter 8

Combining satellite constellation design

In previous chapters, we presented a set of methodologies that can be applied in satellite constellation design. In that respect, we included not only the theory and formulation behind these methodologies, but also multiple examples showing the possibilities of application of each design methodology. However, each technique has been treated separately throughout this work, not presenting, at a first glance, any relation between the different designs, nor how to apply them in a more complex problem.

In this final chapter, we focus on the combination and application of the different constellation design methodologies presented in this thesis. In particular, we deal with the relation that exists between the 2D Necklace Flower Constellations and the Ground-Track Constellations, providing a set of equations that allows to transform the first formulation into the later. Other lattice and necklace formulations can be obtained easily from the set of equations presented in this chapter, and thus, we do not treat them in here.

In addition, and in order to present a clear example of all these methodologies, a basic design and study of an Earth observation constellation based on the designs of the 2D Necklace Flower Constellations and the Ground-Track Constellations is presented. In particular, a constellation whose satellites share the same ground-track is selected, where some satellites of the constellation contain different instruments. This will allow to show the possibilities of design of the Necklace Flower Constellations and the Ground-Track Constellations, and will provide very interesting results from a design point of view.

Finally, the chapter includes a simple study of the constellation generated. This study is separated in three parts. In the first part, the mission concept is presented, including the selection of payloads and the requirements affecting the mission that are considered in this study. Second, we include the definition of the nominal design of the constellation by means of the Flower and Ground-Track Constellations formulations. After this process is done, we provide a description of a couple of launching strategies that allow to build the constellation in orbit. Third, we define a control strategy for the mission and evaluate the orbital maneuvers required by each satellite of the constellation. With all these results, a simple but complete study of an Earth observation constellation mission is shown.

8.1 From Flower Constellations to Ground-Track Constellations

We have seen previously that Necklace Flower Constellations were able to perform uniform distributions of a given set of satellites in the inertial frame of reference. On the other hand, Ground-Track Constellations focused on distribute satellites directly in the Earth Fixed frame of reference, being able to perform any kind of distribution, uniform and non uniform, being its inertial configuration a result of the design in the Earth Fixed. Now, we present a set of expressions that allows to transform the Necklace Flower Constellations into the Ground-Track Constellation formulation. That way, it is possible to determine how satellites are distributed in the Earth Fixed frame of reference.

In that respect, Ground-Track Constellations can only be related to 2D Lattice and Necklace Flower Constellations since in order for a subset of satellites to present the same ground-track, they have to share the semi-major axis, the inclination, the eccentricity and the argument of perigee. In particular, the most general representation of a Ground-Track Constellation distribution is defined as:

$$\begin{aligned} \Delta\Omega_{kq} &= \Delta\Omega_k - \omega_\oplus(t_{kq} - t_0), \\ \Delta M_{kq} &= n(t_{kq} - t_0), \end{aligned} \tag{8.1}$$

where $(t_{kq} - t_0)$ represents the along track distribution of the satellites of the constellation and $\Delta\Omega_k$ is the distribution of the ground-tracks in the Earth Fixed frame of reference. On the other hand, a 2D Lattice Flower Constellation is distributed following this expression:

$$\begin{aligned} \Delta\Omega_{ij} &= \frac{2\pi}{L_\Omega}(i-1), \\ \Delta M_{ij} &= \frac{2\pi}{L_M}(j-1) - \frac{2\pi}{L_M}\frac{L_{M\Omega}}{L_\Omega}(i-1), \end{aligned} \tag{8.2}$$

where L_Ω is the number of orbits of the constellation and L_M is the number of satellites per orbit. Thus, by identification of the distributions in Equations (8.1) and (8.2) we can obtain the relation between Ground-Track and 2D Lattice Flower Constellations:

$$\begin{aligned} \Delta\Omega_k &= 2\pi\left[\left(1 - \frac{\omega_\oplus}{n}\frac{L_{M\Omega}}{L_M}\right)\frac{(i-1)}{L_\Omega} + \frac{\omega_\oplus}{n}\frac{(j-1)}{L_M}\right] \mod (2\pi), \\ (t_{kq} - t_0) &= \frac{2\pi}{n}\left[\frac{(j-1)}{L_M} - \frac{L_{M\Omega}}{L_M}\frac{(i-1)}{L_\Omega}\right], \end{aligned} \tag{8.3}$$

which allows to obtain the distribution of a 2D Lattice Flower Constellation in the Earth Fixed frame of reference.

Moreover, it is possible to establish this relation using the 2D Necklace Flower Constellations formulation. As done in Chapter 2, the positions of the satellites in the different available positions in the orbital planes and in the mean anomaly can be defined by means of the position inside a necklace:

$$\begin{aligned} (i-1) &= \mathcal{G}_\Omega - 1, \\ (j-1) &= \mathcal{G}_M - 1 + S_{M\Omega}(\mathcal{G}_\Omega - 1), \end{aligned} \tag{8.4}$$

which introduced in Equation (8.3) leads to:

$$\begin{aligned}\Delta\Omega_k &= 2\pi\left[\left(1-\frac{\omega_\oplus}{n}\frac{L_{M\Omega}}{L_M}\right)\frac{(\mathcal{G}_\Omega-1)}{L_\Omega}+\frac{\omega_\oplus}{n}\frac{(\mathcal{G}_M-1+S_{M\Omega}(\mathcal{G}_\Omega-1))}{L_M}\right] \mod (2\pi),\\ (t_{kq}-t_0) &= \frac{2\pi}{n}\left[\frac{(\mathcal{G}_M-1+S_{M\Omega}(\mathcal{G}_\Omega-1))}{L_M}-\frac{L_{M\Omega}}{L_M}\frac{(\mathcal{G}_\Omega-1)}{L_\Omega}\right].\end{aligned} \tag{8.5}$$

However, it is interesting to study the case when the constellation is based on repeating ground-track orbits. In those cases, the mean motion n and the Earth spin rate $\omega_\oplus$ can be related with the number of orbit revolutions and days to ground-track repetition (N_p and N_d respectively):

$$n = 2\pi\frac{N_p}{T_c}, \qquad \omega_\oplus = 2\pi\frac{N_d}{T_c}, \tag{8.6}$$

being T_c the time that the constellation satellites require to close their ground-tracks. Thus, introducing this expressions in Equation (8.5):

$$\begin{aligned}\Delta\Omega_k &= 2\pi\left[\left(1-\frac{N_d}{N_p}\frac{L_{M\Omega}}{L_M}\right)\frac{(\mathcal{G}_\Omega-1)}{L_\Omega}+\frac{N_d}{N_p}\frac{(\mathcal{G}_M-1+S_{M\Omega}(\mathcal{G}_\Omega-1))}{L_M}\right] \mod (2\pi),\\ (t_{kq}-t_0) &= \frac{T_c}{N_p}\left[\frac{(\mathcal{G}_M-1+S_{M\Omega}(\mathcal{G}_\Omega-1))}{L_M}-\frac{L_{M\Omega}}{L_M}\frac{(\mathcal{G}_\Omega-1)}{L_\Omega}\right]+A\left(\frac{T_c}{N_p}\right),\end{aligned} \tag{8.7}$$

where A is an unknown integer and, since the ground-tracks are closed, a modular arithmetic in the ground-track distribution is introduced. Another interesting case of study happens when the constellation is distributed in just one ground-track. Since the distribution of the fictitious constellation is uniform, we know that the along track distribution of the constellation is also uniform and thus, we can define the distribution directly in the Earth Fixed frame of reference:

$$(t_{kq}-t_0) = \frac{(q-1)}{N_{st}}T_c = \frac{T_c}{N_p}\left[\frac{(\mathcal{G}_M-1+S_{M\Omega}(\mathcal{G}_\Omega-1))}{L_M}-\frac{L_{M\Omega}}{L_M}\frac{(\mathcal{G}_\Omega-1)}{L_\Omega}\right]+A\left(\frac{T_c}{N_p}\right), \tag{8.8}$$

where $N_{st} = L_\Omega L_M$ is the number of satellites of the constellation. We can simplified the former expression to obtain $(q-1)$ as a function of the distribution in the 2D Necklace Flower Constellation:

$$(q-1) = \frac{N_{st}}{N_p}\left[\frac{(\mathcal{G}_M-1+S_{M\Omega}(\mathcal{G}_\Omega-1))}{L_M}-\frac{L_{M\Omega}}{L_M}\frac{(\mathcal{G}_\Omega-1)}{L_\Omega}\right]+A\left(\frac{N_{st}}{N_p}\right), \tag{8.9}$$

and after performing some basic operations:

$$(q-1) = \frac{1}{N_p}\Big[(\mathcal{G}_M-1+S_{M\Omega}(\mathcal{G}_\Omega-1))L_\Omega-(\mathcal{G}_\Omega-1)L_{M\Omega}\Big]+A\left(\frac{L_\Omega L_M}{N_p}\right). \tag{8.10}$$

It is important to note that $(q-1)$ is always an integer number, since in order to have a 2D Necklace Flower Constellation distributed in just one ground-track, the combination number $L_{M\Omega}$ must be chosen in such a way that the value obtained in Equation (8.10) is an integer number. In addition, Equation (8.10) allows to determine the relative positions of the satellites along the ground-track of the constellation, since a necklace in the along-track distribution has been generated using this

procedure. In such cases, the distribution of the constellation in the right ascension of the ascending node and in the mean anomaly can be rewritten as:

$$\begin{aligned} \Delta\Omega_q &= -2\pi N_d \frac{(q-1)}{N_{st}}, \\ \Delta M_q &= 2\pi N_p \frac{(q-1)}{N_{st}}, \end{aligned} \tag{8.11}$$

where this expression represents the alternative formulation of an uniform distribution in a single ground-track based on the Ground-Track Constellations methodology.

Once the general relation between both constellation design formulations is introduced, we are able to show a simple but complete example of constellation design in the next section. This will allow to not only present some of the possibilities of design of these methodologies but also to show that the design concepts obtained are feasible from an engineering point of view.

8.2 Design and study of an Earth observation constellation

For this study we propose a constellation for Earth observation based on 6 satellites which have to observe the same regions of the Earth under very similar geometries. This property will allow to combine the scientific results of the different satellites and reduce the revisiting time of the mission. In that respect, the chosen constellation is based on the instruments carried by the missions Landsat 7 [47], OCO-2 [48] and CloudSat [1], having each two satellites of the constellation the same or equivalent payloads. This introduces in the problem studied three different families of instruments, which will have some interesting results during the design of the constellation.

Landsat program is the oldest family of satellites that have as their mission the acquisition of satellite imagery of the Earth. The program focuses on monitoring the landmass of the Earth, providing high spatial resolution images both in the visible and the infrared specters of light. The first satellite of the family, the Earth Resources Technology Satellite (later renamed Landsat 1), was launched in 1972 providing nearly three years of operation to the mission. Other satellites of the family followed the program: Landsat 2 (1975−1982), Landsat 3 (1978−1983), Landsat 4 (1982−1993), Landsat 5 (1984−2013), Landsat 6 (1993−1993), Landsat 7 (1999−) and Landsat 8 (2013−). In addition, Landsat 9 is expected to be launched in 2020. In this work we focus on Landsat 7 instrument, the Enhanced Thematic Mapper Plus (ETM+), and the requirements that this instrument imposes to the mission. The ETM+ is an imaging radiometer with eight spectral bands that ranges from the visible blue to the far infrared.

The Orbiting Carbon Observatory (OCO) is a satellite mission that was intended to provide observations on the atmospheric carbon dioxide from a near polar orbit. However, the first satellite of the series, OCO, was lost in a launch failure in 2009. Later, in 2014, OCO-2 was successfully launched to substitute OCO. One interesting property of OCO-2 is that the satellite maintains a loose formation with the A-train (a tandem formation of satellites), providing complementary scientific data to the mentioned constellation. The primary payload of OCO-2 consists of three high resolution grating spectrometers.

The CloudSat mission is part of the Earth Observing System (EOS) Afternoon Constellation, also known as the A-train, a tandem formation actually based on six satellites: Aqua, Aura, CALIPSO, CloudSat, GCOM-W1 and OCO-2. The aim of CloudSat is the study of clouds with the objective of characterizing the role they play in regulating the Earth's climate. The satellite was launched in 2006 and its primary payload is the Cloud Profiling Radar (CPR), a 94-GHz radar with 500-m vertical resolution.

8.2.1 Mission requirements

As it has been said, the mission considered is based on six satellites and two kinds of payloads, two different spectrometers (from Landsat 7 and OCO-2) and a radar (from CloudSat). In addition, each two satellites of the constellation will contain the same or an equivalent payload. This introduces a set of very different mission requirements for each satellite of the constellation that they must fulfill in order to provide scientific data to the mission.

Now, we present the mission requirements for each satellite, showing the constraints that each instrument introduces in the problem as well as the physical properties of the satellites that originally carried these payloads. In that respect, and in order to show the requirements in a clearer manner, we have separated each satellite class in a different point.

8.2.1.1 Landsat 7 class satellites (ETM+)

First of all, and for this mission, we assume that the two Landsat 7 class satellites will be the primary spacecrafts of the mission, since they are the heaviest satellites that we are considering. This means that, during the design, we will focus on the requirements of these two satellites, being the requirements of the other satellites additional constraints that we will apply to this first set of requirements.

The ETM+ is an instrument with a field of view of $\pm 7.5^o$ and a swath of 185 km, which requires to fly in a nominal orbit with an altitude of 705 $km \pm 5\, km$ at the equator. Moreover, this payload requires to perform periodically three different kind of calibrations that affects the selection of the orbit [49, 50, 51]:

- Ground Look Calibration (GLC): this calibration consists on the observation of particular areas of the Earth surface, that, due to their properties of homogeneity and stability over the course of the year, allow to perform measure comparisons. This calibration is carried out each 2 to 6 months during the normal operation of the satellite. Examples of this reference regions are Railroad Valley Playa ((38.5^o N, 115.7^o W)) and White Sands (32.9^o N, 106.4^o W).
- Full aperture Solar Calibration (FASC): this calibration is performed each 4 to 6 weeks during the normal operation of the satellite and consists on the observation of the Sun using a set of mirrors in the instrument while the satellite lays in the frontier between day and night and flies over the polar circle area.
- Partial Aperture Solar Calibration (PASC): this calibration is performed once per day and lasts two minutes. It consists on the measurement of the radiation of the Sun while the satellites has just exit an eclipse and its sub-satellite point is still in a night region.

Additionally, there are two more requirements that the ETM+ must fulfill. First, the local time at ascending node must be between 09:45 and 10:15. Second, and in order to maintain the ground-track of the orbit and the observation geometric properties, the orbit inclination of the satellite must be in the range of $\pm 0.15^o$ from the sun-synchronous inclination.

On the other hand, the spacecraft size and weight of the satellite also influences the dynamic of the satellite. In that respect, we select Landsat 7, as the reference for this class of satellites. Landsat 7 has a mass of 1982 kg, its height is 4 m and presents 2.7 m of diameter [52]. These dimensions will be used in order to evaluate the effect of the atmospheric drag in the satellite.

8.2.1.2 OCO-2 class satellites (grating spectrometer)

The instrument of OCO-2 (a payload consisting of three grating spectrometers), requires a sun-synchronous orbit with a local time at the ascending node between 13:18 and 13:33 and a nominal altitude over the equator of around 705 km. In addition, it requires an inclination control of $\pm 0.1^o$ related to its sun-synchronous inclination.

Furthermore, OCO-2, the reference satellite for this class of satellites, has a weight of 530 kg, a longitude of 2.3 m and 1.4 m of diameter [52].

8.2.1.3 CloudSat class satellites (CPR)

The CPR instrument does not introduce more requirements to the mission (since it share many of the previous constraints presented for Landsat 7 and OCO-2). In that respect, CPR requires also a sun-synchronous orbit with an altitude of around 705 km over the equator. In addition, the reference satellite used in this work, CloudSat, has a mass of 999 kg and the following dimensions: $2.3\,m \times 2.3\,m \times 2.8\,m$ [52].

8.2.1.4 Ground-track maintenance

In addition to the requirements imposed by each instrument of the mission, we are required to maintain the ground-track of the orbit inside some boundaries. This is done primarily for three reasons. The first one is in order to maintain the geometry of the observations from one cycle of repetition to other. This allows to compare the data of different passes, allowing a more in depth insight in the scientific problem considered. The second objective is to be able to maintain the communications with the ground segment in a periodic basis, presenting a geometry between satellite and ground stations that allows the communication for the time required in the mission. Finally, the third objective aims to maintain the structure of the constellation even under the orbital perturbations affecting the constellation.

In that regard, we will assume that all the constellation satellites will have a ground-track control both in plane and in inclination. The boundaries of this control will be the same for all the satellites of the constellation in order to maintain the structure of the system as a constellation. In particular, we assume a dead band of 1.5 km (in each direction) and a range of inclinations of ± 0.01 from the sun-synchronous inclination.

8.2.2 Nominal design of the constellation

Once the mission requirements have been presented, it is time to define the nominal design of the constellation. In order to do that, we first define the reference orbit for the constellation, that is, an orbit that is able to generate the ground-track that we are looking for while fulfilling all the requirements of the mission. Then, the design of the constellation will be performed using the theory of the 2D Necklace Flower Constellations and the Ground-Track Constellations.

First of all, and from the requirements of repetition from the calibration of the ETM+ as well as for convenience of design for data handling and performance of the mission, we select a repeating ground-track sun-synchronous orbit. Moreover, since all the satellites of the constellation require to observe the same regions of the Earth under similar geometries, we impose that all satellites of the constellation share the same ground-track. This means that the nominal values of the eccentricity, inclination, argument of perigee and semi-major axis of all the satellites of the constellation will be the same [22].

However, although the satellites of the constellation are required to fly in an orbit with an altitude of around 705 km, we do not know exactly the semi-major axis of the orbit nor its eccentricity or inclination. In order to obtain them, we impose the requirements of repeating ground-track orbit, sun-synchrony, and that the swath of the ETM+ is able to cover all the Earth at the end of the repeating cycle. By applying these conditions, we can obtain a series of compatible orbits. A summary of them can be seen in Table 8.1. In fact, there are more solutions to the ones presented, however, we focus on the ones that present the minimum repetition time.

Table 8.1: Repetition parameters of some compatible orbits.

$\mathbf{N_p}$	233	262	277	291	306	335	364	379	393	408	422	437
$\mathbf{N_d}$	16	18	19	20	21	23	25	26	27	28	29	30

From Table 8.1 we can observe that the solution with the best repetition time is the one with $N_p = 233$ and $N_d = 16$, thus, we select it as the nominal orbit for the constellation. This means that each satellite of the constellation will repeat its ground-track in 233 orbit revolutions or 16 days. On the other hand, and since we want the orbit to be as stable as possible, we impose that the satellites of the constellation present the frozen orbit property. With these conditions, we are able to obtain the nominal values of the semi-major axis, the eccentricity, the inclination, and the argument of perigee of the orbits. A summary of them can be seen in Table 8.2.

Table 8.2: Orbital parameters of the nominal orbit of the constellation.

Nominal semi-major axis	7077.722 km
Nominal inclination	98.186^o
Nominal eccentricity	0.001043
Nominal argument of perigee	90.000^o
Right ascension of the ascending node and mean anomaly	Dependant on the date and satellite

With the results provided in Table 8.2, we can now focus on the distribution of the constellation. The first step for this is to determine the size of the fictitious constellation that we require to generate. We know from the requirements of Landsat 7 and OCO-2, that they require a local time in the ascending node from 09:45 to 10:15 and from 13:18 to 13:33 respectively. The local time is in fact providing us the information of the angular distance that must exist between the orbital planes of both satellites. In particular, we can separate both orbital planes 51.43^o to fulfill this requirement. This angular distance is chosen to slightly simplify the following calculations, since the value corresponds to the seventh part of the complete rotation ($360^o/7 \approx 51.43^o$). On the other hand, we assume that the CloudSat class satellites do not require any special local solar time to perform their measurements. Thus, with this simple calculation, we have determined that the fictitious constellation must present 7 orbital planes, that is $L_\Omega = 7$ and, since the number of satellites that share instrument is two, we can derive that $N_\Omega = 3$.

The objective now is to determine the number of available positions that can be defined in each orbit in order for all the satellites to have the same ground-track. From the expression in the right ascension of the ascending node of Equation (8.11), if we impose that all the satellites belong to the same inertial orbit:

$$0 = -2\pi N_d \frac{(q-1)}{N_{st}} \mod (2\pi), \tag{8.12}$$

we can derive that the maximum number of available positions in each inertial orbit is equal to N_d (which corresponds to the nodes of the orbit). This means that the fictitious constellation that is compatible with the ground-track of the problem has $L_M = N_d = 16$ available positions in each orbit, where only two positions will be occupied by satellites of the constellation, that is, the number of real satellites per orbit is $N_M = 2$.

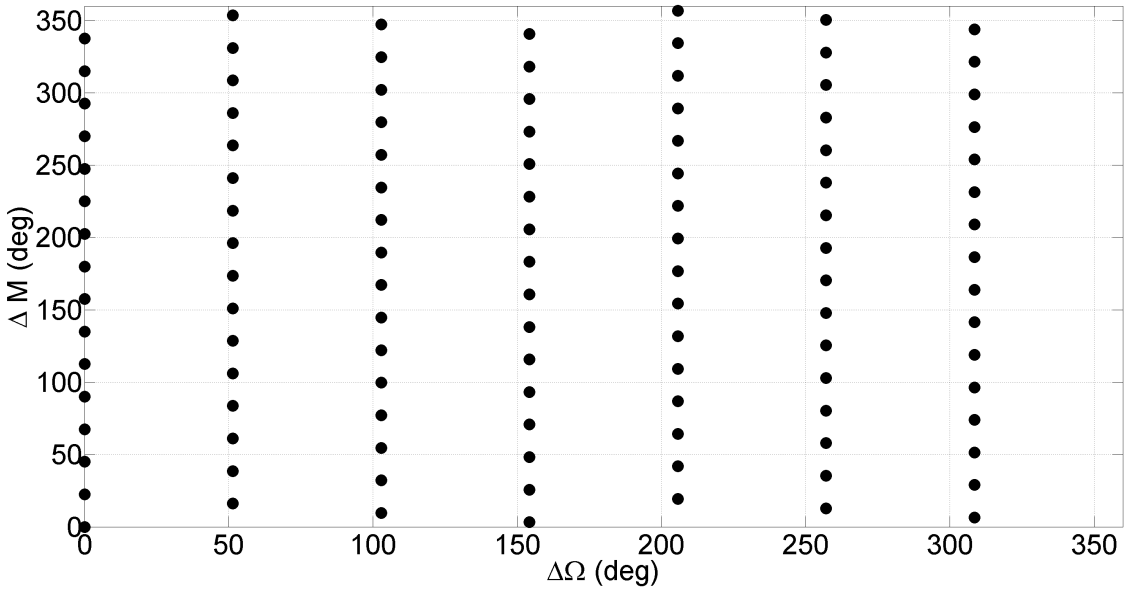

Figure 8.1: Representation of the fictitious constellation in the (Ω, M)-space.

With the dimension of the fictitious constellation already known, that is, L_Ω and L_M, the only parameter of the fictitious constellation that we have to compute is the combination number $L_{M\Omega}$. Its value can be obtained by analyzing Equation (8.10) and imposing that the expression always

generates an integer number. That way, we can derive that the combination number that allows the fictitious constellation to be distributed in only one ground-track is $L_{M\Omega} = 2$. Figure 8.1 shows the distribution of the fictitious constellation in the (Ω, M)-space. It is important to note that the position of the reference satellite of the orbit will depend on the date, since the orbit and the satellites are rotating during the dynamic of the system.

The objective now is to select the positions where the satellites are located, that is, the introduction of necklaces. This process is done in two steps. First, a necklace in the mean anomaly $\mathcal{G}_M$ is introduced and the uniform distributions related to it derived. Then, the necklace in the right ascension of the ascending node is defined, which will constrain the constellation to the orbital planes of interest.

We have to select two satellites from each inertial orbit. In that respect, it is of interest for the mission that the along track distance between both is maximum in order to optimize the revisiting time. Thus, the necklace in the mean anomaly is defined as $\mathcal{G}_M = \{1, 9\}$, where $\mathcal{G}_M(1) = 1$ is the first satellite of each class and $\mathcal{G}_M(2) = 9$ is the second satellite of each class. Then, we obtain the shifting parameter for this configuration by the application of Equation (2.23):

$$8 \mid 7S_{M\Omega} - 2, \tag{8.13}$$

which has as a solution $S_{M\Omega} = 6$. Figure 8.2 shows the resultant configuration, where the filled circles are actual satellites and the emptied and filled circles are the available positions of the fictitious constellation. As it can be seen, the uniformity of the configuration is maintained.

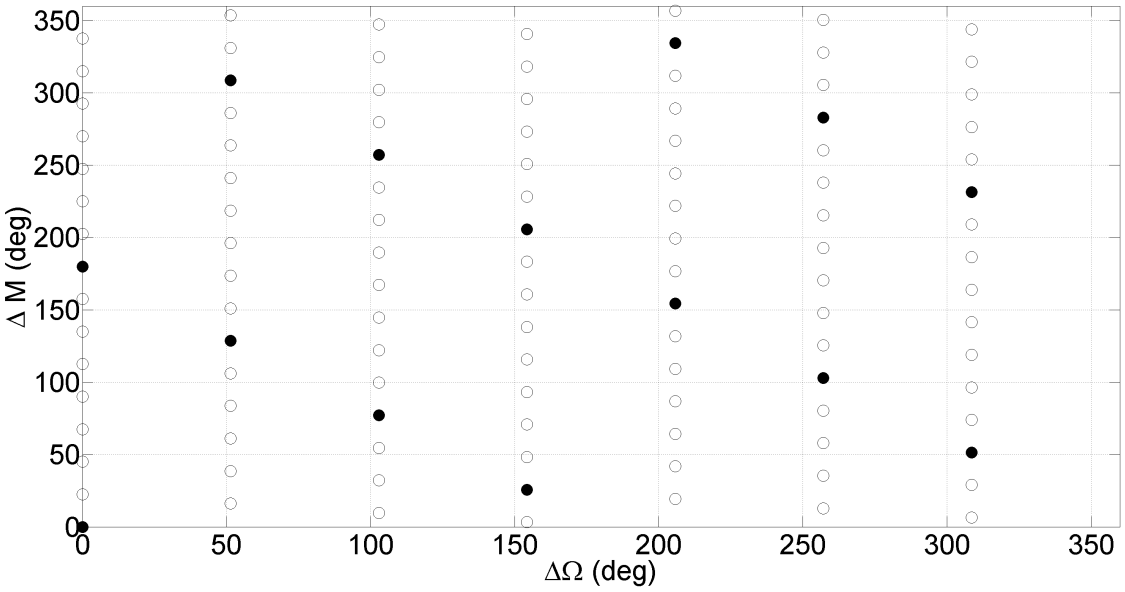

Figure 8.2: Representation of the fictitious constellation with a necklace in the mean anomaly.

After that, we require to include the necklace in the right ascension of the ascending node. In that respect, and since we consider the Landsat 7 class satellites the primary spacecrafts of the mission, we consider their orbital plane as the reference for the constellation. Then, from the mission requirements, we know that the Landsat 7 and OCO-2 class satellites must be in two different planes at an angle of 51.43^o, which represent two consecutive planes of the fictitious constellation. On the

other hand, we locate the orbital plane of the CloudSat class satellites at the same angular distance but on the other direction. That way, the necklace selected is $\mathcal{G}_\Omega = \{1, 2, 7\}$, where $\mathcal{G}_\Omega(1) = 1$ corresponds to the Landsat 7 class satellites, $\mathcal{G}_\Omega(2) = 2$ relate to the OCO-2 class satellites, and $\mathcal{G}_\Omega(3) = 7$ represents the CloudSat class satellites.

Table 8.3: Distribution of the constellation.

	Landsat 7 class $\mathcal{G}_\Omega(1)$		OCO-2 class $\mathcal{G}_\Omega(2)$		CloudSat class $\mathcal{G}_\Omega(3)$	
	$\mathcal{G}_M(1)$	$\mathcal{G}_M(2)$	$\mathcal{G}_M(1)$	$\mathcal{G}_M(2)$	$\mathcal{G}_M(1)$	$\mathcal{G}_M(2)$
$\Delta\Omega$	0.0000^o	0.0000^o	51.4286^o	51.4283^o	308.5714^o	308.5714^o
ΔM	0.0000^o	180.0000^o	128.5714^o	308.5714^o	51.4286^o	231.4286^o

This satellite distribution is summarized in Table 8.3 showing where the different instruments are located. Additionally, Figure 8.3 shows the general distribution of the constellation where the first orbit contains the two Landsat 7 class satellites, the second orbit contains the OCO-2 class satellites and the seventh orbital plane contains the CloudSat class satellites.

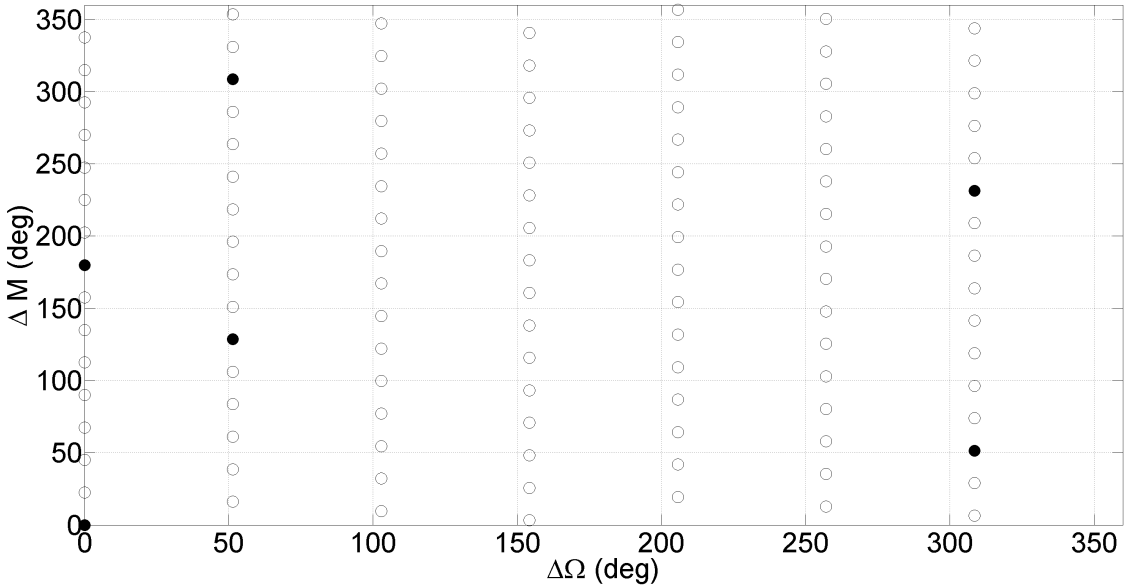

Figure 8.3: Representation of the real constellation in the (Ω, M)-space.

Finally, we determine the order that the satellites follow in their ground-track as well as their along track distance. This is done by using Equation (8.10). It is important to note that Equation (8.10) can be expressed as a Diophantine equation that has only one solution since $q \in \{1, \ldots, L_\Omega L_M\}$. Table 8.4 shows the results of that conversion. As it can be seen, the satellites are sequential, that is, first, an OCO-2 class satellite flies over a given area, then, a Landsat 7 class satellite does so followed by a CloudSat class satellite and again a OCO-2 class satellite, repeating the sequence commented.

Table 8.4: Along track distribution of the constellation.

	Landsat 7 class $\mathcal{G}_\Omega(1)$		OCO-2 class $\mathcal{G}_\Omega(2)$		CloudSat class $\mathcal{G}_\Omega(3)$	
	$\mathcal{G}_M(1)$	$\mathcal{G}_M(2)$	$\mathcal{G}_M(1)$	$\mathcal{G}_M(2)$	$\mathcal{G}_M(1)$	$\mathcal{G}_M(2)$
q	1	57	105	49	65	9

Another important thing to notice is that this is just a possible configuration of the constellation. In that regard, the satellites still have a degree of freedom inside their orbits represented by the available positions of the fictitious constellation. This provides a tool for easily reconfigure the constellation or to fit it to more restrictive requirements or a more concrete mission.

8.2.3 Possible launching strategies

The previous section showed the general distribution of the constellation satellites referenced to one of the Landsat 7 class satellites. However, we did not treat the launching possibilities available nor the strategy to acquire the formation once in orbit. In this section, we describe two launching strategies for the constellation under two different suppositions. In the first one we consider that it is possible to launch two satellites at the same time, while in the second one we assume that each satellite will be launched in different dates.

If it is possible to launch two satellites at the same time, satellites of the same class (that is, that contain the same payload) are launched together, being able to fill the satellites of one orbital plane at the same time. In these cases, a possible strategy consists on injecting the satellites into an orbit that is slightly higher than the nominal. This is done in order to reduce some fuel in the acquisition of the final positions of the satellites in that orbit. In fact, the orbital plane should also be slightly rotated respect to the nominal in order to introduce the effects of the drifting due to the J_2 perturbation during the initial orbit acquisition. The exact values of these modifications depend greatly on the launcher selected, thus, we will not include a study of all these possibilities.

On the other hand, if each satellite is launched separately, we will have two launches per inertial orbit. The first one should aim to the nominal position selected for that particular satellite, that is, one of the nodes of the inertial orbit. However, the second satellite on that orbit must perform other considerations. First of all, one of the nodes of the orbit will be occupied by the first satellite launched. This implies that now there are some nodes in which the injection is not allowed. Second, we have to consider the situations in which a collision may occur between the two satellites. For those reasons, the second satellite should be injected in a lower orbit than the nominal and ahead of the first satellite (see Figure 8.4). This reduced semi-major axis must take into account the launcher injection errors, being sure that the probability that the second satellite and the upper stage of the launcher crosses the orbit of any satellite of the constellation is negligible. Moreover, flying ahead with a lower altitude provides us the certainty that the satellites will move apart each other in the first days of mission.

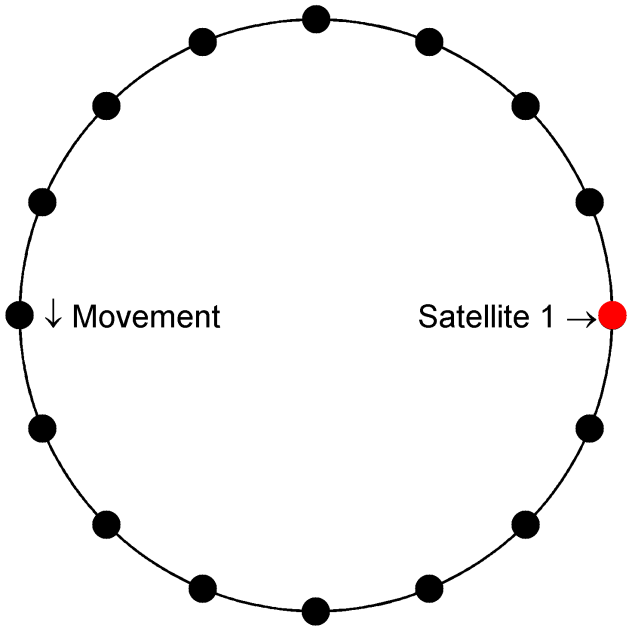

Figure 8.4: Possible injection positions in the orbit.

8.2.4 Control strategy and station keeping

With the nominal values of the orbital elements provided before, it is possible to maintain the orbits without any orbital maneuver under the gravitational potential of the Earth. This is done by transforming the mean elements from the nominal design of the orbit to osculating elements for each particular satellite of the constellation. That way, if only the J_2 perturbation is considered, we can use a transformation like the one of Kozai [28] or Liu [26, 27]. However, if more terms of the Earth gravitational potential are considered, a numerical algorithm is required. An example of this kind of algorithms is the one provided in Chapter 7. Using this transformations, it is possible to maintain a frozen orbit, like the orbits considered, nearly indefinitely under these perturbations, being the maneuvers required negligible compared to other orbital perturbations.

In addition to the Earth gravitational potential, we consider in this study the atmospheric drag, the Sun and Moon as disturbing third bodies and the solar radiation pressure. In that respect, and due to the nature of the problem, we will separate their effects in in plane and out of plane maneuvers, which are more related to the actual control of the satellites.

For this mission, we propose a control box strategy for all the satellites of the constellation. This means that each satellite will have a defined boundary in which it is maintained. From the mission requirements, we have to impose a control in inclination of $\pm 0.01^o$ with respect to the sun-synchronous inclination and a dead band of $\pm 1.5\, km$, which corresponds approximately to the maximum deviation that the control in inclination provokes in the ground-track of the orbits. This control box is applied to all the satellites of the constellation in order to maintain the formation over time.

8.2.4.1 In plane maneuvers

In plane maneuvers have two objectives. The first one aims to counter the decay of the semi-major axis of the orbit due to the atmospheric drag, while its second objective consists on the maintenance of the ground-track of the orbit inside its defined dead band. These two effects are provoked primarily by the atmospheric drag and the Sun and Moon as disturbing third bodies.

In this section we present the results for frequency between in plane maneuvers, size of the maneuvers and impulse in each maneuver for all the satellites of the constellation. As it will be seen, these values depend on the physical properties of each satellite and the date in which the computation is considered. In that respect, we have selected the values of the real Landsat 7, OCO-2 and CloudSat as the references for this study. A summary of their properties is provided in the mission requirements of this chapter. All the in plane maneuvers are assumed to be performed when the satellites are in eclipse in order to not disturb the normal acquisition of images.

On the other hand, and in addition to the expected correction due to the orbital perturbations, a given number of collision avoidance maneuvers per year must be taken into account when defining the fuel budget. However, in most cases those maneuvers require to increase the semi-major axis of the orbit, and thus, do not provoke an increase in the requirements of fuel for the mission (since this fuel is being used to improve the maintenance of the ground-track at the same time). For this reason, we do not treat these cases in the following study.

The results presented in this section are generated using the MSIS-00 model for the atmospheric density, and tabulated data from European Cooperation for Space Standardization (ECSS) for the flux generated in a solar cycle. Moreover, we consider a constant density during each day. In addition, all the figures shown in this section correspond to a complete solar cycle beginning on January of 2020. Note that if information about the mission for other dates not presented in the figures is required, these results can be extrapolated to other dates due to the eleven years periodicity of the solar cycle.

It is important to note that the results presented in this section greatly depend on the ballistic coefficient of the satellites, the local time in their ascending nodes, the solar flux and the drag coefficient of these satellites. In that respect, the values of the solar flux (and thus the atmospheric density) is only a prediction based on past cycles of the Sun, that is constantly updated to include new data. On the other hand the drag coefficient of the satellites is an estimation based on past missions and we are only able to obtain a more precise value once the satellite is in orbit. This means that the calculation presented in this section has a high uncertainty due to these factors. However, these results present a baseline of the strategy and the order of magnitude of the maneuvers expected during the mission of the satellites.

8.2.4.1.1 Landsat 7 class satellites

We start the in plane maneuver study with the results for the Landsat 7 class satellites. In particular, Figures 8.5 shows the maneuver frequency, Figure 8.6, the size of the maneuver, and Figure 8.7, the impulse required in each maneuver.

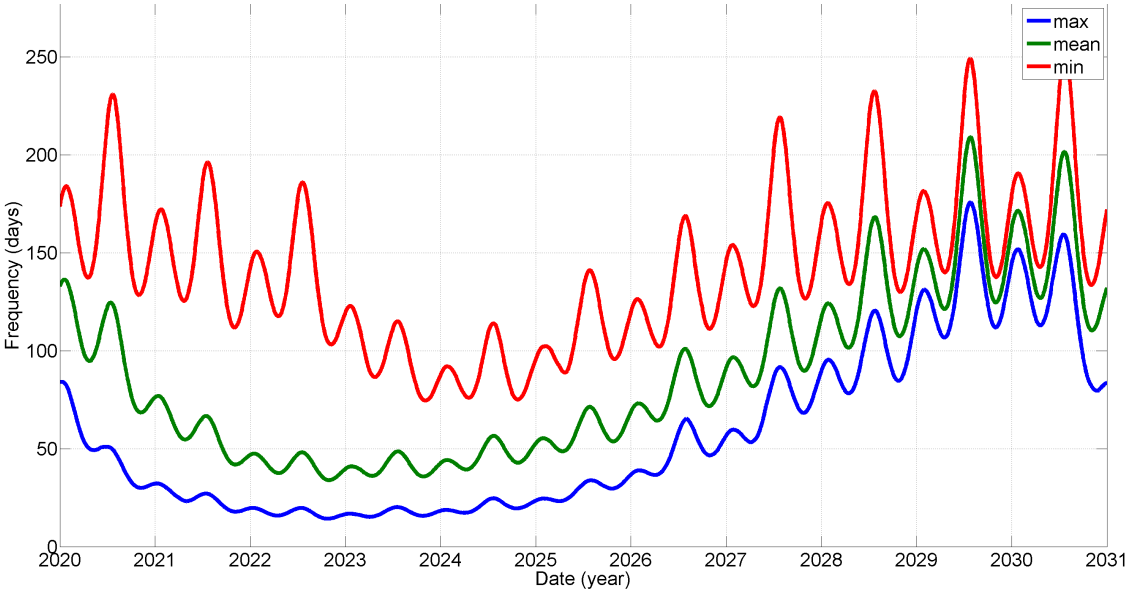

Figure 8.5: Maneuver frequency of the Landsat 7 class satellites.

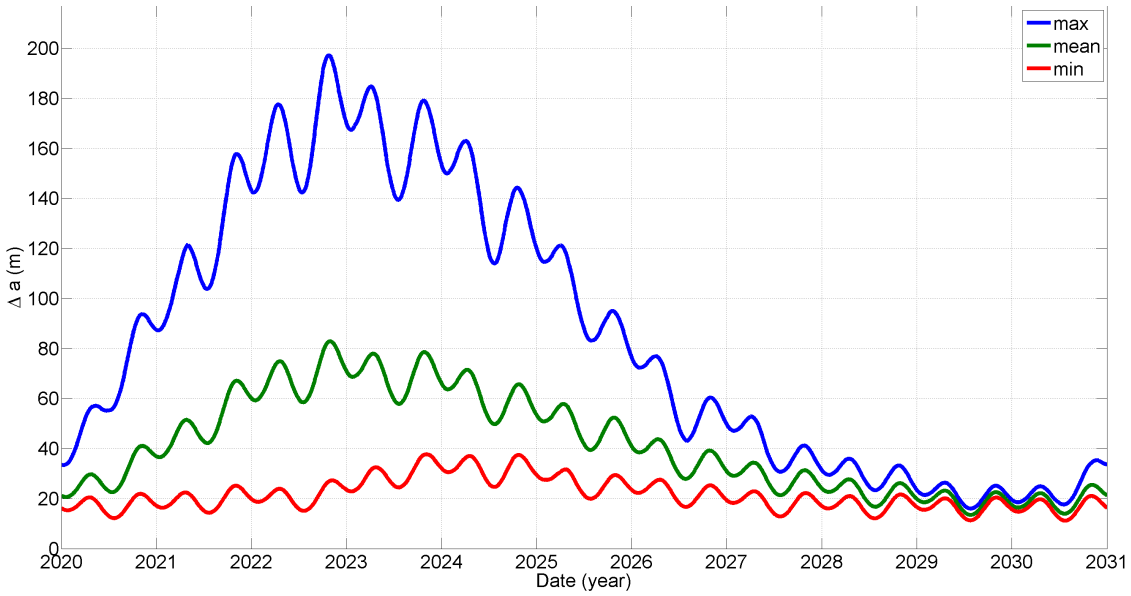

Figure 8.6: Size of the maneuver of the Landsat 7 class satellites.

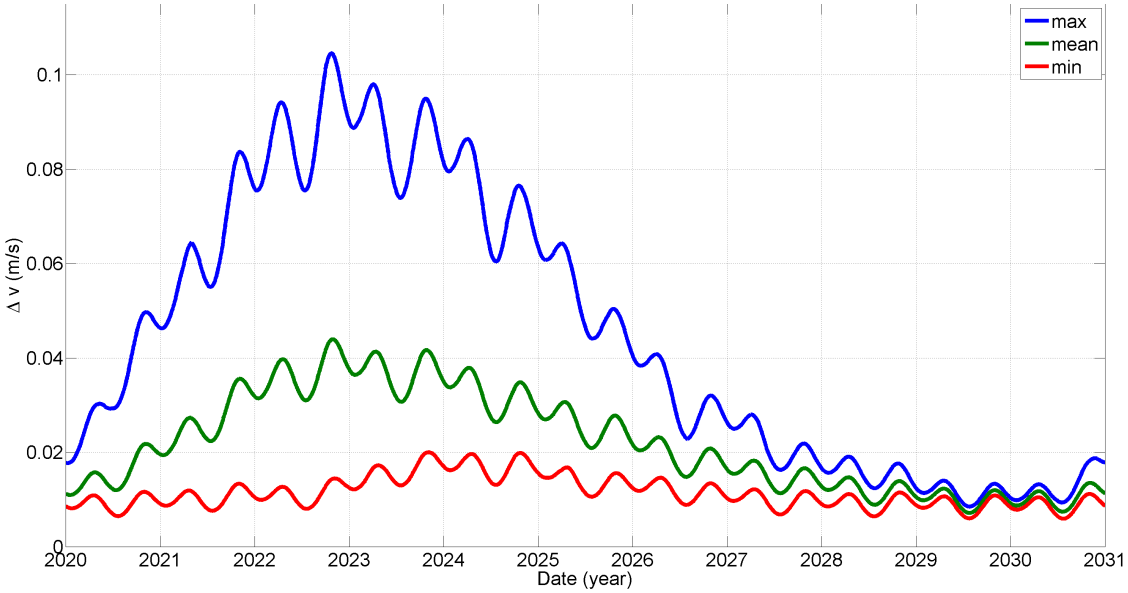

Figure 8.7: Δv per maneuver of the Landsat 7 class satellites.

8.2.4.1.2 OCO-2 class satellites

As done before, the following figures present the results for the OCO-2 class satellites and for a complete solar cycle of eleven years. To be more precise, Figures 8.8 shows the maneuver frequency, Figure 8.9, the size of the maneuver, and Figure 8.10, the impulse required in each maneuver.

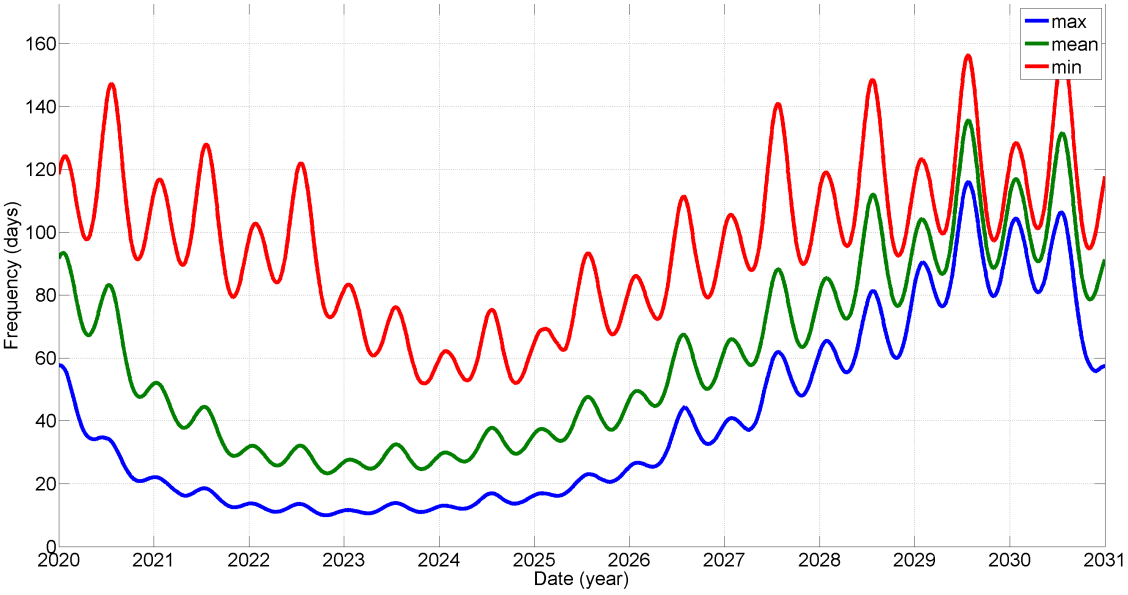

Figure 8.8: Maneuver frequency of the OCO-2 class satellites.

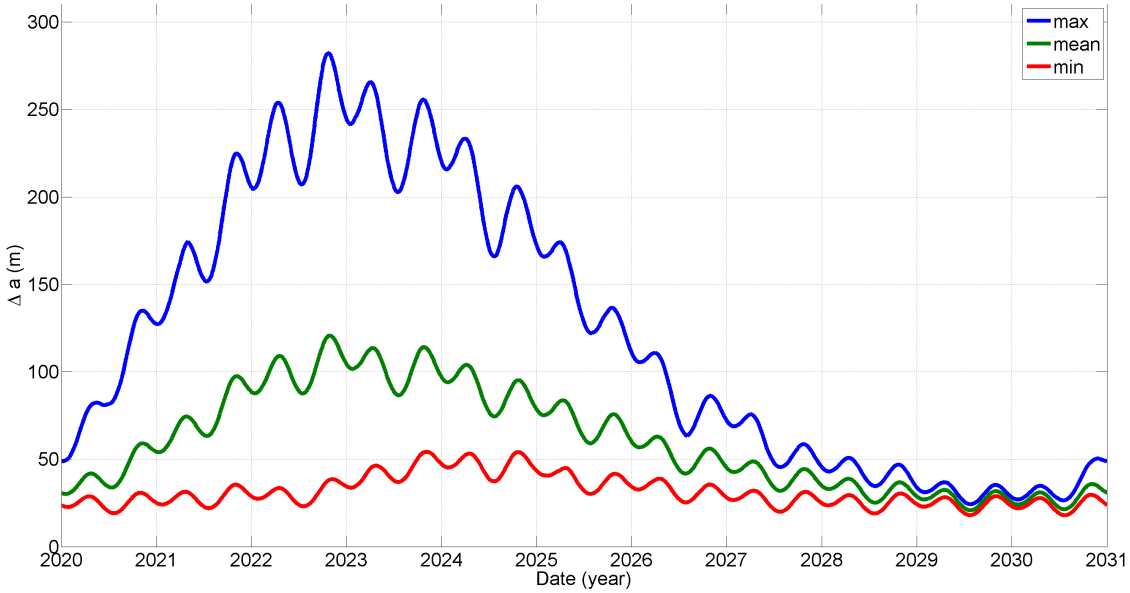

Figure 8.9: Size of the maneuver of the OCO-2 class satellites.

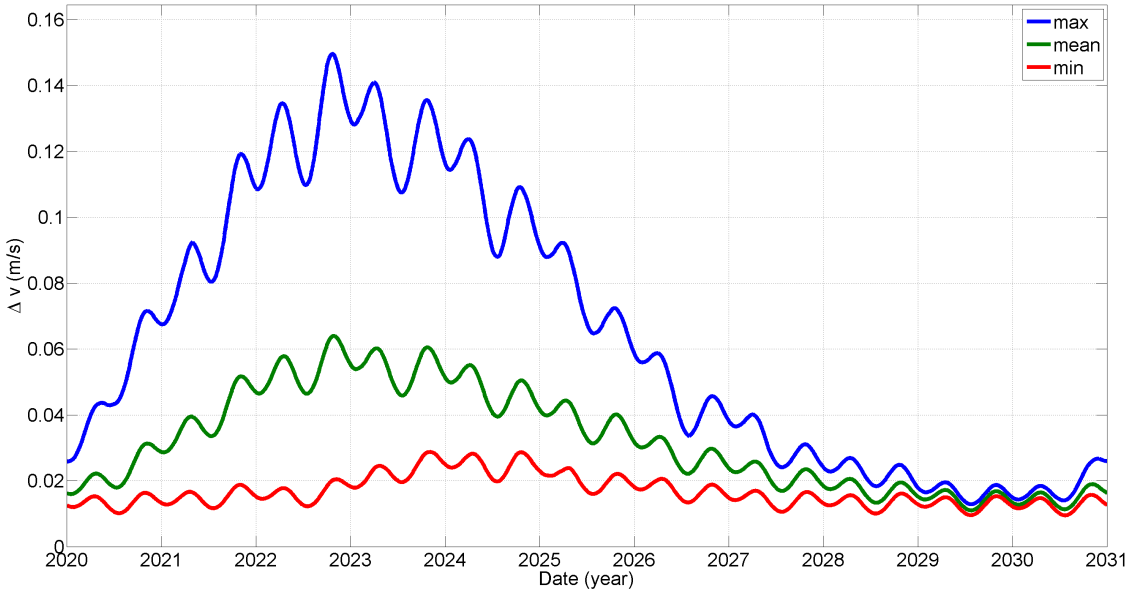

Figure 8.10: Δv per maneuver of the OCO-2 class satellites.

8.2.4.1.3 CloudSat class satellites

Finally, we present the results for the CludSat class satellites. In that regard, Figure 8.11 presents the maneuver frequency, Figure 8.12, the size of the maneuver, and Figure 8.13, the impulse required in each maneuver.

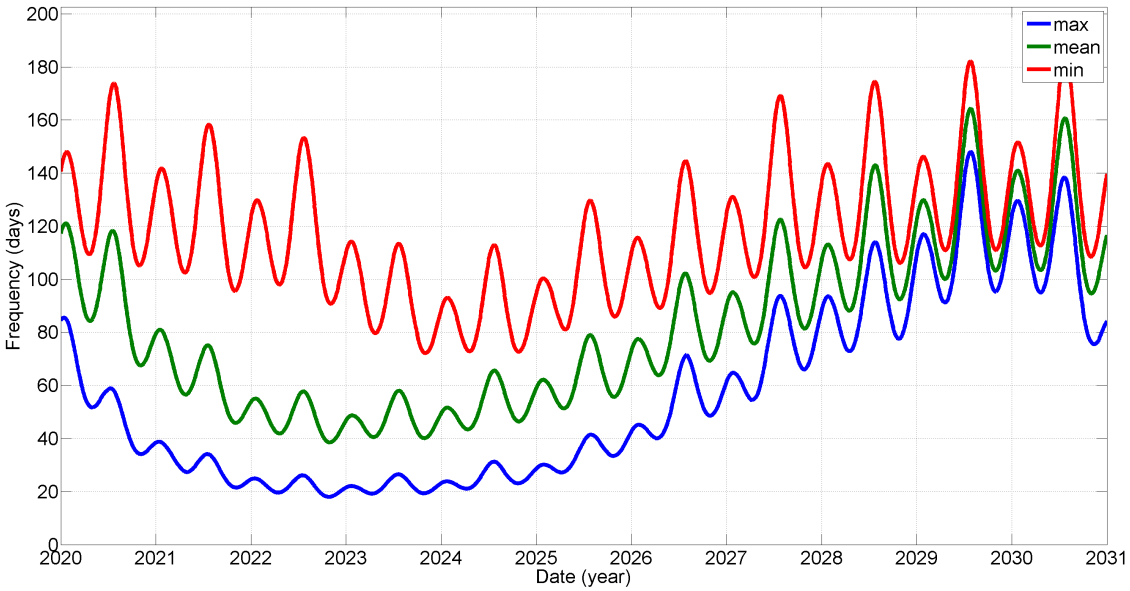

Figure 8.11: Maneuver frequency of the CloudSat class satellites.

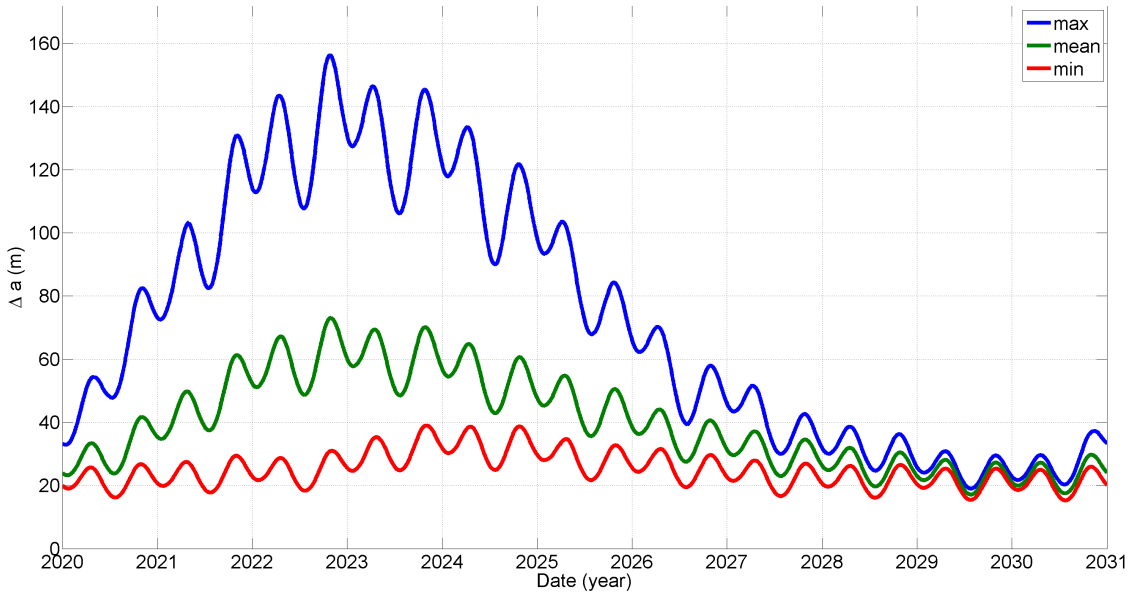

Figure 8.12: Size of the maneuver of the CloudSat class satellites.

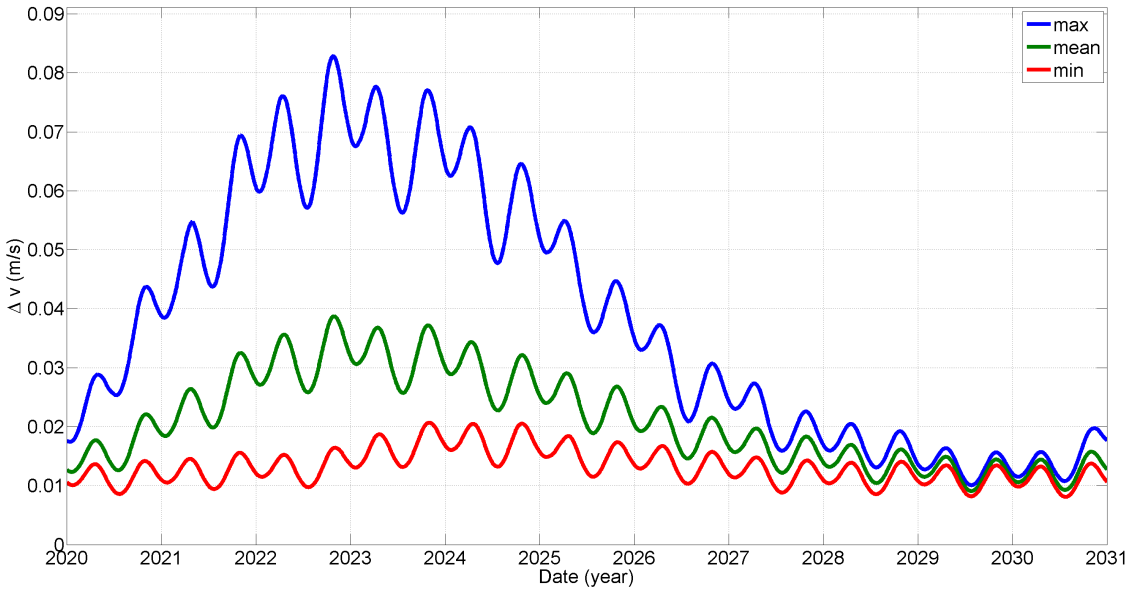

Figure 8.13: Δv per maneuver of the CloudSat class satellites.

As it can be seen from the results presented for each class of satellites, the maneuver frequency and the size and impulse required in each maneuver depends on the satellite considered. In particular, the ballistic coefficient is affecting considerably the results obtained. For instance, focusing on the maneuver frequency, bigger satellites require to perform maneuvers with less frequency, while smaller satellites require more maneuvers for the same time period.

8.2.4.2 Out of plane maneuvers

Out of plane maneuvers aim to ensure the sun-synchrony of the orbit, the mean local solar time, and the maintenance of the ground-track of the constellation. The deviation produced in the inclination of the orbits is provoked primarily by the Sun and Moon as disturbing third bodies and the solar radiation pressure. In this section we present the results of the evolution of the inclination of the orbits under perturbations and the out of plane maneuvers required to maintain the satellites in their defined control boxes.

For this study, we take into account the following perturbations: the Earth gravitational potential up to 4th order terms (including tesseral terms), the Sun and Moon as disturbing third bodies, the solar radiation pressure and the atmospheric drag (using the same model as in the in plane maneuvers). In addition, we assume that the out of plane maneuvers are performed once the satellite has reach the boundary, this means that all the out of plane maneuvers will be based in a change of inclination of 0.02^o, which means that the impulse required is $\Delta v = 2.61957\, m/s$ for each maneuver. Another important thing to notice is that out of plane maneuvers will modify the along track distribution of the constellation and thus, we must expect additional in plane maneuvers following each out of plane maneuver. Since this additional maneuvers are very dependent of the impulsive errors, we do not treat them in this study.

8.2.4.2.1 Landsat 7 class satellites

As before, we begin the study with Landsat 7 class satellites. In that respect, Figure 8.14 shows the evolution of the inclination of the orbit through one year of propagation. From this figure and the numerical data obtained, we can derive that for the inclination boundary considered, that is, $\pm 0.01^o$, an out of plane maneuver should be planed for each Landsat 7 class satellite each 200 days of mission.

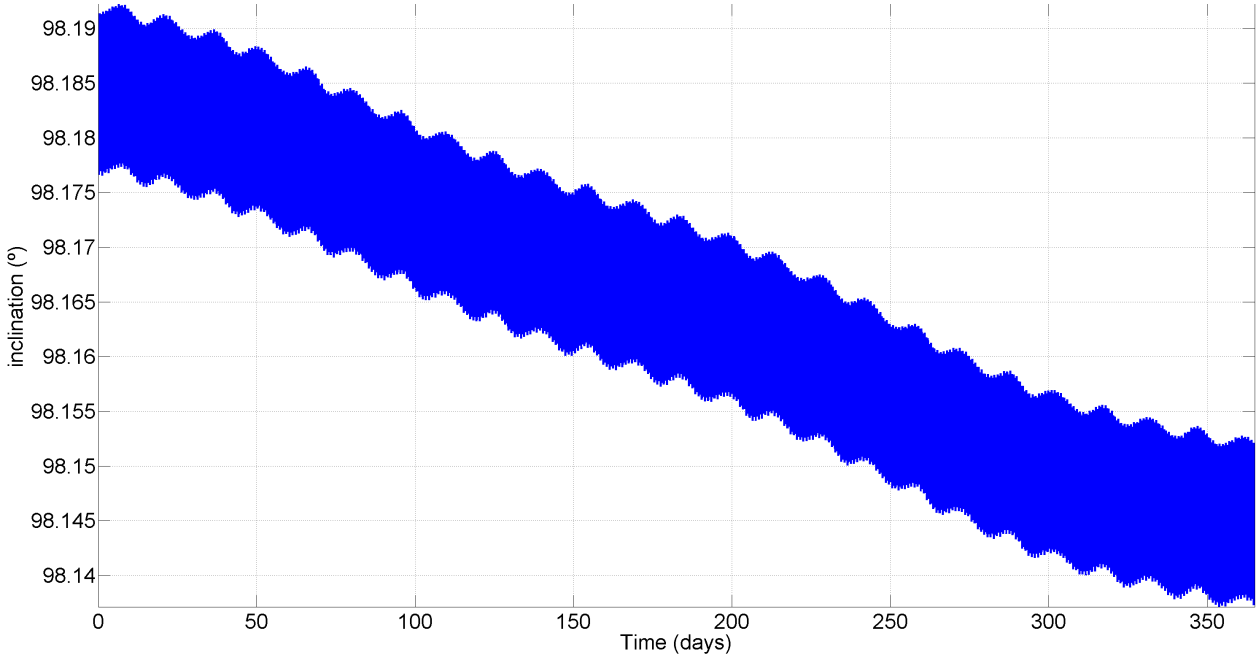

Figure 8.14: Inclination evolution of the Landsat 7 class satellites.

8.2.4.2.2 OCO-2 class satellites

We continue the study about the out of plane maneuvers of the constellation with the OCO-2 class satellites. Figure 8.15 presents the evolution of the inclination (in osculating elements) for one year of propagation of the satellites. From the figure and the numerical data produced during the propagation, we conclude that this class of satellites will require an out of plane maneuver each 260 days in order to fulfill the inclination mission requirements.

Additionally, it is important to note that the secular variation of the inclination suffered by OCO-2 class satellites is positive, compared to the Landsat 7 and CloudSat class satellites which is negative. This effect is produced by the different orientation of the orbit of OCO-2 class satellites with respect to the Sun. In particular, OCO-2 class satellites orbit is the only one with a local solar time in the ascending node greater than the 12:00 hours, more precisely 13:26, which produces this important change in the evolution of the inclination.

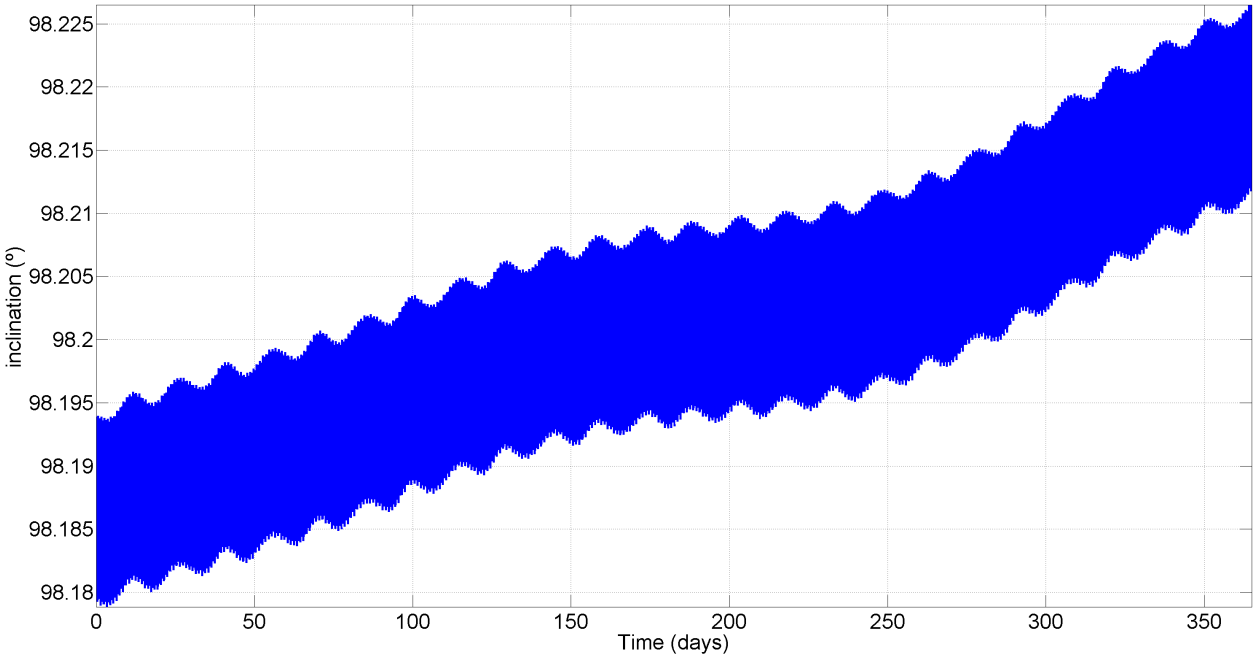

Figure 8.15: Inclination evolution of the OCO-2 class satellites.

8.2.4.2.3 CloudSat class satellites

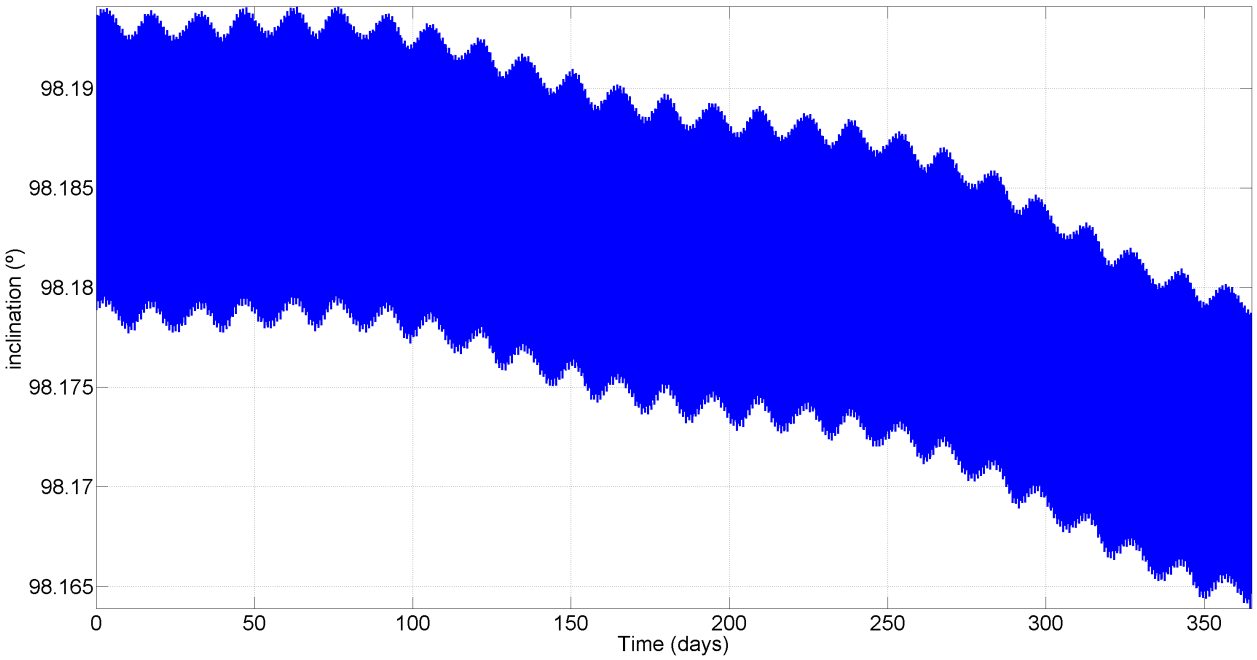

Figure 8.16: Inclination evolution of the CloudSat class satellites.

Finally, Figure 8.16 shows the osculating evolution of the inclination for the CloudSat class satellites for one year of propagation (as in the other cases). However, in this case, after a year of propagation, the satellites are not able to reach the boundaries of the control box. In fact, the computation has been continued, in order to obtain a frequency between out of plane maneuvers. By doing that, we conclude that an out of plane maneuver is required each 600 days of mission.

On the other hand, comparing Landsat 7 class satellites inclination evolution with the one of CloudSat, we can see how CloudSat class satellites require a lesser number of out of plane maneuvers for the same time period. This is provoked due to the gyroscopic effect in the orbit, affecting more intensively to satellites near the 12:00 - 24:00 local solar time at the ascending node. In that respect, the reader should remember that there are two sets of equilibrium points in the inclination. The first one corresponds to the 06:00 - 18:00 orbits which are also know as dusk and dawn orbits (stable configuration); while the second set comprised by the 12:00 - 24:00 orbits is unstable.

8.3 Conclusion

This chapter has introduced a general methodology to relate 2D Necklace Flower Constellations with Ground-Track Constellations. This allows to benefit from both formulations, being able to obtain precise information on the distribution that the constellation presents both in the inertial and in the Earth Fixed frame of reference. In that respect, the chapter focuses on the special case where all the satellites of the constellation share the same ground-track, since this is a very interesting design in many Earth observation an telecommunication missions.

On the other hand, an example of constellation for Earth observation is provided. This constellation design is performed using the methodologies of the Necklace Flower Constellations and the Ground-Track Constellations, which allows to fulfill the mission requirements considered. In that regard, the constellation is based on six satellites containing three different payloads, which means that each instrument introduces new constraints in the problem.

In addition, a complete study of the constellation is performed, including the definition of the nominal orbits of the constellation, the launching strategy and the control strategy for the mission. That way, we present in a clearer manner how all the theory presented in this thesis works together, and how it can be applied to a more complex problem that presents very different mission requirements, showing a possible solution to the problem.

Conclusions

The research presented in this manuscript departs from the Flower Constellations Theory, a general satellite constellation methodology of design based on Number Theory which allows to generate any kind of satellite configuration. In particular, this work centers its attention on its lattice formulations, represented by the 2D and 3D Lattice Flower Constellations, which are the evolution of the initial parametrization of the theory, and the 2D Lattice Flower Constellations using necklaces, which introduced, for the first time, the idea of necklaces in satellite constellation design. Taking these methodologies as a base, this thesis continues that research by generalizing the previous theory and introducing new approaches to the problem.

This work contains the complete Necklace Flower Constellations theory, a new framework for satellite constellation design. The particularity of this new technique lays in the generation of constellation configurations where the satellites are able to create structures that are maintained during their dynamic. In addition, the theory allows to expand the number of different configurations as much as desired, which provides a powerful tool for satellite constellation design.

Necklace Flower Constellations constitutes the evolution and generalization of Lattice Flower Constellations, a methodology that was initially devised to generate uniform and symmetric configurations. In particular, Necklace Flower Constellations allows to increase the size of the searching space, being able to generate a greater number of possible configurations while maintaining the number of satellites of the constellation. This is done by the generation of a fictitious constellation, bigger than the one that we are seeking, from where we select the subset of satellites that fulfills the conditions of symmetry and uniformity. That way, the characteristics of the original Lattice Flower Constellations are maintained in the design.

This methodology has multiple uses. First of all, it allows to expand the number of possibilities that a set of satellites can provide. Second, it presents possible reconfiguration opportunities that a constellation can perform in order to obtain compatible distributions. Third, it allows to define the sequence of launches that a constellation can follow in order to maintain some properties of the structure in each step of the sequence. Finally, the methodology also allows to asses the effect of failure of a satellite in the structure.

This work presents the following Necklace related Flower Constellations:

- 2D Necklace Flower Constellations. This is the basic design of Necklace Flower Constellations where the distribution is performed in the right ascension of the ascending node and the mean anomaly of the satellites. This kind of distribution generates rigid structures that are maintained during the dynamic of the system.

- 3D Necklace Flower Constellations. Compared to the 2D formulation, this technique includes the argument of perigee as the additional distribution variable, which expands the number of possibilities of design while generating rigid structures in the constellation.
- 4D Lattice Flower Constellations. This technique includes the effect of different values of the semi-major axis in satellite constellation design. This means that this methodology is able to bound satellites with very different dynamics, generating a structure as a constellation that presents periodicity.
- 4D Necklace Flower Constellations. This is the greatest generalization of the Necklace Flower Constellation theory which include all the former distributions in its formulation. In addition, it introduces some new concepts in satellite distribution that can be applied to the other Necklace Flower Constellation designs.
- n-Dimensional congruent lattices using necklaces. This theory represents the mathematical foundations of the Lattice and Necklace methodologies of Flower Constellations. It includes the boundaries that the Lattice and Necklace Flower Constellations presents and also the theorems to compute the number of different configuration possibilities that these techniques can provide.

It is important to note that the concepts and methodologies applied to a particular design shown in any of the Necklace Flower Constellations techniques can be applied to the others, since the foundations of these design techniques are the same.

In addition, this work introduces the Ground-Track Constellations, an alternative satellite constellation design performed directly in the Earth Fixed frame of reference. This alternative design philosophy represents the dual definition of the constellation (with respect to the Flower Constellation theory) and presents some advantages compared to other configurations defined in the inertial frame of reference. In particular, the constellation is referenced directly to the objective of most of the missions, the Earth, which simplifies the design process and makes the definition more natural in that reference frame. Moreover, this methodology allows to include orbital perturbations, specially the Earth gravitational potential, in a simple manner in the initial design of the constellation. Finally, this design technique allows to define any kind of distribution, including satellite formations.

All the research presented in this work provides the tools for the design and study of satellite constellations, and includes examples of application for the different methodologies introduced. This includes both simple and more complex studies where these techniques are applied for the definition and study of constellations.

Conclusiones

Los resultados de la investigación presentada en este manuscrito parten de la teoría de las Flower Constellations, una metodología general para el diseño de constelaciones de satélites basada en la Teoría de Números y que permite la generación de cualquier configuración de satélites. En particular, este trabajo centra su atención en las formulaciones basadas en lattices, representadas por las 2D y 3D Lattice Flower Constellations, que son la evolución de la parametrización original de la teoría, y las 2D Lattice Flower Constellations using necklaces, que introdujeron por primera vez la idea de necklaces en el diseño de constelaciones de satélites. Tomando estas metodologías como base, esta tesis continúa esta investigación generalizando la teoría anterior e introduciendo nuevos enfoques al problema.

Este trabajo contiene la teoría completa de las Necklace Flower Constellations, un nuevo marco para el diseño de constelaciones de satélites. La particularidad de esta nueva técnica reside en la generación de constelaciones cuyos satélites permiten crear una estructura que es mantenida durante la dinámica del sistema. Además, la teoría permite expandir el número de configuraciones diferentes obtenidas tanto como se desee, otorgando una herramienta poderosa para el diseño de constelaciones de satélites.

Las Necklace Flower Constellations constituyen la evolución y generalización de las Lattice Flower Constellations, una metodología inicialmente pensada para la generación de configuraciones simétricas y uniformes. En concreto, las Necklace Flower Constellations permiten aumentar el tamaño del espacio de búsqueda, siendo capaces de generar un mayor número de posibles configuraciones mientras se mantiene el número de satélites de la constelación. Esto es posible gracias a la generación de una constelación ficticia, mayor que la que queremos generar, de la que se selecciona el subconjunto de satélites que cumplen las condiciones de simetría y uniformidad. De esta forma, se mantienen las características originales de las Lattice Flower Constellations en el diseño.

Esta metodología tiene múltiples usos. Primero de todo, permite la expansión del número de posibilidades que un conjunto de satélites puede proporcionar. Segundo, presenta posibles oportunidades de reconfiguración que la constelación puede realizar para obtener distribuciones compatibles. Tercero, permite la definición de la secuencia de lanzamientos que una constelación puede seguir para mantener ciertas propiedades de la estructura en cada etapa de la secuencia. Finalmente, la metodología también permite la evaluación del efecto de fallo de un satélite en la estructura.

Este trabajo presenta las siguientes Necklace Flower Constellations:

- 2D Necklace Flower Constellations. Este es el diseño básico de las Necklace Flower Constellations donde la distribución se realiza en el argumento del nodo ascendente y en la anomalía media de los satélites. Este tipo de distribución genera estructuras rígidas que se mantienen durante la dinámica del sistema.
- 3D Necklace Flower Constellations. Comparado con la formulación de las 2D, esta técnica incluye el argumento del perigeo como variable adicional de distribución, la cual expande el número de posibilidades de diseño a la vez que genera estructuras rígidas en la constelación.
- 4D Lattice Flower Constellations. Esta técnica incluye el efecto de diferentes valores del semieje mayor en el diseño de constelaciones de satélites. Ello implica que esta metodología permite relacionar satélites con dinámicas muy distintas, generando una estructura como constelación que presenta periodicidad.
- 4D Necklace Flower Constellations. Esta es la generalización última de la teoría de las Necklace Flower Constellations, e incluye en su formulación todas las distribuciones anteriores. Además, esta metodología introduce nuevos conceptos en distribución de satélites que pueden ser aplicados a otros diseños basados en las Necklace Flower Constellations.
- n-Dimensional congruent lattices using necklaces. Esta teoría representa la base matemática de las metodologías de las Lattice y Necklace Flower Constellations. En concreto, incluye los límites que las Lattice y Necklace Flower Constellations presentan así como los teoremas que permiten la computación del número de posibilidades de configuración que estas metodologías de diseño permiten.

Es importante destacar que los conceptos y metodologías aplicados a diseños particulares mostrados en cualquiera de las técnicas de las Necklace Flower Constellations pueden ser aplicadas a otras, dado que los conceptos base son los mismos en estas técnicas de diseño.

Además, este trabajo introduce las Ground-Track Constellations, un diseño alternativo de constelaciones de satélites que se realiza directamente en el sistema de referencia Earth Fixed. Esta filosofía alternativa de diseño representa la definición dual de la constelación (con respecto a la teoría de las Flower Constellations) y presenta ciertas ventajas comparado con otras configuraciones definidas en el sistema de referencia inercial. En concreto, la constelación se referencia directamente con el objeto de la mayoría de misiones, la Tierra, lo que simplifica el proceso de diseño y consigue que la definición de la constelación sea más natural en este sistema de referencia. Además, esta metodología permite incluir, de un modo sencillo, las perturbaciones orbitales en el diseño inicial de la constelación. Esto es especialmente interesante para el caso del potencial gravitatorio terrestre. Finalmente, esta técnica de diseño permite definir cualquier tipo de distribución, incluyendo formaciones de satélites.

Toda la investigación presentada en este trabajo proporciona las herramientas para el diseño y estudio de constelaciones de satélites, incluyendo ejemplos de aplicación de las distintas metodologías introducidas. Esto incluye tanto estudios simples como más elaborados, en donde estas técnicas son aplicadas para la definición y estudio de constelaciones.

Bibliography

[1] Stephens, G. L.; Vane, D. G.; Boain, R. J.; Mace, G. G.; Sassen, K.; Wang, Z.; Illingworth, A. J.; O'Connor, E. J.; Rossow, W. B.; Durden, S. L.; Miller, S.D.; Austin, R. T.; Benedetti, A.; Mitrescu, C.; and the CloudSat Science Team: *The CloudSat mission and the A-Train: A new dimension of space-based observations of clouds and precipitation*, Bulletin of the American Meteorological Society, Vol. 83, No. 12, 2002, p. 1771-1790. doi: 10.1175/BAMS-83-12-1771.

[2] Krieger, G.; Moreira, A.; Fiedler, H.; Hajnsek, I.; Werner, M.; Younis, M.,; and Zink, M.: *TanDEM-X: a satellite formation for High-Resolution SAR Interferometry*, IEEE Transactions on Geoscience and Remote Sensing, Vol. 45, issue 11, 2007, p. 3317-3341. doi: 10.1109/TGRS.2007.900693.

[3] Walker, J.G.: *Satellite Constellations*, Journal of the British Interplanetary Society, Vol. 37, 1984, p. 559-572. ISSN 0007-084X.

[4] Draim, J. E.: *A common-period four-satellite continuous global coverage constellation*, Journal of Guidance, Control, and Dynamics, Vol. 10, No. 5, 1987, p. 492-499. doi: 10.2514/3.20244.

[5] Mortari, D.; Wilkins, M. P.; and Bruccoleri, C.: *The Flower Constellations*, Journal of the Astronautical Sciences, American Astronautical Society, Vol. 52, issue 1-2, 2004, p. 107-127.

[6] Mortari, D.; and Wilkins, M. P.: *Flower Constellation Set Theory Part I: Compatibility and Phasing*, IEEE Transactions on Aerospace and Electronic Systems, Vol. 44, No. 3, 2008, p. 953-963. doi: 10.1109/TAES.2008.4655355.

[7] Wilkins, M. P.; and Mortari, D.: *Flower Constellation Set Theory Part II: Secondary Paths and Equivalency*, IEEE Transactions on Aerospace and Electronic Systems, Vol. 44, No. 3, 2008, p. 964-976. doi: 10.1109/TAES.2008.4655356.

[8] Avendaño, M. E.; Davis, J. J.; and Mortari, D.: *The 2-D Lattice Theory of Flower Constellations*, Celestial Mechanics and Dynamical Astronomy, Vol. 116, No. 4, 2013, p. 325-337. doi: 10.1007/s10569-013-9493-8.

[9] Davis, J. J.; Avendaño, M. E.; and Mortari, D.: *The 3-D Lattice Theory of Flower Constellations*, Celestial Mechanics and Dynamical Astronomy, Vol. 116, No. 4, 2013, p. 339-356. doi: 10.1007/s10569-013-9494-7.

[10] Sarno, S.; Graziano, M. D.; and D'Errico, M.: *Polar constellations design for discontinuous coverage*, Acta Astronautica, Vol. 127, 2016, p. 367-374. doi: 10.1016/j.actaastro.2016.06.001.

[11] Mazal, L.; and Gurfil, P.: *Cluster flight algorithms for disaggregated satellites*, Journal of Guidance Control and Dynamics, Vol. 36, No. 1, 2013, p. 124-135. doi: 10.2514/1.57180.

[12] Avendaño, M. E.; and Mortari D.: *Rotating Symmetries in Space: The Flower Constellations*, Paper number AAS 09-189, 19^{th} AAS/AIAA Space Flight Mechanics Meeting, Savannah, GA, 2009; also Advances in the Astronautical Science, Vol. 134, 2009, p. 1317-1334.

[13] Avendaño, M. E.; and Mortari, D.: *New Insights on Flower Constellations Theory*, Journal of IEEE Transactions on Aerospace and Electronic Systems, Vol. 48, No. 2, 2012, p. 1018-1030. doi: 10.1109/TAES.2012.6178046.

[14] Casanova, D.; Avendaño, M. E.; and Mortari, D.: *Seeking GDOP-optimal Flower Constellations for global coverage problems through evolutionary algorithms*, Journal of Aerospace Science and Technology, Vol. 39, 2014, p. 331-337. doi: 10.1016/j.ast.2014.09.017.

[15] Casanova, D.; Avendaño, M. E.; and Tresaco, E.: *Lattice-preserving Flower Constellations under J_2 perturbations*, Celestial Mechanics and Dynamical Astronomy, Vol. 121, No. 1, 2014, p. 83-100. doi: 10.1007/s10569-014-9583-2.

[16] Arnas, D.; Casanova, D.; and Tresaco, E.: *Relative and absolute station-keeping for two-dimensional-lattice flower constellations*, Journal of Guidance, Control, and Dynamics, Vol. 39, No. 11, 2016, p. 2596-2602. doi: 10.2514/1.G000358.

[17] Casanova, D.; Avendaño, M. E.; and Mortari, D.: *Design of Flower Constellations using Necklaces*, Journal of IEEE Transactions on Aerospace and Electronic Systems, Vol. 50, issue 2, 2014, p. 1347-1358. doi: 10.1109/TAES.2014.120269.

[18] Casanova, D.; Avendaño, M. E.; and Mortari, D.: *Necklace Theory on Flower Constellations*, Advances in Astronautical Sciences, Vol. 140, 2011, p. 1791-1804.

[19] Arnas, D.; Casanova, D.; and Tresaco, E.: *2D Necklace Flower Constellations*, Acta Astronautica, Vol. 142, p. 18-28, 2018. doi: 10.1016/j.actaastro.2017.10.017.

[20] Arnas, D.; Casanova, D.; Tresaco, E.; and Mortari, D.: *3-Dimensional Necklace Flower Constellations*, Celestial Mechanics and Dynamical Astronomy, Vol. 129, No. 4, p. 433-448, 2017. doi: 10.1007/s10569-017-9789-1.

[21] Arnas, D.; Casanova, D.; Tresaco, E.; and Mortari, D.: *3D Lattice Flower Constellations using necklaces*, Advances in the Astronautical Sciences, Vol. 160, 2017, p. 1681-1700. ISBN: 978-0-87703-638-8; 978-0-87703-637-1.

[22] Arnas, D.; Casanova, D.; and Tresaco, E.: *Time distributions in satellite constellation design*, Celestial Mechanics and Dynamical Astronomy, Vol. 128, No. 2, 2017, p. 197-219. doi: 10.1007/s10569-016-9747-3.

[23] Arnas, D.; Casanova, D.; and Tresaco, E.: *Corrections on repeating ground-track orbits and their applications in satellite constellation design*, Advances in the Astronautical Sciences, Vol. 158, 2016, p. 2823-2840. ISBN: 978-0-87703-634-0.

[24] Deprit, A: *Canonical transformations depending on a small parameter.*, Celestial Mechanics, Vol. 1, No. 1, 1969, p. 12-30.

[25] Brouwer, D: *Solution of the problem of artificial satellite theory without drag.*, Astronomical Journal, Vol. 64, 1959, p. 378.

[26] Liu, J. J. F.: *Satellite Motion about an Oblate Earth*, AIAA Journal, Vol. 12, No. 11, 1974, p. 1511-1516. doi: 10.2514/3.49537.

[27] Liu, J. J. F.; and Alford, R. L.: *Semianalytic theory for a close-Earth artificial satellite*, Journal of Guidance, Control, and Dynamics, Vol. 3, No. 4, 1980, p. 304-311. doi: 10.2514/3.55994.

[28] Kozai, Y.: *Second-order solution of artificial satellite theory without air drag*, The Astronomical Journal, Vol. 67, 1962, p. 446-461.

[29] National Imagery and Mapping Agency: *World Geodetic System 1984*, Third Edition, National Imagery and Mapping Agency, 2000.

[30] Abad, A.: *Astrodinámica*, Bubok Publishing S.L., 2012.

[31] Fortescue, P. W.; Stark, J. P. W.; and Swinerd, G. G.: *Spacecraft Systems Engineering*, Third Edition, Wiley, 2003.

[32] Harris, I.; and Priester, W.: *Theoretical models for the solar-cycle variation of the upper atmosphere*, Journal of Geophysical Research, Vol. 67, No. 12, 1962, p. 4585-4591. doi: 10.1029/JZ067i012p04585.

[33] Harris, I.; and Priester, W.: *Relation between Theoretical and Observational Models of the Upper Atmosphere*, Journal of Geophysical Research, Vol. 68, No. 20, 1963, p. 5891-5894. doi: 10.1029/JZ068i020p05891.

[34] Larson, W. J.; and Wertz, J. R.: *Space Mission Analysis and Design*, Third Edition, Microcosm Press, 1999. ISBN: 1881883108.

[35] Vallado, D.: *Fundamentals of Astrodynamics and Applications*, Space Technology Library, 2001, p. 869-879. ISBN: 978-1-881883-14-2.

[36] Casanova, D.: *Flower Constellations: optimization and applications*, Thesis dissertation, Universidad de Zaragoza, 2013.

[37] Arnas, D.; Fialho, M. A. A.; and Mortari, D.: *Fast and Robust Kernel Generators for Star Trackers*, Acta Astronautica, Vol. 134, 2017, p. 291-302. doi: 10.1016/j.actaastro.2017.02.016.

[38] Arnas, D.; Fialho, M. A. A.; and Mortari, D.: *Robust triad and quad generation algorithms for star trackers*, Advances in the Astronautical Sciences, Vol. 160, 2017, p. 827-846. ISBN: 978-0-87703-638-8; 978-0-87703-637-1.

[39] Tucke, A.: *Applied Combinatorics*, John Wiley and Sons, 2002. ISBN: 0471735078.

[40] Cattell, K.; Ruskey, F.; Sawada, J.; Serra, M.; and Miers, R.: *Fast Algorithms to Generate Necklaces, Unlabeled Necklaces, and Irreducible Polynomials over GF(2)*, Journal of Algorithms, Vol. 37, No. 2, 2000, p. 267-282. doi: 10.1006/jagm.2000.1108.

[41] Sawada, J.: *A fast algorithm to generate necklaces with fixed content*, Theoretical Computer Science, Vol. 301, 2003, p. 277-289. doi: 10.1016/S0304-3975(03)00049-5.

[42] Newman, M.: *Integral matrices*, Academic Press, 1972. ISBN: 9780080873589.

[43] Storjohann, A.; and Labahn, G.: *Asymptotically fast computation of Hermite normal forms of integer matrices*, Proceedings of the 1996 international symposium on Symbolic and algebraic computation, ACM, 1996, p. 259-266. doi: 10.1145/236869.237083.

[44] Wagner, C.: *A Prograde Geosat Exact Repeat Mission?*, Journal of the Astronautical Sciences, Vol. 39, 1991, p. 313-326.

[45] Mortari, D.; Avendaño, M.E.; and Lee, S.: *J2-Propelled Orbits and Constellations*, Journal of Guidance, Control, and Dynamics, Vol. 37, No. 5, 2014, p. 1701-1706. doi: 10.2514/1.G000363.

[46] Schaub, H.; and Alfriend, K.T.: *J_2 Invariant relative orbits for spacecraft formations.*, Celestial Mechanics and Dynamical Astronomy, Vol. 79, issue 2, 2001, p. 77-95. doi: 10.1023/A:1011161811472.

[47] Lee, D. S.; Storey, J. C.; Choate, M. J.; and Hayes, R. W.: *Four years of Landsat-7 on-orbit geometric calibration and performance*, IEEE Transactions on Geoscience and Remote Sensing, Vol. 42, No. 12, 2004, p. 2786-2795. doi: 10.1109/TGRS.2004.836769.

[48] Hammerling, D. M.; Michalak, A. M.; and Kawa, S. R.: *Mapping of CO2 at high spatiotemporal resolution using satellite observations: Global distributions from OCO-2*, Journal of Geophysical Research: Atmospheres, Vol. 117, No. D6, 2012. doi: 10.1029/2011JD017015.

[49] Chander, G.; Markham, B. L.; and Helder, D. L.: *Summary of current radiometric calibration coefficients for Landsat MSS, TM, ETM+, and EO-1 ALI sensors*, Remote sensing of environment, Vol. 113, No. 5, 2009, p. 893-903. doi: 10.1016/j.rse.2009.01.007.

[50] Teillet, P. M.; Barker, J. L.; Markham, B. L.; Irish, R. R.; Fedosejevs, G.; and Storey, J. C.: *Radiometric cross-calibration of the Landsat-7 ETM+ and Landsat-5 TM sensors based on tandem data sets*, Remote sensing of environment, Vol. 78, No. 1, 2001, p. 39-54. doi: 10.1016/S0034-4257(01)00248-6.

[51] Chander, G.; Meyer, D. J.; and Helder, D. L.: *Cross calibration of the Landsat-7 ETM+ and EO-1 ALI sensor*, IEEE Transactions on Geoscience and Remote Sensing, Vol. 42, No. 12, 2004, p. 2821-2831. doi: 10.1109/TGRS.2004.836387.

[52] Parkinson, C. L.; Ward, A.; and King, M. D.: *Earth science reference handbook: a guide to NASA's earth science program and earth observing satellite missions*, National Aeronautics and Space Administration, 277, 2006.